

UC Berkeley
SEMM Reports Series

Title

Analysis of Continuous Box Girder Bridges

Permalink

<https://escholarship.org/uc/item/6z00w953>

Author

Scordelis, Alex

Publication Date

1967-10-01

HIGHWAY PULP APPLICATIONS
LEWIS HALL
UNIVERSITY OF CALIFORNIA
BERKELEY, CALIFORNIA 94720
(415) 642-5113

REPORT NO.
SESM-67-25

STRUCTURES AND MATERIALS RESEARCH
DEPARTMENT OF CIVIL ENGINEERING

ANALYSIS OF CONTINUOUS BOX GIRDER BRIDGES

BY
A. C. SCORDELIS

Report to the Sponsors: Division of Highways, Department
of Public Works, State of California, and the Bureau of
Public Roads, Federal Highway Administration, United States
Department of Transportation.

NOVEMBER 1967

COLLEGE OF ENGINEERING
OFFICE OF RESEARCH SERVICES
UNIVERSITY OF CALIFORNIA
BERKELEY CALIFORNIA

Structures and Materials Research
Department of Civil Engineering
Division of Structural Engineering
and
Structural Mechanics

ANALYSIS OF CONTINUOUS BOX GIRDER BRIDGES

A Report of an Investigation

by

A. C. Scordelis
Professor of Civil Engineering

to

The Division of Highways
Department of Public Works
State of California
Under Research Technical Agreement
No. 13945-14039

and

U.S. Department of Transportation
Federal Highway Administration
Bureau of Public Roads

College of Engineering
Office of Research Services
University of California
Berkeley, California

November 1967

TABLE OF CONTENTS

| | <u>Page</u> |
|---|-------------|
| List of Tables | iv |
| List of Figures | v |
| List of Symbols | x |
| 1. INTRODUCTION | 1 |
| 1.1 Objective | 1 |
| 1.2 General Remarks | 1 |
| 1.3 Previous Studies | 4 |
| 1.4 Scope of Present Investigation | 7 |
| 2. FOLDED PLATE METHOD OF ANALYSIS | 11 |
| 2.1 Introduction | 11 |
| 2.2 General Description of the Method | 12 |
| 2.3 Computer Program - MUPDI | 15 |
| 3. FINITE SEGMENT METHOD OF ANALYSIS | 18 |
| 3.1 Introduction | 18 |
| 3.2 General Description of the Method | 20 |
| 3.3 Derivation of Equations for the Solution of a Single Span Structure by the Finite Segment Method | 24 |
| 3.3.1 Modified Field Matrix for a Beam Segment | 24 |
| 3.3.2 Stiffness matrix for a Beam Segment in Relative Coordinate System | 28 |
| 3.3.3 Fixed Joint Forces Due to Actions at Section k-1 | 32 |
| 3.3.4 Fixed Joint Solution for Actions Z_k in Terms of Actions Z_{k-1} | 33 |
| 3.3.5 Actions Z_k Due to Final Joint Displacements at Center of the Segment | 34 |
| 3.3.6 Fixed Coordinate System and Direct Stiffness Method for One Segment of the Structure | 34 |
| 3.3.7 Boundary Conditions at Two Ends of the Structure and Setup of Actions Vector at the Origin | 36 |
| 3.3.8 Sequence of Matrix Operations | 37 |
| 3.3.9 Equations of Internal Forces and Displacements at Center of Each Segment | 43 |

| | <u>Page</u> |
|---|-------------|
| 3.4 Solution for a Continuous Cellular Folded Plate Structure | 46 |
| 3.5 Direct Stiffness Method Using Complete Segment Stiffness Matrix | 50 |
| 3.6 Advantages and Disadvantages of the Segment Progression Solution as Compared to the Band Matrix Solution | 51 |
| 3.7 Computer Program - SIMPLA | 53 |
| 4. FINITE ELEMENT METHOD OF ANALYSIS | 57 |
| 4.1 Introduction | 57 |
| 4.2 General Description of the Method | 59 |
| 4.3 Development of Finite Element Stiffness by Virtual Work | 65 |
| 4.4 Element Stiffness for Membrane Action-Plane Stress Analysis | 71 |
| 4.4.1 Elasticity Equations for the Plane Stress Problem | 71 |
| 4.4.2 Types of Finite Element Models | 73 |
| 4.4.3 Nodal Point Displacements and Resulting Displacement Patterns | 74 |
| 4.4.4 Derivation of Element Stiffness for Plane Stress | 83 |
| 4.5 Element Stiffness Matrix for Slab Action-Plate Bending Analysis | 90 |
| 4.5.1 Elasticity Equations for the Plate Bending Problem | 90 |
| 4.5.2 Nodal Point Displacements and Resulting Displace- ment Patterns | 93 |
| 4.5.3 Derivation of Element Stiffness for Plate Bending | 96 |
| 4.6 Computer Program - FINPLA | 104 |
| 5. COMPARISON OF RESULTS | 107 |
| 5.1 Introduction | 107 |
| 5.2 Description of Example Bridge and Analytical Models | 107 |
| 5.3 Vertical Deflections | 112 |
| 5.4 Longitudinal Stresses | 112 |
| 5.5 Distribution of Moments to Each Girder | 123 |
| 5.6 Transverse Slab Moments | 130 |
| 5.7 Computer Times | 136 |

| | <u>Page</u> |
|---|-------------|
| 6. STUDY OF 3-CELL AND 6-CELL BRIDGES | 141 |
| 6.1 General Remarks | 141 |
| 6.2 Description of Example Bridges Analyzed | 142 |
| 6.3 Distribution of Moments to Each Girder | 148 |
| 6.3.1 Comparison of Results by Different Methods | 148 |
| 6.3.2 Longitudinal Division of Total Statical Moment Between Positive and Negative Moments | 148 |
| 6.3.3 Transverse Distribution of Moments to Each Girder | 154 |
| 6.4 Midspan Deflections | 156 |
| 7. CONCLUSIONS | 158 |
| 8. ACKNOWLEDGMENTS | 161 |
| 9. REFERENCES | 162 |
| APPENDIX A | |
| Description of IBM 7040/7094 Computer Program for the Analysis of Folded Plate Structures by the Finite Segment Method (Ordinary Theory)---SIMPLA | A-1 |
| APPENDIX B | |
| Description of IBM 7040/7094 Computer Program for the Analysis of Folded Plate Structures by the Finite Element Method (Elasticity Theory)---FINPLA | B-1 |

LIST OF TABLES

| <u>Table</u> | <u>Title</u> | <u>Page</u> |
|--------------|---|-------------|
| 1 | Distribution of Moments to Each Girder for 3-Cell Bridge under Eccentric Load (Fixed-Simple End Support Conditions) | 135 |
| 2 | Summary of Computer Analyses Performed on Example Bridges | 147 |
| 3 | Distribution of Moments to Each Girder for 3-Cell Bridge under Eccentric Load | 150 |
| 4 | Distribution of Moments to Each Girder for 3-Cell Bridge under Center Load | 151 |
| 5 | Distribution of Moments to Each Girder for 6-Cell Bridge under Eccentric Load | 152 |
| 6 | Distribution of Moments to Each Girder for 6-Cell Bridge under Center Load | 153 |
| 7 | Midspan Vertical Deflections in Ft. x 10 ⁴ for Eccentric and Center Loads on 3 and 6-Cell Bridges | 157 |

LIST OF FIGURES

| <u>Figure</u> | <u>Title</u> | <u>Page</u> |
|---------------|---|-------------|
| 1 | Reinforced Concrete Box Girder Bridges | 3 |
| 2 | Cross-section of a Composite Steel-Concrete Box Girder Bridge | 3 |
| 3 | Folded Plate Method of Analysis of Continuous Box Girder Bridge | 14 |
| 4 | Finite Segment Analytical Model | 19 |
| 5a | Positive Directions of Finite Segment Forces and Moments in the Relative Coordinate System | 23 |
| 5b | Positive Directions of Finite Segment Displacements in the Relative Coordinate System | 23 |
| 6 | Finite Segments of a Folded Plate Structure | 25 |
| 7 | Positive Directions of Actions for a Beam Segment | 25 |
| 8 | Edge Force Patterns for a Beam Segment | 27 |
| 9 | Positive Segment Edge Forces and Displacements in the Relative Coordinate System | 35 |
| 10 | Positive Joint Forces and Displacements in the Fixed Coordinate System | 35 |
| 11 | Positive Segment Edge Forces and Displacements in the Fixed Coordinate System | 35 |
| 12 | Folded Plate Structure with One Interior Rigid Diaphragm | 52 |
| 13 | Makeup of Structure Stiffness Matrix Using Complete Segment Stiffness Matrix | 52 |
| 14 | Finite Element Analytical Model | 61 |
| 15 | Global (Fixed) XYZ and Local (Relative) xyz Coordinate Systems and Finite Element Dimensions | 61 |
| 16 | Positive Internal Forces and Displacements in a Finite Element | 61 |

| <u>Figure</u> | <u>Title</u> | <u>Page</u> |
|---------------|--|-------------|
| 17 | Positive Directions for Coordinate Axes, External Forces, Displacements and Internal Stresses | 72 |
| 18 | Notation and Positive Directions for Displacements and Forces at a Typical Nodal Point | 76 |
| 19 | Displacement and Damping Functions | 76 |
| 20 | Displacement Pattern for Nodal Point Displacement u_i | 78 |
| 21 | Displacement Pattern for Nodal Point Displacement v_i | 78 |
| 22 | Displacement Pattern for Nodal Point Displacement θ_{zi} | 79 |
| 23 | Rotations and Shear Distortions in Four Elements Meeting at a Typical Nodal Point | 82 |
| 24 | Positive Directions for Coordinate Axes, External Forces, Displacements, and Internal Moments and Forces | 91 |
| 25 | Notation and Positive Directions for Displacements and Forces at a Typical Nodal Point | 95 |
| 26 | Displacement Pattern for Nodal Point Displacement θ_{yi} | 95 |
| 27 | Displacement Pattern for Nodal Point Displacement θ_{xi} | 95 |
| 28 | Displacement Pattern for Nodal Point Displacement w_i | 95 |
| 29 | Dimensions and Loading for Example Bridge | 109 |
| 30 | Folded Plate Analytical Model | 109 |
| 31 | Finite Element Analytical Model - Mesh 1 | 111 |
| 32 | Finite Element Analytical Model - Mesh 2 | 111 |
| 33 | Finite Segment Analytical Model - Mesh 1 | 113 |
| 34 | Finite Segment Analytical Model - Mesh 2 | 113 |
| 35 | Vertical Deflections Along Longitudinal Line at Top of Girder R_2 | 114 |
| 36 | Vertical Deflections Along Longitudinal Line at Top of Girder R_1 | 115 |
| 37 | Vertical Deflections Along Longitudinal Line at Top of Girder L_1 | 116 |

| <u>Figure</u> | <u>Title</u> | <u>Page</u> |
|---------------|---|-------------|
| 38 | Vertical Deflections Along Longitudinal Line at Top of Girder L_2 | 117 |
| 39 | Vertical Deflections at Transverse Sections | 118 |
| 40 | Longitudinal Distribution of Longitudinal Stress σ_x (PSF) in Top Slab | 120 |
| 41 | Longitudinal Distribution of Longitudinal Stress σ_x (PSF) in Bottom Slab | 121 |
| 42 | Longitudinal Distribution of Longitudinal Stress σ_x (PSF) in External Web | 122 |
| 43 | Transverse Distribution of Longitudinal Stress σ_x (PSF) in Top Slab at Midspan Section | 124 |
| 44 | Transverse Distribution of Longitudinal Stress σ_x (PSF) in Bottom Slab at Midspan Section | 125 |
| 45 | Transverse Distribution of Longitudinal Stress σ_x (PSF) in Webs at Midspan Section | 126 |
| 46 | Transverse Distribution of Longitudinal Stress σ_x (PSF) in Top Slab at Fixed End Support | 127 |
| 47 | Transverse Distribution of Longitudinal Stress σ_x (PSF) in Bottom Slab at Fixed End Support | 128 |
| 48 | Transverse Distribution of Longitudinal Stress σ_x (PSF) in Webs at Fixed End Support | 129 |
| 49 | Longitudinal Distribution of Transverse Moment M_y (FT-LB/FT) in Top Slab | 131 |
| 50 | Longitudinal Distribution of Transverse Moment M_y (FT-LB/FT) in Bottom Slab | 132 |
| 51 | Longitudinal Distribution of Transverse Moment M_y (FT-LB/FT) at Top of External Web | 133 |
| 52 | Longitudinal Distribution of Transverse Moment M_y (FT-LB/FT) at Bottom of External Web | 134 |
| 53 | Transverse Distribution of Transverse Slab Moment M_y (FT-LB/FT) in Top Slab at Midspan | 137 |
| 54 | Transverse Distribution of Transverse Slab Moment M_y (FT-LB/FT) in Bottom Slab at Midspan | 138 |
| 55 | Transverse Distribution of Transverse Slab Moment M_y (FT-LB/FT) in Webs at Midspan | 139 |

| <u>Figure</u> | <u>Title</u> | <u>Page</u> |
|---------------|---|-------------|
| 56 | Transverse Section Dimensions and Load Positions for Example Bridges | 143 |
| 57 | End Conditions for Example Bridges | 143 |
| 58 | Transverse Element Subdivisions for Analysis of 3-Cell Bridges | 145 |
| 59 | Transverse Element Subdivision of 6-Cell Bridge Under Eccentric Load for Folded Plate and Finite Segment Analyses | 146 |
| 60 | Transverse Element Subdivision of 6-Cell Bridge Under Central Load for Folded Plate and Finite Segment Analyses | 146 |
| 61 | Beam Moment Diagram for Simple-Simple Case | 149 |
| 62 | Beam Moment Diagram for Fixed-Simple Case | 149 |
| 63 | Beam Moment Diagram for Fixed-Fixed Case | 149 |

APPENDIX A

| | | |
|----|--|------|
| A1 | Longitudinal Elevation and Loading | A-11 |
| A2 | General View of Structure | A-11 |
| A3 | Cross-Section Idealization Using Element, Plate Type, and Joint Numbers | A-12 |
| A4 | Positive Joint Actions in Fixed Coordinate System | A-12 |
| A5 | Sign Convention for Element Projection and Corresponding Positive Direction of Element Relative Coordinate Axes and Positive Plate Edge Forces | A-12 |
| A6 | Positive Internal Beam End and Plate Edge Forces and Displacements | A-13 |

| <u>Figure</u> | <u>Title</u> | <u>Page</u> |
|---------------|--|-------------|
| APPENDIX B | | |
| B1 | Longitudinal Elevation and Loading | B-10 |
| B2 | General View of Structure Showing Right Hand Global Coordinate System | B-10 |
| B3 | First Interval Cross-Section Idealization Using Element, Element Type, and Nodal PointNumbers | B-11 |
| B4 | Positive Direction of All External Loads and Displacements . . | B-11 |
| B5 | Sign Convention for Element Projections and Corresponding Positive Direction of Local Element Coordinate Axes | B-11 |
| B6 | Positive Internal Element Forces, Moments and Stresses | B-12 |

LIST OF SYMBOLS

The alphabetic list of symbols is separated into three parts corresponding to the different methods of analysis.

1. FOLDED PLATE METHOD OF ANALYSIS

| | |
|----------------|---|
| [F] | Flexibility matrix |
| P | External loads |
| X | Redundant forces |
| { δ } | Displacement vector |
| { δ_o } | Displacement vector due to external loads |
| { δ }_x | Displacement vector due to redundant forces |

2. FINITE SEGMENT METHOD OF ANALYSIS

| | |
|-------|--|
| [a] | Sub-vectors obtained by partitioning $[D_o]$ |
| {a} | Sub-vectors obtained by partitioning $\{D_o\}$ |
| [A] | Displacement transformation matrix |
| b | Plate thickness |
| [b] | Sub-matrix obtained by partitioning $[D_o]$ |
| {b} | Sub-vectors obtained by partitioning $\{\tilde{D}_o\}$ |
| [B] | Matrix representing plate edge displacements, v_p , in terms of the unknown actions at origin |
| {B} | Column vector representing plate edge displacements, v_p , due to known actions at origin and previous segments. |
| [C] | Matrix relating beam actions $\{Z_{k-1}\}$ to fixed joint forces $\{S_p\}_F$. |
| [c] | Matrix product of $[b] [d]^{-1}$ |
| d | Plate width |
| {d} | Sub-vectors obtained by partitioning $\{Z_o^T\}$ |
| {d}_o | Displacement actions at section e only due to unknown actions at origin |

| | |
|-----------------------|---|
| $[D_i]$ | Matrix representing plate actions at section i in terms of the unknown actions at origin |
| $\{\tilde{D}_i\}$ | Column vector representing plate actions at section i due to known actions at origin and previous segments |
| E | Modulus of elasticity |
| $\{e\}$ | Subscript denotes actions at section e |
| $[E]$ | Matrix representing the fixed joint forces in terms of the unknown actions at origin |
| $\{\tilde{E}\}$ | Column vector representing the fixed joint forces due to known actions at origin and previous segments |
| $\{f\}$ | Sub-vectors obtained by partitioning $\{Z_o^T\}$ |
| $\{f_o\}$ | Force actions at section e only due to unknown actions at origin |
| $\{\tilde{f}\}_{d=0}$ | Force actions at section e due to loads at span I assuming the structure is fixed at e |
| $\{ \}_F$ | Subscript F refers to fixed joint actions |
| F_K | Field matrix of segment k |
| G | Shearing modulus |
| $[G]$ | Matrix representing the final joint displacements in terms of the unknown actions at origin |
| $\{\tilde{G}\}$ | Column vector representing the final joint displacements due to known actions at origin and previous segments |
| $[H]$ | Matrix relating joint actions $\{Z_{k-1}\}$ to fixed joint actions $\{Z_k\}_F$ |
| I | Moment of inertia = $(1/12)bd^3$ |
| I_s | Moment of inertia of a slab strip of unit width = $b^3/12$ |
| $[J]$ | Matrix relating final joint displacements $\{v_p\}$ to actions $\{Z_k\}_v$ |
| K | Constant |
| $[K_p]$ | Plate stiffness matrix |
| $[K_s]$ | Slab stiffness matrix |
| $\{ \}_{kn}$ | Subscript kn refers to known vector |

| | |
|--|--|
| L | Segment length |
| \bar{L} | Half segment length = $\frac{1}{2} L$ |
| [L] | Coefficient matrix in which each column contains a single 1 and the rest of the elements are zeros |
| $[L_e^T]$ | Matrix representing plate actions after an interior rigid diaphragm, Section e, in terms of a new set of unknowns which contain the diaphragm reactions and the non-restrained displacements |
| $[L_e^T]$ | Column vector representing plate actions after an interior rigid diaphragm due to loads at previous spans and known diaphragm restraints |
| M | In-plane bending moment, or transverse slab moment about the longitudinal edge of a segment |
| $\left. \begin{matrix} M_i \\ M_j \end{matrix} \right\}$ | Transverse slab moment at i-edge, j-edge, per unit width |
| $[M^m]$ | Matrix product of $[C^T] [L^T]$ |
| $\{\tilde{M}^m\}$ | Matrix product of $[C^T] [Z_o^m]_{kn}$ |
| N | Axial force |
| $[N^1], [\tilde{N}^1]$ | Matrix product of $[A]^T [M^1]$ or $[A]^T [\tilde{M}^1]$ for plate element 1 |
| P | Transverse membrane force normal to the edge of a segment |
| P' | Symmetrical transverse membrane edge force per unit length |
| P'' | Anti-symmetrical transverse membrane edge force per unit length |
| Q | Shear force, or shear force normal to the plate at the edge of a segment |
| $\{r_n\}$ | Final joint displacement vector at joint n |
| $\{R\}$ | Final joint force vector |
| $\{R\}_A$ | External applied joint force vector |
| $\{\tilde{R}\}_A$ | Vector difference, $\{R\}_A - \{E\}$ |
| $\{R\}_F$ | Fixed joint forces of a whole transverse section |

| | |
|--|---|
| $\{\bar{S}_n^\Sigma\}$ | Fixed joint force vector in fixed coordinate system at joint n . Σ denotes the sum over all elements connecting to the joint n |
| $\{S_p\}$ | Plate force vector |
| $\{S_s\}$ | Force vector of slab action |
| $\{\bar{S}\}_F$ | Fixed joint force vector in the fixed coordinate system |
| T | Membrane shear force along the edge of a segment |
| T' | Symmetrical membrane edge shear force per unit length |
| T'' | Anti-symmetrical membrane edge shear force per unit length |
| $[^T]$ | Superscript T inside brackets refers to total plate elements in a cross-section |
| $[]^T$ | Superscript T outside of brackets refers to matrix transpose |
| u | Axial displacement corresponding to N , or in-plane displacement corresponding to T along the edge of a segment |
| \bar{u} | Displacement at center of segment due to T' , or, internal beam displacement at center of segment due to u_i and u_j |
| $\{ \}_{unk}$ | Subscript unk refers to unknown vector |
| v | Shear displacement corresponding to Q , or transverse displacement corresponding to P normal to the edge of a segment |
| \bar{v} | Displacement at center of segment due to T'' , or internal beam displacement at center of segment due to u_i and u_j |
| v' | Transverse extension at segment edge due to P' , or displacement defined as $(v_i - v_j)$ |
| $\{v_p\}$ | Plate displacement vector, or final joint displacements at center of the segment, or displacement vector in relative coordinate system corresponding to plate stiffness |
| $\{v_s\}$ | Displacement vector of slab action, or displacement vector in relative coordinate system corresponding to slab stiffness |
| $\{\bar{v}_d\}$ | Displacement vector defined as the difference between the final edge displacements and the edge displacements carried over from the previous $(k-1)$ section |
| $\left. \begin{matrix} v_i \\ v_j \end{matrix} \right\}$ | Shear force normal to slab at i -edge, j -edge, per unit width |

| | |
|--------------------------|--|
| w | Shear displacement normal to the plate at the edge of a segment |
| w_i w_j | Deflection due to shear force V_i, V_j |
| Z_k Z_{k-1} | |
| Z_o^m | Action at origin of plate m |
| β | Coefficient = $6EIK/L^2GA$ |
| $\bar{\beta}$ | Coefficient = 4β |
| θ | Transverse slab rotation corresponding to M about the longitudinal edge of a segment |
| θ_i θ_j | Rotation due to slab moment M_i, M_j |
| Ψ | |
| $\bar{\Psi}$ | Displacement at center of segment due to P'' , or internal beam rotation at center of segment due to u_i and u_j |

3. FINITE ELEMENT METHOD OF ANALYSIS

| | |
|---------|---|
| a | Element dimension in x-direction |
| [a] | Displacement transformation matrix |
| [A] | Generalized coordinate transformation matrix |
| b | Element dimension in y-direction |
| $[B_p]$ | Matrix relating generalized coordinates α_p to strain ϵ |
| $[B_s]$ | Matrix relating generalized coordinates α_s to curvatures κ |
| D | Plate stiffness = $Eh^3/12(1-\nu^2)$ |
| [D] | Matrix containing material constants |
| E | Elastic modulus |

| | |
|---------------|--|
| F_{xi} | Nodal point force at i corresponding to u_i |
| F_{yi} | Nodal point force at i corresponding to v_i |
| F_{zi} | Nodal point force at i corresponding to w_i |
| $F(x,y)$ | Displacement functions |
| h | Element thickness |
| $[k]$ | Element stiffness matrix in local coordinates |
| $[\bar{k}]$ | Element stiffness matrix in global coordinates |
| $[\tilde{k}]$ | Element stiffness matrix relating generalized forces β to generalized coordinates α |
| $[k_p]$ | Element in-plane stiffness matrix |
| $[k_s]$ | Element slab stiffness matrix |
| $[k]$ | Structure stiffness matrix |
| M_x | } Plate bending moments |
| M_y | |
| M_{xy} | |
| M_{xi} | Moment at node i corresponding to θ_{xi} |
| M_{yi} | Moment at node i corresponding to θ_{yi} |
| M_{zi} | Moment at node i corresponding to θ_{zi} |
| N_x | } Membrane forces |
| N_y | |
| N_{xy} | |
| Q_x | } Plate transverse shears |
| Q_y | |
| r | Nodal point displacements corresponding to R (global coordinates) |
| R | External forces and moments (global coordinates) |
| S | Internal forces (local coordinates) |
| \bar{S} | Internal forces (global coordinates) |

| | |
|---------------|--|
| S_p | Internal in-plane forces |
| S_s | Internal slab forces |
| u_i | Displacement of node i in x-direction |
| v | Internal displacements (local coordinates) |
| \bar{v} | Internal displacements (global coordinates) |
| v_i | Displacement of node i in y-direction |
| v_p | Internal in-plane displacements |
| v_s | Internal slab displacements |
| w_i | Displacement of node i in z-direction |
| W_E | External virtual work |
| W_I | Internal virtual work |
| X_n | } Displacement functions in x, y -directions (n-order of polynomial) |
| Y_n | |
| α | Generalized coordinates |
| β | Generalized forces corresponding to general coordinates α |
| ϵ | Strains |
| ϵ_x | } Strain components |
| ϵ_y | |
| γ_{xy} | |
| θ_{xi} | Rotation of node i about x-axis |
| θ_{yi} | Rotation of node i about y-axis |
| θ_{zi} | Rotation of node i about z-axis |
| K | Curvatures |
| ν | Poisson's ratio |

ρ_x }
 ρ_y } Radii of curvatures
 ρ_{xy} }

σ_x }
 σ_y } Stress components
 τ_{xy} }

1. INTRODUCTION

1.1 Objective

The objective of this investigation was the development of general methods of analysis for continuous box girder bridges. The study was concerned with the elastic analysis of these structures by methods suited to the application of digital computers. The ultimate goal of the investigation was the development of general computer programs capable of accurately determining displacements and internal forces in prismatic cellular box girder bridges having arbitrary cross-sections and end support conditions. These programs were to be designed to require a minimum amount of input information and be able to meet a variety of loading and boundary conditions.

1.2 General Remarks

The present expansion of the highway network, in the State of California and elsewhere, is largely the result of the great increase in traffic, population, and the extensive growth of metropolitan urban areas. This expansion has led to many changes in the use and development of various kinds of bridges. In recent years bridges having cellular cross-sections of various types have been proposed and used as economic and aesthetic solutions for the over crossings, under crossings, separation structures and viaducts found in today's modern highway system.

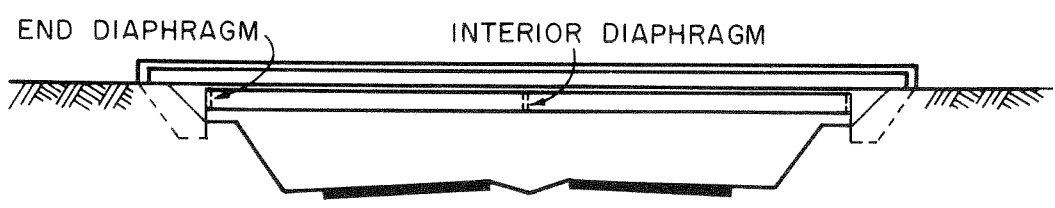
In California, the most widely used cellular type bridge is the reinforced concrete box girder bridge, Fig. 1. In recent years, roughly 60% of California's concrete bridges (computed on the basis of deck area) have been of this variety. The very large torsional rigidity of the box girder's closed cellular section provides structural efficiency, while its broad unbroken soffit, viewed from beneath, provides a pleasing appearance.

These bridges have found wide usage both as simple span and continuous structures, Figs. 1a, 1b, primarily in the span ranges between 60 and 100 feet. Transverse diaphragms are placed at the end and interior support points and in some cases additional interior diaphragms are utilized between supports. For continuous bridges interior supports are often provided by single column bents to give a graceful appearance to the structure.

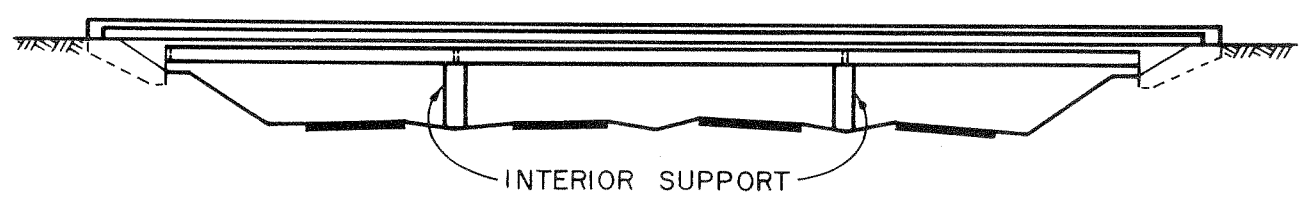
The typical cross-section of a reinforced concrete box girder bridge, Fig. 1c, consists of a top and bottom slab connected monolithically by vertical webs to form a cellular or box-like structure. In some of the more recent designs, efforts have been directed toward making box girder bridges even more attractive by incorporating sloping or rounded exterior girder webs, Fig. 1c. This improvement in aesthetic qualities has been accompanied, however, by some increases in the complexity of construction, and of design by specifications which were established for simpler configurations of cross-sections.

For longer spans up to 160 feet, cast-in-place, simply supported, post-tensioned box girders have been used extensively. In the past few years this type of bridge has comprised almost half of all the prestressed highway structures built in California.

Another type of cellular bridge which has recently received considerable attention is the composite steel-concrete box girder bridge, Fig. 2. This bridge consists of a concrete deck acting integrally with cellular steel boxes. The individual steel boxes are spaced uniformly over the width of the bridge. Each box consists of two narrow top flange plates welded to two inclined web plates and a wide bottom flange plate connecting the two webs to form the steel box.



a) ELEVATION OF TYPICAL SIMPLE SPAN BRIDGE



b) ELEVATION OF TYPICAL CONTINUOUS BRIDGE



c) TYPICAL CROSS - SECTIONS

FIG. 1 REINFORCED CONCRETE BOX GIRDER BRIDGES

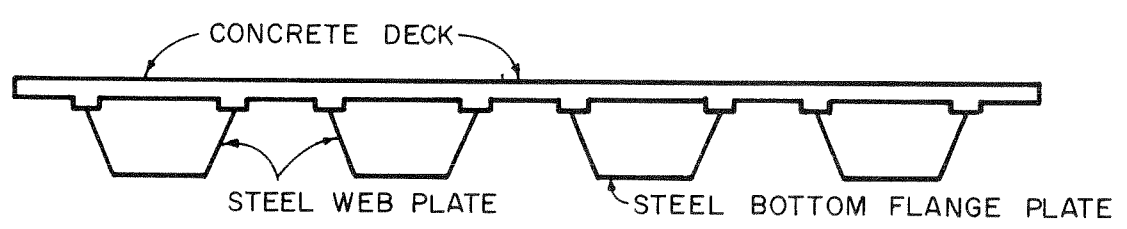


FIG. 2 CROSS-SECTION OF A COMPOSITE STEEL-CONCRETE BOX GIRDER BRIDGE

Present design methods for continuous box girder bridges are based on taking a typical repeating segment of the cross-section and treating it as an independent longitudinal beam. For wheel loads placed on the bridge deck, empirical formulas are used to determine the load distribution to the independent beam, which is then analyzed as a continuous beam to determine positive and negative beam moments and thence longitudinal stresses. While this procedure may provide some measure of accuracy regarding the distribution of the positive moments across the width of the bridge, it is difficult to justify the use of this same distribution for the negative moments at the supports. In addition to the design for overall longitudinal bending of the bridge, each slab or plate element is designed to carry transverse and longitudinal slab bending moments, calculated again by empirical formulas.

The true distribution of internal forces and moments in a continuous box girder bridge is obviously a highly indeterminate problem and is dependent on the geometry of the bridge and the makeup and connection of its various structural elements. It is highly desirable that accurate and general solutions be developed which can be used to analyze cellular type bridges of general configurations. Because of the complexity of these analyses, they must be programmed for solution by a digital computer to be of practical use. These programs may then be used directly in design or they may be used to study the effect of various parameters on the distributions of internal forces and moments in order to develop improved simplified design procedures similar to those presently being used.

1.3 Previous Studies

The present investigation is a continuation of the research previously conducted on the analysis of simply supported box girder bridges reported on by Scordelis [1]. In that research, the box girder bridge was treated

as a series of rectangular plates interconnected along longitudinal joints to form a cellular structure, simply supported at the end diaphragms. A folded plate analysis was developed for the structure using elastic plate theory for loads normal to the plane of the plates and two-dimensional plane-stress theory for loads in the plane of the plates. The solution was based on a direct stiffness method in which a harmonic analysis using Fourier series was utilized to analyze structures with arbitrary loading and boundary conditions. Because of the need to use a harmonic analysis, the solution is restricted to bridges which are simply supported at the ends. Using this method a general computer program was written for the analysis of simply supported box girder bridges. Input into the program consists of the span; geometry and material properties of the plates; the loading conditions; and the boundary conditions at the longitudinal joints. Both concentrated and distributed loads can be treated by the program. Final output for the program includes joint displacements, reactions and all of the internal forces and moments at selected points in the structure.

The results of two other research investigations dealing with box girder bridges have also been published during the past year. The first, reported on by Wright, Abel-Samad and Robinson [2] of the University of Illinois, discusses three methods of analysis for closed section girder bridges. The first method, called the "plate element method" is similar to the folded plate method described above [1]. The second method, named the "generalized coordinate method", is based on Vlasov's [3] theory for thin walled beams. This theory makes certain simplifying, but reasonable, assumptions regarding the behavior of the cellular structure. The third method, termed the "B.E.F. Method", utilizes an analogy to the theory of beams on elastic foundations to obtain an approximate analysis procedure for cellular structures with or without diaphragms or cross braces.

A second recent research investigation reported on by Mattock and Johnston [4] [5] of the University of Washington consists of an analytical and experimental study of composite steel-concrete box girder bridges. Based on these studies, formulas are given for determining wheel load distribution for this type of bridge.

A box girder bridge may be thought of as a cellular folded plate structure. While a large number of papers have been written on the analysis of simply supported folded plate structures (see bibliography in [6]), the extension to continuous structures has only recently received the attention of several investigators because of the complicating factors introduced by continuity in the longitudinal direction. Folded plate analyses are usually based on either the "ordinary theory" or the "elasticity theory" [7]. The ordinary theory assumes that the membrane stresses in each plate can be calculated by elementary beam theory and that slab bending is defined by means of transverse one-way slab action only. The elasticity theory utilizes plane stress elasticity theory and classical two-way thin plate bending theory to determine the membrane stresses and slab moments in each plate.

The analysis of continuous folded plate roofs has been studied by Gruber [8] based on a simplified theory. Yitzhaki [9] presented an approximate solution based on the ordinary theory for certain special cases of end conditions. Beaufait [10] used the same theory in an attempt to extend the solution to arbitrary end conditions. The general validity of several of the assumptions used by Beaufait appears questionable. Recently Pultar [11] and Lee [12] have developed solutions for continuous folded plate roofs based on the elasticity theory. Pultar's solution, which is applicable only to structures with simply supported ends, uses a harmonic analysis together with a force method in which the reactions at the interior supports are

taken as redundants. A finite difference technique was used by Lee to analyze structures with arbitrary end conditions in which an extrapolation procedure was utilized to improve the accuracy of the solution.

During the past year, the application of a finite element analysis to an open section folded plate was presented by Rockey and Evans [17] in which they used a rectangular element possessing 8 degrees of freedom for in-plane stresses and 12 degrees of freedom for plate bending to develop an element stiffness matrix for the folded plate problem.

Two recent Ph.D. dissertations by Abu Ghazaleh [13] and Lo [14], written under the direction of Scordelis, form the basis for the methods used in the present investigation for the analysis of continuous box girder bridges and certain parts of these dissertations will be described in detail in this report.

1.4 Scope of Present Investigation

This investigation was concerned with the elastic analysis of continuous box girder bridges under concentrated and distributed loads. Three analytical approaches were used in the investigation. The first approach, designated the "folded plate method", utilized the folded plate analysis developed for simply supported box girder bridges as a starting point. A combination of a displacement (stiffness) and a force (flexibility) method is used in the solution. A primary structure is selected consisting of the loaded structure simply supported at its ends with a large number of unknown redundant forces existing at the interior supports. Displacements due to each effect are evaluated by a direct stiffness solution and then compatibility equations are used to evaluate the unknown redundants. The original structure is then analyzed subjected to the known loading and known redundants to determine the final stresses and displacements in the continuous box girder system.

In this analysis the basic structural element used is a single plate having a width equal to the distance between longitudinal joints and a length equal to the overall length of the bridge. This method, which has already been described in the initial report [1], is briefly reviewed in Chapter 2. The method is based on the elasticity theory and is applicable to a box girder, continuous over several supports, but simply supported at its extreme ends. While each of the plates, which are interconnected at the longitudinal joints to make up the bridge, may have different geometric and material properties, there can be no variation in these properties, longitudinally or transversely within a single plate.

The second approach, hereafter called the "finite segment method", is based on the ordinary theory for folded plates and will be described in detail in Chapter 3. In this analysis the basic structural element used is formed by dividing each plate element into a finite number of segments longitudinally. Compatibility and equilibrium conditions are then satisfied at selected points along the four edges of each segment in the structure. Each segment is assumed to have 14 degrees of freedom. A matrix progression procedure is used in solving the problem. Unlike the folded plate method, the finite segment method has the advantage that it can be applied to a structure with arbitrary boundary conditions at its extreme ends. The finite segment lengths may be varied along the span as desired. Imposed loadings or displacements may be specified at any point and interior diaphragm supports may be used at sections between the two ends of the bridge. The method has the disadvantage that it is necessary in its application to use the approximations of the ordinary theory as opposed to the more exact elasticity theory used in the folded plate method.

The third approach, hereafter specified as the "finite element method", is based on satisfying as closely as possible the assumptions of the elasticity theory for folded plates. This approach will be described in detail in Chapter 4. The basic structural element used is obtained by dividing each plate element transversely as well as longitudinally into an assemblage of smaller rectangular finite elements. Element stiffness matrices are developed based on 24 degrees of freedom for each element. These degrees of freedom are related to six nodal point displacements, three translational and three rotational, at each of the four corners of the rectangular finite element. A direct stiffness solution is used in which the initial objective is to find all of the unknown nodal point displacements and forces. Once these are known the internal element forces and moments may then be determined. This method is perhaps the most versatile of those presently available. It can be used for arbitrary loadings and boundary conditions. It also can treat the cases of varying dimensional and material properties throughout the structure, as well as the cases of cutouts in the plates. It has the disadvantage that the sizes of the matrices involved in the solution are much larger than by the finite segment method which uses the width of the plate as the width of the segment. Thus computer storage capacity and times required for solution become limiting criteria with respect to the size of the problem that can be treated. In addition, while both the folded plate method and the finite element method are based on elasticity theory, the first approach treats the structure as a continuum while the latter approximates it as an assemblage of finite elements and its accuracy is dependent on the fineness of mesh used in subdividing the structure.

Each of the three methods of analysis described above were used to write general computer programs for continuous box girder bridges. Basic

input consists of the overall length of the structure; boundary conditions at the ends and at interior support points; geometry and material properties of the structural elements and their interconnections; and the loading conditions. Final output from the programs includes joint displacements, reactions and the internal forces, moments and displacements at selected points in the structure. A detailed comparison of the results obtained by the three methods for the general case of a 3-cell box girder bridge under an eccentric concentrated load is given in Chapter 5.

In order to evaluate the effect of continuity on the load distribution in box girder bridges a total of 23 cases were studied using the computer programs developed. The results of these parameter studies are presented in Chapter 6. A 3-cell and a 6-cell cross-section were selected as the two basic bridge types for the parameter study. A single span of 60 feet was analyzed with three different sets of end conditions assumed to bracket the variations found in spans of a continuous bridge. End conditions treated were simple-simple, fixed-fixed, and fixed-simple. Two loading conditions were used involving a single unit load placed at midspan first, at a central lateral position and second, at an extreme eccentric lateral position over an exterior web.

2. FOLDED PLATE METHOD OF ANALYSIS

2.1 Introduction

This method has been described in detail in the initial report by Scordelis [1] and by Lo [14] and will only be briefly reviewed here with respect to its application to continuous box girder bridges.

The basic assumptions used are as follows:

- (a) Each plate of the box girder is rectangular, of uniform thickness and is made of an elastic isotropic and homogeneous material.
- (b) The relation between forces and deformations is linear, so that superposition is valid.
- (c) The structure is simply supported at its extreme ends.
- (d) Transverse diaphragms at the end and interior supports are infinitely rigid in their own plane, but perfectly flexible normal to their own plane.
- (e) The stresses and displacements in each plate element due to loads normal to the plate (slab action) are determined by means of the classical thin plate bending theory applied to plates supported along all four edges.
- (f) The stresses and displacements in each plate element due to loads in the plane of the plate (membrane action) are determined by means of elasticity equations defining the plane stress problem.

This method is ideally suited to continuous box girder bridges which have simple supports at the two ends since a harmonic analysis using Fourier series can be used to analyze bridges under both concentrated and distributed loads. For these support conditions it permits an "exact solution" within

the assumptions of the elasticity theory and thus it may be used as a standard of comparison for other more general methods based on simplifying, but reasonable assumptions.

2.2 General Description of the Method

A force method of analysis is used which is similar in concept to that used to analyze a continuous beam, Fig. 3. A primary structure is selected, Fig. 3a, in which the redundants X are taken as the reaction forces at the interior supports. Since a rigid transverse diaphragm is assumed to exist at the interior support, the displacements and rotations in the plane of the diaphragm of all points on this cross section of the bridge should be zero under the influence of the external load P and the redundant forces X .

The redundant forces X are represented by a set of three joint forces at each longitudinal joint, Fig. 3e, consisting of vertical, horizontal and rotational components in the plane of the transverse diaphragm and a set of four plate forces for each plate, Fig. 3f, consisting of distributed normal and tangential forces having triangular variations between the two longitudinal edges of the plate. The 3-cell box girder continuous over one interior support which is shown in Fig. 3 has 8 longitudinal joints and 10 plate elements and thus would have a total of $(8 \times 3) + (10 \times 4) = 64$ redundants. For two interior supports, therefore a 3-span continuous bridge, the number of redundants would double. All of the redundant forces are assumed to be uniformly distributed in the longitudinal span direction over a length equal to the transverse diaphragm thickness specified at the interior support. The condition of zero displacement of the entire cross-section at the interior support is closely approximated by requiring that the displacements be zero on this cross-section at each of the longitudinal joints in the vertical, horizontal, and rotational directions and at the third points between joints in directions normal and tangential to the plane of each plate.

The analysis is carried out in the following sequence of steps:

1. With the redundants set equal to zero, Fig. 3b, the structure is analyzed under the given external loading P . Because of the simple supports at the two ends a harmonic analysis using a direct stiffness solution of the folded plate method by the elasticity theory [1] [14] may be used to determine displacements at any desired points on the bridge. A displacement vector is found for this case which defines the displacements at the points where the redundants are to act.

$$\{\delta\} = \begin{Bmatrix} \delta_1 \\ \delta_2 \\ \cdot \\ \cdot \\ \delta_c \end{Bmatrix} \quad (2.1)$$

For the bridge shown in Fig. 3, there would be 64 displacement components to evaluate for this vector.

2. The structure is then analyzed for unit values of each of the redundant forces X , Fig. 3c, and the corresponding flexibility matrix is formed.

$$\begin{Bmatrix} \delta_1 \\ \delta_2 \\ \cdot \\ \cdot \\ \delta_c \end{Bmatrix}_X = \begin{bmatrix} F_{11} & F_{12} & \cdot & F_{1c} \\ F_{21} & F_{22} & \cdot & F_{2c} \\ \cdot & \cdot & \cdot & \cdot \\ \cdot & \cdot & \cdot & \cdot \\ F_{c1} & F_{c2} & \cdot & F_{cc} \end{bmatrix} \begin{Bmatrix} X_1 \\ X_2 \\ \cdot \\ \cdot \\ X_c \end{Bmatrix} \quad (2.2)$$

or simply:

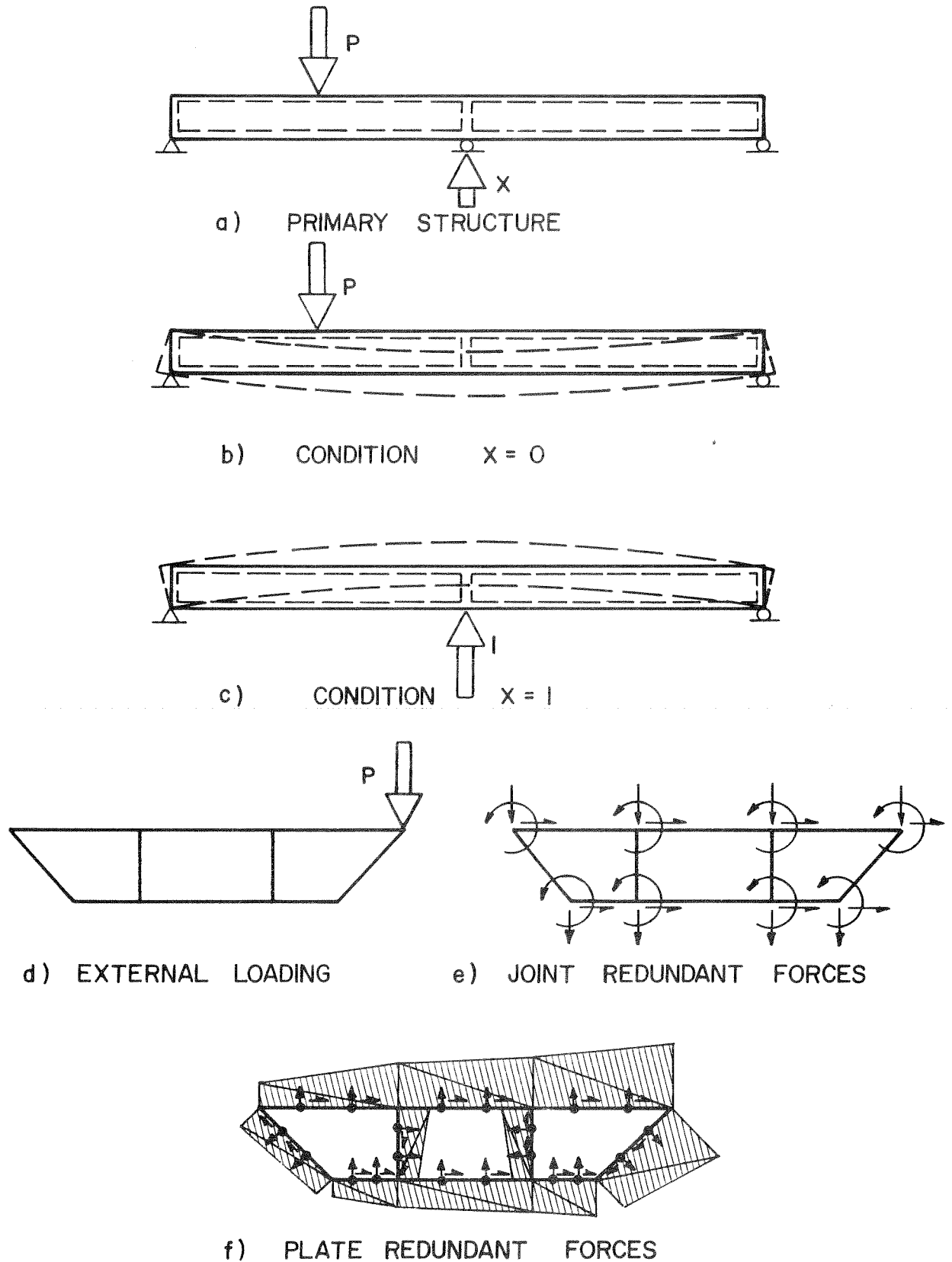


FIG. 3 FOLDED PLATE METHOD OF ANALYSIS OF CONTINUOUS BOX GIRDER BRIDGE

$$\{\delta\}_x = [F] \{X\} \quad (2.2a)$$

For the bridge shown in Fig. 3 the flexibility matrix would have a size of 64 x 64.

3. The total displacement under the superposition of the external loading P and the redundants X must be zero at each of the points where the redundants exist.

$$\{\delta\} = \{\delta\}_o + \{\delta\}_x = 0 \quad (2.3)$$

4. Substituting Eq. (2.2a) into (2.3) the redundants may be found.

$$\begin{aligned} \{\delta\}_o + [F] \{X\} &= 0 \\ \{X\} &= - [F]^{-1} \{\delta\}_o \end{aligned} \quad (2.4)$$

5. The simply supported structure can now be analyzed, subjected to the known loading and the known redundant forces, to determine the final stresses and displacements in the continuous box girder bridge.

The above description merely outlines the basic conceptual steps in the solution. The detailed analysis is quite complex [1] [14] and requires a large amount of computation which can only be carried out with the aid of a digital computer.

2.3 Computer Program - MUPDI

A general computer program has been written to perform the analysis by the folded plate method described above. The program, entitled MUPDI, was written in FORTRAN IV language for the IBM 7094 computer. Detailed

descriptions* of the input, output, sign conventions, and limitations and restrictions of this program are given in the initial report [1].

A brief description of the program is given below

(a) Input Data

1. Geometry and dimensions of the structure in terms of the span, number of plates, joints, and interior supports.
2. Dimensions and material properties of each plate element.
3. Magnitudes and locations of externally applied loads.
4. Location and thickness of each interior support diaphragm and indices defining restraints corresponding to redundants selected for each joint or plate element.
5. Desired locations for final results in output.

(b) Output Data

1. The complete input data is properly labelled and printed as a check.
2. The calculated redundant forces at the interior support for each joint and plate element are printed.
3. Resulting horizontal, vertical, rotational and longitudinal joint displacements are given at specified locations along the span.

*These detailed descriptions together with the FORTRAN listing for the program have been placed on file with the American Concrete Institute and may be obtained at the cost of reproduction and handling by writing to the American Concrete Institute, P.O. Box 4754, Redford Station, Detroit, Michigan 48219.

4. For each plate element all internal forces, moments and displacements are printed for each transverse section specified across the plate width and at the x-coordinates along the plate length.

(c) Limitations, Restrictions and Remarks

1. The maximum number of plate elements and longitudinal joints are 30 and 20 respectively.
2. Up to 100 non-zero terms of the appropriate Fourier series may be used to express the loads.
3. The maximum absolute difference between the two longitudinal joint numbers of any plate element is 4.
4. The maximum number of interior diaphragm supports along the span is 4.
5. The total number of redundant forces existing at the support points must not exceed 120.

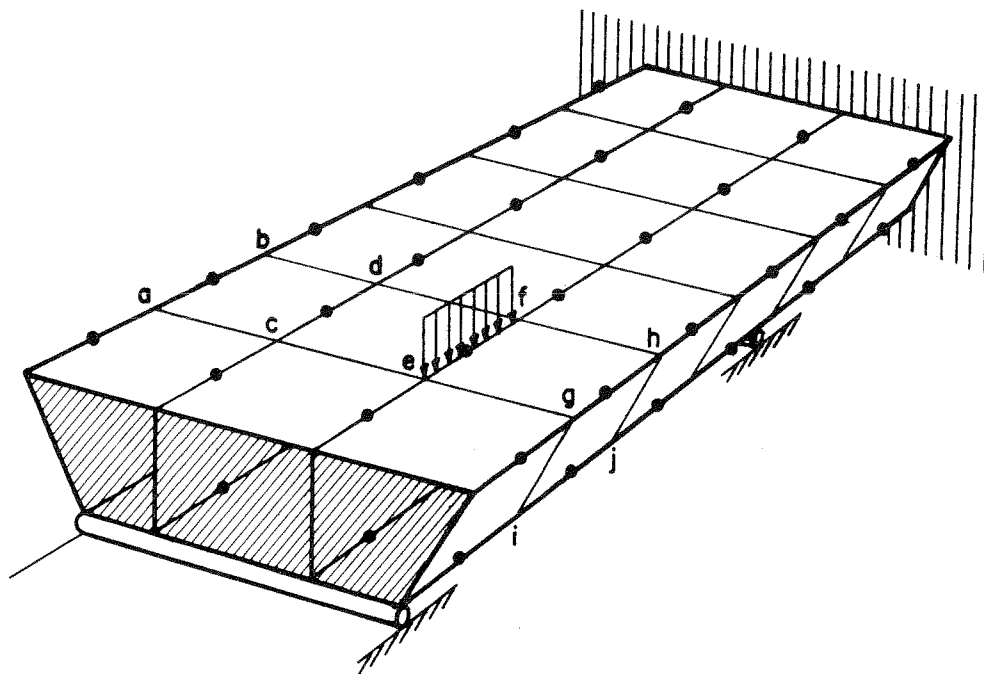
3. FINITE SEGMENT METHOD OF ANALYSIS

3.1 Introduction

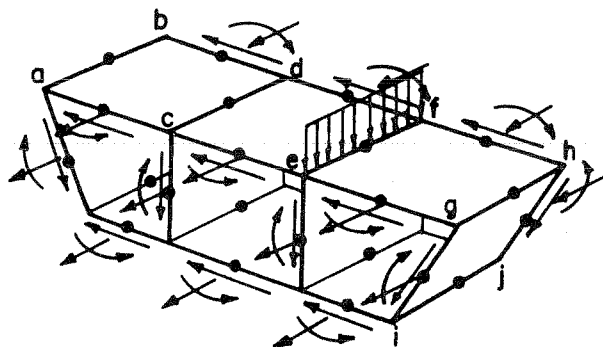
The approach described in the preceding chapter is limited to box girder bridges simply supported at the two ends. For a system with other end conditions the analysis is not applicable. In this chapter a finite segment method of analysis will be developed and described which can be applied to structures with arbitrary boundary conditions at the two ends. The basic structural element used in this method is a finite segment which is formed by dividing each plate element into a finite number of segments longitudinally (Fig. 4). These finite segments each have a width equal to the transverse distance between the longitudinal joints of the plate. In the analysis, the finite segments are first interconnected transversely at one end of the bridge to form a full transverse segment of the entire bridge cross-section (Fig. 4b). The solution proceeds by a segment progression method along the span to connect one transverse segment to the next until the far end of the bridge is reached. The boundary conditions at the two ends of the bridge provide sufficient equations to determine all the unknowns needed in the solution of the problem.

The basic assumptions used are as follows:

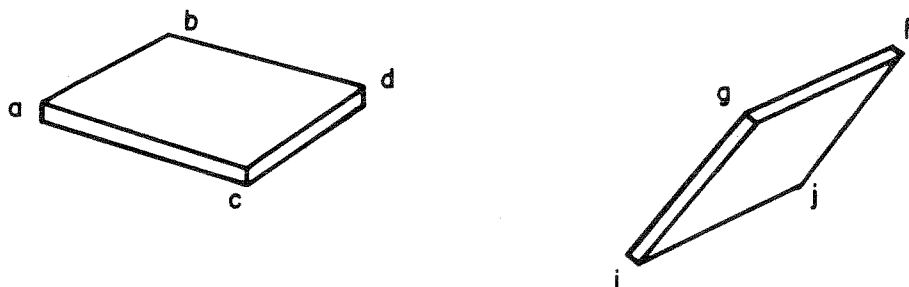
- (a) Each finite segment is rectangular, of uniform thickness and is made of an elastic, isotropic and homogeneous material.
- (b) The relation between forces and deformations is linear, so that superposition is valid.



a) TOTAL BRIDGE SYSTEM



b) TYPICAL FULL TRANSVERSE SEGMENT



c) TYPICAL FINITE SEGEMENTS

FIG.4 FINITE SEGMENT ANALYTICAL MODEL

- (c) The stresses and displacements in each finite segment due to loads normal to the plate (slab action) are determined by the behavior of transverse one way slab strips spanning between longitudinal joints. Thus, torsional and longitudinal slab moments are neglected.
- (d) The stresses and displacements in each finite segment due to loads in the plane of the plate (membrane action) are calculated by elementary beam theory applied to individual finite segments. Thus, the longitudinal stresses vary linearly over the width of each segment between joints.
- (e) Poisson's ratio is zero.

Assumptions c, d and e above are those of the ordinary theory for folded plates. The approximations involved in these assumptions should be accurate enough for most box girder bridges since each ^{plate} generally has a large longitudinal span to transverse width ratio. In the immediate vicinity of a concentrated load, however, the stresses obtained can only be considered to be approximate.

3.2 General Description of the Method

The problem to be solved may be stated simply as: given a continuous box girder bridge subjected to distributed line loads at the longitudinal joints; find the resulting internal forces, moments and stresses and the joint displacements. Of particular interest are the longitudinal stress distribution at any transverse section, the membrane shears in each plate and the transverse slab bending moments. It should be noted that only joint loads are considered and they are assumed to be uniformly distributed over the length of each segment.

If a single finite segment is taken as a free body it is similar to a rectangular plate on elastic supports along its four sides. The boundary conditions at the two longitudinal ends of the segment require that continuity and equilibrium with the next segment along the span or with a support condition must be satisfied. Along the two longitudinal edges of the segment, line loads are acting on the edges. These line loads produce both transverse one way slab bending and also in-plane membrane stresses. At each longitudinal joint, equilibrium requires that the sum of all the line loads on the segments connected to the joint must be equal to the externally applied line load acting on the joint. In addition these segments must all have the same joint displacements to satisfy compatibility.

A typical finite segment taken from the structure is shown in Figs. 5a and 5b with the positive directions of the forces and corresponding displacements shown. At each longitudinal end of the segment, therefore at sections $k-1$ and k , there exist three stress resultants: an axial force N , a shear force Q , and an in-plane bending moment M . The three corresponding displacements at each end are u , v and Ψ . It is assumed that plane sections remain plane at each end of the segment when satisfying continuity. Along the longitudinal edges i and j , plate edge forces, uniformly distributed along the length of the segment, are assumed to exist. These forces per unit length of edge are: a membrane shear force T along the edge, a transverse membrane force P normal to the edge, a shear force V normal to the plate, and a transverse slab moment M about the longitudinal edge (shown as a vector using the right hand rule). The four corresponding displacements u , v , w and θ are taken at the midpoint of the two ends of the segments. Thus in the solution compatibility conditions with respect to these displacements

on the longitudinal joints are satisfied only at the center points of each segment.

An inspection of Figs. 5a and 5b indicates that each finite segment has 14 degrees of displacement freedom and 14 corresponding forces. A segment progression solution based on the transfer matrix method [15] is adopted in the analysis. This has certain advantages over a direct stiffness solution for this type of problem which will be discussed in a later section.

A folded plate structure simply supported at the left end, fixed at the right end, and with one interior support is shown in Fig. 6. To describe the segment progression solution, consider a segment k between sections $k-1$ and k taken as a free body from a plate element. This free body is subjected to the actions, forces and displacements, shown in Figs. 5a and 5b. The actions at section k depend on the actions at sections $k-1$ and the uniformly distributed line loads at the two longitudinal edges i and j of the segment. The magnitudes of the edge line loads are determined so as to satisfy compatibility and equilibrium conditions of a whole transverse cross-section. They can be expressed in terms of the actions of all plate elements at section $k-1$ and the externally applied joint loads on segment k . After the edge line loads are found in these terms, the actions at section k can then be expressed in terms of the actions at section $k-1$ and the externally applied joint loads on this segment. Repeating this procedure for the first segment at the origin to the last segment at the far end of the structure, the relation between the actions at the two ends of the structure is obtained. Where an interior support condition is encountered at a particular section, proper account is taken of the boundary conditions imposed when passing from one segment to the next. By satisfying the boundary conditions at the two ends, sufficient equations are available to determine the unknown actions at

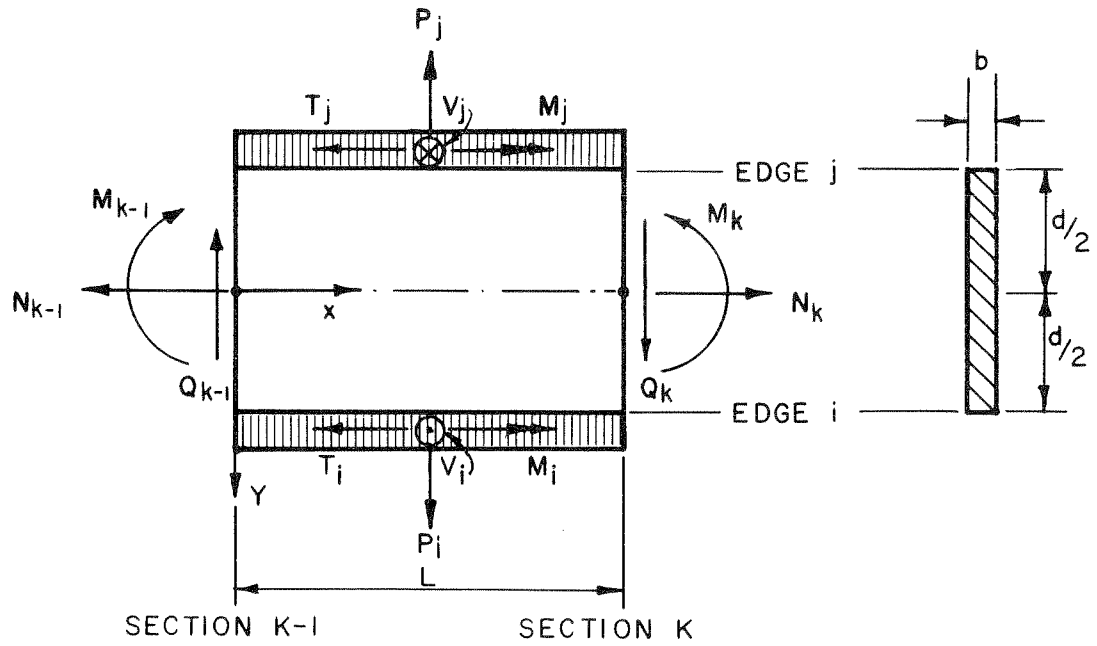


FIG.5a POSITIVE DIRECTIONS OF FINITE SEGMENT FORCES AND MOMENTS IN THE RELATIVE COORDINATE SYSTEM

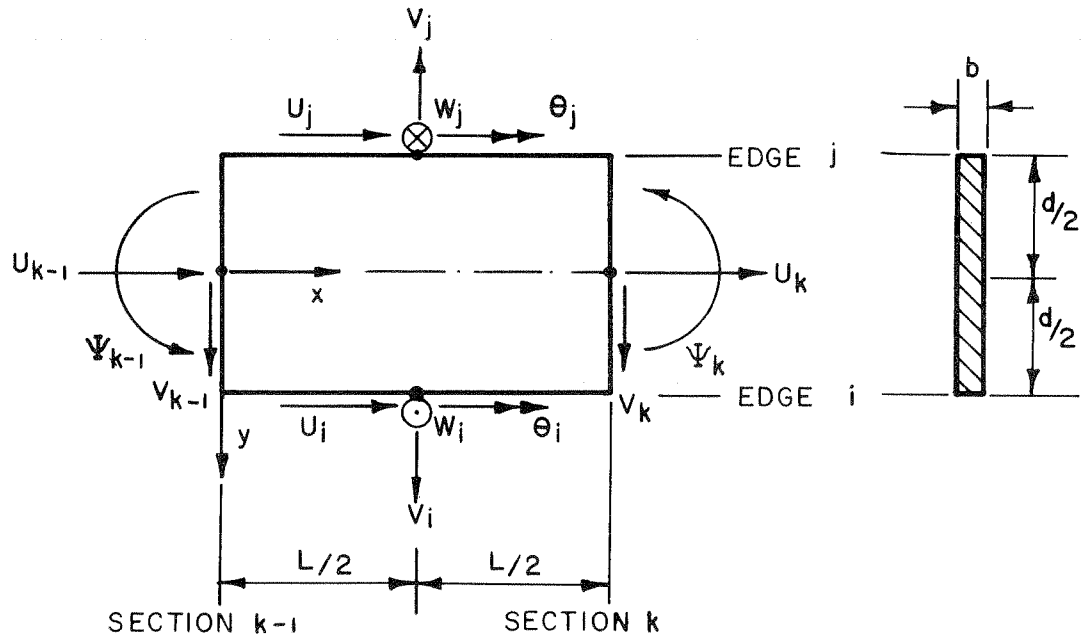


FIG.5b POSITIVE DIRECTIONS OF FINITE SEGMENT DISPLACEMENTS IN THE RELATIVE COORDINATE SYSTEM

the two ends and then the final internal forces and displacements can be found by progressing along the structure once again.

3.3 Derivation of Equations for the Solution of a Single Span Structure by the Finite Segment Method

A detailed development of the equations necessary for the analysis of a single span and then a continuous structure are presented in the remainder of this chapter. The development of these equations is taken from the Ph.D. dissertation by Lo [14].

3.3.1 Modified Field Matrix for a Beam Segment

From a plate element in Fig. 6, consider a typical segment k , between sections $k-1$ and k , which is subjected to the actions at its two ends shown in Fig. 7. The relation between the actions at the two ends of a beam segment can be written by a matrix which is called the field matrix [15]. Including the shear effect on the deflection of the beam, the field matrix is given as.

$$\begin{Bmatrix} u \\ v \\ \psi \\ M \\ Q \\ N \end{Bmatrix}_k = \begin{bmatrix} 1 & 0 & 0 & 0 & 0 & \frac{L}{AE} \\ 0 & 1 & -L & \frac{-L^2}{2EI} & \frac{-L^3}{6EI}(1-\beta) & 0 \\ 0 & 0 & 1 & \frac{L}{EI} & \frac{L^2}{2EI} & 0 \\ 0 & 0 & 0 & 1 & 1 & 0 \\ 0 & 0 & 0 & 0 & 1 & 0 \\ 0 & 0 & 0 & 0 & 0 & 1 \end{bmatrix} \begin{Bmatrix} u \\ v \\ \psi \\ M \\ Q \\ N \end{Bmatrix}_{k-1} \quad (3.1)$$

where

$$I = \frac{1}{12} bd^3, \quad A = bd, \quad L = \text{length of the segment and} \quad \beta = \frac{6EIK}{L^2GA}$$

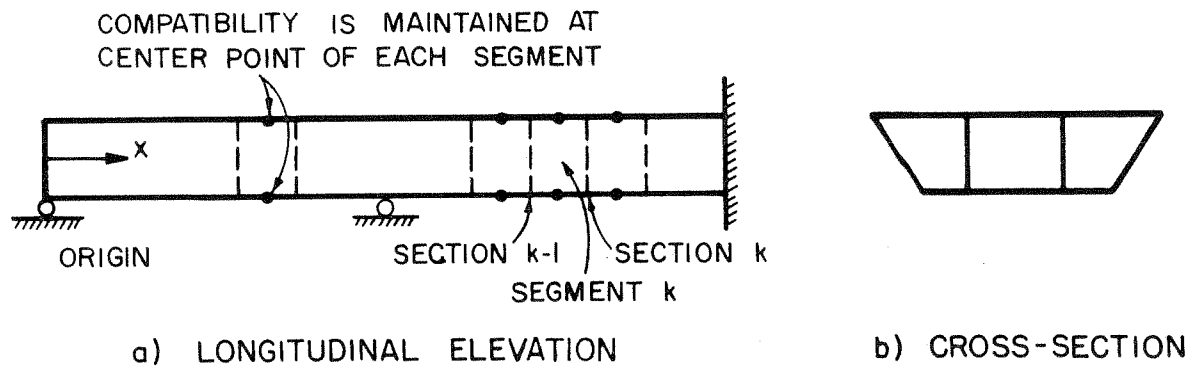


FIG. 6 FINITE SEGMENTS OF A FOLDED PLATE STRUCTURE

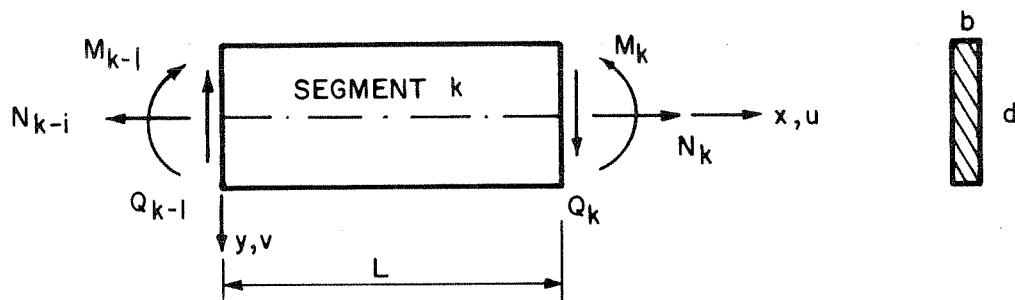


FIG. 7 POSITIVE DIRECTIONS OF ACTIONS FOR A BEAM SEGMENT

With Poisson's ratio equal to zero and $K = 6/5$ for a rectangular section, the coefficient β can be simplified to $\beta = (6/5)(d^2/L^2)$. The positive directions of the actions are shown in Fig. 5. The rotation Ψ is positive as the beam rotates counterclockwise. Equation 3.1 can be written in symbolic form as

$$Z_k = F_k Z_{k-1} \quad (3.1a)$$

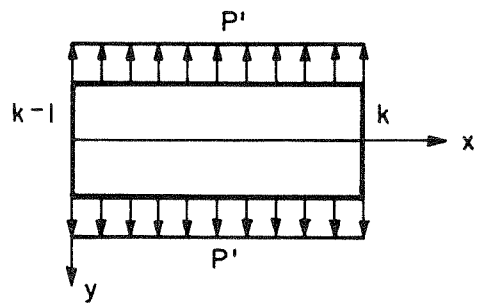
The actions Z_k at section k must be modified if the beam segment is subjected to uniform edge forces. Three force patterns are considered.

They are:

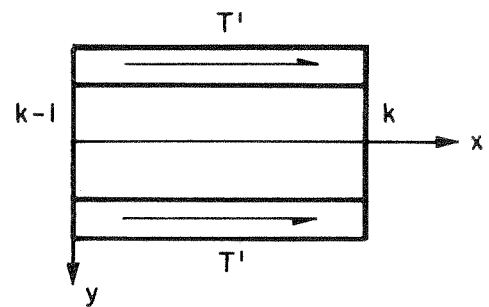
1. Symmetrical longitudinal membrane edge shear forces which will produce longitudinal extension of the plate.
2. Antisymmetrical transverse membrane edge forces which will produce both flexural and shear deformations.
3. Antisymmetrical longitudinal membrane edge shear forces which will produce pure flexural deformation.

These three force patterns and their positive directions are shown in Figs. (8b, 8c and 8d). Assuming all the actions (forces and displacements) at section $k-1$ are zero, the actions at section k due to these distributed edge forces can be determined using ordinary beam theory. They are summarized in the following matrix equation:

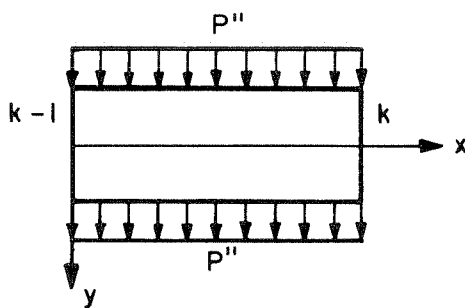
$$\begin{Bmatrix} u \\ v \\ \Psi \\ M \\ Q \\ N \end{Bmatrix}_k = \begin{bmatrix} \frac{-L^2}{AE} & 0 & 0 \\ 0 & \frac{L^3 d}{6EI} & \frac{L^4}{12EI} (1-2\beta) \\ 0 & \frac{-L^2 d}{2EI} & \frac{-L^3}{3EI} \\ 0 & -Ld & -L^2 \\ 0 & 0 & -2L \\ -2L & 0 & 0 \end{bmatrix} \begin{Bmatrix} T' \\ T'' \\ P'' \end{Bmatrix} \quad (3.2)$$



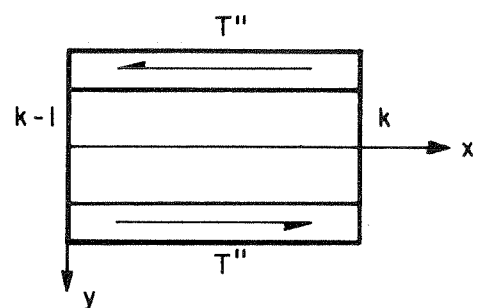
a) SYMMETRICAL TRANSVERSE
MEMBRANE EDGE FORCES



b) SYMMETRICAL MEMBRANE
EDGE SHEAR FORCES



c) ANTISYMMETRICAL TRANSVERSE
MEMBRANE EDGE FORCES



d) ANTISYMMETRICAL
MEMBRANE EDGE
SHEAR FORCES

FIG. 8 EDGE FORCE PATTERNS FOR A BEAM SEGMENT

Note that the forces T' , T'' and P'' are forces per unit length.

Combining Eqs. (3.1) and (3.2), the actions at section k due to actions at section $k-1$ and segment edge forces may be written in the following form:

$$\begin{Bmatrix} u \\ v \\ \Psi \\ M \\ Q \\ N \end{Bmatrix}_k = \begin{bmatrix} 1 & 0 & 0 & 0 & 0 \\ 0 & 1 & -L & \frac{-L^2}{2EI} & \frac{-L^3}{6EI}(1-\beta) \\ 0 & 0 & 1 & \frac{L}{EI} & \frac{L^2}{2EI} \\ 0 & 0 & 0 & 1 & L \\ 0 & 0 & 0 & 0 & 1 \\ 0 & 0 & 0 & 0 & 0 \end{bmatrix} \begin{Bmatrix} u \\ v \\ \Psi \\ M \\ Q \\ N \end{Bmatrix}_{k-1} + \begin{bmatrix} \frac{-L^2}{AE} & 0 & 0 \\ 0 & \frac{L^3 d}{6EI} & \frac{L^4}{12EI}(1-2\beta) \\ 0 & \frac{-L^2 d}{2EI} & \frac{-L^3}{3EI} \\ 0 & -Ld & -L^2 \\ 0 & 0 & -2L \\ -2L & 0 & 0 \end{bmatrix} \begin{Bmatrix} T' \\ T'' \\ P'' \end{Bmatrix} \quad (3.3)$$

3.3.2 Stiffness Matrix for a Beam Segment in Relative Coordinate System

Considering the transverse action of a finite segment, the slab stiffness and the plate stiffness are independent of each other. Referring to Fig. 9, the slab stiffness matrix may be determined from the slope deflection equations,

$$\begin{Bmatrix} M_i \\ M_j \\ V_i \\ V_j \end{Bmatrix} = \begin{bmatrix} 4 & 2 & 6/d & 6/d \\ 2 & 4 & 6/d & 6/d \\ 6/d & 6/d & 12/d^2 & 12/d^2 \\ 6/d & 6/d & 12/d^2 & 12/d^2 \end{bmatrix} \frac{EI_s}{d} \begin{Bmatrix} \theta_i \\ \theta_j \\ w_i \\ w_j \end{Bmatrix} \quad (3.4)$$

or symbolically,

$$\{S_s\} = [k_s] \{v_s\} \quad (3.4a)$$

In Eq. (3.4), I_s is the moment inertia of a slab strip of unit width and is equal to $b^3/12$. M and V are the transverse moment and normal shear per unit width.

The plate stiffness matrix of a beam segment is defined by the relation of the uniform edge forces to the edge displacements at center of the edges under the condition that the actions Z_{k-1} at section $k-1$ are zero. The stiffness matrix can be found by first referring to the symmetrical and antisymmetrical force patterns. From Eq. (3.2) the displacements at center of segment due to edge forces are given as

$$\begin{Bmatrix} \bar{u} \\ \bar{v} \\ \bar{\psi} \end{Bmatrix} = \begin{bmatrix} \frac{-\bar{L}^2}{AE} & & \\ 0 & \frac{\bar{L}^3 d}{6EI} & \frac{\bar{L}^4}{12EI}(1-2\bar{\beta}) \\ 0 & \frac{-\bar{L}^2 d}{2EI} & \frac{-\bar{L}^3}{3EI} \end{bmatrix} \begin{Bmatrix} T' \\ T'' \\ P'' \end{Bmatrix} \quad (3.5)$$

in which,

$$\bar{L} = \frac{1}{2} L, \quad \text{and} \quad \bar{\beta} = 4\beta.$$

The bar refers to quantities at center of the segment. An additional force pattern which corresponds to the transverse extension of the plate segment must be included. This force pattern is shown in Fig. 8a. The relation of the transverse extension v' (at each edge) to the symmetrical force P' is given by the following equation:

$$v' = \frac{d}{2Eb} P' \quad (3.6)$$

Now, Eqs. (3.5) and (3.6) can be combined as

$$\begin{Bmatrix} \bar{u} \\ v' \\ \bar{v} \\ \bar{\Psi} \end{Bmatrix} = \begin{bmatrix} \frac{-\bar{L}^{-2}}{AE} & 0 & 0 & 0 \\ 0 & \frac{d}{2Eb} & 0 & 0 \\ 0 & 0 & \frac{\bar{L}^{-3}d}{6EI} & \frac{\bar{L}^{-4}}{12EI}(1-2\bar{\beta}) \\ 0 & 0 & \frac{-\bar{L}^{-2}d}{2EI} & \frac{-\bar{L}^{-3}}{3EI} \end{bmatrix} \begin{Bmatrix} T' \\ P' \\ T'' \\ P'' \end{Bmatrix} \quad (3.7)$$

The inversion of the matrix gives,

$$\begin{Bmatrix} T' \\ P' \\ T'' \\ P'' \end{Bmatrix} = \begin{bmatrix} \frac{-AE}{\bar{L}^2} & 0 & 0 & 0 \\ 0 & \frac{2Eb}{d} & 0 & 0 \\ 0 & 0 & \frac{24EI}{(1+6\bar{\beta})d\bar{L}^3} & \frac{6(1-2\bar{\beta})EI}{(1+6\bar{\beta})d\bar{L}^2} \\ 0 & 0 & \frac{-36EI}{(1+6\bar{\beta})\bar{L}^4} & \frac{-12EI}{(1+6\bar{\beta})\bar{L}^3} \end{bmatrix} \begin{Bmatrix} \bar{u} \\ v' \\ \bar{v} \\ \bar{\Psi} \end{Bmatrix} \quad (3.8)$$

Eq. (3.8) can be transformed to yield the plate stiffness matrix corresponding to the segment edge forces and displacements as defined in Figs. 5 and 9. Note that the sign convention is such that the longitudinal membrane forces T and the corresponding longitudinal edge displacements u are chosen positive in opposite directions. This is done in order to obtain a symmetric plate stiffness matrix. The two transformation matrix equations will be

$$\begin{Bmatrix} \bar{u} \\ v' \\ \bar{v} \\ \bar{\Psi} \end{Bmatrix} = \begin{bmatrix} \frac{1}{2} & \frac{1}{2} & 0 & 0 \\ 0 & 0 & \frac{1}{2} & \frac{1}{2} \\ 0 & 0 & \frac{1}{2} & \frac{-1}{2} \\ \frac{1}{d} & \frac{-1}{d} & 0 & 0 \end{bmatrix} \begin{Bmatrix} u_i \\ u_j \\ v_i \\ v_j \end{Bmatrix} \quad (3.9)$$

$$\begin{Bmatrix} T_i \\ T_j \\ P_i \\ P_j \end{Bmatrix} = \begin{bmatrix} -1 & 0 & -1 & 0 \\ -1 & 0 & 1 & 0 \\ 0 & 1 & 0 & 1 \\ 0 & 1 & 0 & -1 \end{bmatrix} \begin{Bmatrix} T' \\ P' \\ T'' \\ P'' \end{Bmatrix} \quad (3.10)$$

Substitute Eq. (3.9) into Eq. (3.8),

$$\begin{Bmatrix} T' \\ P' \\ T'' \\ P'' \end{Bmatrix} = \begin{bmatrix} \frac{-AE}{2L^2} & \frac{-AE}{2L^2} & 0 & 0 \\ 0 & 0 & \frac{AE}{d^2} & \frac{AE}{d^2} \\ \frac{6(1-2\bar{\beta})EI}{(1+6\bar{\beta})d^2L^2} & \frac{-6(1-2\bar{\beta})EI}{(1+6\bar{\beta})d^2L^2} & \frac{12EI}{(1+6\bar{\beta})dL^3} & \frac{-12EI}{(1+6\bar{\beta})dL^3} \\ \frac{-12EI}{(1+6\bar{\beta})dL^3} & \frac{12EI}{(1+6\bar{\beta})dL^3} & \frac{-18EI}{(1+6\bar{\beta})L^4} & \frac{18EI}{(1+6\bar{\beta})L^4} \end{bmatrix} \begin{Bmatrix} u_i \\ u_j \\ v_i \\ v_j \end{Bmatrix} \quad (3.11)$$

The plate stiffness matrix may be obtained by substituting Eq. (3.11) into Eq. (3.10),

$$\begin{Bmatrix} T_i \\ T_j \\ P_i \\ P_j \end{Bmatrix} = \begin{bmatrix} \left(\frac{4\bar{\beta}}{(1+6\bar{\beta})} \frac{AE}{L^2} \right) & & & \\ \left(\frac{1+2\bar{\beta}}{(1+6\bar{\beta})} \frac{AE}{L^2} \right) \left(\frac{4\bar{\beta}}{(1+6\bar{\beta})} \frac{AE}{L^2} \right) & \text{Sym.} & & \\ \left(\frac{-AEd}{(1+6\bar{\beta})L^3} \right) \left(\frac{AEd}{(1+6\bar{\beta})L^3} \right) \left(\frac{AE}{d^2} - \frac{18EI}{(1+6\bar{\beta})L^4} \right) & & & \\ \left(\frac{AEd}{(1+6\bar{\beta})L^3} \right) \left(\frac{-AEd}{(1+6\bar{\beta})L^3} \right) \left(\frac{AE}{d^2} + \frac{18EI}{(1+6\bar{\beta})L^4} \right) \left(\frac{AE}{d^2} - \frac{18EI}{(1+6\bar{\beta})L^4} \right) & & & \end{bmatrix} \begin{Bmatrix} u_i \\ u_j \\ v_i \\ v_j \end{Bmatrix} \quad (3.12)$$

or in symbolic form,

$$\{S_p\} = [k_p] \{v_p\} \quad (3.12a)$$

Eqs. (3.4) and (3.12) can be combined to give the total segment stiffness matrix,

$$\begin{Bmatrix} S_s \\ S_p \end{Bmatrix} = \begin{bmatrix} k_s & 0 \\ 0 & k_p \end{bmatrix} \begin{Bmatrix} v_s \\ v_p \end{Bmatrix} \quad (3.13)$$

It should again be emphasized that Eq. (3.13) relates the uniformly distributed force quantities M , V , P and T at each longitudinal edge, Fig. 5a, to the corresponding displacement quantities θ , w , v and u at the center point of each longitudinal edge, Fig. 5b, under the special condition that the actions (forces and displacements) Z_{k-1} at section $k-1$ are zero.

3.3.3 Fixed Joint Forces due to Actions at Section $k-1$.

The fixed joint forces represent the uniform joint forces required to restrain the longitudinal edges of a segment against any displacements at the center point. The fixed joint forces of a beam segment due to actions at section $k-1$ can be obtained as the following. From Eq. (3.3) the displacements at center of the segment are given as

$$\begin{Bmatrix} \bar{u} \\ \bar{v} \\ \bar{\psi} \end{Bmatrix} = \begin{bmatrix} 1 & 0 & 0 & 0 & 0 & \frac{\bar{L}}{AE} \\ 0 & 1 & -\bar{L} & \frac{-\bar{L}^2}{2EI} & \frac{-\bar{L}^3}{6EI}(1-\bar{\beta}) & 0 \\ 0 & 0 & 1 & \frac{\bar{L}}{EI} & \frac{\bar{L}^2}{2EI} & 0 \end{bmatrix} \{Z_{k-1}\} + \begin{bmatrix} \frac{-\bar{L}^2}{AE} & 0 & 0 \\ 0 & \frac{\bar{L}^3 d}{6EI} & \frac{\bar{L}^4}{12EI}(1-2\bar{\beta}) \\ 0 & \frac{-\bar{L}^2 d}{2EI} & \frac{-\bar{L}^3}{3EI} \end{bmatrix} \begin{Bmatrix} T' \\ T'' \\ P'' \end{Bmatrix} \quad (3.14)$$

The displacements are set to zero, and the joint forces are solved in terms of the actions Z_{k-1} , then

$$\begin{Bmatrix} T' \\ T'' \\ P'' \end{Bmatrix}_F = - \begin{bmatrix} \frac{-AE}{\bar{L}^2} & 0 & 0 & 0 & \frac{-1}{\bar{L}} \\ 0 & \frac{24EI}{(1+6\bar{\beta})d\bar{L}^3} & \frac{-6(3+2\bar{\beta})EI}{(1+6\bar{\beta})d\bar{L}^2} & \frac{-6(1+2\bar{\beta})}{(1+6\bar{\beta})d\bar{L}} & 0 \\ 0 & \frac{-36EI}{(1+6\bar{\beta})\bar{L}^4} & \frac{24EI}{(1+6\bar{\beta})\bar{L}^3} & \frac{6}{(1+6\bar{\beta})\bar{L}^2} & 0 \end{bmatrix} \{Z_{k-1}\} \quad (3.15)$$

The subscript F refers to fixed joint forces. Substitute the above equation with $P' = 0$ into Eq. (3.10),

$$\left\{ \begin{array}{c} T_i \\ T_j \\ P_i \\ P_j \end{array} \right\}_F = \left[\begin{array}{ccccc} \frac{AE}{\bar{L}^2} & \frac{-24EI}{(1+6\bar{\beta})d\bar{L}^3} & \frac{6(3+2\bar{\beta})EI}{(1+6\bar{\beta})d\bar{L}^2} & \frac{6(1+2\bar{\beta})}{(1+6\bar{\beta})d\bar{L}} & \frac{(1+2\bar{\beta})}{(1+6\bar{\beta})d} \\ \frac{AE}{\bar{L}^2} & \frac{24EI}{(1+6\bar{\beta})d\bar{L}^3} & \frac{-6(3+2\bar{\beta})EI}{(1+6\bar{\beta})d\bar{L}^2} & \frac{-6(1+2\bar{\beta})}{(1+6\bar{\beta})d\bar{L}} & \frac{-(1+2\bar{\beta})}{(1+6\bar{\beta})d} \\ 0 & \frac{-36EI}{(1+6\bar{\beta})\bar{L}^4} & \frac{24EI}{(1+6\bar{\beta})\bar{L}^3} & \frac{6}{(1+6\bar{\beta})\bar{L}^2} & \frac{-6\bar{\beta}}{(1+6\bar{\beta})\bar{L}} \\ 0 & \frac{36EI}{(1+6\bar{\beta})\bar{L}^4} & \frac{-24EI}{(1+6\bar{\beta})\bar{L}^3} & \frac{-6}{(1+6\bar{\beta})\bar{L}^2} & \frac{6\bar{\beta}}{(1+6\bar{\beta})\bar{L}} \end{array} \right] \frac{1}{\bar{L}} \{Z_{k-1}\} \quad (3.16)$$

or symbolically,

$$\{S_p\}_F = [C] \{Z_{k-1}\} \quad (3.16a)$$

3.3.4 Fixed Joint Solution for Actions Z_k in Terms of Actions Z_{k-1}

Substituting Eq. (3.15) into Eq. (3.3) with the identities $\bar{L} = 1/2 L$ and $\bar{\beta} = 4\beta$, the fixed joint solution for actions Z_k is given by the following equation:

$$\{Z_k\}_F = [H] \{Z_{k-1}\} \quad (3.17)$$

in which

$$[H] = \left[\begin{array}{ccccc} -3 & 0 & 0 & 0 & 0 \\ 0 & \frac{17-18\bar{\beta}}{(1+6\bar{\beta})} & \frac{(-5+10\bar{\beta})L}{(1+6\bar{\beta})} & \frac{(-1+4\bar{\beta})L^2}{2(1+6\bar{\beta})EI} & \frac{\bar{\beta}(3-2\bar{\beta})L^3}{8(1+6\bar{\beta})EI} \\ 0 & \frac{-96}{(1+6\bar{\beta})L} & \frac{29-18\bar{\beta}}{(1+6\bar{\beta})} & \frac{(3-6\bar{\beta})L}{(1+6\bar{\beta})EI} & \frac{-2\bar{\beta}L^2}{(1+6\bar{\beta})EI} \\ 0 & \frac{-384EI}{(1+6\bar{\beta})L^2} & \frac{24(5-2\bar{\beta})EI}{(1+6\bar{\beta})L} & \frac{(13-18\bar{\beta})}{(1+6\bar{\beta})} & \frac{-8\bar{\beta}L}{(1+6\bar{\beta})} \\ 0 & \frac{-1152EI}{(1+6\bar{\beta})L^3} & \frac{384EI}{(1+6\bar{\beta})L^2} & \frac{48}{(1+6\bar{\beta})L} & \frac{(1-18\bar{\beta})}{(1+6\bar{\beta})} \\ \frac{-8AE}{L} & 0 & 0 & 0 & 0 \end{array} \right] \begin{array}{c} \frac{-L}{AE} \\ 0 \\ 0 \\ 0 \\ 0 \\ -3 \end{array} \quad (3.17a)$$

3.3.5 Actions Z_k due to Final Joint Displacements at Center of the Segment

Letting v_p be the final joint displacements at center of the segment, Eq. (3.11) gives the corresponding edge forces. Substituting Eq. (3.11) with $P' = 0$ into Eq. (3.2) and simplifying, the following equation is found:

$$\begin{Bmatrix} u \\ v \\ \psi \\ M \\ Q \\ N_k \end{Bmatrix} = \begin{bmatrix} 2 & 2 & 0 & 0 \\ \frac{-4(1+\bar{\beta})L}{(1+6\bar{\beta})d} & \frac{4(1+\bar{\beta})L}{(1+6\bar{\beta})d} & \frac{-8+12\bar{\beta}}{(1+6\bar{\beta})} & \frac{8-12\bar{\beta}}{(1+6\bar{\beta})} \\ \frac{(20+24\bar{\beta})}{(1+6\bar{\beta})d} & \frac{-(20+24\bar{\beta})}{(1+6\bar{\beta})d} & \frac{48}{(1+6\bar{\beta})L} & \frac{-48}{(1+6\bar{\beta})L} \\ \frac{(72+48\bar{\beta})EI}{(1+6\bar{\beta})dL} & \frac{-(72+48\bar{\beta})EI}{(1+6\bar{\beta})dL} & \frac{192EI}{(1+6\bar{\beta})L^2} & \frac{-192EI}{(1+6\bar{\beta})L^2} \\ \frac{192EI}{(1+6\bar{\beta})dL^2} & \frac{-192EI}{(1+6\bar{\beta})dL^2} & \frac{576EI}{(1+6\bar{\beta})L^3} & \frac{-576EI}{(1+6\bar{\beta})L^3} \\ \frac{4AE}{L} & \frac{4AE}{L} & 0 & 0 \end{bmatrix} \begin{Bmatrix} u_i \\ u_j \\ v_i \\ v_j \end{Bmatrix} \quad (3.18)$$

or in symbolic form,

$$\{Z_k\}_v = [J] \{v_p\} \quad (3.18a)$$

3.3.6 Fixed Coordinate System and Direct Stiffness Method for One Segment of the Structure

A fixed coordinate system for the joint and segment edge forces and displacements is defined and shown in Figs. 10 and 11.

A displacement transformation matrix A which relates the segment edge displacements in the relative coordinate system to those in the fixed coordinate system may be readily written in terms of the geometry of cross-section. The matrix equations for the solutions of the joint displacements due to joint loads for one transverse segment of the structure are essentially the same as those used in the folded plate method described in Chapter 2 and

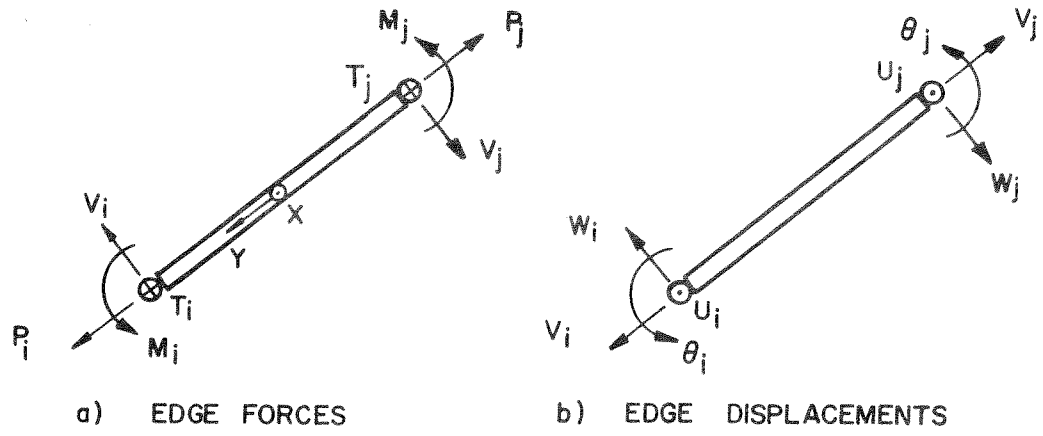


FIG. 9 POSITIVE SEGMENT EDGE FORCES AND DISPLACEMENTS IN THE RELATIVE COORDINATE SYSTEM

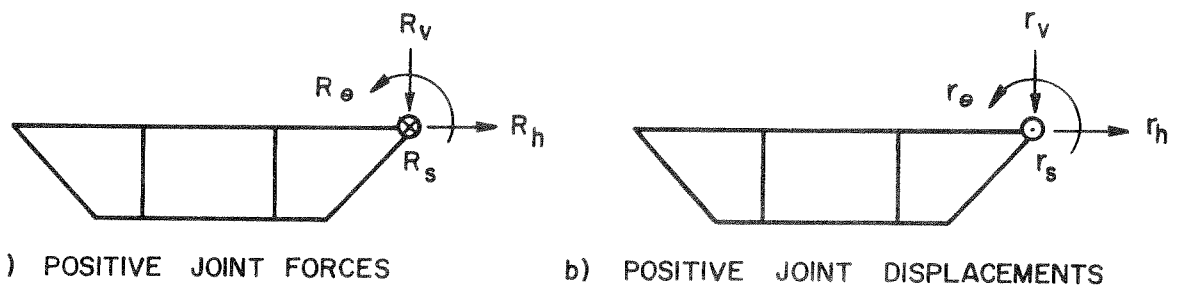


FIG. 10 POSITIVE JOINT FORCES AND DISPLACEMENTS IN THE FIXED COORDINATE SYSTEM

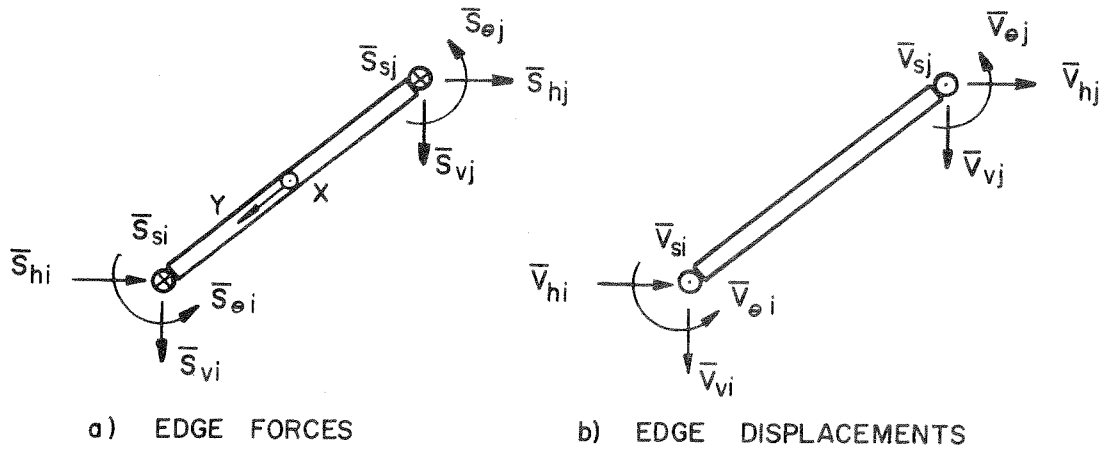


FIG. 11 POSITIVE SEGMENT EDGE FORCES AND DISPLACEMENTS IN THE FIXED COORDINATE SYSTEM

the initial report [1], and thus they will not be repeated here. However, it must be pointed out that in finding the joint displacements in the present finite segment method the actions at section $k-1$ are assumed to be zero.

3.3.7 Boundary Conditions at Two Ends of the Structure and Set Up of Actions Vector at the Origin.

There are 6 actions at each end of a plate element. They are 3 displacements and 3 forces as shown in Eq. (3.1) and for each plate end 3 actions are known while the other 3 are unknowns. Whenever a force is known, the corresponding displacement is unknown and vice versa. In matrix form, this can be written as

$$\begin{matrix} \{Z\} \\ 6 \times 1 \end{matrix} = \begin{matrix} [L] \\ 6 \times 3 \end{matrix} \begin{matrix} \{Z\}_{\text{unk.}} \\ 3 \times 1 \end{matrix} + \begin{matrix} \{Z\}_{\text{kn.}} \\ 6 \times 1 \end{matrix} \quad (3.19)$$

where $\{Z\}_{\text{unk.}}$ has the three unknown actions and $\{Z\}_{\text{kn.}}$ has three known actions (can be zeros) and three zeros for the unknown actions. $[L]$ is a coefficient matrix in which each column contains a single 1 and the rest of the elements are zeros.

If there are m plate elements in the structure, the actions of the structure at the origin can be written as

$$\begin{Bmatrix} Z_o^1 \\ Z_o^2 \\ \vdots \\ Z_o^m \end{Bmatrix} = \begin{bmatrix} L^1 & & & \\ & L^2 & & \\ & & \ddots & \\ & & & L^m \end{bmatrix} \begin{Bmatrix} Z_o^1 \\ Z_o^2 \\ \vdots \\ Z_o^m \end{Bmatrix}_{\text{unk.}} + \begin{Bmatrix} Z_o^1 \\ Z_o^2 \\ \vdots \\ Z_o^m \end{Bmatrix}_{\text{kn.}} \quad (3.20)$$

or

$$\{Z_o^T\} = [L^T] \{Z_o^T\}_{\text{unk.}} + \{Z_o^T\}_{\text{kn.}} \quad (3.20a)$$

The superscripts, 1 . . . m, refer to element numbers.

3.3.8 Sequence of Matrix Operations

1. The actions of the structure at the origin are formed as given in Eq. (3.20a).

2. The fixed joint forces for segment one are established. Equation (3.16a) gives the fixed joint forces for one element, and for the whole structure the equation can be enlarged to

$$\left\{ \begin{array}{c} S_p^1 \\ S_p^2 \\ \cdot \\ \cdot \\ S_p^m \end{array} \right\}_F = \left[\begin{array}{c} C^1 \\ C^2 \\ \cdot \\ \cdot \\ C^m \end{array} \right] \left\{ \begin{array}{c} Z_o^1 \\ Z_o^2 \\ \cdot \\ \cdot \\ Z_o^m \end{array} \right\} \quad (3.21)$$

The superscripts, 1 . . . m, refer to the element numbers of the structure. Substitute Eq. (3.20) into the above equation and carry out the matrix multiplication, the following matrix equation is obtained:

$$\left\{ \begin{array}{c} S_p^1 \\ S_p^2 \\ \cdot \\ \cdot \\ S_p^m \end{array} \right\}_F = \left[\begin{array}{c} M^1 \\ M^2 \\ \cdot \\ \cdot \\ M^m \end{array} \right] \left\{ \begin{array}{c} \tilde{M}^1 \\ \tilde{M}^2 \\ \cdot \\ \cdot \\ \tilde{M}^m \end{array} \right\} + \left\{ \begin{array}{c} Z_o^T \\ \text{unk.} \end{array} \right\}_{3m \times 1} \quad (3.22)$$

$4m \times 1$ $4m \times 3m$ $4m \times 1$

For each element the joint forces have to be transformed into the fixed coordinate system and the joint forces corresponding to the same joint must be summed up. Using the transpose of the displacement transformation matrix A , the fixed joint forces \bar{S}_F in the fixed coordinate system for an element can be written as

$$\{\bar{S}\}_F = [A]^T \{S\}_F \quad (3.23)$$

Assuming no normal slab loads exist between two joints of the element then,

$$\{S_s\}_F = 0 \quad (3.24)$$

and Eq. (3.23) becomes

$$\begin{Bmatrix} \bar{S}_i \\ \bar{S}_j \end{Bmatrix}_F = [A]^T \begin{Bmatrix} 0 \\ S_p \end{Bmatrix}_F \quad (3.25)$$

where i and j are the two joint numbers of the element. Equation (3.22) can be separated into m submatrix equations of the form

$$\begin{Bmatrix} S_p^1 \end{Bmatrix} = [M^1] \begin{Bmatrix} Z_o^T \end{Bmatrix}_{\text{unk.}} + \begin{Bmatrix} \tilde{M}^1 \end{Bmatrix}, \text{ etc.} \quad (3.26)$$

4x1 4x3m 3mx1 4x1

Substituting Eq. (3.26) into Eq. (3.25),

$$\begin{Bmatrix} \bar{S}_i^1 \\ \bar{S}_j^1 \end{Bmatrix}_F = [N^1] \begin{Bmatrix} Z_o^T \end{Bmatrix}_{\text{unk.}} + \begin{Bmatrix} \tilde{N}^1 \end{Bmatrix}, \text{ etc.} \quad (3.27)$$

8x1 8x3m 3mx1 8x1

The fixed joint forces R_F of the whole transverse segment are obtained by the summation of all joint forces from each element,

$$\{R\}_F = \begin{Bmatrix} R_1 \\ R_2 \\ \vdots \\ R_n \end{Bmatrix}_F = \begin{Bmatrix} \bar{S}_1^\Sigma \\ \bar{S}_2^\Sigma \\ \vdots \\ \bar{S}_n^\Sigma \end{Bmatrix} \quad (3.28)$$

here n represents the total number of joints and the Σ sign means the sum over all elements connecting the same joint. Since the fixed joint forces are in terms of the unknown actions at origin, Eq. (3.28) finally will be written in the following form:

$$\begin{matrix} \{R\}_F & = & [E] & \{Z_O^T\}_{\text{unk.}} & + & \{\tilde{E}\} \\ 4n \times 1 & & 4n \times 3m & 3m \times 1 & & 4n \times 1 \end{matrix} \quad (3.29)$$

3. Let R_A be the external applied joint forces, then the final joint forces R are given as

$$\{R\} = \{R\}_A - \{R\}_F \quad (3.30)$$

or using Eq. (3.29),

$$\{R\} = - [E] \{Z_O^T\}_{\text{unk.}} + \{\tilde{R}\}_A \quad (3.31)$$

where

$$\{\tilde{R}\}_A = \{R\}_A - \{\tilde{E}\} .$$

4. Joint displacements at center of the transverse segment are found using a recursive procedure to solve the equations similar to that used in the folded plate method. However, the joint forces are not just a vector now but are given by Eq. (3.31) and the final joint displacements are in terms of the actions at origin and given as

$$\begin{matrix} \left\{ \begin{matrix} r_1 \\ r_2 \\ \cdot \\ \cdot \\ r_n \end{matrix} \right\} & = & \left[\begin{matrix} G_1 \\ G_2 \\ \cdot \\ \cdot \\ G_n \end{matrix} \right] & \{Z_O^T\}_{\text{unk.}} & + & \left\{ \begin{matrix} \tilde{G}_1 \\ \tilde{G}_2 \\ \cdot \\ \cdot \\ \tilde{G}_n \end{matrix} \right\} \\ 4n \times 1 & & 4n \times 3m & 3m \times 1 & & 4n \times 1 \end{matrix} \quad (3.32)$$

or

$$\{r\} = [G] \{Z_o^T\}_{\text{unk.}} + \{\tilde{G}\} \quad (3.32a)$$

5. After the joint displacements are solved, the actions at the next section can be determined by two contributions: a) the fixed joint solution and b) solution due to final joint displacements.

Referring to Eq. (3.17), the fixed joint solution can be written as

$$\begin{Bmatrix} Z_1^1 \\ Z_1^2 \\ \vdots \\ Z_1^m \end{Bmatrix}_F = \begin{bmatrix} H^1 & & \\ & H^2 & \\ & & \ddots \\ & & & H^m \end{bmatrix} \begin{Bmatrix} Z_o^1 \\ Z_o^2 \\ \vdots \\ Z_o^m \end{Bmatrix} \quad (3.33)$$

Equation (3.18) gives the actions due to final joint displacements in relative coordinate system. In order to calculate the actions at next section, the joint displacements given in Eq. (3.32) must be transformed into the relative coordinate system. From Eq. (3.32), a submatrix equation for the two joint displacements of an element can be rewritten as

$$\begin{Bmatrix} \bar{v}_i \\ \bar{v}_j \end{Bmatrix} = \begin{Bmatrix} r_i \\ r_j \end{Bmatrix} = \begin{bmatrix} G_i \\ G_j \end{bmatrix} \{Z_o^T\}_{\text{unk.}} + \begin{Bmatrix} \tilde{G}_i \\ \tilde{G}_j \end{Bmatrix} \quad (3.34)$$

These joint displacements can be transformed to the relative coordinate system by the displacement transformation matrix A,

$$\begin{Bmatrix} v_s \\ v_p \end{Bmatrix} = [A] \begin{Bmatrix} \bar{v}_i \\ \bar{v}_j \end{Bmatrix} \quad (3.35)$$

Substituting Eq. (3.34) into Eq. (3.35) the joint displacements v_p can be represented by

$$\begin{matrix} \{v_p\} \\ 4 \times 1 \end{matrix} = [B] \begin{matrix} \{Z_o^T\}_{\text{unk.}} \\ 3 \times 3 \end{matrix} + \{\tilde{B}\} \quad (3.36)$$

For all elements Eq. (3.36) becomes

$$\begin{matrix} \left\{ \begin{matrix} v_p^1 \\ v_p^2 \\ \vdots \\ v_p^m \end{matrix} \right\} \\ 4 \times 1 \end{matrix} = \begin{matrix} \left[\begin{matrix} B^1 \\ B^2 \\ \vdots \\ B^m \end{matrix} \right] \\ 4 \times 3 \end{matrix} \begin{matrix} \{Z_o^T\}_{\text{unk.}} \\ 3 \times 1 \end{matrix} + \begin{matrix} \left\{ \begin{matrix} \tilde{B}^1 \\ \tilde{B}^2 \\ \vdots \\ \tilde{B}^m \end{matrix} \right\} \\ 3 \times 1 \end{matrix} \quad (3.37)$$

From Eq. (3.18), the actions due to joint displacements are

$$\begin{matrix} \left\{ \begin{matrix} Z_1^1 \\ Z_1^2 \\ \vdots \\ Z_1^m \end{matrix} \right\}_v \\ 3 \times 1 \end{matrix} = \begin{matrix} \left[\begin{matrix} J^1 \\ J^2 \\ \vdots \\ J^m \end{matrix} \right] \\ 3 \times 4 \end{matrix} \begin{matrix} \left\{ \begin{matrix} v_p^1 \\ v_p^2 \\ \vdots \\ v_p^m \end{matrix} \right\} \\ 4 \times 1 \end{matrix} \quad (3.38)$$

The final actions at section 1 are obtained by the combination of Eqs. (3.33) and (3.38),

$$\begin{aligned} \begin{matrix} \left\{ \begin{matrix} Z_1^1 \\ Z_1^2 \\ \vdots \\ Z_1^m \end{matrix} \right\} \\ 3 \times 1 \end{matrix} &= \begin{matrix} \left\{ \begin{matrix} Z_1^1 \\ Z_1^2 \\ \vdots \\ Z_1^m \end{matrix} \right\}_F \\ 3 \times 1 \end{matrix} + \begin{matrix} \left\{ \begin{matrix} Z_1^1 \\ Z_1^2 \\ \vdots \\ Z_1^m \end{matrix} \right\}_v \\ 3 \times 1 \end{matrix} \\ &= \begin{matrix} \left[\begin{matrix} H^1 \\ H^2 \\ \vdots \\ H^m \end{matrix} \right] \\ 3 \times 3 \end{matrix} \{Z_o^T\} + \begin{matrix} \left[\begin{matrix} J^1 \\ J^2 \\ \vdots \\ J^m \end{matrix} \right] \\ 3 \times 4 \end{matrix} \begin{matrix} \left\{ \begin{matrix} v_p^1 \\ v_p^2 \\ \vdots \\ v_p^m \end{matrix} \right\} \\ 4 \times 1 \end{matrix} \end{matrix} \quad (3.39)$$

Substituting Eqs. (3.20) and (3.37) into the above equation and simplifying,

$$\begin{Bmatrix} Z_1^1 \\ Z_1^2 \\ \cdot \\ \cdot \\ Z_1^m \end{Bmatrix} = \begin{matrix} [D_1] & \{Z_o^T\}_{\text{unk.}} & + & \{\tilde{D}_1\} \\ 6 \times 3 \text{m} & 3 \times 1 & & 6 \times 1 \end{matrix} \quad (3.40)$$

6. Repeat steps 2 through 5 for the second segment and then for all segments until the last one. The following changes have to be made for segment number k :

(a) Z_o^T and Z_1^T are changed to Z_{k-1}^T and Z_k^T respectively.

(b) From the preceding segment, Eq. (3.40) should be written as

$$\{Z_{k-1}^T\} = [D_{k-1}] \{Z_o^T\}_{\text{unk.}} + \{\tilde{D}_{k-1}\} \quad (3.40a)$$

This equation, (3.40a), is used for substitution into Eqs. (3.21) and (3.39) instead of Eq. (3.20).

7. For the last segment e , Eq. (3.40) becomes

$$\begin{matrix} \{Z_e^T\} \\ 6 \times 1 \end{matrix} = \begin{matrix} [D_e] & \{Z_o^T\}_{\text{unk.}} & + & \{\tilde{D}_e\} \\ 6 \times 3 \text{m} & 3 \times 1 & & 6 \times 1 \end{matrix} \quad (3.41)$$

The actions Z_e^T at end of the structure have $3m$ known and $3m$ unknown actions. Considering the known actions of Z_e^T , Eq. (3.41) can be condensed to

$$\begin{matrix} \{Z_e\}_{\text{kn.}} \\ 3 \times 1 \end{matrix} = \begin{matrix} [D] & \{Z_o^T\}_{\text{unk.}} & + & \{\tilde{D}\} \\ 3 \times 3 \text{m} & 3 \times 1 & & 3 \times 1 \end{matrix} \quad (3.42)$$

Solving Eq. (3.42) for the unknown actions at the origin,

$$\{Z_o^T\}_{\text{unk.}} = [D]^{-1} \left(\{Z_e\}_{\text{kn.}} - \{\tilde{D}\} \right) \quad (3.43)$$

8. Final internal forces and displacements at the center of each segment are calculated by progressing over the structure once again after the actions at the origin are known as Z_o^T .

3.3.9 Equations for Internal Forces and Displacements at Center of Each Segment

After the unknown actions at the origin are found from Eq. (3.43), the actions at section $k-1$ are calculated by Eq. (3.40a),

$$\{Z_{k-1}^T\} = [D_{k-1}] \{Z_o^T\} + \{\tilde{D}_{k-1}\} \quad (3.44)$$

and the final joint displacements at center of segment k can be obtained using Eq. (3.32a),

$$\{r\}_k = [G]_k \{Z_o^T\} + \{\tilde{G}\}_k \quad (3.45)$$

For any particular element between joints i and j , the joint displacements \bar{v}_i and \bar{v}_j can be taken out from the displacement vector r and the edge displacements in the relative coordinate system are given by Eq. (3.35),

$$\begin{Bmatrix} v_s \\ v_p \end{Bmatrix} = [A] \begin{Bmatrix} \bar{v}_i \\ \bar{v}_j \end{Bmatrix} \quad (3.35)$$

From Eq. (3.9) the internal beam displacements at center of segment are

$$\begin{Bmatrix} \bar{u} \\ \bar{v} \\ \bar{\psi} \end{Bmatrix} = \begin{bmatrix} \frac{1}{2} & \frac{1}{2} & 0 & 0 \\ 0 & 0 & \frac{1}{2} & \frac{-1}{2} \\ \frac{1}{d} & \frac{-1}{d} & 0 & 0 \end{bmatrix} \begin{Bmatrix} u_i \\ u_j \\ v_i \\ v_j \end{Bmatrix} \quad (3.46)$$

A displacement vector \bar{v}_d defined as the difference between the final edge displacements and the edge displacements carried over from the actions at section $k-1$ can be calculated by

$$\{\bar{v}_d\} = \begin{Bmatrix} u_d \\ v_d \\ \psi_d \end{Bmatrix} = \begin{Bmatrix} \bar{u} \\ \bar{v} \\ \bar{\psi} \end{Bmatrix} - \begin{bmatrix} 1 & 0 & 0 & 0 & 0 & \frac{\bar{L}}{AE} \\ 0 & 1 & -\bar{L} & \frac{-\bar{L}^2}{2EI} & \frac{-\bar{L}^3(1-\bar{\beta})}{6EI} & 0 \\ 0 & 0 & 1 & \frac{\bar{L}}{EI} & \frac{\bar{L}^2}{2EI} & 0 \end{bmatrix} \{Z_{k-1}\} \quad (3.47)$$

From Eq. (3.8) the final edge forces are,

$$\begin{Bmatrix} T' \\ T'' \\ P'' \end{Bmatrix} = \begin{bmatrix} \frac{-AE}{\bar{L}^2} & 0 & 0 \\ 0 & \frac{24EI}{(1+6\bar{\beta})d\bar{L}^3} & \frac{6(1-2\bar{\beta})EI}{(1+6\bar{\beta})d\bar{L}^2} \\ 0 & \frac{-36EI}{(1+6\bar{\beta})\bar{L}^4} & \frac{-12EI}{(1+6\bar{\beta})\bar{L}^3} \end{bmatrix} \begin{Bmatrix} u_d \\ v_d \\ \psi_d \end{Bmatrix} \quad (3.48)$$

The internal beam forces at center of the segment can be determined by two contributions: 1) actions at section k-1 and 2) the final edge forces obtained by Eq. (3.48). Therefore, referring to Eq. (3.3),

$$\begin{Bmatrix} M \\ Q \\ N \end{Bmatrix}_{\text{center of segment}} = \begin{bmatrix} 1 & \bar{L} & 0 \\ 0 & 1 & 0 \\ 0 & 0 & 1 \end{bmatrix} \begin{Bmatrix} M \\ Q \\ N \end{Bmatrix}_{k-1} + \begin{bmatrix} 0 & -\bar{L}d & -\bar{L}^2 \\ 0 & 0 & -2\bar{L} \\ -2\bar{L} & 0 & 0 \end{bmatrix} \begin{Bmatrix} T' \\ T'' \\ P'' \end{Bmatrix} \quad (3.49)$$

Substituting Eq. (3.48) into Eq. (3.49),

$$\begin{Bmatrix} M \\ Q \\ N \end{Bmatrix}_{\text{center of segment}} = \begin{bmatrix} 1 & \bar{L} & 0 \\ 0 & 1 & 0 \\ 0 & 0 & 1 \end{bmatrix} \begin{Bmatrix} M \\ Q \\ N \end{Bmatrix}_{k-1} + \begin{bmatrix} 0 & \frac{12EI}{(1+6\bar{\beta})\bar{L}^2} & \frac{(6+12\bar{\beta})EI}{(1+6\bar{\beta})\bar{L}} \\ 0 & \frac{72EI}{(1+6\bar{\beta})\bar{L}^3} & \frac{24EI}{(1+6\bar{\beta})\bar{L}^2} \\ \frac{2AE}{\bar{L}} & 0 & 0 \end{bmatrix} \begin{Bmatrix} u_d \\ v_d \\ \psi_d \end{Bmatrix} \quad (3.50)$$

The edge forces corresponding to one-way slab bending are given by Eq. (3.4a),

$$\{S_s\} = [k_s] \{v_s\} \quad (3.4a)$$

Equation (3.48) can be extended to include the transverse extension of the plate,

$$\begin{Bmatrix} T' \\ P' \\ T'' \\ P'' \end{Bmatrix} = \begin{bmatrix} \frac{-AE}{\bar{L}^2} & 0 & 0 & 0 \\ 0 & \frac{2Eb}{d} & 0 & 0 \\ 0 & 0 & \frac{24EI}{(1+6\bar{\beta})d\bar{L}^3} & \frac{6(1-2\bar{\beta})EI}{(1+6\bar{\beta})d\bar{L}^2} \\ 0 & 0 & \frac{-36EI}{(1+6\bar{\beta})\bar{L}^4} & \frac{-12EI}{(1+6\bar{\beta})\bar{L}^3} \end{bmatrix} \begin{Bmatrix} u_d \\ v' \\ v_d \\ \psi_d \end{Bmatrix} \quad (3.51)$$

in which

$$v' = \frac{1}{2} (v_i + v_j)$$

The edge forces corresponding to in-plane stress problem can be obtained by substituting Eq. (3.51) into Eq. (3.10).

$$\begin{Bmatrix} T_i \\ T_j \\ P_i \\ P_j \end{Bmatrix} = \begin{bmatrix} \frac{AE}{\bar{L}^2} & 0 & \frac{-24EI}{(1+6\bar{\beta})d\bar{L}^3} & \frac{-6(1-2\bar{\beta})EI}{(1+6\bar{\beta})d\bar{L}^2} \\ \frac{AE}{\bar{L}^2} & 0 & \frac{24EI}{(1+6\bar{\beta})d\bar{L}^3} & \frac{6(1-2\bar{\beta})EI}{(1+6\bar{\beta})d\bar{L}^2} \\ 0 & \frac{2Eb}{d} & \frac{-36EI}{(1+6\bar{\beta})\bar{L}^4} & \frac{-12EI}{(1+6\bar{\beta})\bar{L}^3} \\ 0 & \frac{2Eb}{d} & \frac{36EI}{(1+6\bar{\beta})\bar{L}^4} & \frac{12EI}{(1+6\bar{\beta})\bar{L}^3} \end{bmatrix} \begin{Bmatrix} u_d \\ v' \\ v_d \\ \psi_d \end{Bmatrix} \quad (3.52)$$

3.4 Solution for a Continuous Cellular Folded Plate Structure

If the folded plate structure is continuous over interior rigid columns connected at the joints only, the matrix equations listed in preceding section can be used directly with the following assumptions. First of all, the column reactions are idealized as uniformly distributed over the column length in longitudinal direction and restraint displacements are considered at the center point only. A segment whose length in longitudinal direction equals the length of the column support is chosen. The problem is solved if the restrained zero displacements are specified when solving the unknown joint displacements of that segment under step 4 described earlier in Section 3.3.8.

For the case in which interior rigid diaphragms exist, the following assumptions are made:

1. Since each plate element is treated as a longitudinal beam, the restraint conditions for each plate element are in terms of 3 displacements: longitudinal axial displacement, transverse beam displacement, and longitudinal beam rotation.
2. The restraint forces are concentrated line forces at the section of the diaphragm. Corresponding to the 3 beam displacements the 3 forces are: longitudinal axial force, transverse beam shear, and longitudinal beam moment.
3. There are no restraints assumed at the longitudinal joints of the folded plate structure for this case.

For the interior rigid diaphragm, some plate elements are restrained against displacement. If a displacement action is zero at the diaphragm, a reaction must exist and the corresponding force action is discontinuous. After the interior diaphragm a new set of unknown actions is chosen instead of the unknowns at the origin of the structure. The new set of unknowns contains the diaphragm reactions with those displacement actions which are not restrained by the diaphragm.

A structure with one interior rigid diaphragm is used as illustration (Fig. 12). Using equations developed in last section, the actions at section e (interior diaphragm) of span I are given by Eq. (3.41).

$$\{Z_e^T\} = [D_e] \{Z_o^T\}_{\text{unk.}} + \{\tilde{D}_e\} \quad (3.41)$$

The complete action vector Z_e^T can be rearranged into displacement and force sub-vectors d and f , so Eq. (3.41) can be written as

$$\left\{ \begin{array}{c} -d \\ f \end{array} \right\} = \left[\begin{array}{c} -a \\ b \end{array} \right] \{Z_o^T\}_{\text{unk.}} + \left\{ \begin{array}{c} \tilde{a} \\ \tilde{b} \end{array} \right\} \quad (3.53)$$

or,

$$\{d\} = [a] \{Z_o^T\}_{\text{unk.}} + \{\tilde{a}\} \quad (3.53a)$$

$$\{f\} = [b] \{Z_o^T\}_{\text{unk.}} + \{\tilde{b}\} \quad (3.53b)$$

in which d and f represent all the displacement and force actions at section e , respectively.

The force actions corresponding to zero displacements at the interior diaphragm are first calculated. Setting Eq. (3.53a) to zero,

$$\{Z_o^T\}_{\text{unk.}} = -[a]^{-1} \{\tilde{a}\} \quad (3.54)$$

and substitute into Eq. (3.53b),

$$\{\tilde{f}\}_{d=0} = -[b] [a]^{-1} \{\tilde{a}\} + \{\tilde{b}\} \quad (3.55)$$

$\tilde{f}_{d=0}$ represent the force actions at section e due to loads at span I assuming the structure is fixed at e .

Neglecting the surface loading the relation between the displacement and force actions, d_o and f_o , at section e and the unknown actions at origin is given by (refer to Eq. (3.53)),

$$\left\{ \begin{array}{c} d_o \\ f_o \end{array} \right\} = \left[\begin{array}{c} a \\ b \end{array} \right] \{Z_o^T\}_{\text{unk.}} \quad (3.56)$$

or,

$$\{d_o\} = [a] \{Z_o^T\}_{\text{unk.}} \quad (3.56a)$$

$$\{f_o\} = [b] \{Z_o^T\}_{\text{unk.}} \quad (3.56b)$$

Based on Eq. (3.56), d_o and f_o are not independent of each other, they are related by the following equation:

$$\{f_o\} = [b] [a]^{-1} \{d_o\} \quad (3.57)$$

or

$$\{f_o\} = [c] \{d_o\} \quad (3.57a)$$

where

$$[c] = [b] [a]^{-1}$$

Let $\{d\}_{\text{unk.}}$ be the unknown displacement actions at section e , then the complete actions at section e can be represented by the following matrix equation:

$$\left\{ \begin{array}{c} d \\ f \end{array} \right\} = \left[\begin{array}{c} 1 \\ c \end{array} \right] \{d\}_{\text{unk.}} + \left\{ \begin{array}{c} o \\ f \end{array} \right\}_{d=0} \quad (3.58)$$

Due to the restraint conditions at the diaphragm, Eq. (3.58) must be modified in the following way. If a displacement action d_i in $\{d\}_{\text{unk.}}$ is zero, the corresponding reaction, defined as R_i , is an unknown and d_i in the vector $\{d\}_{\text{unk.}}$ will be replaced by R_i . The corresponding 1 (i^{th} row, i^{th} column) in the unit matrix will become zero, and the corresponding i^{th} column vector in matrix c is substituted by a vector containing 1 in the i^{th} row and zeros in the other elements. After all modifications due to restraints have been performed, the equation can be rearranged into the order corresponding to the actions of each plate element. It can be represented as

$$\{Z_e^T\} = [L_e^T] \{Z_e^T\}_{\text{unk.}} + \{\tilde{L}_e^T\} \quad (3.59)$$

which is similar to Eq. (3.20a) and the equations developed in the last section can be used for calculations while progressing along the segments in span II. Note that $\{Z_e^T\}_{\text{unk.}}$ now contains the unknown displacements of the plate elements and unknown reactions from the rigid diaphragm at the section of the support.

Due to the given boundary conditions at the far end of the folded plate structure, $\{Z_e^T\}_{\text{unk.}}$ is first solved following the equations in the preceding section. In order to obtain the solution for $\{Z_o^T\}_{\text{unk.}}$, the displacement vector d at section e is formed and $\{Z_o^T\}_{\text{unk.}}$ is determined from the solution of Eq. (3.53a). Therefore,

$$\{Z_o^T\}_{\text{unk.}} = [a]^{-1} (\{d\} - \{\tilde{a}\}) \quad (3.60)$$

and the problem is solved.

It should be mentioned that for a large folded plate system, the coefficients relating the actions at the two ends of the structure become very sensitive and the solution is not accurate. To avoid this sensitivity, the displacement actions at certain sections within the structure are used as intermediate unknowns while progressing along the system. Such a section is termed as a stopover. At each stopover, Eq. (3.58) is formed and then the rows of the matrices are rearranged in an order according to the actions of each element as

$$\{Z^T\} = [L^T] \{d\}_{\text{unk.}} + \{\tilde{L}^T\} \quad (3.61)$$

So the displacements at the stopover are used as unknown actions for the next group of segments until another stopover, interior diaphragm, or the far end of the structure is reached. A back substitution procedure using

equations such as Eq. (3.60) is needed to solve for all the unknown displacements at a stopover, as well as the unknowns at any interior diaphragm and finally the unknown actions at the origin.

3.5 Direct Stiffness Method Using Complete Segment Stiffness Matrix

Based on the assumptions and simplifications mentioned in Section 3.1, each segment may be treated as a finite element of the folded plate structure and direct stiffness method can be used. The direct stiffness method for structural analysis is well known, and in fact it has been utilized in the folded plate method described in Chapter 2. Only a brief description of the procedure is given here.

1. The structure is divided longitudinally into a finite number of segments.
2. The segment stiffness matrix based on relative or segment coordinate system is calculated.
3. The segment stiffness matrix is transformed from the relative coordinate system to a fixed coordinate system of the structure.
4. The total stiffness matrix of the structure is obtained by assembling the segment stiffness matrices. This stiffness matrix relates the external forces to the corresponding displacements of the entire structure.
5. The unknown displacements of the structure are solved.
6. The segment internal forces and displacements are calculated.

The most important step is the determination of the segment stiffness matrix. There are 14 degrees of freedom for each segment: 4 at each edge of the two longitudinal edges and 3 at each end of the segment. Ten out of the 14 correspond to the in-plane stiffness while the other 4 correspond to transverse one-way slab bending. The complete 14 x 14 segment stiffness matrix has been derived by Lo [14], but will not be presented here.

The total stiffness matrix of the structure is symmetrical and it can be arranged into a band matrix form. For a structure of m elements and n

joints, the maximum band width will be $6m + 4n$ as shown in Fig. 13.

Since the stiffness coefficients at upper right triangle of the sub-matrix relating quantities at sections $k-1$ and k are zeros, the band width becomes $3(m+1) + 4n$ (Fig. 13). The unknown displacements of the system can be determined by solving this band stiffness matrix.

3.6 Advantages and Disadvantages of the Segment Progression Solution as Compared to the Band Matrix Solution

The advantages of the segment progression solution are:

1. It requires less storage. The computer program (discussed in the next section) needs two big coefficient matrices of the sizes $6m \times (3m+1)$ and $4n \times (3m+1)$ for a structure of m elements and n joints. The storage of these two matrices will be $18m^2 + 6m + 12nm + 4n$, or approximately $30m^2 + 10m$ if $m = n$.

When the direct stiffness method, as presented in Section 3.5, is used, the storage of a band matrix with band width of $3(m+1) + 4n$ and $(3m + 4n)$ rows will be $9m^2 + 16n^2 + 24mn + 9m + 12n$ or approximately $49m^2 + 21m$ if $m = n$.

2. In progressing from one section to the next one, the calculation of the element actions requires approximately $(288m^2 + 150m)$ multiplications in the computer program. Here n is assumed to be equal to m and only the non-zero terms in the matrix equations are programmed. This corresponds to the steps including Eq. (3.21) through Eq. (3.40).

In the band matrix solution (Fig. 13) of the direct stiffness method, in order to eliminate the unknowns of one section and one segment ($3m + 4n$ unknowns), the number of multiplication or division will be approximately equal to $7m \times (7m + 3)^2 \times 1/2 \approx 172m^3 + 150m$. Here n is again assumed to be equal to m .

It is believed that the above steps take into account most of the computation times for each of the two different methods, and from these estimates the segment progression solution should involve less computation time than the band matrix solution. However, this comparison can only give a rough idea because the back substitution procedure and the calculation of segment

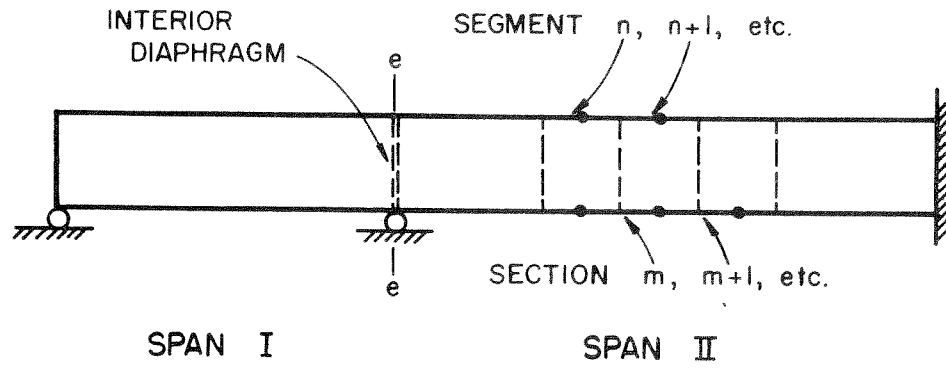


FIG. 12 FOLDED PLATE STRUCTURE WITH ONE INTERIOR RIGID DIAPHRAGM.

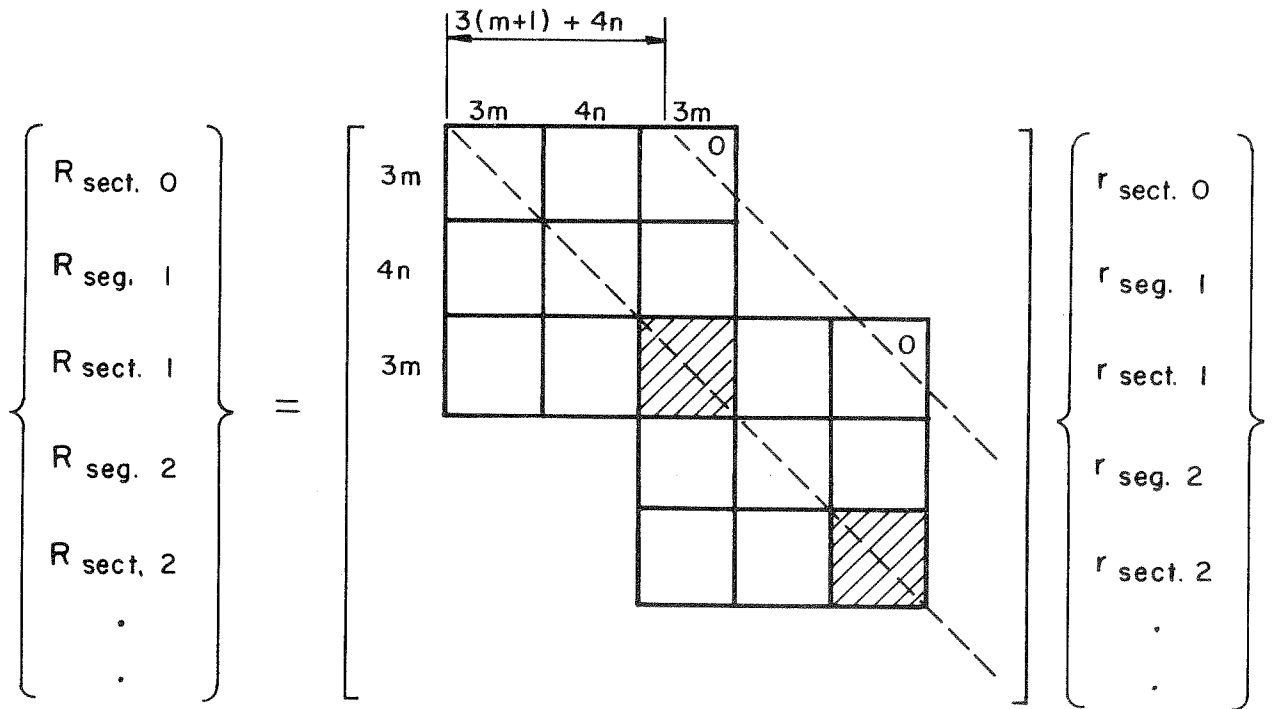


FIG. 13 MAKEUP OF STRUCTURE STIFFNESS MATRIX USING COMPLETE SEGMENT STIFFNESS MATRIX.

forces and displacements are not included. Only the segment progression solution is presently programmed for solution, therefore no accurate time comparisons can be made.

The disadvantages of the segment progression solution are:

1. As discussed in the last paragraph of Section 3.4, for a big system stopovers are needed because of sensitivity problem. For each stopover this requires an inversion of a $3m \times 3m$ matrix and a number of additional computations. Therefore, as the number of stopovers increases, the computation time will increase.

2. In writing the computer program, it has been found that double precision is advisable. Thus both the computation time and required storage will increase.

3.7 Computer Program - SIMPLA

A general computer program based on the segment progression solution, entitled SIMPLA, has been written in FORTRAN IV language for the IBM 7094 digital computer. It provides a solution for a folded plate structure with arbitrary conditions (with respect to the end conditions of a beam for each element) at the two ends and with or without interior rigid column or diaphragm supports. Only joint loads may be applied to the structure. The resulting joint displacements of the structure together with the edge forces and displacements and internal forces and displacements for each segment are determined. A detailed description of the input, output, sign conventions and limitations and restrictions of the program are given in Appendix A. A brief description of the program is given below

a. Input Data:

(1) The geometry and dimensions of the structure in terms of the number of plates, joints, segments, etc.

(2) Dimensions and material properties for each plate (beam) element.

(3) Boundary conditions at the two ends of the structure. The boundary conditions may consist of any combination of known forces and displacements referred to the plate elements which are treated as longitudinal beams.

(4) Applied uniform joint loads and/or given zero displacements at the joints of each segment of the structure.

(5) Indicators for restraint conditions on each plate element if a rigid diaphragm exists.

b. Computer Output:

(1) The complete input data is properly labelled and printed for a check.

(2) Final plate actions (forces and displacements) for each plate element at the two ends of the structure as well as at the stopovers and interior rigid diaphragms are printed.

(3) For each segment final joint and plate forces and displacements at the center of the segment are printed.

c. Limitations, Remarks and Restrictions:

(1) The maximum number of plate elements and joints for a cross-section is 15 and 16, respectively.

(2) The longitudinal span can be divided into any arbitrary number of segment lengths.

(3) The joint loads are uniformly distributed over each segment length, however, each segment of the structure can have different loading conditions.

(4) Each interior rigid diaphragm can have its own restraint conditions on the structure.

(5) The number and locations of the stopovers are arbitrary. The minimum number required to give an accurate result depends on the size of the structure and for a suitable choice, experience is needed.

d. Logical Steps:

- (1) Read and print input data.
- (2) Set up total actions in terms of the boundary conditions at the origin of the structure.
- (3) For each segment of the structure,
 - (a) Compute stiffness and coefficient matrices for each type of plate segment.
 - (b) Assemble the stiffness matrix for one transverse segment of the folded plate structure. If the segment length is the same as a previous one, the total stiffness matrix will be read from a tape.
 - (c) Calculate fixed joint forces due to actions at preceding section. Add external applied joint forces.
 - (d) Solve for the joint displacements.
 - (e) Calculate actions at the end of this segment.
- (4) If there is a stopover or interior rigid diaphragm,
 - (a) The actions of the structure are changed to be in terms of a new set of unknowns which contain the unknown displacements and/or diaphragm reactions at this section.
 - (b) Progress to next segment of the structure.
- (5) After progression to the last segment, set up the boundary conditions at the end of the structure.

(6) Calculate and print final plate forces and displacements at the end, stopovers, rigid diaphragms and the origin of the structure.

(7) For each segment the joint (edge) forces and displacements and the final internal plate forces and displacements are calculated and printed.

4. FINITE ELEMENT METHOD OF ANALYSIS

4.1 Introduction

The finite element method can be thought of as a numerical procedure by means of which the solution of a problem in continuum mechanics may be approximated by analyzing a structure consisting of an assemblage of finite elements interconnected at a finite number of nodal points, in which selected internal stress or displacement patterns are assumed in the elements to satisfy certain required conditions. During the past decade this method has been applied successfully to a variety of problems involving plates subjected to in-plane or normal loadings, axi-symmetric solids and axi-symmetric shells. More recently attention has been focused on applying the method to general thin shell problems and to the general three dimensional analysis of solids. No attempt will be made here to review the extensive literature on this subject. An excellent book by Zienkiewicz [16] has been recently published (1967) which gives a comprehensive discussion of the theory and application of the finite element method to the problems mentioned above. It also contains an extensive set of references.

Of particular interest in the present investigation is the application of the finite element method to the analysis of prismatic cellular folded plate structures such as the box girder bridge. The basic structural element used in this method is a finite element which is formed by dividing each rectangular plate element transversely as well as longitudinally into an assemblage of smaller rectangular finite elements, Fig. 14. The size, thickness and material properties of these rectangular finite elements can be varied as desired throughout the structure. Thus in zones near concentrated loads, Fig. 14, a finer mesh can be used to more accurately determine the

stresses and moments which are rapidly changing in this vicinity. Arbitrary loading or boundary conditions may be selected at each nodal point. In the development to be described it is assumed that each nodal point has six degrees of freedom. For each of these, a known external force or a known displacement may exist. If a certain force is known, the corresponding displacement is unknown, and vice versa. A direct stiffness solution can be used to find all of the unknown nodal point displacements and forces. Once these are known, the internal forces and stresses for each finite element can be determined. The key step in this approach is the development of element stiffness matrices for the individual finite elements which can accurately approximate the behavior of the continuum when they are assembled to form the structure stiffness matrix needed in the direct stiffness solution. This step will be discussed in detail in the later sections of this chapter.

The basic assumptions used are as follows:

- (a) Each finite element is rectangular, of uniform thickness and is made of an elastic, isotropic and homogeneous material.
- (b) The relation between forces and deformations is linear, so that superposition is valid.
- (c) The in-plane displacements within each rectangular finite element (membrane action) are obtained by the superposition of 12 displacement patterns. These patterns can be uniquely defined by three nodal point displacement components at each corner of the element, which are taken as two in-plane translations and one rotation about a normal to the plane of the element.

- (d) In-plane stresses within each finite element are determined from the in-plane displacements by means of the elasticity equations defining the plane stress problem.
- (e) The normal displacements within each rectangular finite element (slab action) are obtained by the superposition of 12 displacement patterns. These patterns can be uniquely defined by three nodal point displacement components at each corner of the element, which are taken as two rotations about in-plane axes and a displacement normal to the plane of the plate.
- (f) The plate bending and torsional moments within each finite element are determined from the normal displacements by means of the classical thin plate bending theory.

The assumptions of (d) and (f) above for each element are those of the elasticity theory for folded plates, however, it should be remembered that the complete structure assembled from the finite elements only approximates the true continuum since equilibrium and compatibility are satisfied only at the nodal points and not along the entire interfaces of adjacent elements. In general the independent displacement patterns chosen for the individual elements are selected so as to closely as possible satisfy compatibility across these interfaces. In addition, to achieve accuracy in the solution, the displacement patterns should include all possible rigid body modes and uniform straining modes of displacement for the element.

4.2 General Description of the Method

Consider the structure shown in Fig. 14, subjected to a given loading and set of boundary conditions as shown. It is desired to find the resulting nodal point displacements and the internal forces and moments in each finite

element. Reference is made to two right coordinate systems shown in Figs. 14 and 15, the global (fixed) system XYZ and the local (relative) system xyz . The global system is the same for all elements with the XY plane being horizontal and the Z axis vertical down. The local system varies from element to element and depends on the angle θ defining the inclination of the element with the horizontal plane.

All external loads and nodal point displacements are referred to the global system. Each nodal point has six degrees of displacement freedom, three translational and three rotational. The positive directions of the external forces or moments R and corresponding nodal point displacements r are defined by the positive directions of the global XYZ axes. The right hand vector rule should be used for moments and rotations. Similarly the internal element nodal point forces and displacements, six at each corner of the rectangular element shown in Fig. 15, may be defined in either a local system as S and v or in a global system as \bar{S} and \bar{v} . A simple transformation matrix involving the angle θ shown in Fig. 15 relates the two systems. Positive directions of these quantities are defined by the positive directions of the local axes xyz or the global axes XYZ . Each finite element has 24 degrees of freedom.

The positive directions of the final desired internal forces and moments at any point in the structure are shown in Fig. 16. These consist of the membrane forces N_x, N_y, N_{xy} and the slab forces $M_x, M_y, M_{xy}, Q_x,$ and Q_y .

The analysis of the structure is carried out by means of a direct stiffness solution and involves the following steps.

- (1) External distributed surface loadings on the structure are converted to equivalent nodal point forces by a simple tributary area concept and they are added to the other existing nodal point loads to form the known loads on

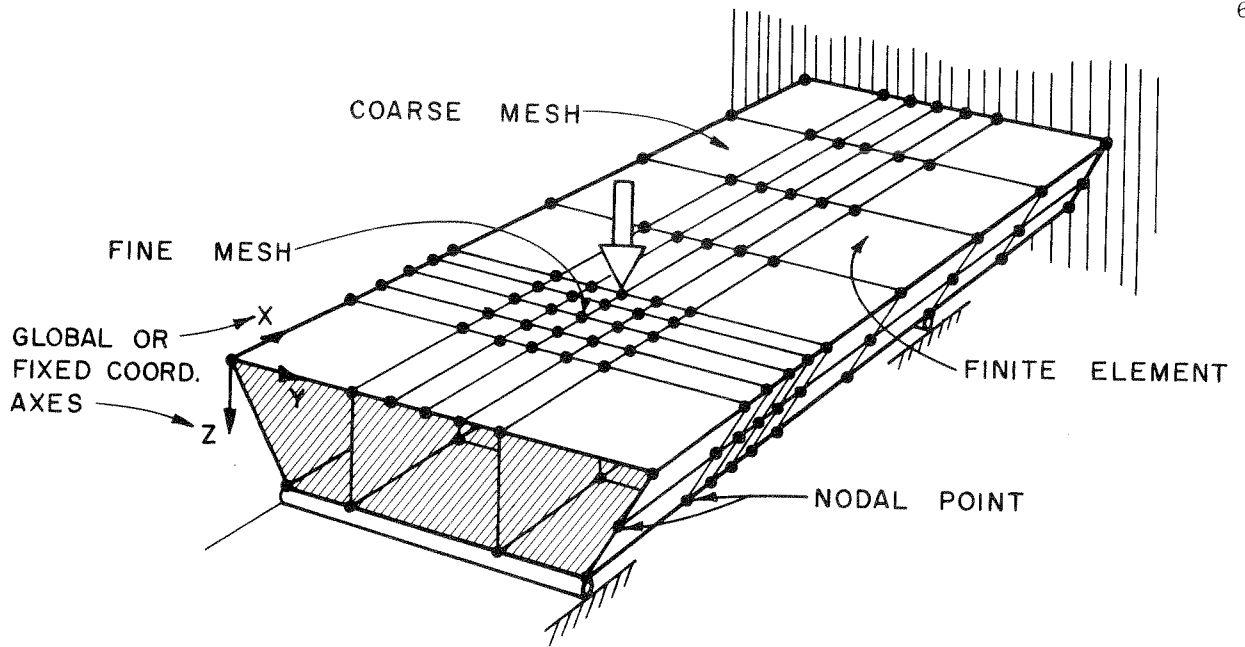


FIG. 14 FINITE ELEMENT ANALYTICAL MODEL

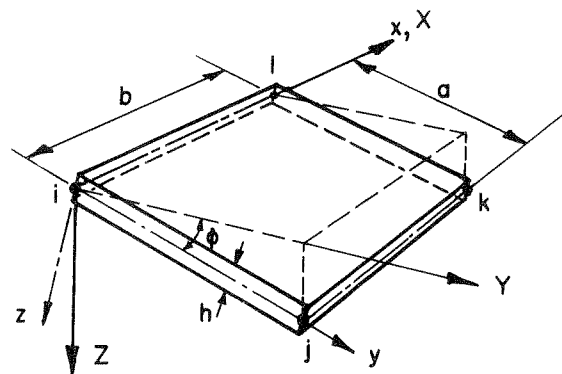


FIG. 15 GLOBAL (FIXED) XYZ AND LOCAL (RELATIVE) xyz COORDINATE SYSTEMS AND FINITE ELEMENT DIMENSIONS

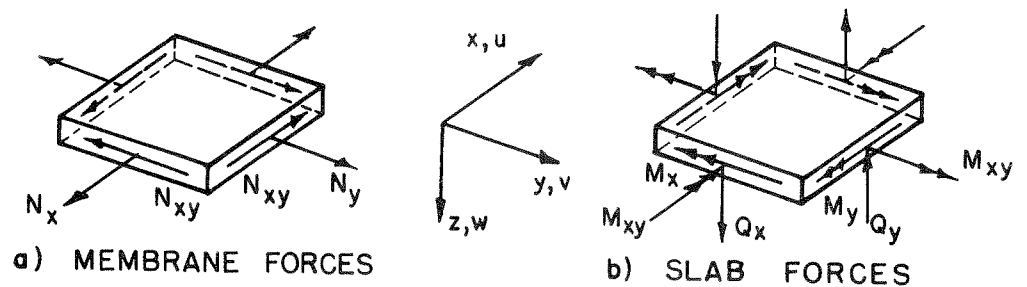


FIG. 16 POSITIVE INTERNAL FORCES AND DISPLACEMENTS IN A FINITE ELEMENT

the structure. Specified known displacements will also exist at some joints. For each degree of freedom, if a known force exists, a corresponding unknown displacement will exist and vice-versa. An external load vector R and a displacement vector r are formed containing these known and unknown quantities.

- (2) Stiffness matrices based on carefully selected displacement patterns are derived in the local coordinate system for membrane action k_p and for slab action k_s in a typical finite element,

$$\begin{Bmatrix} S_p \\ S_s \end{Bmatrix}_{24 \times 1} = \begin{bmatrix} k_p & 0 \\ 0 & k_s \end{bmatrix}_{24 \times 24} \begin{Bmatrix} v_p \\ v_s \end{Bmatrix}_{24 \times 1} \quad (4.1)$$

or simply

$$\{S\} = [k] \{v\} \quad (4.1a)$$

Since membrane action and slab action in an element are uncoupled, the 12×12 matrix k_p and the 12×12 matrix k_s may be derived independently of each other by considering independently the plane stress problem and the plate bending problem. Each of these will be considered in detail in subsequent sections in this chapter.

- (3) The element nodal point forces S and displacements v in the local coordinate system are transformed into a global coordinate system \bar{S} and \bar{v} , by means of a displacement transformation matrix a and its transpose a^T .

$$\{v\} = [a] \{\bar{v}\} \quad (4.2)$$

$$\{\bar{S}\} = [a]^T \{S\} \quad (4.3)$$

- (4) The element stiffness matrix in the global coordinate system is determined by substituting Eqs. (4.2) and (4.3) into (4.1a).

$$\{\bar{S}\} = [a]^T [k] [a] \{\bar{v}\} \quad (4.4a)$$

or

$$\{\bar{S}\} = [\bar{k}] \{\bar{v}\} \quad (4.4b)$$

where

$$[\bar{k}] = [a]^T [k] [a] \quad (4.5)$$

The matrix \bar{k} is a 24 x 24 element stiffness matrix and one such matrix is evaluated for each finite element in the structure.

- (5) Equation (4.4b) is partitioned as follows

$$\begin{Bmatrix} \bar{S}_i \\ \bar{S}_j \\ \bar{S}_k \\ \bar{S}_l \end{Bmatrix} = \begin{bmatrix} \bar{k}_{ii} & \bar{k}_{ij} & \bar{k}_{ik} & \bar{k}_{il} \\ \bar{k}_{ji} & \bar{k}_{jj} & \bar{k}_{jk} & \bar{k}_{jl} \\ \bar{k}_{ki} & \bar{k}_{kj} & \bar{k}_{kk} & \bar{k}_{kl} \\ \bar{k}_{li} & \bar{k}_{lj} & \bar{k}_{lk} & \bar{k}_{ll} \end{bmatrix} \begin{Bmatrix} \bar{v}_i \\ \bar{v}_j \\ \bar{v}_k \\ \bar{v}_l \end{Bmatrix} \quad (4.6)$$

where i, j, k and l represent the four nodal points at the corners of the rectangular finite element shown in Fig. 15. Each of the resulting 6 x 6 submatrices \bar{k}_{mn} relate the six nodal point forces \bar{S} produced at a corner m by a set of unit nodal point displacements \bar{v} at a corner n .

- (6) Static equilibrium at any nodal point requires that the external nodal point forces at a joint must equal the sum of the element forces acting on the same joint. For example assuming four elements are connected to joint i .

$$\{R_i\} = \{\bar{S}_i^1\} + \{\bar{S}_i^2\} + \{\bar{S}_i^3\} + \{\bar{S}_i^4\} \quad (4.7)$$

where the superscript refers to the element number.

- (7) Geometric compatibility at any nodal point requires that the external joint displacements must equal the element nodal point displacements in the global system.

$$\{r_i\} = \{\bar{v}_i^1\} = \{\bar{v}_i^2\} = \{\bar{v}_i^3\} = \{\bar{v}_i^4\} \quad (4.8)$$

- (8) The structure stiffness matrix K for the entire structure can now be assembled by properly adding the element stiffness sub-matrices of Eq. (4.6)

$$\begin{matrix} \{R\} = [K] \{r\} \\ 6n \times 1 \quad 6n \times 6n \quad 6n \times 1 \end{matrix} \quad (4.9)$$

The structure stiffness matrix K will be extremely large for problems of this type and will have a size $6n \times 6n$ in which n is the number of nodal points. By adopting a proper sequence for numbering the nodal points, such that the maximum difference in the nodal point numbers of any finite element is minimized, advantage may be taken of the topology of the structure to yield the minimum band width possible for the K matrix. In the computer program to be described later, advantage is taken of the prismatic nature of the structure by requiring only the

numbering of the nodal points on the cross-section at $x = 0$. The computer then automatically assigns nodal point numbers to the other specified sections along the span, which define the locations of nodal points.

- (9) A tri-diagonalization method is used to solve the large system of equations represented by Eq. (4.9). This is the most time consuming part of the problem in the computer.
- (10) With the nodal point displacements r known, the finite element nodal point displacements v in the local coordinate system may be found through the use of Eqs. (4.8) and (4.2).
- (11) Internal forces and displacements, Fig. 16, in each finite element are calculated at selected points by expressions relating these quantities to the nodal point displacements.

4.3 Development of Finite Element Stiffness by Virtual Work

The derivation of the element stiffness matrices for membrane action and slab action can be accomplished either by a direct geometric approach or by using the principle of virtual work. General descriptions of both of these approaches, which have become well known, may be found in the book by Zinkiewicz [16]. The virtual work procedure is adopted here and is outlined below for the plane stress and plate bending effects occurring in the rectangular finite element to be used. The outline is based on the description given by Abu-Ghazaleh [13].

- (1) Express the internal displacements V in terms of displacement functions F .

$$\{V(x,y)\} = [F(x,y)] \{\alpha\} \quad (4.10)$$

- a. The in-plane displacements u and v are used for the plane stress problem and the normal displacement w is used for the plate bending problem.
 - b. A total of 24 linearly independent coefficients α , 12 for plane stress and 12 for plate bending, are used as the generalized coordinates for the system. The number of degrees of freedom assigned to the element is also taken equal to 24.
 - c. The functions contained in $\{V(x,y)\}$, Eq. (4.10), may be thought of as the superposition of a number of independent displacement patterns equal to the number of degrees of freedom assigned to the element.
- (2) Define a set of generalized displacements V_i which have the following properties.
- a. Capable of uniquely expressing the connectivity between different elements.
 - b. The boundary displacement field should be uniquely determined by means of these generalized displacements.
 - c. In the present development the nodal point displacements (translations and rotations) at the four corners of the rectangular element are selected as the generalized displacements.

- (3) Evaluate the nodal point displacements in terms of the generalized coordinates.

$$\{V_i\} = [A] \{\alpha\} \quad (4.11)$$

The A matrix can be found using Eq. (4.10) by appropriately defining V_i and substituting in the nodal point coordinates.

- (4) a. For a plane stress problem, evaluate the element strains ϵ by appropriate differentiation of the displacement functions of Eq. (4.10).
- b. For a plate bending problem, evaluate the element curvatures κ by appropriate differentiation of the displacement functions of Eq. (4.10).

$$\left. \begin{aligned} \{\epsilon(x,y)\} &= [B_p(x,y)] \{\alpha_p\} \\ \{\kappa(x,y)\} &= [B_s(x,y)] \{\alpha_s\} \end{aligned} \right\} \quad (4.12)$$

- (5) a. For a plane stress problem, evaluate the element stresses σ from the assumed stress-strain law.
- b. For a plate bending problem, evaluate the element moments M from the assumed moment-curvature law.

$$\left. \begin{aligned} \{\sigma(x,y)\} &= [D_p] \{\epsilon(x,y)\} \\ \{M(x,y)\} &= [D_s] \{\kappa(x,y)\} \end{aligned} \right\} \quad (4.13)$$

The matrix D in each case contains the appropriate elastic constants.

- (6) Substituting Eqs. (4.12) into Eqs. (4.13)

$$\left. \begin{aligned} \{\sigma(x,y)\} &= [D_p] [B_p(x,y)] \{\alpha_p\} \\ \{M(x,y)\} &= [D_s] [B_s(x,y)] \{\alpha_s\} \end{aligned} \right\} \quad (4.14)$$

- (7) a. For a plane stress problem, introduce sets of virtual strain fields $\bar{\epsilon}$ such that the corresponding generalized coordinates have unit values, i.e. $\bar{\alpha}_p = I$ (identity matrix) in Eq. (4.12).
- b. For a plate bending problem, introduce sets of virtual curvature fields $\bar{\kappa}$ such that the generalized coordinates have unit values, i.e. $\bar{\alpha}_s = I$ (identity matrix) in Eq. (4.12).
- c. The internal virtual work done in a differential volume of the element is

$$\left. \begin{aligned} dW_I &= \bar{\epsilon}^T \sigma dV \\ dW_I &= \bar{\kappa}^T M dV \end{aligned} \right\} \quad (4.15)$$

- d. Taking transposes of both sides of Eqs. (4.12)

$$\left. \begin{aligned} \{\bar{\epsilon}(x,y)\}^T &= \{\bar{\alpha}_p\}^T [B_p(x,y)]^T \\ \{\bar{\kappa}(x,y)\}^T &= \{\bar{\alpha}_s\}^T [B_s(x,y)]^T \end{aligned} \right\} \quad (4.16)$$

- c. Substituting Eqs. (4.16) and (4.13) into (4.15) and dropping the matrix brackets and x,y for simplified notation.

$$dW_I = \bar{\alpha}^T B^T DB \alpha dV \quad (4.17)$$

$$W_I = \int_V \bar{\alpha}^T B^T DB \alpha dV \quad (4.18)$$

Since $\bar{\alpha}$ and α are independent of the variables of integration

$$W_I = \bar{\alpha}^T \left[\int_V B^T D B \, dV \right] \alpha \quad (4.19)$$

$$W_I = \bar{\alpha}^T \tilde{k} \alpha$$

where

$$\tilde{k} = \int_V B^T D B \, dV \quad (4.20)$$

- (8) Defining β as the generalized forces corresponding to the generalized coordinates α , the external virtual work W_E done during the virtual displacements $\bar{\alpha} = I$ is

$$W_E = \bar{\alpha}^T \beta \quad (4.21)$$

- (9) Since the external virtual work must equal the internal virtual work

$$W_E = W_I \quad (4.22)$$

which gives using Eqs. (4.21) and (4.19)

$$\bar{\alpha}^T \beta = \bar{\alpha}^T \tilde{k} \alpha \quad (4.23)$$

but since $\bar{\alpha} = I$ (identity matrix) this may be simplified to

$$\beta = \tilde{k} \alpha \quad (4.24)$$

in which \tilde{k} is the element stiffness matrix relating the generalized forces β to the generalized coordinates α .

- (10) Since the number of linear independent coefficients α is equal to the number of degrees of freedom of the element, the element stiffness matrix k relating nodal point forces S_i to nodal point displacements V_i may be obtained as follows.

- (a) From Eq. (4.11) using brackets only where needed for clarity

$$\alpha = [A^{-1}] V_i \quad (4.25)$$

the A matrix can be inverted for this case since it is a square non-singular matrix.

- (b) The A^{-1} matrix represents the displacement transformation matrix relating generalized coordinates α to nodal point displacements V_i . Thus the relation between nodal point forces S_i and generalized forces β may be written as follows

$$S_i = [A^{-1}]^T \beta \quad (4.26)$$

- (c) Combining Eqs. (4.24) (4.25) and (4.26)

$$S_i = [A^{-1}]^T \beta = [A^{-1}]^T \tilde{k} \alpha = [A^{-1}]^T \tilde{k} [A^{-1}] \quad (4.27)$$

or simply

$$S_i = k V_i \quad (4.28)$$

where

$$k = [A^{-1}]^T \tilde{k} [A^{-1}] \quad (4.29)$$

Once k is known for all elements the direct stiffness solution outlined in the preceding section may be used to analyze the total structure.

For rectangular elements the necessary integration involved in finding \tilde{k} in Eq. (4.20) can usually be carried out in a formal mathematical manner.

Abu Ghazaleh has made an extensive study [12] of element stiffnesses for rectangular elements. He compared the properties of five different plane stress finite elements and two different plate bending finite elements.

Based on a comparison of the results obtained in applying these to problems of plane stress and plate bending with known solutions, he selects one plane stress finite element and one plate bending finite element as being the most accurate and the most suitable for combining to solve prismatic folded plate problems. The stiffness matrices for these latter two elements will be developed in detail in the next two sections based on the dissertation by Abu Ghazaleh [13].

4.4 Element Stiffness for Membrane Action - Plane Stress Analysis

4.4.1 Elasticity Equations for the Plane Stress Problem

For a plane stress problem, an exact elasticity solution should satisfy the conditions given below. The standard notation, sign convention and direction of coordinate axes based on Timoshenko and Goodier [18], are shown in Fig. 17.

(1) Equilibrium requirements:

$$\frac{\partial \sigma_x}{\partial x} + \frac{\partial \tau_{xy}}{\partial y} + X = 0 \quad (4.30a)$$

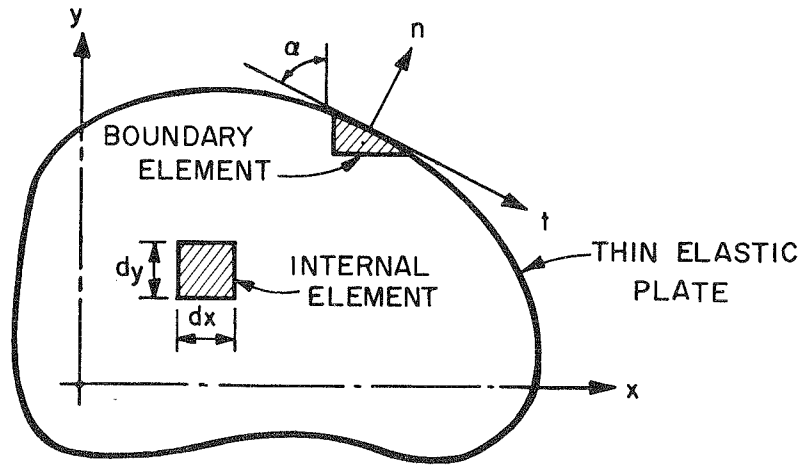
$$\frac{\partial \tau_{xy}}{\partial x} + \frac{\partial \sigma_y}{\partial y} + Y = 0 \quad (4.30b)$$

(2) Stress-strain law:

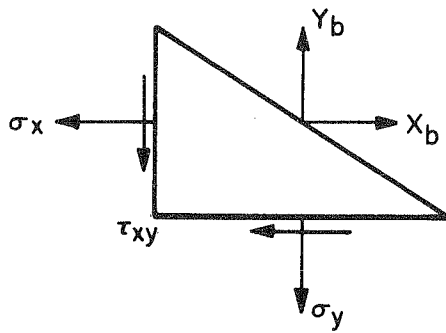
$$e_x = \frac{1}{E} [\sigma_x - \nu \sigma_y] \quad (4.31a)$$

$$e_y = \frac{1}{E} [\sigma_y - \nu \sigma_x] \quad (4.31b)$$

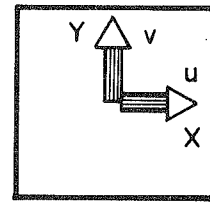
$$\gamma_{xy} = 2(1+\nu) \frac{1}{E} \tau_{xy} = \frac{\tau_{xy}}{G} \quad (4.31c)$$



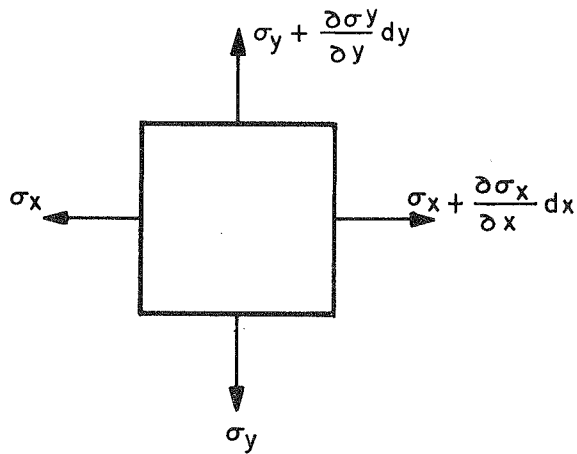
a) ELASTIC BODY AND REFERENCE AXIS



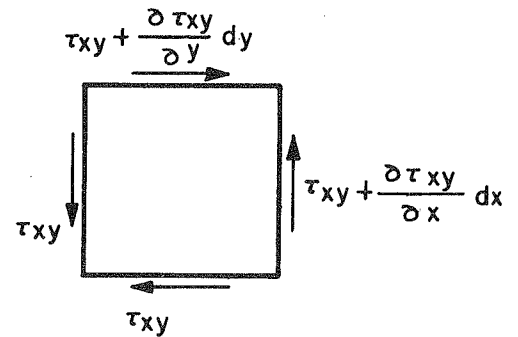
b) BOUNDARY ELEMENT



c) EXTERNAL FORCES AND DISPLACEMENTS



d) NORMAL STRESSES



e) SHEAR STRESSES

FIG. 17 POSITIVE DIRECTIONS FOR COORDINATE AXES, EXTERNAL FORCES, DISPLACEMENTS AND INTERNAL STRESSES.

(3) Compatibility conditions:

$$\epsilon_x = \frac{\partial u}{\partial x} \quad (4.32a)$$

$$\epsilon_y = \frac{\partial v}{\partial y} \quad (4.32b)$$

$$\gamma_{xy} = \frac{\partial u}{\partial y} + \frac{\partial v}{\partial x} \quad (4.32c)$$

eliminating u and v in these equations gives

$$\frac{\partial^2 \epsilon_x}{\partial y^2} + \frac{\partial^2 \epsilon_y}{\partial x^2} = \frac{\partial^2 \gamma_{xy}}{\partial x \partial y} \quad (4.32d)$$

(4) Boundary conditions:

(a) Displacements

$$u \text{ (internal)} = \bar{u} \text{ (external)} \quad (4.33a)$$

$$v \text{ (internal)} = \bar{v} \text{ (external)} \quad (4.33b)$$

(b) Forces

$$X_b = \sigma_x \cos\alpha + \tau_{xy} \sin\alpha \quad (4.34a)$$

$$Y_b = \sigma_y \sin\alpha + \tau_{xy} \cos\alpha \quad (4.34b)$$

A solution which satisfies Eqs. (4.30) through (4.34) over the entire domain of the problem may be termed an exact solution to the plane stress problem. Often this exact solution is difficult to obtain for many practical problems because of the complexities of irregular boundary conditions, cutouts etc.

4.4.2 Types of Finite Element Models

In the finite element method, a certain internal behavior of the elements is selected which satisfies some, but not all, of the conditions defined by Eqs. (4.30) through (4.34). Three types of finite elements and the conditions they satisfy may be described as follows:

- (1) A compatible element model satisfies:
 - (a) Internal compatibility, Eq. (4.32)
 - (b) Boundary continuity of displacements, Eq. (4.33), at both element and external boundaries
 - (c) Stress-strain law, Eq. (4.31)
- (2) An equilibrium element model satisfies:
 - (a) Internal equilibrium, Eq. (4.30)
 - (b) Boundary continuity of forces, Eq. (4.34) at both element and external boundaries
 - (c) Stress-strain law, Eqs. (4.31)
- (3) A mixed model which satisfies partially some of the conditions under (1) and (2).

In general, investigators have chosen formulations based on the use of compatible elements because they have yielded excellent results and because their properties are more easily derived than those of equilibrium elements. Sometimes difficulties are also encountered in developing fully compatible finite elements. In these cases discontinuities of certain displacement quantities which have a secondary effect are permitted at the element interfaces and good results are still achieved.

4.4.3 Nodal Point Displacements and Resulting Displacement Patterns

For plane stress in the present investigation, a finite element is selected in which a physical interpretation may be utilized to visualize the nodal point displacements and the resulting displacement patterns over the element. The nodal points are taken at the four corners of the rectangular element and each node is assumed to have three degrees of freedom, Fig. 18.

Note that a different sign convention from that shown in Fig. 15 is adopted in Fig. 18 for purposes of the present derivation. The displacements at a typical node i are:

(1) A displacement in the x direction, u_i (4.35a)

(2) A displacement in the y direction, v_i (4.35b)

(3) An averaged rotation about the z -axis, θ_{zi} defined by

$$\theta_{zi} = \frac{1}{2} \left[\left(\frac{\partial v}{\partial x} \right)_i - \left(\frac{\partial u}{\partial y} \right)_i \right] \quad (4.35c)$$

The corresponding nodal point forces are forces in the x and y directions, F_{xi} and F_{yi} , and a moment about the z -axis, M_{zi} . The inclusion of the rotation about the z -axis, which has not been used by other investigators, gives a complete set of physical displacements corresponding to those found in the usual structural analysis problem of a rigid frame loaded in its own plane. It also permits a simple and accurate coupling with the plate bending element, to be described later, for use in the solution of the prismatic folded plate problem.

The displacement pattern over the surface of the element due to each nodal point displacement may be built up from an assumed variation defined by a function along one edge of the rectangular element which is damped to a zero value at the far edge by a damping function. The functions used for this purpose are shown in Fig. 19 and consist of a linear function; a beam rotation function which has the deflected shape of a beam subjected to a unit rotation at one end and fixed at the far end; and a beam displacement function which has the deflected shape of a beam subjected to a unit displacement at one end with both ends fixed against rotation. A similar set of functions in the x and y directions is required for all four nodal points and a complete list of these is as follows:

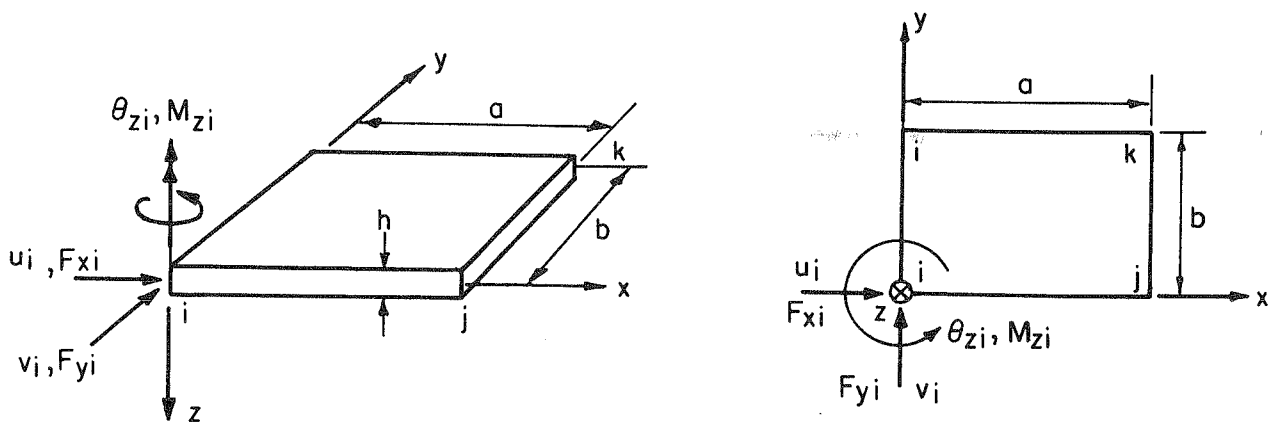


FIG. 18 NOTATION AND POSITIVE DIRECTIONS FOR DISPLACEMENTS AND FORCES AT A TYPICAL NODAL POINT

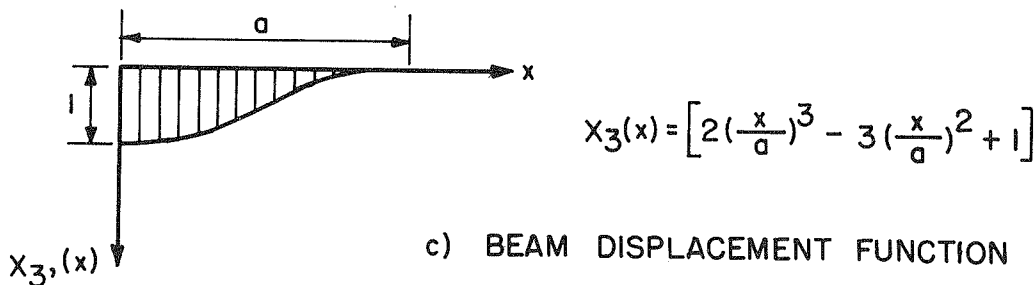
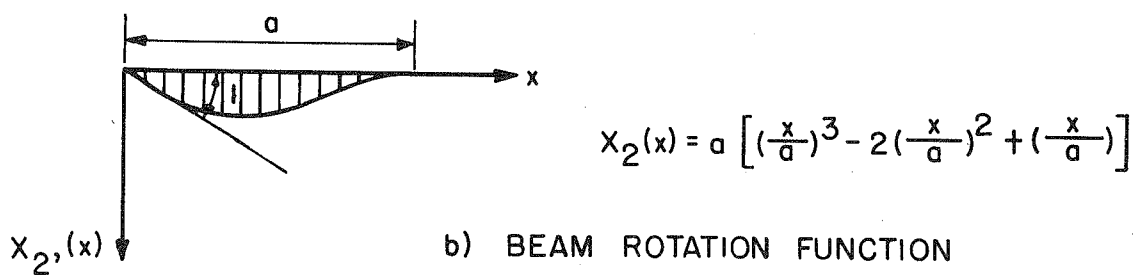
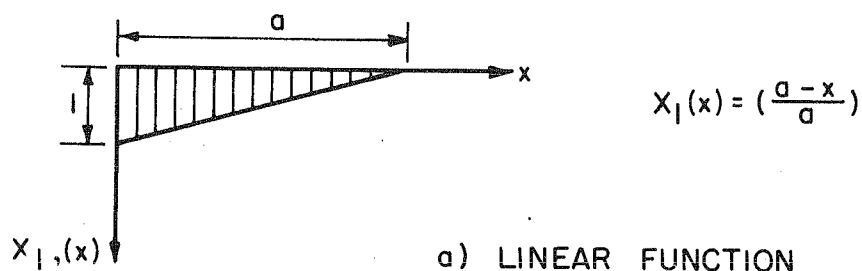


FIG. 19 DISPLACEMENT AND DAMPING FUNCTIONS.

(1) Linear function

$$\left. \begin{aligned} X_1(x) &= \left(\frac{a-x}{a}\right) \\ X_1(a-x) &= \left(\frac{x}{a}\right) \\ Y_1(y) &= \left(\frac{b-y}{b}\right) \\ Y_1(b-y) &= \left(\frac{y}{b}\right) \end{aligned} \right\} \quad (4.36)$$

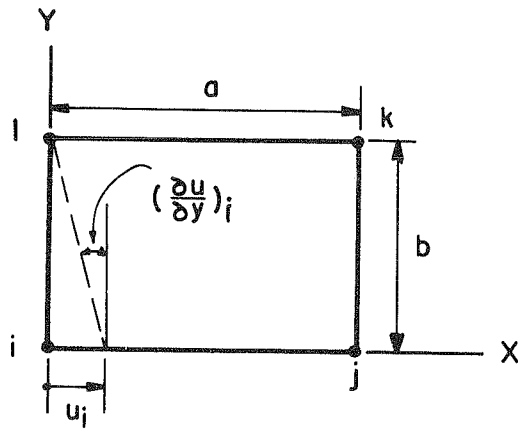
(2) Beam rotation function

$$\left. \begin{aligned} X_2(x) &= a \left[\left(\frac{x}{a}\right)^3 - 2\left(\frac{x}{a}\right)^2 + \left(\frac{x}{a}\right) \right] \\ X_2(a-x) &= a \left[-\left(\frac{x}{a}\right)^3 + \left(\frac{x}{a}\right)^2 \right] \\ Y_2(y) &= b \left[\left(\frac{y}{b}\right)^3 - 2\left(\frac{y}{b}\right)^2 + \left(\frac{y}{b}\right) \right] \\ Y_2(b-y) &= b \left[-\left(\frac{y}{b}\right)^3 + \left(\frac{y}{b}\right)^2 \right] \end{aligned} \right\} \quad (4.37)$$

(3) Beam displacement function

$$\left. \begin{aligned} X_3(x) &= \left[2\left(\frac{x}{a}\right)^3 - 3\left(\frac{x}{a}\right)^2 + 1 \right] \\ X_3(a-x) &= \left[-2\left(\frac{x}{a}\right)^3 + 3\left(\frac{x}{a}\right)^2 \right] \\ Y_3(y) &= \left[2\left(\frac{y}{b}\right)^3 - 3\left(\frac{y}{b}\right)^2 + 1 \right] \\ Y_3(b-y) &= \left[-2\left(\frac{y}{b}\right)^3 + 3\left(\frac{y}{b}\right)^2 \right] \end{aligned} \right\} \quad (4.38)$$

The first step in the development of the finite element stiffness may now be initiated by specifying the displacements u and v in terms of the above functions. The displacement patterns assumed for nodal point displacements u_i , v_i , and θ_{zi} are shown graphically in Figs. 20, 21, and 22.



a) PLAN VIEW

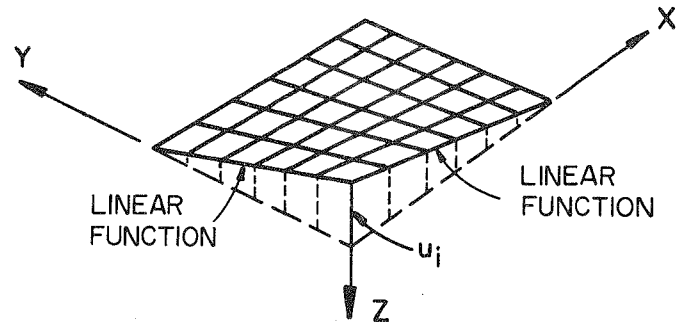
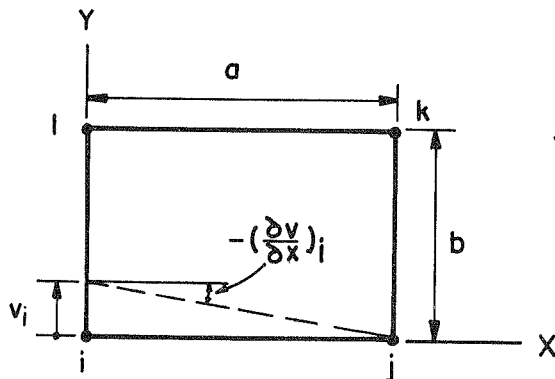
b) VARIATION OF u OVER SURFACE

FIG. 20 DISPLACEMENT PATTERN FOR NODAL POINT DISPLACEMENT u_i



a) PLAN VIEW

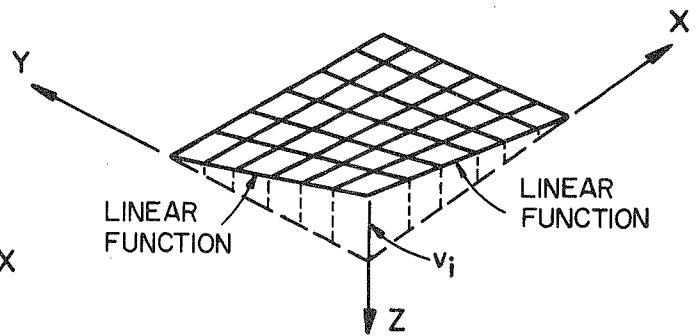
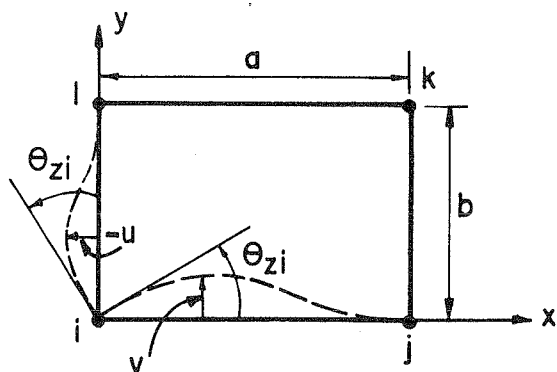
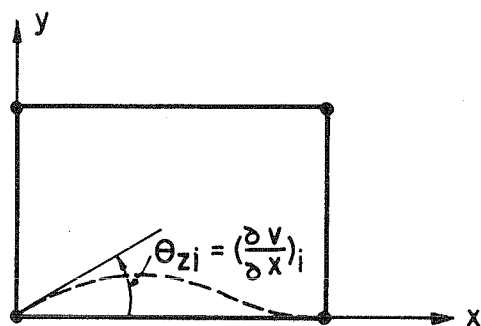
b) VARIATION OF v OVER SURFACE

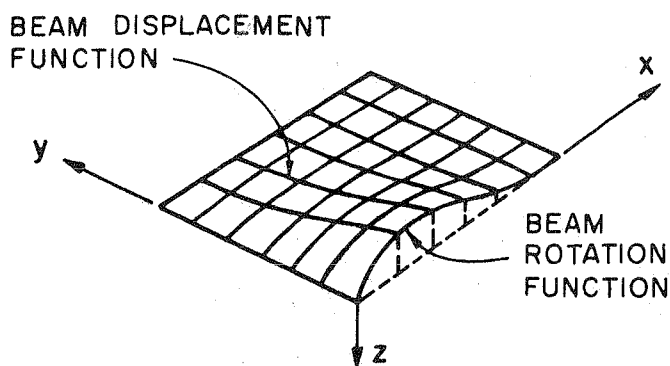
FIG. 21 DISPLACEMENT PATTERN FOR NODAL POINT DISPLACEMENT v_i



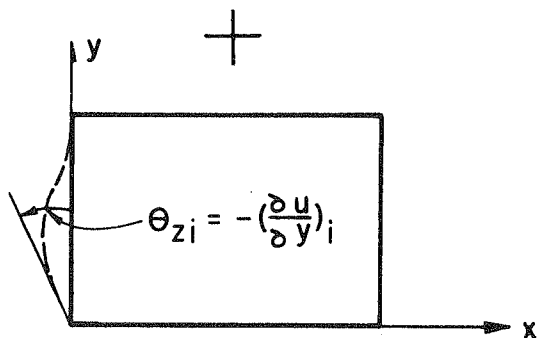
a) θ_{zi} PRODUCES u AND v DISPLACEMENTS



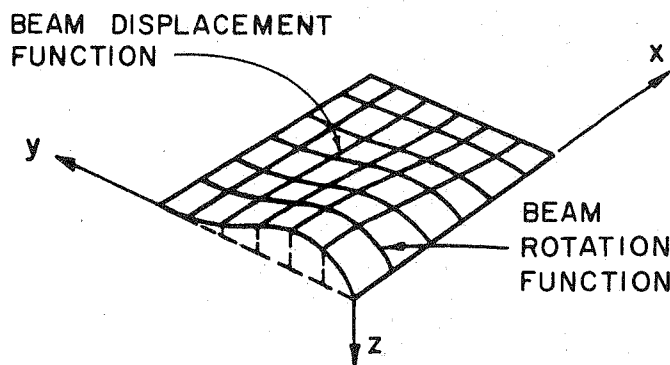
b) PLAN VIEW OF v DISPLACEMENT



c) VARIATION OF v OVER SURFACE



d) PLAN VIEW OF u DISPLACEMENT



e) VARIATION OF u OVER SURFACE

FIG.22 DISPLACEMENT PATTERN FOR NODAL POINT DISPLACEMENT

A similar set of displacement patterns exist for nodal points j , k , and l giving a total of 12 displacement patterns to be superposed. Note from Fig. 22 that the nodal point displacement θ_{zi} produces both u and v displacements within the element and that the displacement patterns corresponding to u_i and v_i shown in Figs. 20 and 21 will also contribute to the total θ_{zi} .

Equation (4.10) may now be written out totally in the following form in terms of 12 generalized coordinates α_1 to α_{12} .

$$\begin{array}{rcl}
 & \begin{array}{c} \text{Nodal Point Translation} \\ \text{in x-direction} \end{array} & \begin{array}{c} \text{Nodal Point Rotation} \\ \text{about z-axis} \end{array} \\
 u(x,y) = & \begin{array}{l} \alpha_1 X_1(x) Y_1(y) \\ +\alpha_4 X_1(a-x) Y_1(y) \\ +\alpha_7 X_1(a-x) Y_1(b-y) \\ +\alpha_{10} X_1(x) Y_1(b-y) \end{array} & \begin{array}{l} -\alpha_3 X_3(x) Y_2(y) \\ -\alpha_6 X_3(a-x) Y_2(y) \\ +\alpha_9 X_3(a-x) Y_2(b-y) \\ +\alpha_{12} X_3(x) Y_2(b-y) \end{array} & \begin{array}{l} \text{Nodal Point } i \\ \text{Nodal Point } j \\ \text{Nodal Point } k \\ \text{Nodal Point } l \end{array} \\
 & & & (4.39)
 \end{array}$$

$$\begin{array}{rcl}
 & \begin{array}{c} \text{Nodal Point Translation} \\ \text{in y-direction} \end{array} & \begin{array}{c} \text{Nodal Point Rotation} \\ \text{about z-axis} \end{array} \\
 v(x,y) = & \begin{array}{l} \alpha_2 X_1(x) Y_1(y) \\ +\alpha_5 X_1(a-x) Y_1(y) \\ +\alpha_8 X_1(a-x) Y_1(b-y) \\ +\alpha_{11} X_1(x) Y_1(b-y) \end{array} & \begin{array}{l} +\alpha_3 X_2(x) Y_3(y) \\ -\alpha_6 X_2(a-x) Y_3(y) \\ -\alpha_9 X_2(a-x) Y_3(b-y) \\ +\alpha_{12} X_2(x) Y_3(b-y) \end{array} & \begin{array}{l} \text{Nodal Point } i \\ \text{Nodal Point } j \\ \text{Nodal Point } k \\ \text{Nodal Point } l \end{array} \\
 & & & (4.40)
 \end{array}$$

When Eqs. (4.36), (4.37), and (4.38) are substituted into Eqs. (4.39) and (4.40) a polynomial expression is obtained for u and v in terms of x , y and the generalized coordinates α_1 to α_{12} .

A comment should be made regarding the compatibility properties of the nodal point displacements and the displacement functions chosen for the finite element. Consider a typical nodal point i joining four adjacent

rectangular elements, Fig. 23. Restating the definitions of the shearing strain γ_i and the nodal point displacement θ_{zi} defined earlier.

$$\gamma_i = \left(\frac{\partial v}{\partial x} \right)_i + \left(\frac{\partial u}{\partial y} \right)_i \quad (4.32c)$$

$$\theta_{zi} = \frac{1}{2} \left[\left(\frac{\partial v}{\partial x} \right)_i - \left(\frac{\partial u}{\partial y} \right)_i \right] \quad (4.35c)$$

it is apparent that even though the averaged rotations θ_{zi} for each of the four elements joined at nodal point i are made to have the same value, there will be an angular discontinuity between the common edges of adjacent elements which is proportional to the difference in shear strain existing in the elements joined at nodal point i . Four possibilities are illustrated in Fig. 23. In Fig. 23a, it is assumed that the shear distortion in all four elements is zero, in which case full compatibility is achieved. In Fig. 23b, it is assumed that the shear distortion in all four elements is the same, in which case full compatibility is again achieved. In Fig. 23c, it is assumed that only equal pure shear distortions of opposite signs occur in adjacent elements. For this case $\theta_{zi} = 0$ for all four elements, but angular discontinuities will exist between adjacent elements. Finally in Fig. 23d, in the general case where rotation plus a different shear distortion exist in the four elements, angular discontinuities occur even though θ_{zi} is the same for all four elements. From the results of numerical studies it has been found that effect of these discontinuities is very small and that the element chosen above for the present investigation gives more accurate results for a given mesh size than does a fully compatible element used by other investigators, which includes only the two degrees of freedom u_i and v_i at each nodal point shown in Figs. 20 and 21.

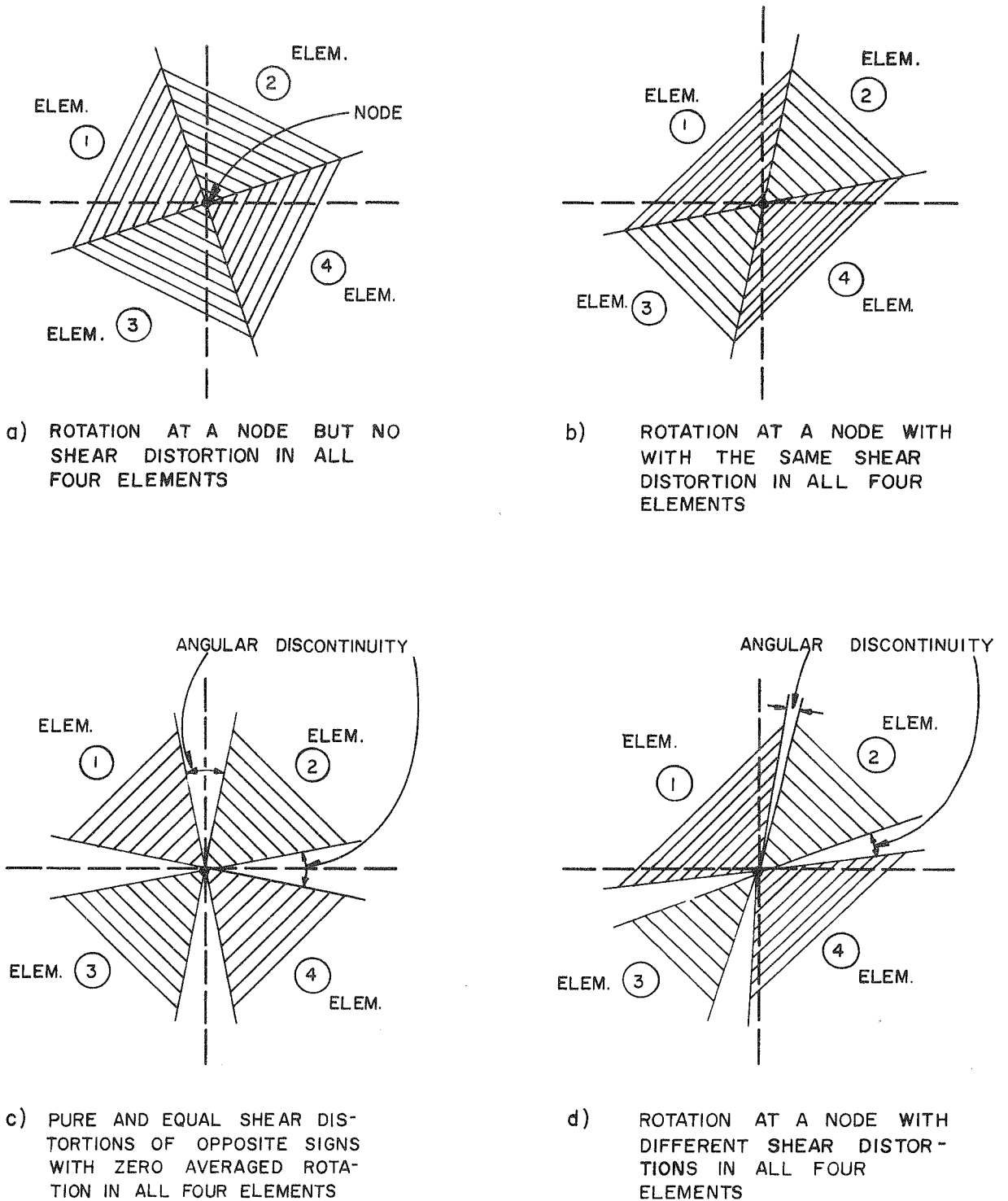


FIG. 23 ROTATIONS AND SHEAR DISTORTIONS IN FOUR ELEMENTS MEETING AT A TYPICAL NODAL POINT

4.4.4 Derivation of Element Stiffness for Plane Stress

The necessary steps required to derive the element stiffness matrix for plane stress k_p relating the nodal point forces S_p to nodal point forces v_p , Fig. 18, have been given in Section 4.3. Rewriting Eqs. (4.28), (4.29), and (4.20) specifically for the plane stress problem.

$$\begin{matrix} \{S_p\} \\ 12 \times 1 \end{matrix} = \begin{matrix} [k_p] \\ 12 \times 12 \end{matrix} \begin{matrix} \{V_p\} \\ 12 \times 1 \end{matrix} \quad (4.41)$$

where

$$k_p = [A_p^{-1}]^T \tilde{k}_p [A_p^{-1}] \quad (4.42)$$

and

$$\tilde{k}_p = \int_V B_p^T D_p B_p dV \quad (4.43)$$

The A_p matrix relates the nodal point displacements V_p to the generalized coordinates α_p .

$$\begin{matrix} \{V_p\} \\ 12 \times 1 \end{matrix} = \begin{matrix} [A_p] \\ 12 \times 12 \end{matrix} \begin{matrix} \{\alpha_p\} \\ 12 \times 1 \end{matrix} \quad (4.44)$$

The elements of the A_p matrix may be found from the definitions of the nodal point displacements, Eqs. (4.35), and the displacement functions of Eqs. (4.39) and (4.40). When the appropriate differentiations and substitutions of the nodal point coordinates are made, the following result is obtained.

$$\left\{ \begin{array}{c} u_i \\ v_i \\ \theta_{zi} \\ u_j \\ v_j \\ \theta_{zj} \\ u_k \\ v_k \\ \theta_{zk} \\ u_l \\ v_l \\ \theta_{zl} \end{array} \right\} = \begin{bmatrix} 1 & 0 & 0 & 0 & 0 & 0 & 0 & 0 & 0 & 0 & 0 & 0 \\ 0 & 1 & 0 & 0 & 0 & 0 & 0 & 0 & 0 & 0 & 0 & 0 \\ \frac{1}{2b} & -\frac{1}{2a} & 1 & 0 & \frac{1}{2a} & 0 & 0 & 0 & 0 & -\frac{1}{2b} & 0 & 0 \\ 0 & 0 & 0 & 1 & 0 & 0 & 0 & 0 & 0 & 0 & 0 & 0 \\ 0 & 0 & 0 & 0 & 1 & 0 & 0 & 0 & 0 & 0 & 0 & 0 \\ 0 & -\frac{1}{2a} & 0 & \frac{1}{2b} & \frac{1}{2a} & 1 & -\frac{1}{2b} & 0 & 0 & 0 & 0 & 0 \\ 0 & 0 & 0 & 0 & 0 & 0 & 1 & 0 & 0 & 0 & 0 & 0 \\ 0 & 0 & 0 & 0 & 0 & 0 & 0 & 1 & 0 & 0 & 0 & 0 \\ 0 & 0 & 0 & \frac{1}{2b} & 0 & 0 & -\frac{1}{2b} & \frac{1}{2a} & 1 & 0 & -\frac{1}{2a} & 0 \\ 0 & 0 & 0 & 0 & 0 & 0 & 0 & 0 & 0 & 1 & 0 & 0 \\ 0 & 0 & 0 & 0 & 0 & 0 & 0 & 0 & 0 & 0 & 1 & 0 \\ \frac{1}{2b} & 0 & 0 & 0 & 0 & 0 & 0 & \frac{1}{2a} & 0 & -\frac{1}{2b} & -\frac{1}{2a} & 1 \end{bmatrix} \left\{ \begin{array}{c} \alpha_1 \\ \alpha_2 \\ \alpha_3 \\ \alpha_4 \\ \alpha_5 \\ \alpha_6 \\ \alpha_7 \\ \alpha_8 \\ \alpha_9 \\ \alpha_{10} \\ \alpha_{11} \\ \alpha_{12} \end{array} \right\} \quad (4.44a)$$

The B_p matrix in Eq. (4.43) relates the internal strains ϵ in the element to the generalized coordinates α_p .

$$\left\{ \begin{array}{c} \epsilon(x,y) \\ \epsilon_x \\ \epsilon_y \\ \gamma_{xy} \end{array} \right\} = \begin{bmatrix} B_p(x,y) \\ 3 \times 12 \end{bmatrix} \left\{ \begin{array}{c} \alpha_p \\ 12 \times 1 \end{array} \right\} \quad (4.45)$$

The elements of the B_p matrix may be obtained by appropriate differentiation of Eqs. (4.39) and (4.40) and by noting from Eqs. (4.32) that

$$\left\{ \begin{array}{c} \epsilon_x \\ \epsilon_y \\ \gamma_{xy} \end{array} \right\} = \left\{ \begin{array}{c} \frac{\partial u}{\partial x} \\ \frac{\partial v}{\partial y} \\ \frac{\partial u}{\partial y} + \frac{\partial v}{\partial x} \end{array} \right\} \quad (4.45a)$$

Performing these differentiations, the following results are obtained for the elements of the 3×12 B_p matrix. A prime indicates a differentiation of that function with respect to its variable.

$$\begin{array}{ll}
 B_p(1,1) = X_1'(x)Y_1(y) & B_p(2,7) = 0 \\
 B_p(1,2) = 0 & B_p(2,8) = X_1(a-x)Y_1'(b-y) \\
 B_p(1,3) = -X_1'(x)Y_2(y) & B_p(2,9) = -X_2(a-x)Y_3'(b-y) \\
 B_p(1,4) = X_1'(a-x)Y_1(y) & B_p(2,10) = 0 \\
 B_p(1,5) = 0 & B_p(2,11) = X_1(x)Y_1'(b-y) \\
 B_p(1,6) = X_3'(a-x)Y_2(y) & B_p(2,12) = X_2(x)Y_3'(b-y) \\
 B_p(1,7) = X_1'(a-x)Y_1(b-y) & B_p(3,1) = X_1(x)Y_1'(y) \\
 B_p(1,8) = 0 & B_p(3,2) = X_1'(x)Y_1(y) \\
 B_p(1,9) = X_3'(a-x)Y_2(b-y) & B_p(3,3) = -X_3(x)Y_2'(y) + X_2'(x)Y_3(y) \\
 B_p(1,10) = X_1'(x)Y_1(b-y) & B_p(3,4) = X_1(a-x)Y_1'(y) \\
 B_p(1,11) = 0 & B_p(3,5) = X_1'(a-x)Y_1(y) \\
 B_p(1,12) = X_3'(x)Y_2(b-y) & B_p(3,6) = -X_3(a-x)Y_2'(y) - X_2'(a-x)Y_3(y) \\
 B_p(2,1) = 0 & B_p(3,7) = X_1(a-x)Y_1'(b-y) \\
 B_p(2,2) = X_1(x)Y_1'(y) & B_p(3,8) = X_1'(a-x)Y_1(b-y) \\
 B_p(2,3) = X_2(x)Y_3'(y) & B_p(3,9) = X_3(a-x)Y_2'(b-y) - X_2'(a-x)Y_3(b-y) \\
 B_p(2,4) = 0 & B_p(3,10) = X_1(x)Y_1'(b-y) \\
 B_p(2,5) = X_1(a-x)Y_1'(y) & B_p(3,11) = X_1'(x)Y_1(b-y) \\
 B_p(2,6) = -X_2(a-x)Y_3'(y) & B_p(3,12) = X_3(x)Y_2'(b-y) + X_2'(x)Y_3(b-y)
 \end{array}$$

Internal stresses may be expressed in terms of internal strains to form the D_p matrix.

$$\begin{array}{ccc}
 \{\sigma(x,y)\} & = & [D_p] \{\epsilon(x,y)\} \\
 3 \times 1 & & 3 \times 3 \quad 3 \times 1
 \end{array} \tag{4.46}$$

$$\begin{Bmatrix} N_x \\ N_y \\ N_{xy} \end{Bmatrix} = \begin{Bmatrix} \sigma_x h \\ \sigma_y h \\ \tau_{xy} h \end{Bmatrix} = \frac{Eh}{(1-\nu^2)} \begin{bmatrix} 1 & \nu & 0 \\ \nu & 1 & 0 \\ 0 & 0 & (1-\nu)/2 \end{bmatrix} \begin{Bmatrix} \epsilon_x \\ \epsilon_y \\ \gamma_{xy} \end{Bmatrix} \quad (4.46a)$$

in which h is the plate thickness.

With the elements of the A_p , B_p , and D_p matrices now defined in Eqs. (4.44), (4.45) and (4.46), the element stiffness matrix k_p in Eq. (4.41) can now be determined.

$$k_p = [A_p^{-1}]^T \left[\int_0^b \int_0^a B_p^T D_p B_p dx dy \right] [A_p^{-1}] \quad (4.47)$$

and

$$\{S_p\} = [k_p] \{v_p\} = \left(\frac{Eh}{1-\nu^2} \right) [KP] \{v_p\} \quad (4.48)$$

in which KP is a 12×12 matrix of coefficients obtained by performing the tedious integration and matrix multiplication indicated in Eq. (4.47). The sequence of nodal point forces and corresponding displacements in Eq. (4.48) is as follows:

$$\begin{Bmatrix} F_{xi} \\ F_{yi} \\ M_{zi} \\ F_{xj} \\ F_{yj} \\ M_{zj} \\ F_{xk} \\ F_{yk} \\ M_{zk} \\ F_{xl} \\ F_{yl} \\ M_{zl} \end{Bmatrix} = \left(\frac{Eh}{1-\nu^2} \right) \begin{bmatrix} 12 \times 12 \text{ KP matrix} \end{bmatrix} \begin{Bmatrix} u_i \\ v_i \\ \theta_{zi} \\ u_j \\ v_j \\ \theta_{zj} \\ u_k \\ v_k \\ \theta_{zk} \\ u_l \\ v_l \\ \theta_{zl} \end{Bmatrix} \quad (4.48a)$$

The expressions derived for the elements of the symmetrical KP matrix by Eq. (4.47), are as follows, using the notation and sign convention given in Fig. 18:

$$KP(1,1) = \frac{123}{350} \frac{b}{a} + \frac{41}{175} \frac{a}{b} (1-\nu)$$

$$KP(1,2) = \frac{9}{80} + \frac{11}{80} \nu$$

$$KP(1,3) = -\frac{9}{175} \frac{b^2}{a} - \frac{393}{8400} a + \frac{743}{8400} \nu a$$

$$KP(1,4) = -\frac{123}{350} \frac{b}{a} + \frac{57}{1400} \frac{a}{b} (1-\nu)$$

$$KP(1,5) = -\frac{9}{80} + \frac{29}{80} \nu$$

$$KP(1,6) = \frac{9}{175} \frac{b^2}{a} + \frac{183}{8400} a - \frac{533}{8400} \nu a$$

$$KP(1,7) = -\frac{26}{175} \frac{b}{a} - \frac{57}{1400} \frac{a}{b} (1-\nu)$$

$$KP(1,8) = -KP(1,2)$$

$$KP(1,9) = -\frac{67}{2100} \frac{b^2}{a} + \frac{183}{8400} a + \frac{167}{8400} \nu a$$

$$KP(1,10) = \frac{26}{175} \frac{b}{a} - \frac{41}{175} \frac{a}{b} (1-\nu)$$

$$KP(1,11) = -KP(1,5)$$

$$KP(1,12) = \frac{67}{2100} \frac{b^2}{a} - \frac{393}{8400} a + \frac{43}{8400} \nu a$$

$$KP(2,2) = \frac{123}{350} \frac{a}{b} + \frac{41}{175} \frac{b}{a} (1-\nu)$$

$$KP(2,3) = \frac{9}{175} \frac{a^2}{b} + \frac{393}{8400} b - \frac{743}{8400} \nu b$$

$$KP(2,4) = -KP(1,5)$$

$$KP(2,5) = \frac{26}{175} \frac{a}{b} - \frac{41}{175} \frac{b}{a} (1-\nu)$$

$$KP(2,6) = -\frac{67}{2100} \frac{a^2}{b} + \frac{393}{8400} b - \frac{43}{8400} \nu b$$

$$KP(2,7) = KP(1,8)$$

$$KP(2,8) = -\frac{26}{175} \frac{a}{b} - \frac{57}{1400} \frac{b}{a} (1-\nu)$$

$$KP(2,9) = \frac{67}{2100} \frac{a^2}{b} - \frac{183}{8400} b - \frac{167}{8400} \nu b$$

$$KP(2,10) = KP(1,5)$$

$$KP(2,11) = -\frac{123}{350} \frac{a}{b} + \frac{57}{1400} \frac{b}{a} (1-\nu)$$

$$KP(2,12) = -\frac{9}{175} \frac{a^2}{b} - \frac{183}{8400} b + \frac{533}{8400} \nu b$$

$$KP(3,3) = \frac{2}{175} \left(\frac{a^3}{b} + \frac{b^3}{a} \right) + \frac{83}{2100} ab - \frac{5}{84} \nu ab$$

$$KP(3,4) = KP(1,6)$$

$$KP(3,5) = -KP(2,6)$$

$$KP(3,6) = -\frac{2}{175} \frac{b^3}{a} - \frac{3}{350} \frac{a^3}{b} + \frac{13}{1050} ab + \frac{8}{1050} \nu ab$$

$$KP(3,7) = -KP(1,9)$$

$$KP(3,8) = -KP(2,9)$$

$$KP(3,9) = \frac{3}{350} \left(\frac{b^3}{a} + \frac{a^3}{b} \right) - \frac{1}{70} ab - \frac{6}{1050} \nu ab$$

$$KP(3,10) = -KP(1,12)$$

$$KP(3,11) = KP(2,12)$$

$$KP(3,12) = -\frac{3}{350} \frac{b^3}{a} - \frac{2}{175} \frac{a^3}{b} + \frac{13}{1050} ab + \frac{8}{1050} \nu ab$$

$$\begin{array}{ll}
\text{KP}(4,4) = \text{KP}(1,1) & \text{KP}(6,12) = \text{KP}(3,9) \\
\text{KP}(4,5) = -\text{KP}(1,2) & \text{KP}(7,7) = \text{KP}(1,1) \\
\text{KP}(4,6) = \text{KP}(1,3) & \text{KP}(7,8) = \text{KP}(1,2) \\
\text{KP}(4,7) = \text{KP}(1,10) & \text{KP}(7,9) = -\text{KP}(1,3) \\
\text{KP}(4,8) = \text{KP}(1,5) & \text{KP}(7,10) = \text{KP}(1,4) \\
\text{KP}(4,9) = \text{KP}(1,12) & \text{KP}(7,11) = \text{KP}(1,5) \\
\text{KP}(4,10) = \text{KP}(1,7) & \text{KP}(7,12) = -\text{KP}(1,6) \\
\text{KP}(4,11) = \text{KP}(1,2) & \text{KP}(8,8) = \text{KP}(2,2) \\
\text{KP}(4,12) = \text{KP}(1,9) & \text{KP}(8,9) = \text{KP}(5,6) \\
\text{KP}(5,5) = \text{KP}(2,2) & \text{KP}(8,10) = \text{KP}(2,4) \\
\text{KP}(5,6) = -\text{KP}(2,3) & \text{KP}(8,11) = \text{KP}(2,5) \\
\text{KP}(5,7) = \text{KP}(2,4) & \text{KP}(8,12) = \text{KP}(3,5) \\
\text{KP}(5,8) = \text{KP}(2,11) & \text{KP}(9,9) = \text{KP}(3,3) \\
\text{KP}(5,9) = -\text{KP}(2,12) & \text{KP}(9,10) = -\text{KP}(3,4) \\
\text{KP}(5,10) = \text{KP}(1,2) & \text{KP}(9,11) = \text{KP}(2,6) \\
\text{KP}(5,11) = \text{KP}(2,8) & \text{KP}(9,12) = \text{KP}(3,6) \\
\text{KP}(5,12) = \text{KP}(3,8) & \text{KP}(10,10) = \text{KP}(1,1) \\
\text{KP}(6,6) = \text{KP}(3,3) & \text{KP}(10,11) = -\text{KP}(1,2) \\
\text{KP}(6,7) = \text{KP}(3,10) & \text{KP}(10,12) = -\text{KP}(1,3) \\
\text{KP}(6,8) = -\text{KP}(2,12) & \text{KP}(11,11) = \text{KP}(2,2) \\
\text{KP}(6,9) = \text{KP}(3,12) & \text{KP}(11,12) = \text{KP}(2,3) \\
\text{KP}(6,10) = \text{KP}(3,7) & \text{KP}(12,12) = \text{KP}(3,3) \\
\text{KP}(6,11) = \text{KP}(2,9) &
\end{array}$$

As a check on the above derived expressions for KP they were used together with Eq. (4.48a) to perform equilibrium checks on the element by taking $\sum F_x$, $\sum F_y$ and $\sum M_z$ of the nodal point forces produced by unit values of each of the nodal point displacements. In all cases these summations equalled zero providing a check on the derivations.

4.5 Element Stiffness Matrix for Slab Action - Plate Bending Analysis

4.5.1 Elasticity Equations for the Plate Bending Problem

For a plate bending problem, an exact solution by the classical thin plate theory should satisfy the equations given below. The standard notation, sign convention and direction of coordinate axes, based on Timoshenko and Woinowsky-Krieger [19], are shown in Fig. 24.

(1) Equilibrium requirements:

$$\frac{\partial M_{xy}}{\partial x} + \frac{\partial M_y}{\partial y} + Q_y = 0 \quad (4.49a)$$

$$\frac{\partial M_{yx}}{\partial y} + \frac{\partial M_x}{\partial x} + Q_x = 0 \quad (4.49b)$$

$$\frac{\partial Q_x}{\partial x} + \frac{\partial Q_y}{\partial y} + Z = 0 \quad (4.49c)$$

(2) Displacement - curvature conditions:

$$\kappa_x = \frac{1}{\rho_x} = \frac{\partial^2 w}{\partial x^2} \quad (4.50a)$$

$$\kappa_y = \frac{1}{\rho_y} = \frac{\partial^2 w}{\partial y^2} \quad (4.50b)$$

$$\kappa_{xy} = \frac{1}{\rho_{xy}} = \frac{\partial^2 w}{\partial x \partial y} \quad (4.50c)$$

from which it follows that:

$$\frac{\partial^2 \kappa_x}{\partial y^2} - \frac{2\partial^2 \kappa_{xy}}{\partial x \partial y} + \frac{\partial^2 \kappa_y}{\partial x^2} = 0 \quad (4.50d)$$

(3) Moment - curvature relationships:

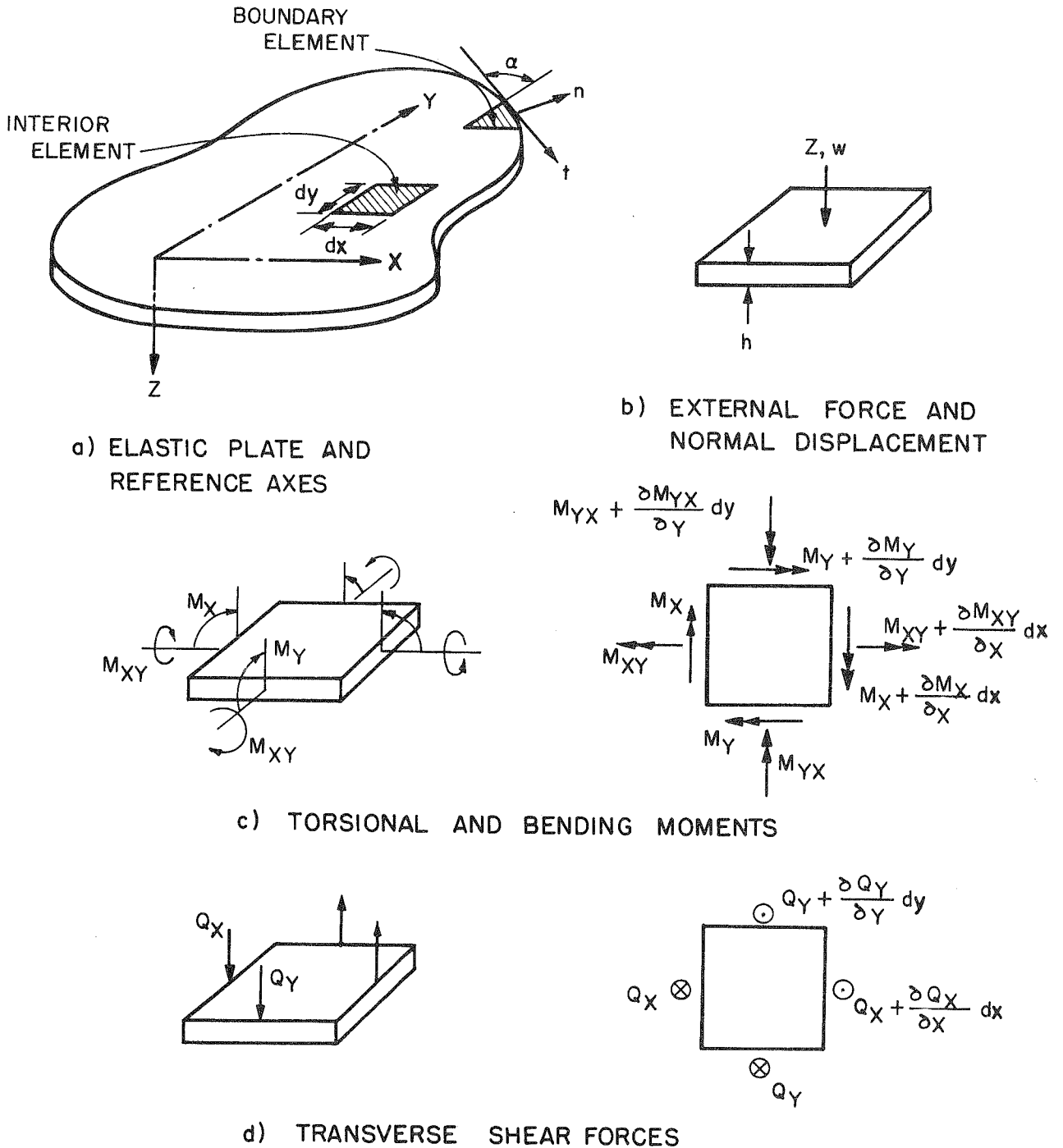


FIG. 24 POSITIVE DIRECTIONS FOR COORDINATE AXES, EXTERNAL FORCES, DISPLACEMENTS, AND INTERNAL MOMENTS AND FORCES.

$$M_x = D \left[\frac{1}{\rho_x} + \frac{\nu}{\rho_y} \right] \quad (4.51a)$$

$$M_y = D \left[\frac{1}{\rho_y} + \frac{\nu}{\rho_x} \right] \quad (4.51b)$$

$$M_{xy} = D (1-\nu) \left[\frac{1}{\rho_{xy}} \right] \quad (4.51c)$$

in which

$$D = \frac{Eh^3}{12(1-\nu^2)} \quad (4.51d)$$

(4) Boundary conditions:

(a) Displacements

$$w \text{ (internal)} = \bar{w} \text{ (external)} \quad (4.52a)$$

$$\frac{\partial w}{\partial n} \text{ (internal)} = \frac{\partial \bar{w}}{\partial n} \text{ (external)} \quad (4.52b)$$

(b) Moments and forces:

$$M_n \text{ (internal)} = \bar{M}_n \text{ (external)} \quad (4.53a)$$

$$M_{nt} \text{ (internal)} = \bar{M}_{nt} \text{ (external)} \quad (4.53b)$$

$$Q_n \text{ (internal)} = \bar{Q}_n \text{ (external)} \quad (4.53c)$$

The three conditions expressed by Eqs. (4.53) are reduced to two sufficient conditions by using Kirchoff's relationship.

$$V_n = Q_n - \frac{\partial M_{nt}}{\partial t} \quad (4.53d)$$

A solution which satisfies Eqs. (4.49) through (4.53) over the entire domain of the problem may be termed an exact solution within the assumptions of the classical thin plate theory.

4.5.2 Nodal Point Displacements and Resulting Displacement Patterns

For plate bending, a finite element model is selected which closely approximates the properties of a compatible element model (see Section 4.4.2).

The nodal points are taken at the four corners of the rectangular element and each node is assumed to have three degrees of freedom (Fig. 25). Note that a different sign convention from that shown in Fig. 15 is adopted in Fig. 25 for purposes of the present derivation. The displacements at a typical node i are:

- (1) A rotation about the x -axis, θ_{xi} , defined by:

$$\theta_{xi} = \left(\frac{\partial w}{\partial y} \right)_i \quad (4.54a)$$

- (2) A rotation about the y -axis, θ_{yi} , defined by:

$$\theta_{yi} = \left(\frac{\partial w}{\partial x} \right)_i \quad (4.54b)$$

- (3) A displacement in the z -direction, w_i (4.54c)

The corresponding nodal point forces are moments about x and y axes, M_{xi} and M_{yi} , and a force in the z -direction, F_{zi} .

The displacement pattern over the surface of the element due to each nodal point displacement may be built up from an assumed variation defined by a function along one edge of the rectangular element which is damped to a zero value at the far edge by a damping function. The functions to be used are the same as those used in the derivation of the element stiffness matrix for membrane action. These are given in Eqs. (4.36), (4.37), and (4.38) and are shown in Fig. 19.

The first step in the development of the finite element stiffness may now be initiated by specifying the displacement w in terms of the above

functions. The displacement patterns assumed for nodal point displacements θ_{xi} , θ_{yi} , and w_i are shown graphically in Figs. 26, 27, and 28. A similar set of displacement patterns exists for nodal points j , k , and l giving a total of 12 displacement patterns to be superposed. Note that the displacement pattern corresponding to w_i shown in Fig. 28 is a pure twist pattern and also that it will contribute to the total θ_{xi} and θ_{yi} displacements.

Equation (4.10) may now be written out totally in the following form in terms of the generalized coordinates α_{13} to α_{24} .

| <u>Nodal Point Rotation about y-axis</u> | <u>Nodal Point Rotation about x-axis</u> | <u>Nodal Point Translation in z-direction</u> | |
|--|--|---|-------------------|
| $w(x,y) = \alpha_{13} X_2(x) Y_3(y)$ | $+ \alpha_{14} X_3(x) Y_2(y)$ | $+ \alpha_{15} X_1(x) Y_1(y)$ | <u>Nodal Pt i</u> |
| $- \alpha_{16} X_2(a-x) Y_3(y)$ | $+ \alpha_{17} X_3(a-x) Y_2(y)$ | $+ \alpha_{18} X_1(a-x) Y_1(y)$ | <u>Nodal Pt j</u> |
| $- \alpha_{19} X_2(a-x) Y_3(b-y)$ | $- \alpha_{20} X_3(a-x) Y_2(b-y)$ | $+ \alpha_{21} X_1(a-x) Y_1(b-y)$ | <u>Nodal Pt k</u> |
| $+ \alpha_{22} X_2(x) Y_3(b-y)$ | $- \alpha_{23} X_3(x) Y_2(b-y)$ | $+ \alpha_{24} X_1(x) Y_1(b-y)$ | <u>Nodal Pt l</u> |
| | | | (4.55) |

When Eqs. (4.36), (4.37), and (4.38) are substituted into Eq. (4.55) a polynomial expression is obtained for w in terms of x , y and the generalized coordinates α_{13} to α_{24} .

It can be shown [13] that the displacement function chosen in Eq. (4.55) will provide complete compatibility along the entire common edge between adjacent elements with respect to displacements and slopes parallel to the edge. However, for slopes normal to the edge, compatibility is maintained at the common edge only at the nodal points and at the midpoints between nodal points. From the results of numerical studies it has been

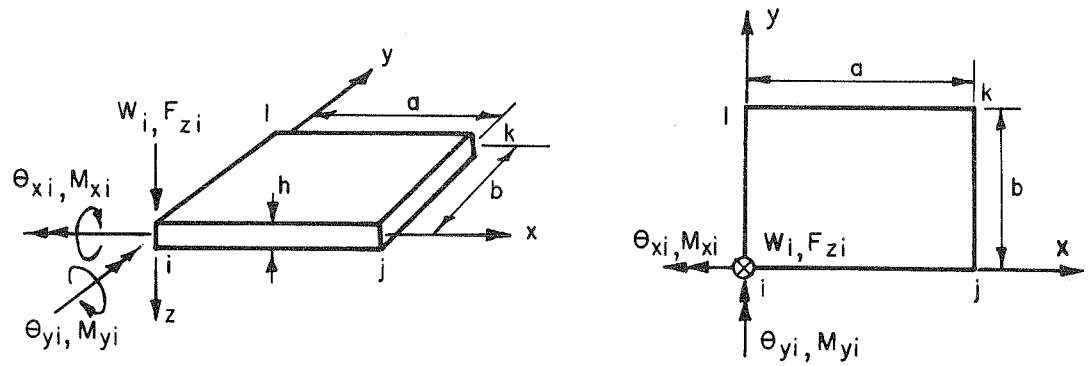


FIG. 25 NOTATION AND POSITIVE DIRECTIONS FOR DISPLACEMENTS AND FORCES AT A TYPICAL NODAL POINT

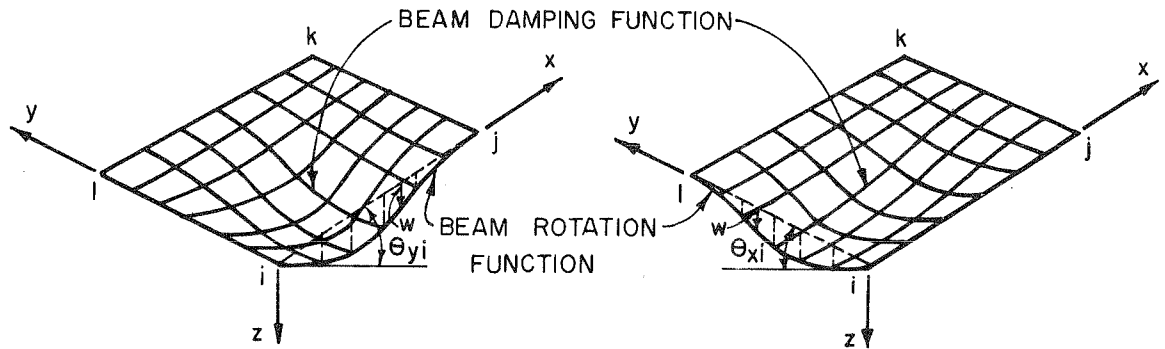


FIG. 26 DISPLACEMENT PATTERN FOR NODAL POINT DISPLACEMENT θ_{yi}

FIG. 27 DISPLACEMENT PATTERN FOR NODAL POINT DISPLACEMENT θ_{xi}

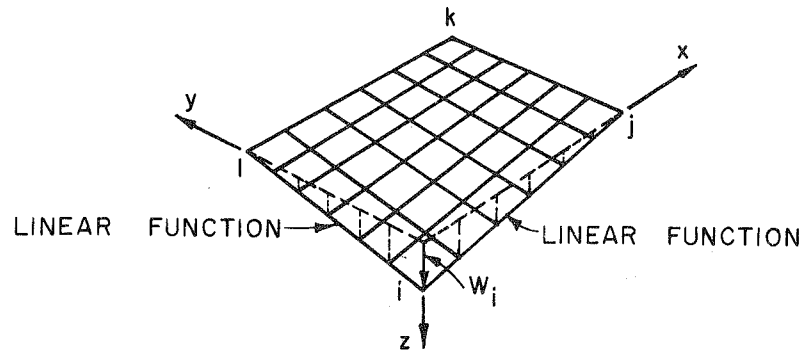


FIG. 28 DISPLACEMENT PATTERN FOR NODAL POINT DISPLACEMENT W_i

found that the effect of this discontinuity is small and that accurate results can be obtained in plate bending problems using a reasonable mesh size.

4.5.3 Derivation of Element Stiffness for Plate Bending

The necessary steps to derive the element stiffness matrix for plate bending k_s relating nodal point forces to nodal point displacements have been given in Section 4.3. Rewriting Eqs. (4.28), (4.29) and (4.20) specifically for the plate bending problem

$$\begin{matrix} \{S_s\} \\ 12 \times 1 \end{matrix} = \begin{matrix} [k_s] \\ 12 \times 12 \end{matrix} \begin{matrix} \{v_s\} \\ 12 \times 1 \end{matrix} \quad (4.56)$$

where

$$k_s = [A_s^{-1}]^T \tilde{k}_s [A_s^{-1}] \quad (4.57)$$

and

$$\tilde{k}_s = \int_V B_s^T D_s B_s dV \quad (4.58)$$

The A_s matrix relates the nodal point displacements V_s to the generalized coordinates α_s .

$$\begin{matrix} \{V_s\} \\ 12 \times 1 \end{matrix} = \begin{matrix} [A_s] \\ 12 \times 12 \end{matrix} \begin{matrix} \{\alpha_s\} \\ 12 \times 1 \end{matrix} \quad (4.59)$$

The elements of the A_s matrix may be found from the definitions of the nodal point displacements, Eqs. (4.54), and the displacement functions, Eq. (4.55). When the appropriate differentiations and substitutions of the nodal point coordinates are made, the following result is obtained.

$$\begin{Bmatrix} \theta_{yi} \\ \theta_{xi} \\ w_i \\ \theta_{yj} \\ \theta_{xj} \\ w_j \\ \theta_{yk} \\ \theta_{xk} \\ w_k \\ \theta_{yl} \\ \theta_{xl} \\ w_l \end{Bmatrix} = \begin{bmatrix} 1 & 0 & -\frac{1}{a} & 0 & 0 & \frac{1}{a} & 0 & 0 & 0 & 0 & 0 & 0 \\ 0 & 1 & -\frac{1}{b} & 0 & 0 & 0 & 0 & 0 & 0 & 0 & 0 & \frac{1}{b} \\ 0 & 0 & 1 & 0 & 0 & 0 & 0 & 0 & 0 & 0 & 0 & 0 \\ 0 & 0 & -\frac{1}{a} & 1 & 0 & \frac{1}{a} & 0 & 0 & 0 & 0 & 0 & 0 \\ 0 & 0 & 0 & 0 & 1 & -\frac{1}{b} & 0 & 0 & \frac{1}{b} & 0 & 0 & 0 \\ 0 & 0 & 0 & 0 & 0 & 1 & 0 & 0 & 0 & 0 & 0 & 0 \\ 0 & 0 & 0 & 0 & 0 & 0 & 1 & 0 & \frac{1}{a} & 0 & 0 & -\frac{1}{a} \\ 0 & 0 & 0 & 0 & 0 & -\frac{1}{b} & 0 & 1 & \frac{1}{b} & 0 & 0 & 0 \\ 0 & 0 & 0 & 0 & 0 & 0 & 0 & 0 & 1 & 0 & 0 & 0 \\ 0 & 0 & 0 & 0 & 0 & 0 & 0 & 0 & \frac{1}{a} & 1 & 0 & -\frac{1}{a} \\ 0 & 0 & -\frac{1}{b} & 0 & 0 & 0 & 0 & 0 & 0 & 0 & 1 & \frac{1}{b} \\ 0 & 0 & 0 & 0 & 0 & 0 & 0 & 0 & 0 & 0 & 0 & 1 \end{bmatrix} \begin{Bmatrix} \alpha_{13} \\ \alpha_{14} \\ \alpha_{15} \\ \alpha_{16} \\ \alpha_{17} \\ \alpha_{18} \\ \alpha_{19} \\ \alpha_{20} \\ \alpha_{21} \\ \alpha_{22} \\ \alpha_{23} \\ \alpha_{24} \end{Bmatrix} \quad (4.59a)$$

The B_s matrix in Eq. (4.58) relates the internal curvatures K in the element to the generalized coordinates α_s .

$$\begin{matrix} \{K(x,y)\} \\ 3 \times 1 \end{matrix} = \begin{matrix} [B_s(x,y)] \\ 3 \times 12 \end{matrix} \begin{matrix} \{\alpha_s\} \\ 12 \times 1 \end{matrix} \quad (4.60)$$

The elements of the B_s matrix may be obtained by appropriate differentiation of Eq. (4.55) and by noting from Eq. (4.50) that

$$\{\kappa(x,y)\} = \begin{Bmatrix} \kappa_x \\ \kappa_y \\ 2\kappa_{xy} \end{Bmatrix} = \begin{Bmatrix} \frac{1}{\rho_x} \\ \frac{1}{\rho_y} \\ \frac{2}{\rho_{xy}} \end{Bmatrix} = \begin{Bmatrix} \frac{\partial^2 w}{\partial x^2} \\ \frac{\partial^2 w}{\partial y^2} \\ \frac{2\partial^2 w}{\partial x \partial y} \end{Bmatrix} \quad (4.60a)$$

In specifying the generalized curvatures above, note that a factor of 2 has been added to the twisting curvature. This factor of 2 is needed to account for the virtual work done in Eq. (4.58) by the torsional moments on both of the adjacent faces of the differential element shown in Fig. 24c.

Performing the necessary differentiations, the following results are obtained for the elements of the $3 \times 12 B_s$ matrix. A prime indicates a differentiation of the function with respect to its variable.

$$\begin{aligned} B_s(1,1) &= X_2''(x)Y_3(y) & B_s(1,7) &= -X_2''(a-x)Y_3(b-y) \\ B_s(1,2) &= X_3''(x)Y_2(y) & B_s(1,8) &= -X_3''(a-x)Y_2(b-y) \\ B_s(1,3) &= X_1''(x)Y_1(y) & B_s(1,9) &= X_1''(a-x)Y_1(b-y) \\ B_s(1,4) &= -X_2''(a-x)Y_3(y) & B_s(1,10) &= X_2''(x)Y_3(b-y) \\ B_s(1,5) &= X_3''(a-x)Y_2(y) & B_s(1,11) &= -X_3''(x)Y_2(b-y) \\ B_s(1,6) &= X_1''(a-x)Y_1(y) & B_s(1,12) &= X_1''(x)Y_1(b-y) \end{aligned}$$

$$\begin{aligned}
B_s(2,1) &= X_2(x)Y_3''(y) & B_s(3,1) &= 2X_2'(x)Y_3'(y) \\
B_s(2,2) &= X_3(x)Y_2''(y) & B_s(3,2) &= 2X_3'(x)Y_2'(y) \\
B_s(2,3) &= X_1(x)Y_1''(y) & B_s(3,3) &= 2X_1'(x)Y_1'(y) \\
B_s(2,4) &= -X_2(a-x)Y_3''(y) & B_s(3,4) &= -2X_2'(a-x)Y_3'(y) \\
B_s(2,5) &= X_3(a-x)Y_2''(y) & B_s(3,5) &= 2X_3'(a-x)Y_2'(y) \\
B_s(2,6) &= X_1(a-x)Y_1''(y) & B_s(3,6) &= 2X_1'(a-x)Y_1'(y) \\
B_s(2,7) &= -X_2(a-x)Y_3''(b-y) & B_s(3,7) &= -2X_2'(a-x)Y_3'(b-y) \\
B_s(2,8) &= -X_3(a-x)Y_2''(b-y) & B_s(3,8) &= -2X_3'(a-x)Y_2'(b-y) \\
B_s(2,9) &= X_1(a-x)Y_1''(b-y) & B_s(3,9) &= 2X_1'(a-x)Y_1'(b-y) \\
B_s(2,10) &= X_2(x)Y_3''(b-y) & B_s(3,10) &= 2X_2'(x)Y_3'(b-y) \\
B_s(2,11) &= -X_3(x)Y_2''(b-y) & B_s(3,11) &= -2X_3'(x)Y_2'(b-y) \\
B_s(2,12) &= X_1(x)Y_1''(b-y) & B_s(3,12) &= 2X_1'(x)Y_1'(b-y)
\end{aligned}$$

Internal bending and torsional moments may be expressed in terms of curvatures and twists to form the D_s matrix

$$\{M(x,y)\} = [D_s] \{\kappa(x,y)\} \quad (4.61)$$

$$\begin{Bmatrix} M_x \\ M_y \\ M_{xy} \end{Bmatrix} = \frac{Eh^3}{12(1-\nu^2)} \begin{bmatrix} 1 & \nu & 0 \\ \nu & 1 & 0 \\ 0 & 0 & \frac{(1-\nu)}{2} \end{bmatrix} \begin{Bmatrix} \kappa_x \\ \kappa_y \\ 2\kappa_{xy} \end{Bmatrix} \quad (4.61a)$$

in which h is the plate thickness.

With the elements of the A_s , B_s , and D_s matrices now defined in Eqs. (4.59), (4.60) and (4.61), the element stiffness matrix k_s in Eq. (4.57) can now be determined

$$k_s = [A_s^{-1}]^T \left[\int_0^b \int_0^a B_s^T D_s B_s \, dx dy \right] [A_s^{-1}] \quad (4.62)$$

and

$$\{S_s\} = [k_s] \{V_s\} = \left(\frac{Eh^3}{12(1-\nu^2)} \right) [KS] \{V_s\} \quad (4.63)$$

in which KS is a 12×12 matrix of coefficients obtained by performing the tedious integration and matrix multiplication indicated in Eq. (4.62). The sequence of nodal point forces and corresponding displacements in Eq. (4.63) is as follows:

$$\begin{Bmatrix} M_{yi} \\ M_{xi} \\ F_{zi} \\ M_{yj} \\ M_{xj} \\ F_{zj} \\ M_{yk} \\ M_{xk} \\ F_{zk} \\ M_{yl} \\ M_{xl} \\ F_{zl} \end{Bmatrix} = \frac{Eh^3}{12(1-\nu^2)} \begin{bmatrix} 12 \times 12 \text{ KS matrix} \end{bmatrix} \begin{Bmatrix} \theta_{yi} \\ \theta_{xi} \\ w_i \\ \theta_{yj} \\ \theta_{xj} \\ w_j \\ \theta_{yk} \\ \theta_{xk} \\ w_k \\ \theta_{yl} \\ \theta_{xl} \\ w_l \end{Bmatrix} \quad (4.63a)$$

The expressions derived for the elements of the symmetrical KS matrix by Eq. (4.62) are as follows, using the notation and sign convention given in Fig. 25:

$$KS(1,1) = \frac{52}{35} \frac{b}{a} + \frac{8}{25} \frac{a}{b} + \frac{4}{35} \frac{a^3}{b^3}$$

$$KS(1,2) = \frac{11}{35} \frac{a^2}{b^2} + \frac{11}{35} \frac{b^2}{a^2} + 1.2 \nu + 0.2$$

$$KS(1,3) = \frac{23}{35} \frac{a^2}{b^3} + \frac{33}{14} \frac{b}{a^2} + \frac{7}{25} \frac{1}{b} + 1.3 \frac{\nu}{b}$$

$$KS(1,4) = \frac{26}{35} \frac{b}{a} - \frac{2}{25} \frac{a}{b} - \frac{3}{35} \frac{a^3}{b^3}$$

$$KS(1,5) = \frac{13}{70} \frac{a^2}{b^2} - \frac{11}{35} \frac{b^2}{a^2} - \frac{\nu}{10} - 0.02$$

$$KS(1,6) = -\frac{33}{14} \frac{b}{a^2} + \frac{12}{35} \frac{a^2}{b^3} - \frac{7}{25} \frac{1}{b} - 0.1 \frac{\nu}{b}$$

$$KS(1,7) = \frac{9}{35} \frac{b}{a} + \frac{2}{25} \frac{a}{b} + \frac{3}{35} \frac{a^3}{b^3}$$

$$KS(1,8) = \frac{13}{70} \frac{b^2}{a^2} + \frac{13}{70} \frac{a^2}{b^2} - 0.02$$

$$KS(1,9) = -\frac{9}{14} \frac{b}{a^2} - \frac{12}{35} \frac{a^2}{b^3} + \frac{7}{25} \frac{1}{b} + 0.1 \frac{\nu}{b}$$

$$KS(1,10) = \frac{18}{35} \frac{b}{a} - \frac{8}{25} \frac{a}{b} - \frac{4}{35} \frac{a^3}{b^3}$$

$$KS(1,11) = \frac{11}{35} \frac{a^2}{b^2} - \frac{13}{70} \frac{b^2}{a^2} + \frac{\nu}{10} + 0.02$$

$$KS(1,12) = \frac{9}{14} \frac{b}{a^2} - \frac{23}{35} \frac{a^2}{b^3} - \frac{7}{25} \frac{1}{b} - 1.3 \frac{\nu}{b}$$

$$KS(2,2) = \frac{52}{35} \frac{a}{b} + \frac{8}{25} \frac{b}{a} + \frac{4}{35} \frac{b^3}{a}$$

$$KS(2,3) = \frac{23}{35} \frac{b^2}{a^3} + \frac{33}{14} \frac{a}{b^2} + \frac{7}{25} \frac{1}{a} + 1.3 \frac{v}{a}$$

$$KS(2,4) = -KS(1,5)$$

$$KS(2,5) = -\frac{8}{25} \frac{b}{a} + \frac{18}{35} \frac{a}{b} - \frac{4}{35} \frac{b^3}{a^3}$$

$$KS(2,6) = -\frac{23}{35} \frac{b^2}{a^3} + \frac{9}{14} \frac{a}{b^2} - \frac{7}{25} \frac{1}{a} - 1.3 \frac{v}{a}$$

$$KS(2,7) = KS(1,8)$$

$$KS(2,8) = \frac{3}{35} \frac{b^3}{a^3} + \frac{9}{35} \frac{a}{b} + \frac{2}{25} \frac{b}{a}$$

$$KS(2,9) = -\frac{12}{35} \frac{b^2}{a^3} - \frac{9}{14} \frac{a}{b^2} + \frac{7}{25} \frac{1}{a} + 0.1 \frac{v}{a}$$

$$KS(2,10) = -KS(1,11)$$

$$KS(2,11) = -\frac{3}{35} \frac{b^3}{a^3} + \frac{26}{35} \frac{a}{b} - \frac{2}{25} \frac{b}{a}$$

$$KS(2,12) = \frac{12}{35} \frac{b^2}{a^3} - \frac{33}{14} \frac{a}{b^2} - \frac{7}{25} \frac{1}{a} - 0.1 \frac{v}{a}$$

$$KS(3,3) = \frac{176}{35} \frac{a}{b^3} + \frac{176}{35} \frac{b}{a^3} + \frac{78}{25} \frac{1}{ab} + 0.8 \frac{v}{ab}$$

$$KS(3,4) = -KS(1,6)$$

$$KS(3,5) = KS(2,6)$$

$$KS(3,6) = -\frac{176}{35} \frac{b}{a^3} + \frac{34}{35} \frac{a}{b^3} - \frac{78}{25} \frac{1}{ab} - 0.8 \frac{v}{ab}$$

$$KS(3,7) = -KS(1,9)$$

$$KS(3,8) = -KS(2,9)$$

$$KS(3,9) = -\frac{34}{35} \frac{a}{b^3} - \frac{34}{35} \frac{b}{a^3} + \frac{78}{25} \frac{1}{ab} + 0.8 \frac{v}{ab}$$

$$KS(3,10) = KS(1,12)$$

$$KS(3,11) = -KS(2,12)$$

$$KS(3,12) = \frac{34}{35} \frac{b}{a^3} - \frac{176}{35} \frac{a}{b^3} - \frac{78}{25} \frac{1}{ab} - 0.8 \frac{v}{ab}$$

$$KS(4,4) = KS(1,1) \quad KS(6,11) = -KS(2,9)$$

$$KS(4,5) = -KS(1,2) \quad KS(6,12) = KS(3,9)$$

$$KS(4,6) = -KS(1,3) \quad KS(7,7) = KS(1,1)$$

$$KS(4,7) = KS(1,10) \quad KS(7,8) = KS(1,2)$$

$$KS(4,8) = -KS(1,11) \quad KS(7,9) = -KS(1,3)$$

$$KS(4,9) = -KS(1,12) \quad KS(7,10) = KS(1,4)$$

$$KS(4,10) = KS(1,7) \quad KS(7,11) = KS(1,5)$$

$$KS(4,11) = -KS(1,8) \quad KS(7,12) = -KS(1,6)$$

$$KS(4,12) = -KS(1,9) \quad KS(8,8) = KS(2,2)$$

$$KS(5,5) = KS(2,2) \quad KS(8,9) = -KS(2,3)$$

$$KS(5,6) = KS(2,3) \quad KS(8,10) = KS(2,4)$$

$$KS(5,7) = KS(1,11) \quad KS(8,11) = KS(2,5)$$

$$KS(5,8) = KS(2,11) \quad KS(8,12) = -KS(2,6)$$

$$KS(5,9) = KS(2,12) \quad KS(9,9) = KS(3,3)$$

$$KS(5,10) = -KS(1,8) \quad KS(9,10) = KS(1,6)$$

$$KS(5,11) = KS(2,8) \quad KS(9,11) = -KS(2,6)$$

$$KS(5,12) = KS(2,9) \quad KS(9,12) = KS(3,6)$$

$$KS(6,6) = KS(3,3) \quad KS(10,10) = KS(1,1)$$

$$KS(6,7) = -KS(1,12) \quad KS(10,11) = -KS(1,2)$$

$$KS(6,8) = -KS(2,12) \quad KS(10,12) = KS(1,3)$$

$$KS(6,9) = KS(3,12) \quad KS(11,11) = KS(2,2)$$

$$KS(6,10) = KS(1,9) \quad KS(11,12) = -KS(2,3)$$

$$KS(12,12) = KS(3,3)$$

As a check on the above derived expressions for KS they were used together with Eq. (4.63a) to perform equilibrium checks on the element by taking $\sum M_x$, $\sum M_y$ and $\sum F_z$ of the nodal point forces produced by unit values of each of the nodal point displacements. In all cases these summations equalled zero providing a check on the derivations.

4.6 Computer Program - FINPLA

A general computer program, called FINPLA, has been written to perform the finite element analysis described in this chapter. The program has been written in FORTRAN IV language for the IBM 7094 computer. For detailed descriptions of the input, output, sign conventions, limitations, and usage see Appendix B. A brief description is given below.

(a) Input Data:

- (1) Geometry and dimensions of the structure and its finite element mesh idealization.
- (2) Dimensions and material properties of each finite element type.
- (3) Magnitude and location of uniform surface loads on the elements.
- (4) Magnitude and location of concentrated or line loads along joints or at nodal points.
- (5) Boundary conditions of the structure.
- (6) Location, geometry and properties of diaphragms.
- (7) Desired locations for final results in output.

(b) Output Data:

- (1) The complete input data are properly labelled and printed as a check.
- (2) The six final displacement components are printed for each nodal point of the structure.
- (3) Internal forces, consisting of the inplane quantities N_x , N_y , N_{xy} , and the bending and torsional moments M_x , M_y , M_{xy} , are printed out at the nodal points and at intermediate points wherever desired.
- (4) The execution times for the different links of the program conclude the output.

(c) Limitations, Restrictions, and Remarks:

- (1) The maximum number of nodal points in one cross-section is 20. The maximum absolute nodal point difference of one element is 5.
- (2) There may be up to 28 elements in one cross-section and up to 40 elements subdivision along the span of the whole structure.
- (3) Each finite element must belong to one of up to 90 different element types, characterized by its geometry, material properties, and uniform loading.
- (4) Up to 150 concentrated or distributed line loads or displacements may be specified at the longitudinal joints.
- (5) There may be up to 25 boundary displacement components specified, which are applied to any number of nodal points in a cross-section.
- (6) The maximum number of transverse diaphragms is 5.
- (7) The internal forces of adjoining elements may be averaged if desired.

(d) Logical Steps:

- (1) Read and print input data.
- (2) Set up the total force and displacement arrays for the structure, containing the complete or final input forces or displacements of each nodal point. An indicator array which is set up shows if a force or displacement is specified.

- (3) Calculate the element stiffnesses for each element type in global coordinates.
- (4) Form and invert the total structure stiffness for one longitudinal segment at a time.
- (5) Print out final joint displacements.
- (6) Calculate all desired internal forces and average the results of adjacent elements if desired.
- (7) Print out internal forces.
- (8) Calculate and print internal forces in diaphragms.
- (9) Print execution times.

5. COMPARISON OF RESULTS

5.1 Introduction

Three different methods for analyzing continuous box girder bridges have been presented in the preceding chapters. The assumptions, limitations, advantages and disadvantages have also been discussed for each of the methods. The general computer programs, MUPDI, SIMPLA, and FINPLA, developed to perform these analyses provide a powerful means for the analysis of continuous box girder bridges as well as a variety of other problems.

In order to check the validity of the assumptions and the accuracy of the three methods of analysis, it is desirable to analyze a general case by the three methods and to compare the results obtained. A two span continuous bridge with a cross-section consisting of three cells was selected as the example structure to be analyzed. Extensive results were obtained from the computer output with respect to displacements, internal forces and moments at various sections along the span. Only selected results will be presented for discussion. Comparisons will be made of vertical deflections, longitudinal stresses, percentage of total moment at a section taken by each girder, and transverse slab moments. In addition a summary of computer times required for each solution will be given, so that this factor may be considered in evaluating the advantages and disadvantages of one method over another.

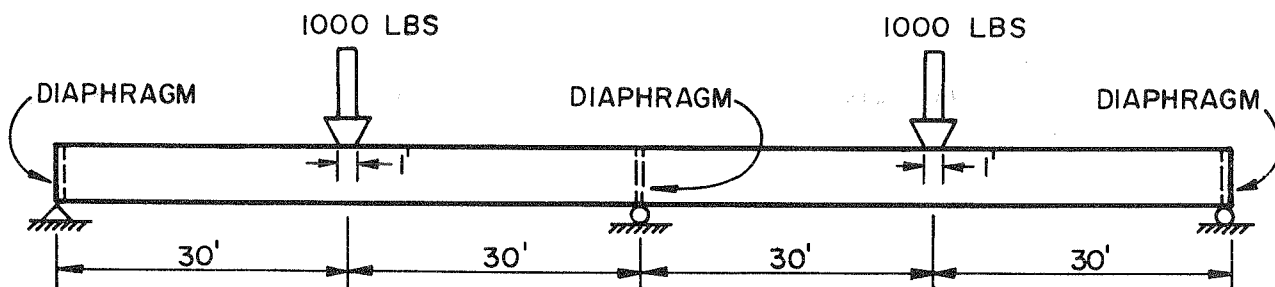
5.2 Description of Example Bridge and Analytical Models

The dimensions and loading for the example bridges are shown in Fig. 29. Rigid diaphragms are assumed to exist at each of the three support points. The cross-sectional dimensions of the 3-cell bridge are the same as those used for one of the example bridges in the initial report on simply supported bridges [1]. By subjecting each of the two 60 ft. spans to a midspan load of 1,000 lb. distributed over a 1 ft. length and placed over an exterior web,

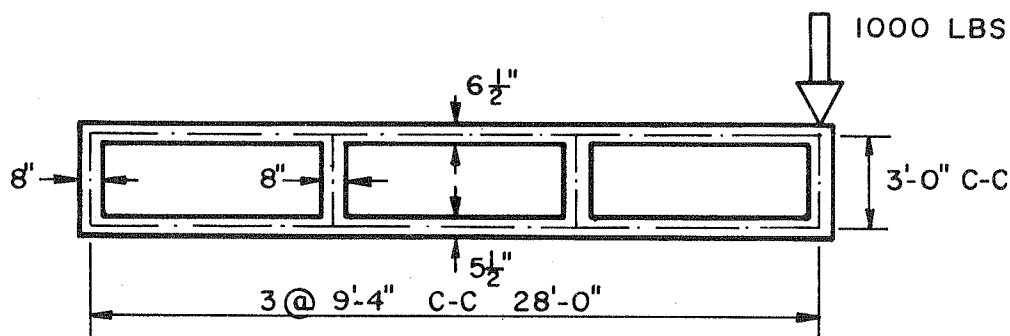
symmetry is obtained in the longitudinal direction about the middle support. Thus, instead of the two span continuous bridge, a single 60 ft. span can be analyzed, if desired, which has boundary conditions consisting of a fixed support at one end and a simple support at the other end.

Five separate computer analyses were made of the example bridge: one by the folded plate method; two by the finite element method, using two different element subdivisions; and two by the finite segment method, using two different segment subdivisions. The results of the folded plate analysis are used as a standard for comparison, since it is considered to be the most accurate of the methods of analysis used. The modulus of elasticity was assumed to be 3,000,000 psi in all analyses. Poisson's ratio was taken as 0.15 for the folded plate and finite element analyses and as zero in the finite segment analyses as necessitated by its assumptions.

The folded plate analytical model was taken as a two span continuous structure with simple supports at the two extreme ends. A rigid diaphragm 1 ft. thick was assumed to exist at the interior support. The cellular folded plate system was subdivided into 11 plates interconnected at 9 longitudinal joints, Fig. 30. Note that a longitudinal joint was included in the top slab midway between the two interior webs. This was done so that the same subdivision could also be used for a central concentrated load as well as for the eccentric one shown. In the analyses, displacements of the folded plate system at the rigid diaphragm over the interior support were set to zero at all possible joint and plate restraint points. A total of $[(9 \times 3) + (11 \times 4)] = 71$ redundant reaction forces at the section over the interior support resulted from these imposed restraints. Both the applied concentrated 1,000 lb. loads and the reaction forces at the interior support were represented by the sum of the first 99 harmonics of the appropriate Fourier series.

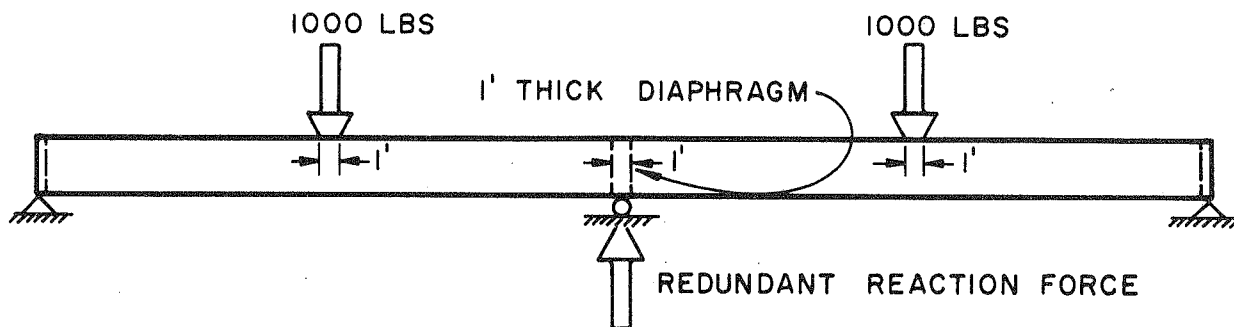


a) LONGITUDINAL ELEVATION

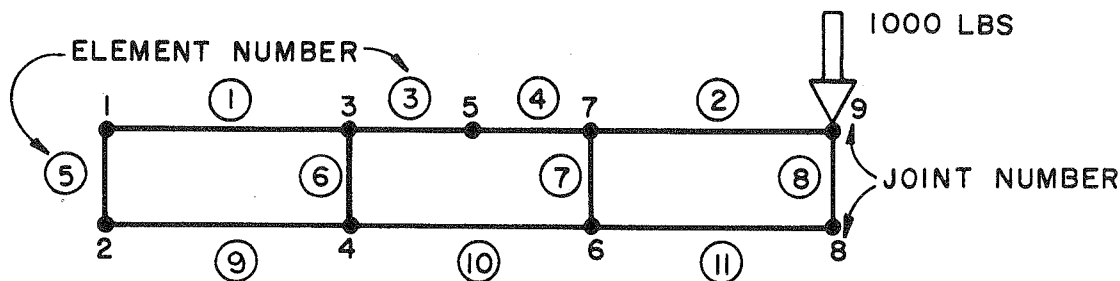


b) TRANSVERSE SECTION

FIG. 29 DIMENSIONS AND LOADING FOR EXAMPLE BRIDGE



a) LONGITUDINAL ELEVATION



b) TYPICAL TRANSVERSE SECTION

FIG. 30 FOLDED PLATE ANALYTICAL MODEL

Because of longitudinal symmetry this involved 50 non-zero harmonics. The computer program MUPDI was used to perform the analysis by the folded plate method.

Two element subdivisions were used in the finite element analysis. The first subdivision, designated Mesh 1, is shown in Fig. 31. A single span, fixed at one end and simply supported at the other end, was used in the analysis. For Mesh 1, a typical transverse section, Fig. 31b, had 10 finite elements and 8 nodal points. Longitudinally, the structure was divided into 14 segments resulting in 15 sections containing nodal points, Fig. 31a. Thus the total number of finite elements in the structure was 140 and the total number of nodal points was 120. Since each nodal point has 6 degrees of freedom, this resulted in a structure stiffness matrix with a total of 720 degrees of freedom. The maximum band width in the structure stiffness matrix was equal to 66. This is defined as being equal to the number of degrees of freedom per nodal point times the sum of the maximum absolute difference between the nodal point numbers on a typical cross-section for any single finite element plus the number of nodal points on the cross-section plus one. In the computer program for the finite element method, FINPLA, a major portion of the computer time is expended in solving Eq. (4.9) which contains the structure stiffness matrix. As an approximate guide, the time required for the solution of the equations increases directly with the total number of degrees of freedom and as the square of the maximum band width.

The second subdivision, used in the finite element analysis, designated Mesh 2, is shown in Fig. 32. The same number of subdivisions, as in Mesh 1, were used longitudinally, Fig. 32a. However, a typical transverse section, Fig. 32b, had 15 finite elements and 13 nodal points and, as can be seen,

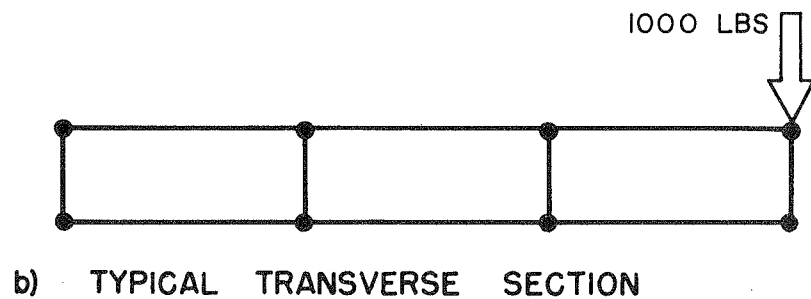
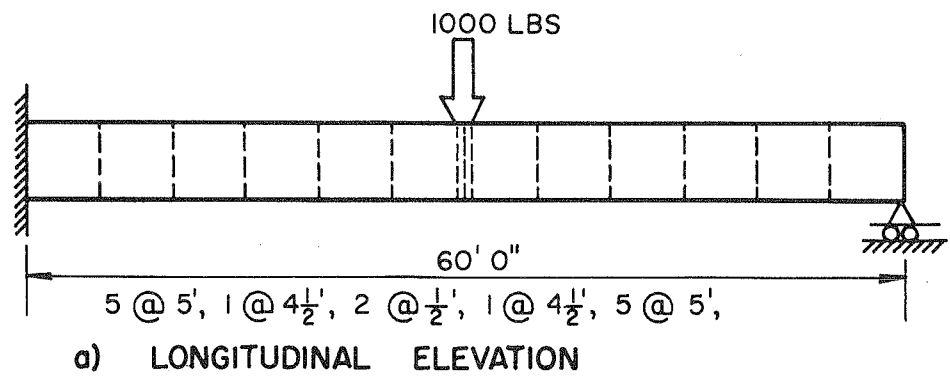


FIG. 31 FINITE ELEMENT ANALYTICAL MODEL - MESH 1

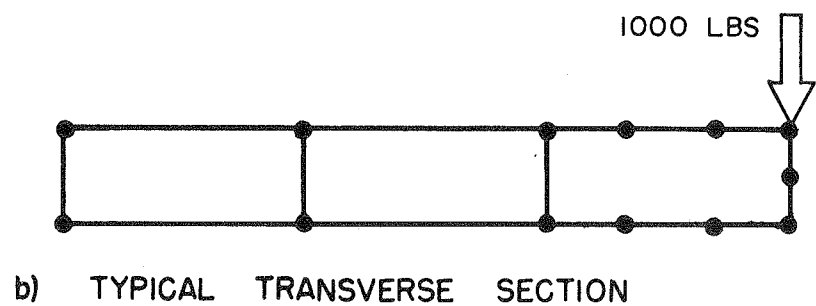
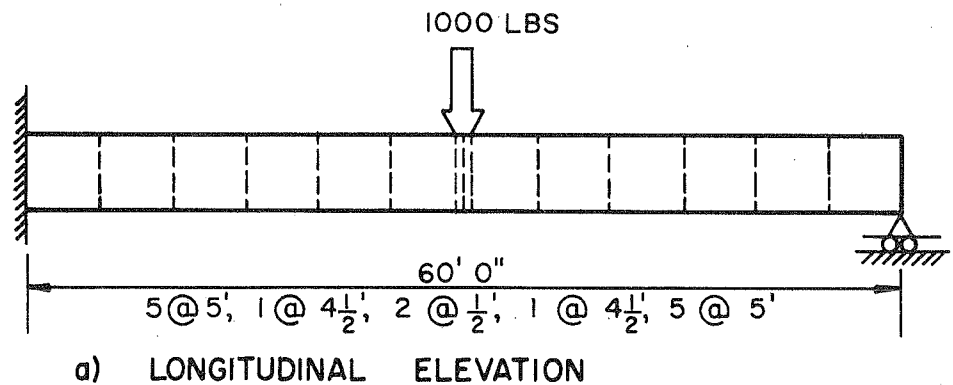


FIG. 32 FINITE ELEMENT ANALYTICAL MODEL - MESH 2

the finer mesh was used only in the loaded cell. Mesh 2 had a total of 210 finite elements, 195 nodal points, 1170 degrees of freedom and a maximum band width of 96.

The two element subdivisions used in the finite segment analysis, designated Mesh 1 and Mesh 2, are shown in Figs. 33 and 34. It can be seen that these are identical with those used in the finite element analysis with the exception that at midspan, one 1 ft. long longitudinal segment was used in place of two 1/2 ft. long segments. In the analysis by the computer program SIMPLA, longitudinal stopovers, as discussed in Section 3.4, were specified at the end of every other segment.

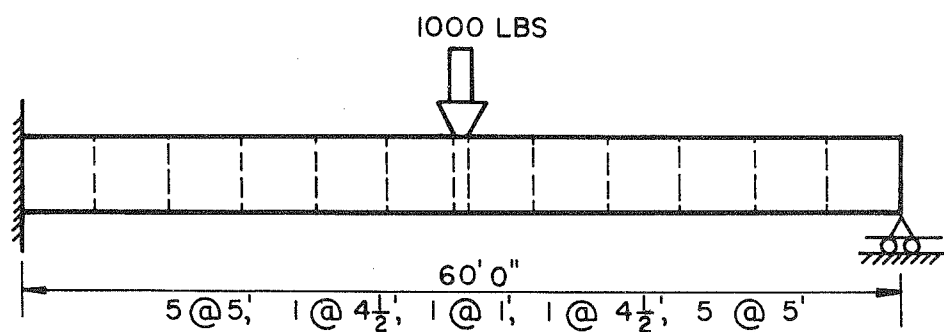
5.3 Vertical Deflections

Results for the vertical deflections along longitudinal lines at the top of each of the four webs are depicted in Figs. 35 to 38. Good agreement exists between the results of the five analyses. The vertical deflections are generally the least sensitive of the results obtained and even the coarse Mesh 1 used for the finite element and the finite segment methods gave results which compare favorably with the folded plate results. As would be expected the shapes of the deflected curves are all similar in form to that of a beam fixed at one end and simply supported at the other end,

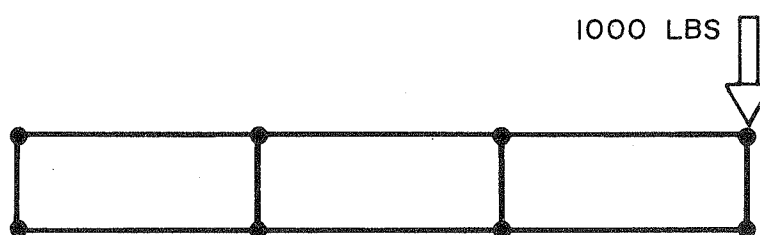
The distribution of vertical deflections across transverse sections at $x = 17.5$ ft, $x = 30.0$ ft. (midspan), and $x = 42.5$ ft. from the fixed end support are shown in Fig. 39. The deflections at the midspan section exhibit the greatest non-uniformity due to the effect of the concentrated load at midspan.

5.4 Longitudinal Stresses

In evaluating the longitudinal stresses from the computer output, plots of stress σ_x at each element edge versus distance from the fixed support

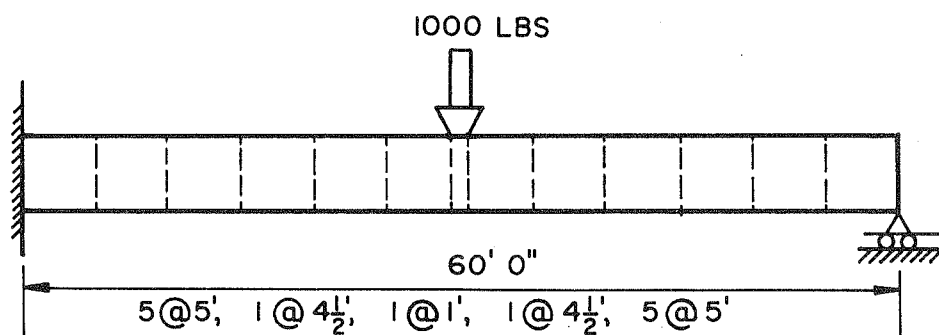


a) LONGITUDINAL ELEVATION

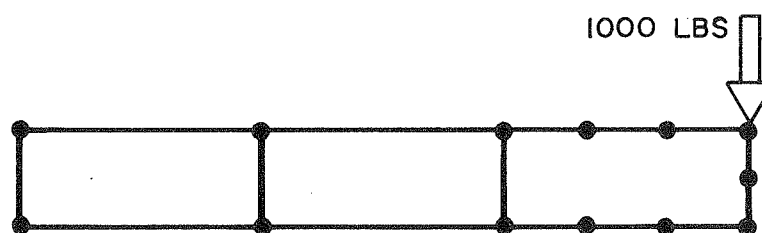


b) TYPICAL TRANSVERSE SECTION

FIG. 33 FINITE SEGMENT ANALYTICAL MODEL - MESH 1



a) LONGITUDINAL ELEVATION



b) TYPICAL TRANSVERSE SECTION

FIG. 34 FINITE SEGMENT ANALYTICAL MODEL - MESH 2

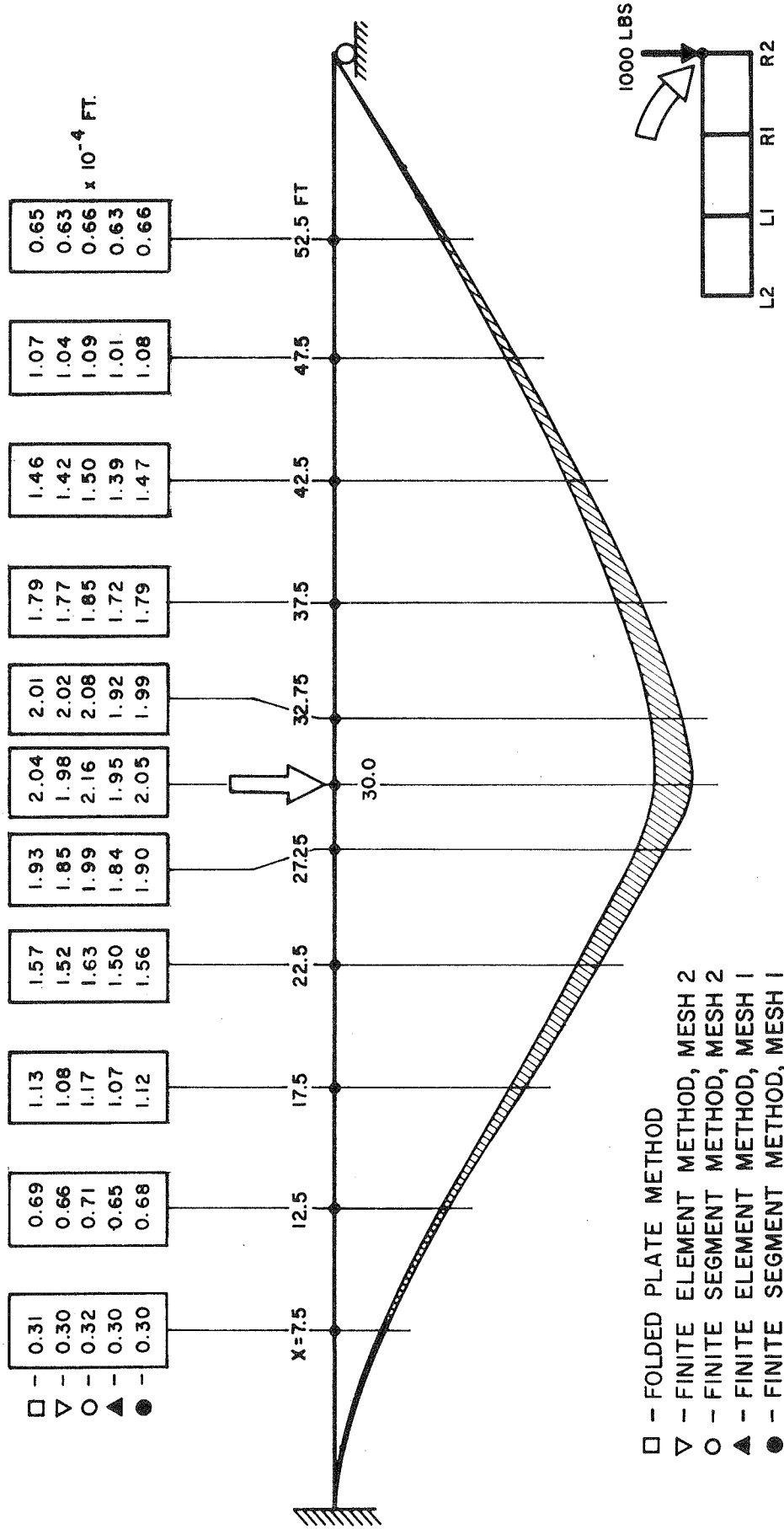
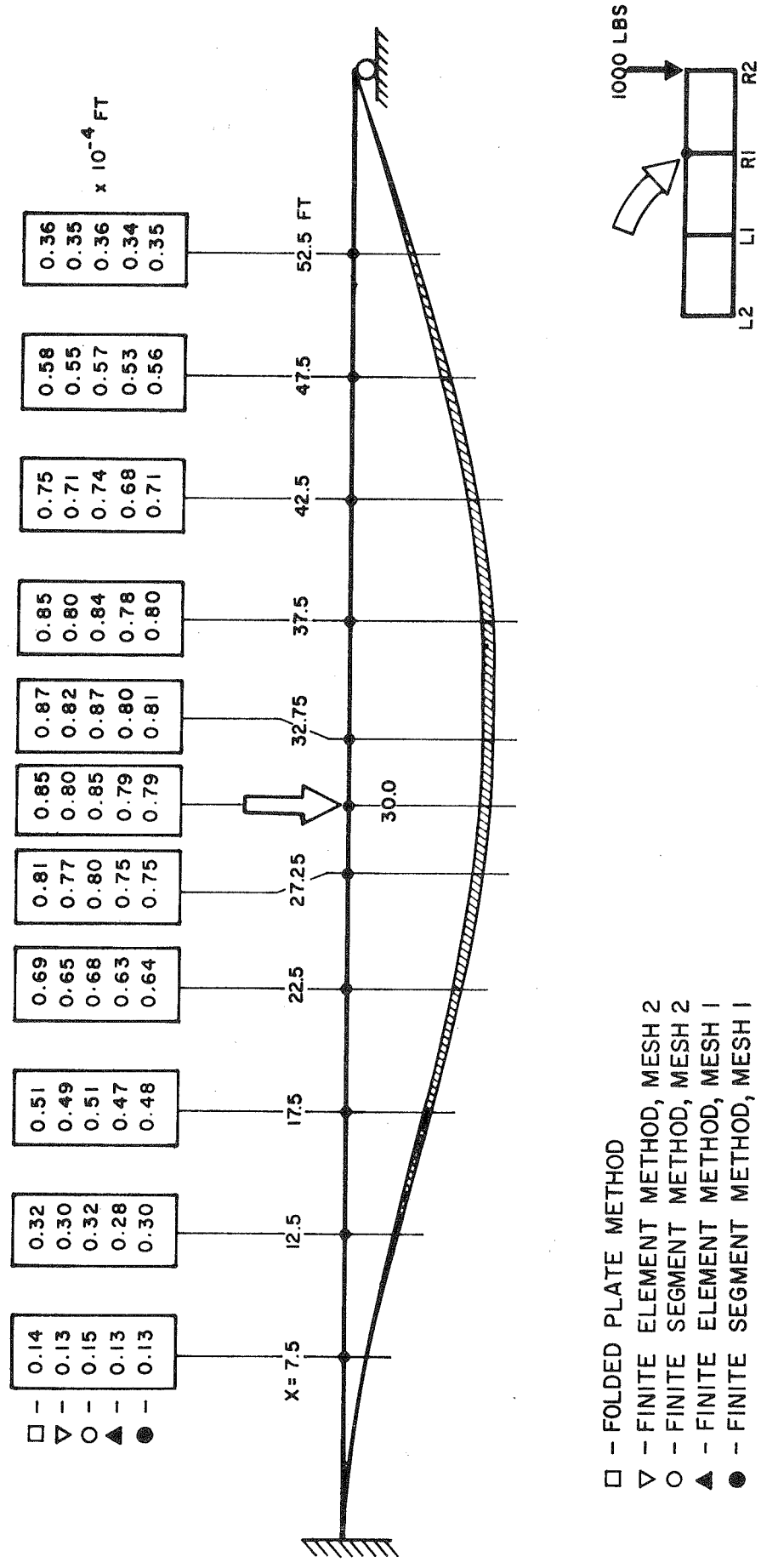


FIG. 35 VERTICAL DEFLECTION ALONG LONGITUDINAL LINE AT TOP OF GIRDER R₂



- - FOLDED PLATE METHOD
- ▽ - FINITE ELEMENT METHOD, MESH 2
- - FINITE SEGMENT METHOD, MESH 2
- ▲ - FINITE ELEMENT METHOD, MESH 1
- - FINITE SEGMENT METHOD, MESH 1

FIG. 36 VERTICAL DEFLECTION ALONG LONGITUDINAL LINE AT TOP OF GIRDER R₁

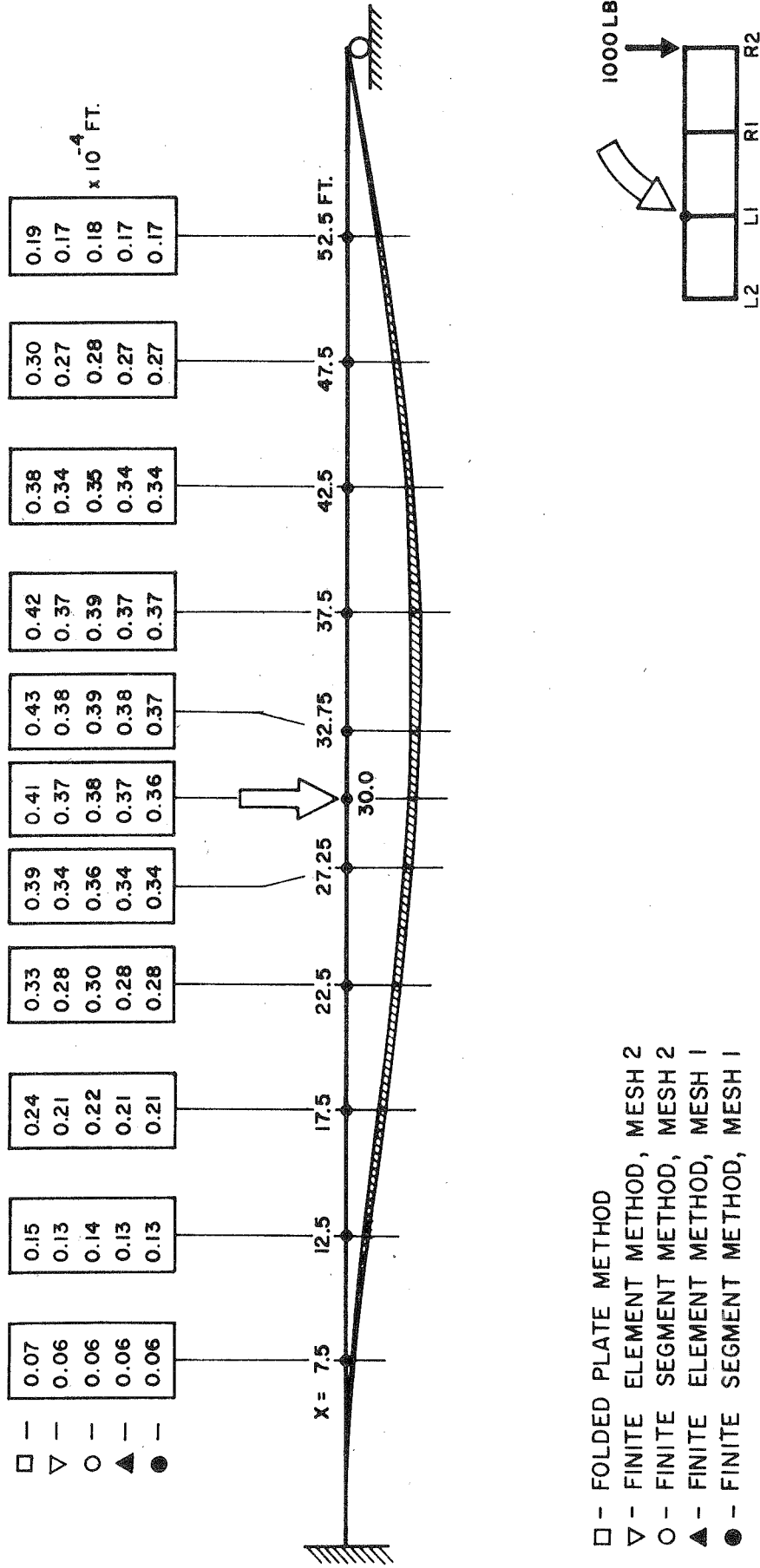
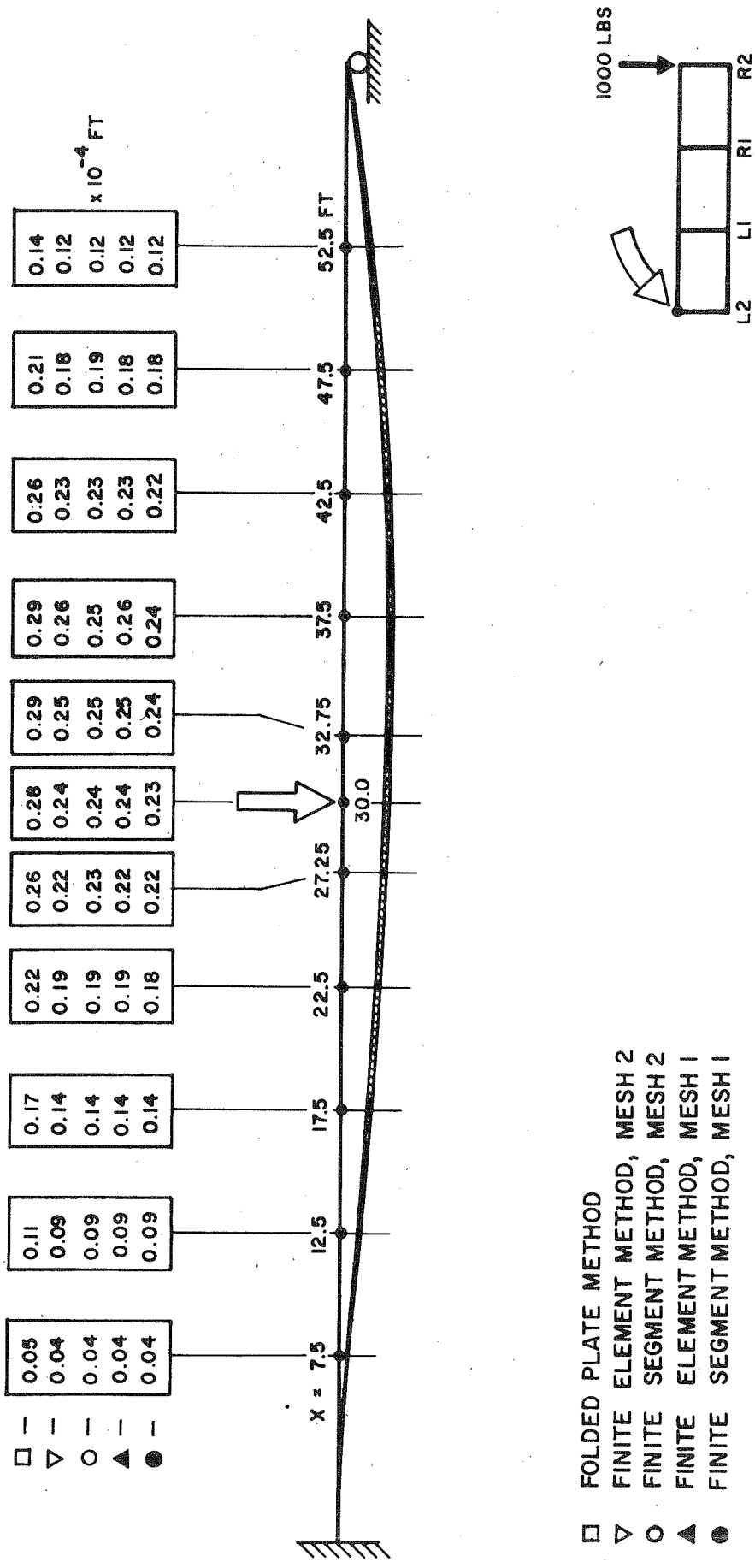


FIG. 37 VERTICAL DEFLECTION ALONG LONGITUDINAL LINE AT TOP OF GIRDER L1



- FOLDED PLATE METHOD
- ▽ FINITE ELEMENT METHOD, MESH 2
- FINITE SEGMENT METHOD, MESH 2
- ▲ FINITE ELEMENT METHOD, MESH 1
- FINITE SEGMENT METHOD, MESH 1

FIG. 38 VERTICAL DEFLECTION ALONG LONGITUDINAL LINE AT TOP OF GIRDER L2

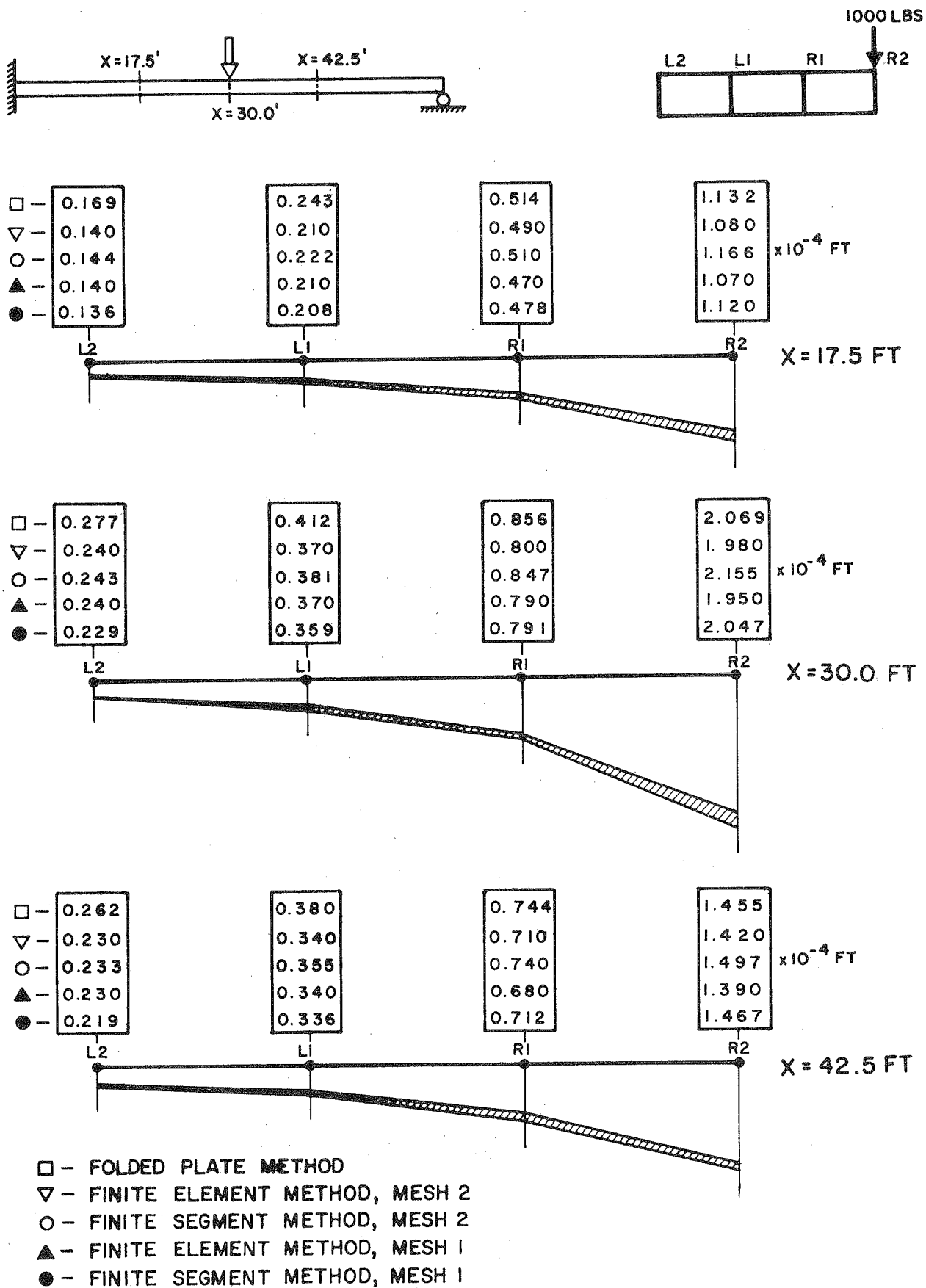


FIG. 39 VERTICAL DEFLECTION AT TRANSVERSE SECTIONS

were made for all elements in the cross-section. Typical plots of this type are shown in Figs. 40, 41, and 42 for points on the top slab, bottom slab and exterior web of the loaded cell.

In making these plots it should be noted that each of the methods of analysis used involves different assumptions regarding the longitudinal variation of stress along an element edge. The folded plate method assumes a continuous variation along the entire span based on the sum of the harmonic contributions. Thus results by this method may be plotted directly from the computer output at specified sections. The assumed displacement patterns used in the finite element method, Figs. 20 to 22, result in a uniform variation in longitudinal strain along the longitudinal edges of a finite element. Thus the results for σ_x by this method, from the computer output, indicate essentially uniform stress along the longitudinal edge of each element, with sudden jumps at each nodal point. In interpreting these results the simplest procedure is to average the values longitudinally at each nodal point. This was done in plotting the curves shown in Figs. 40 to 42. Essentially the same curves are obtained from a plot of the stresses at the midpoints of each longitudinal element edge. The curves were extrapolated to the support and to midspan to obtain stresses at these sections. The finite segment method assumes a linear stress variation along a longitudinal edge of a segment. Values at the midpoints and at the ends of the segments were used in plotting the curves shown in Figs. 40 to 42. In all three methods the plotted stresses on the top and bottom slabs at a longitudinal joint were taken as the average transversely of the stresses in the elements on either side of the joint.

A study of Figs. 40 to 42 indicates general agreement between the results of all five analyses except in the sensitive vicinity of the concentrated load. In this vicinity, a refinement of the mesh from Mesh 1 to Mesh 2 for

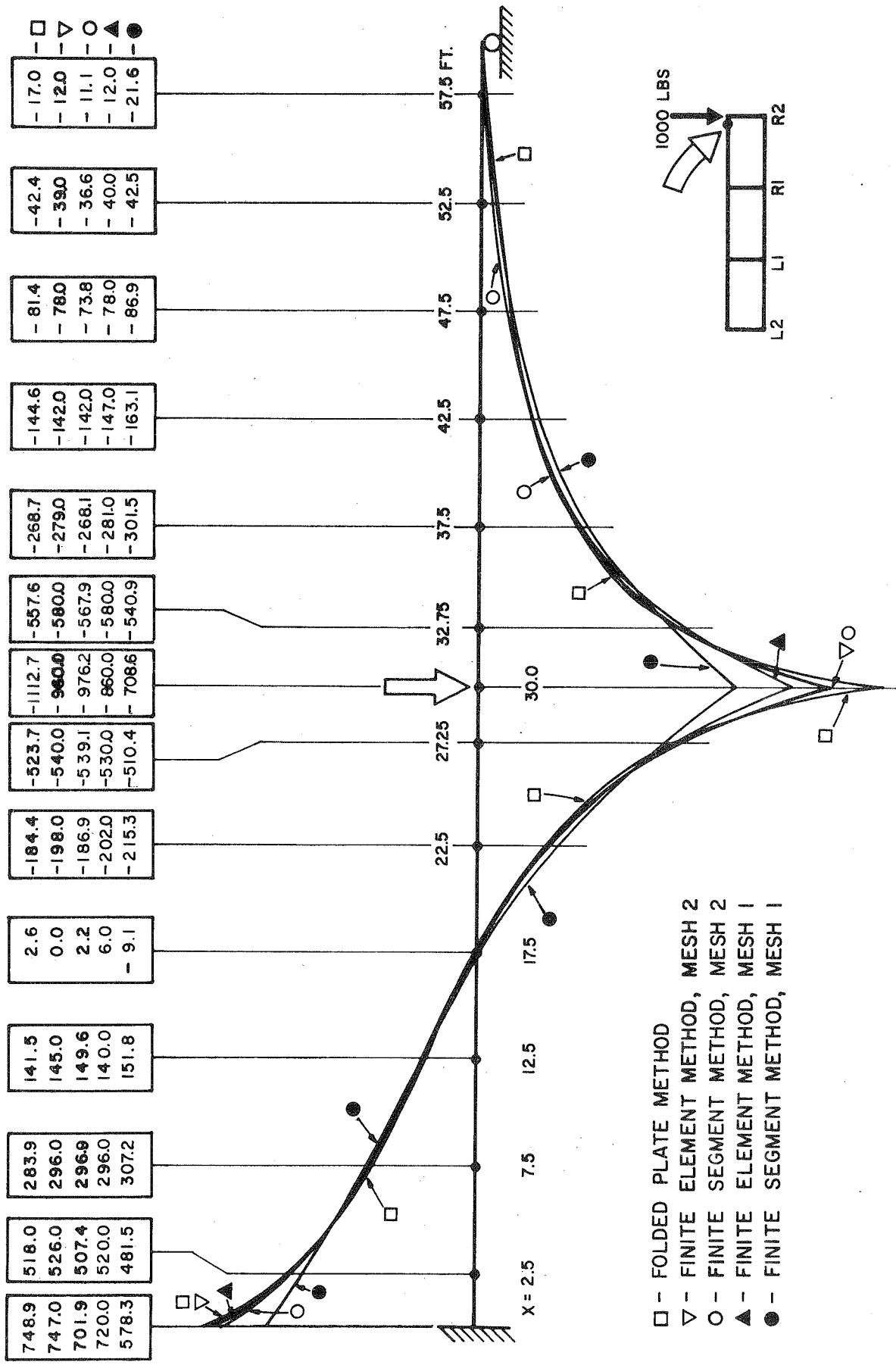


FIG. 40 LONGITUDINAL DISTRIBUTION OF LONGITUDINAL STRESS σ_x (PSF) IN TOP SLAB

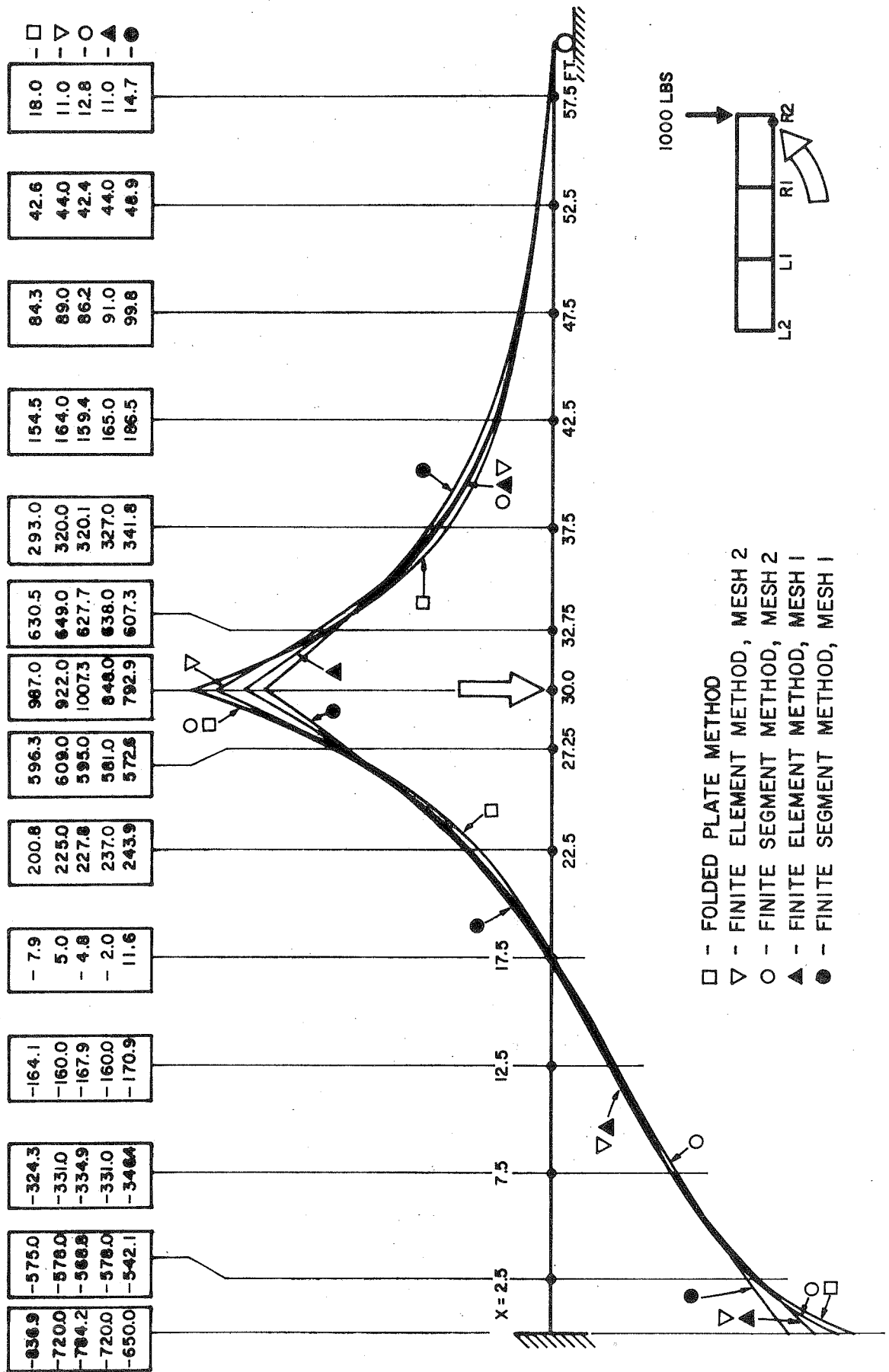


FIG. 41 LONGITUDINAL DISTRIBUTION OF LONGITUDINAL STRESS σ_x (PSF) IN BOTTOM SLAB

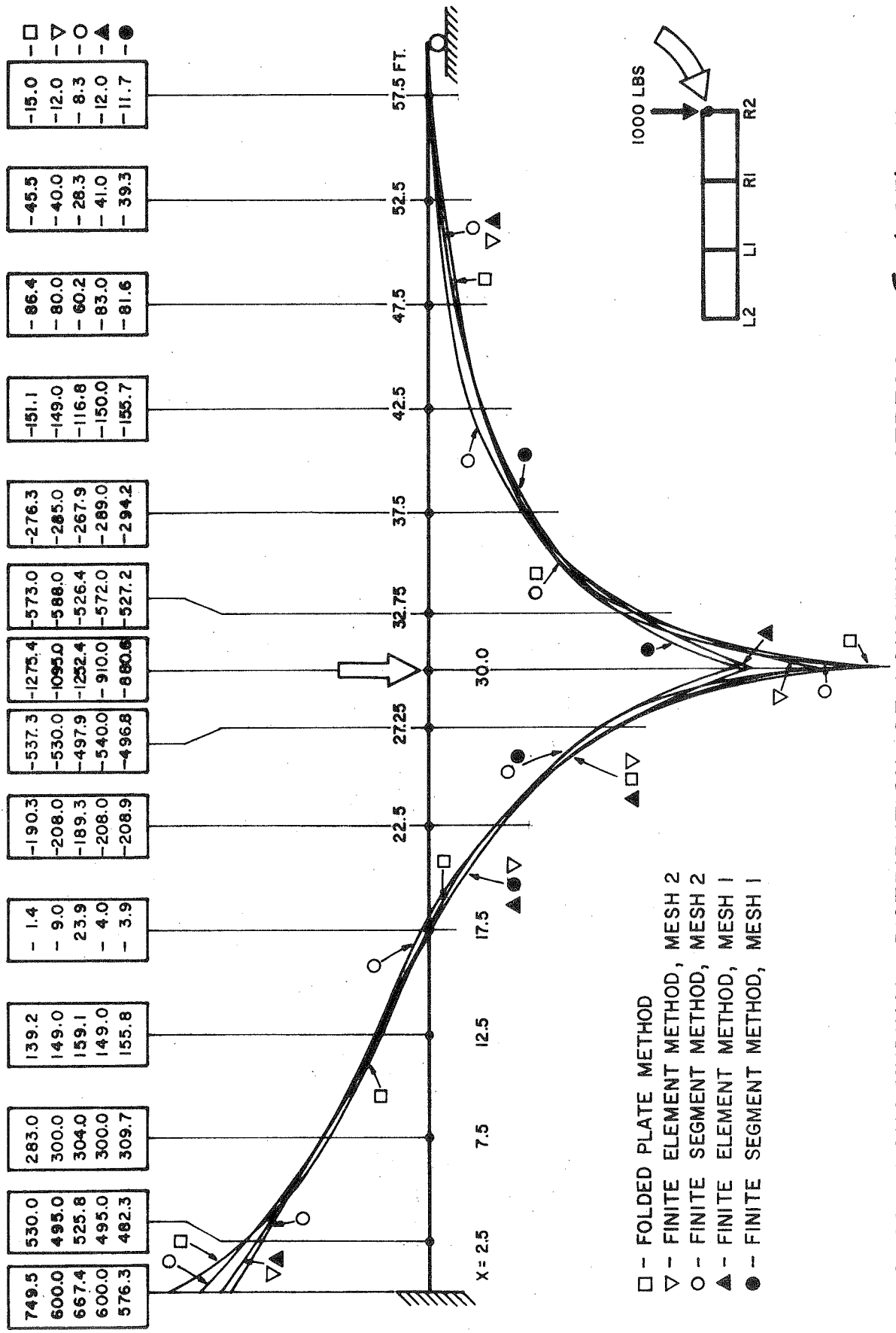


FIG. 42 LONGITUDINAL DISTRIBUTION OF LONGITUDINAL STRESS σ_x (PSF) IN EXTERNAL WEB

both the finite element and finite segment methods improves the comparison with the results of the folded plate method.

The transverse distribution of longitudinal stresses at midspan and at the fixed support are shown in Figs. 43 to 48. The folded plate method gives a continuous transverse variation of stress and results in longitudinal stress concentrations directly under the midspan concentrated load and at the slab-web junctures at the fixed end support reactions. For both the finite element and finite segment methods a linear transverse variation of stresses exists between joint locations and it is apparent that as the mesh is refined from Mesh 1 to Mesh 2 the distributions by both methods begin to approach each other and that obtained by the folded plate method. The assumptions of both the folded plate and the finite segment methods automatically insure that statics at a section are satisfied, thus the stresses obtained by the finite segment method represent a best "fit", within the restriction of a linear variation between joints, of the stresses found by the folded plate method. The assumptions of the finite element method do not insure that statics at a section are satisfied, however, as the mesh is made finer and finer, this condition is approached.

5.5 Distribution of Moments to Each Girder

The actual box girder cross-section is first divided into individual girders consisting of a web and top and bottom flanges. The flanges are taken equal in width to the distance between the midpoint of the cells on adjacent sides of the web. Thus for the example bridge, shown in Fig. 29, all the interior girders have flange widths twice those of the exterior girders.

The girder moment at any section taken by an individual girder can be found by integrating the stresses, shown in Figs. 43 to 48, over the proper

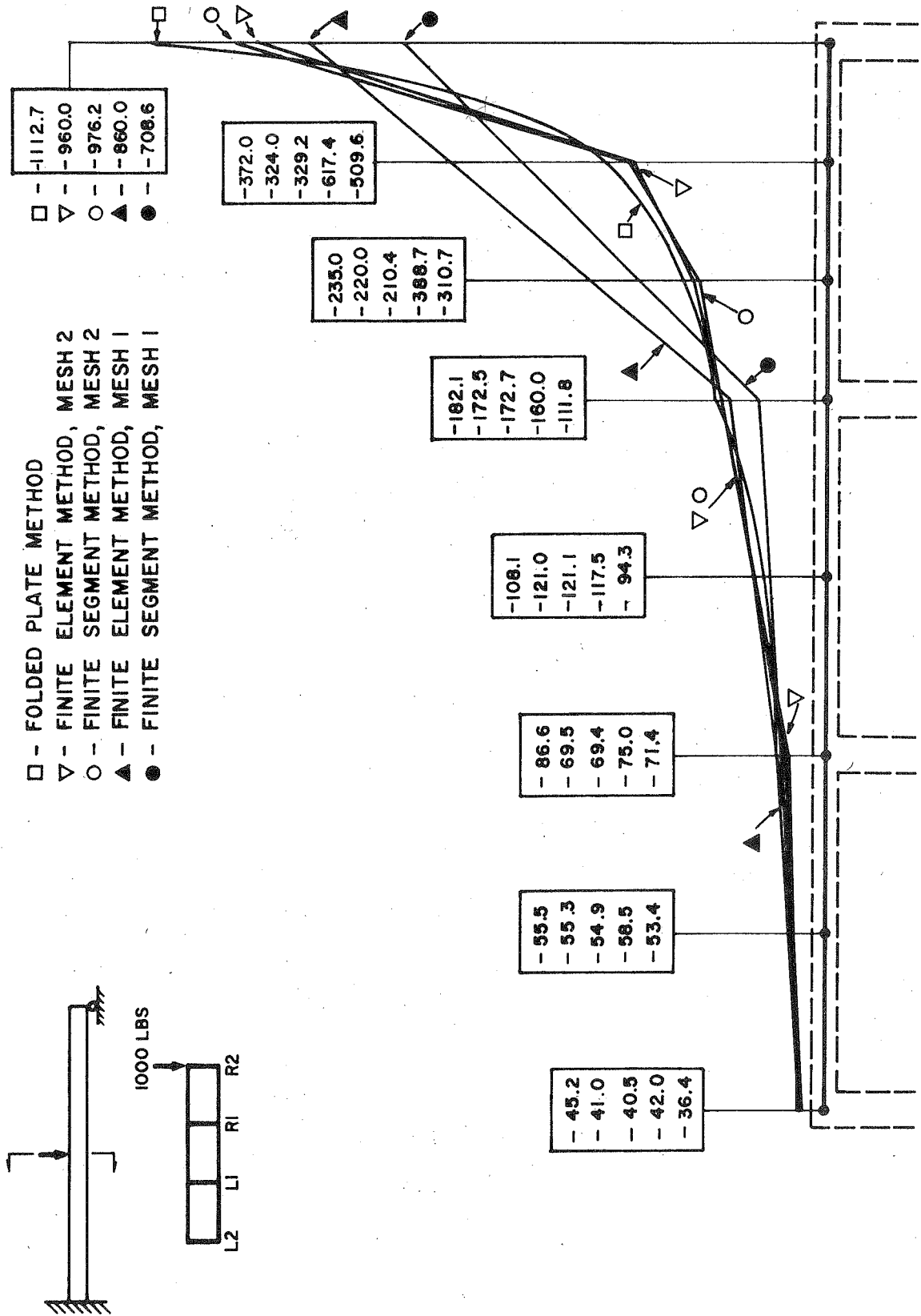


FIG. 43 TRANSVERSE DISTRIBUTION OF LONGITUDINAL STRESS σ_x (PSF) IN TOP SLAB AT MIDSPAN SECTION

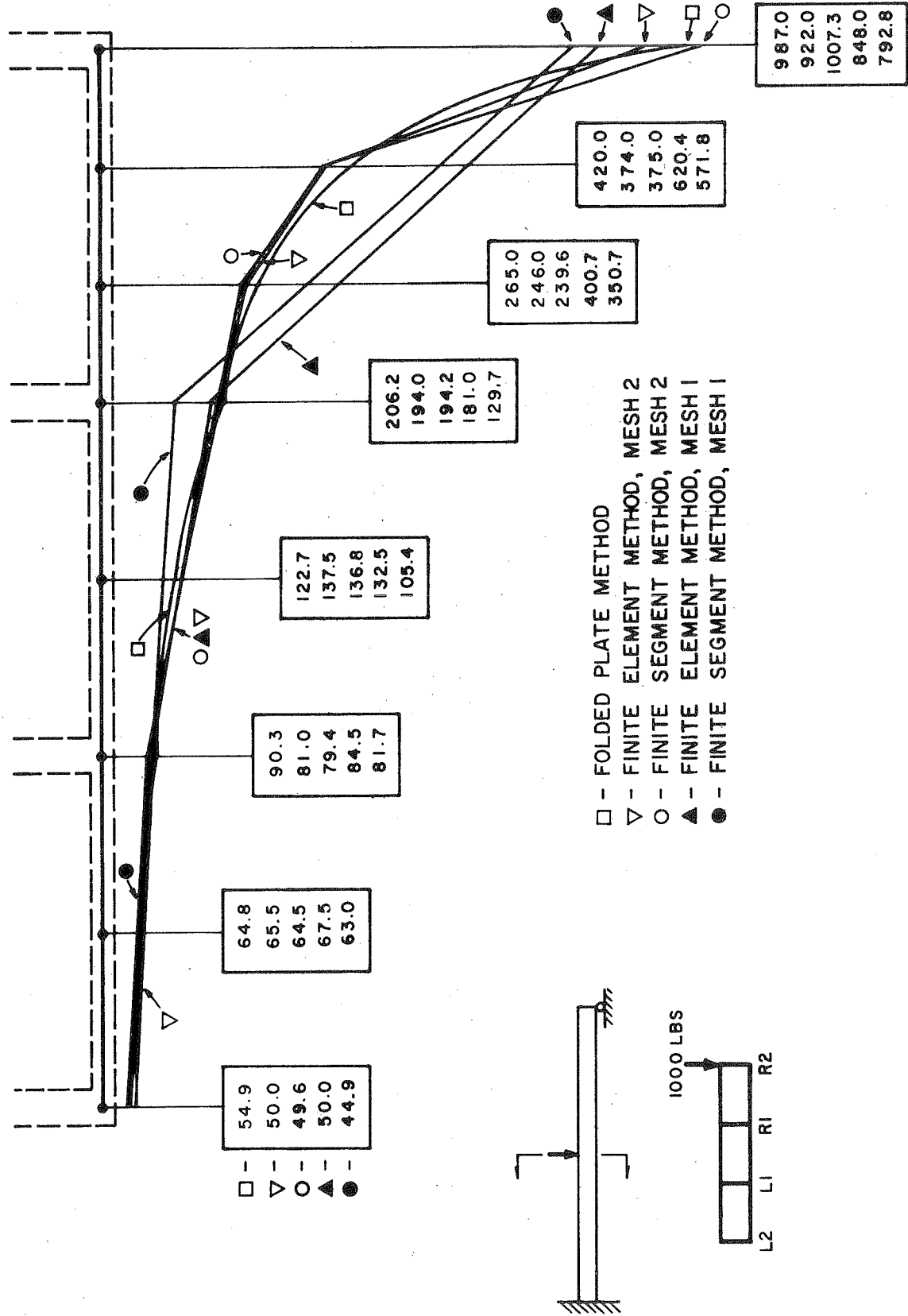


FIG. 44 TRANSVERSE DISTRIBUTION OF LONGITUDINAL STRESS σ_x (PSF) IN BOTTOM SLAB AT MIDSPAN

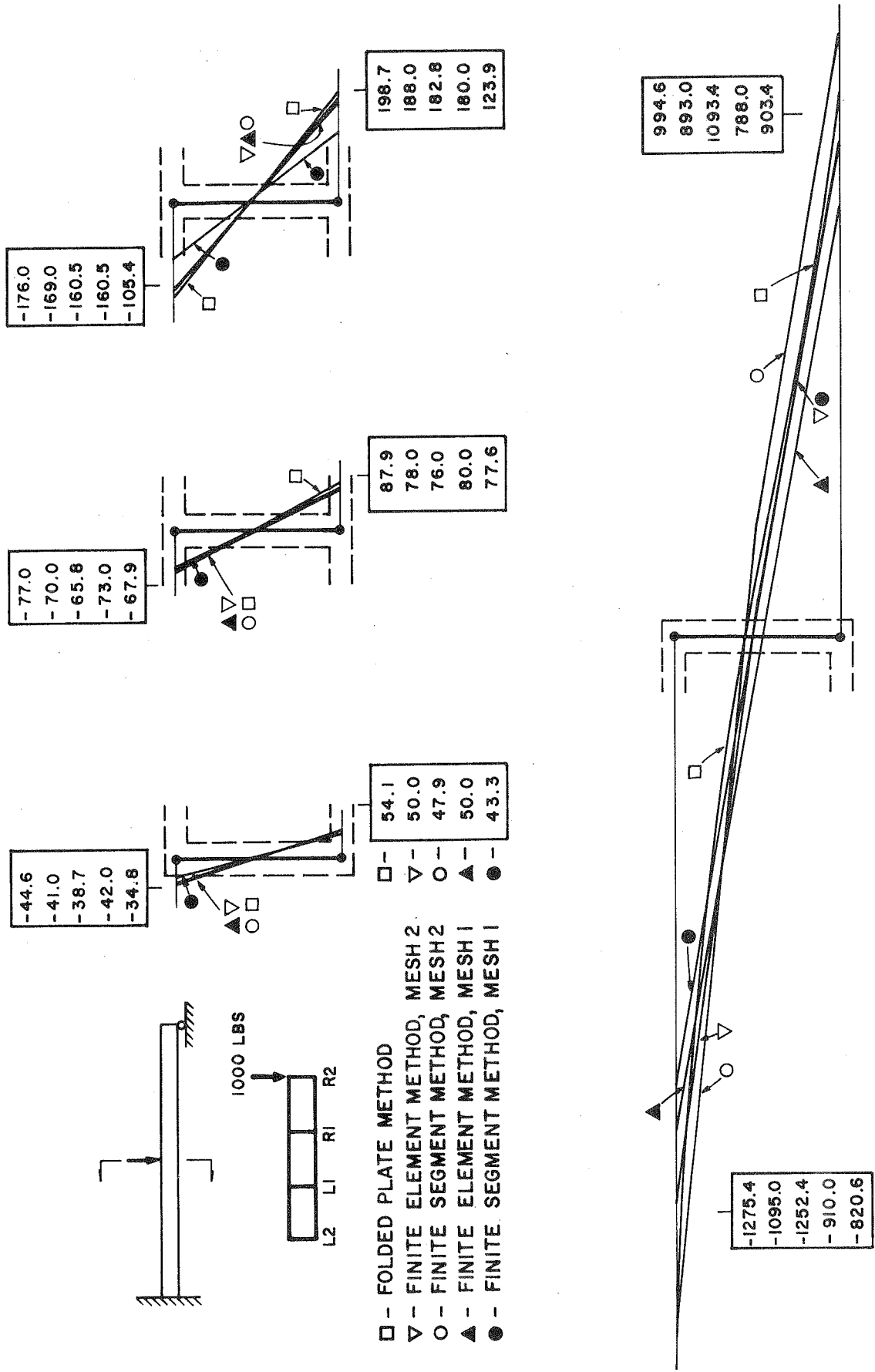


FIG. 45 TRANSVERSE DISTRIBUTIONS OF LONGITUDINAL STRESS σ_x (PSF) IN WEBS AT MIDSPAN SECTION

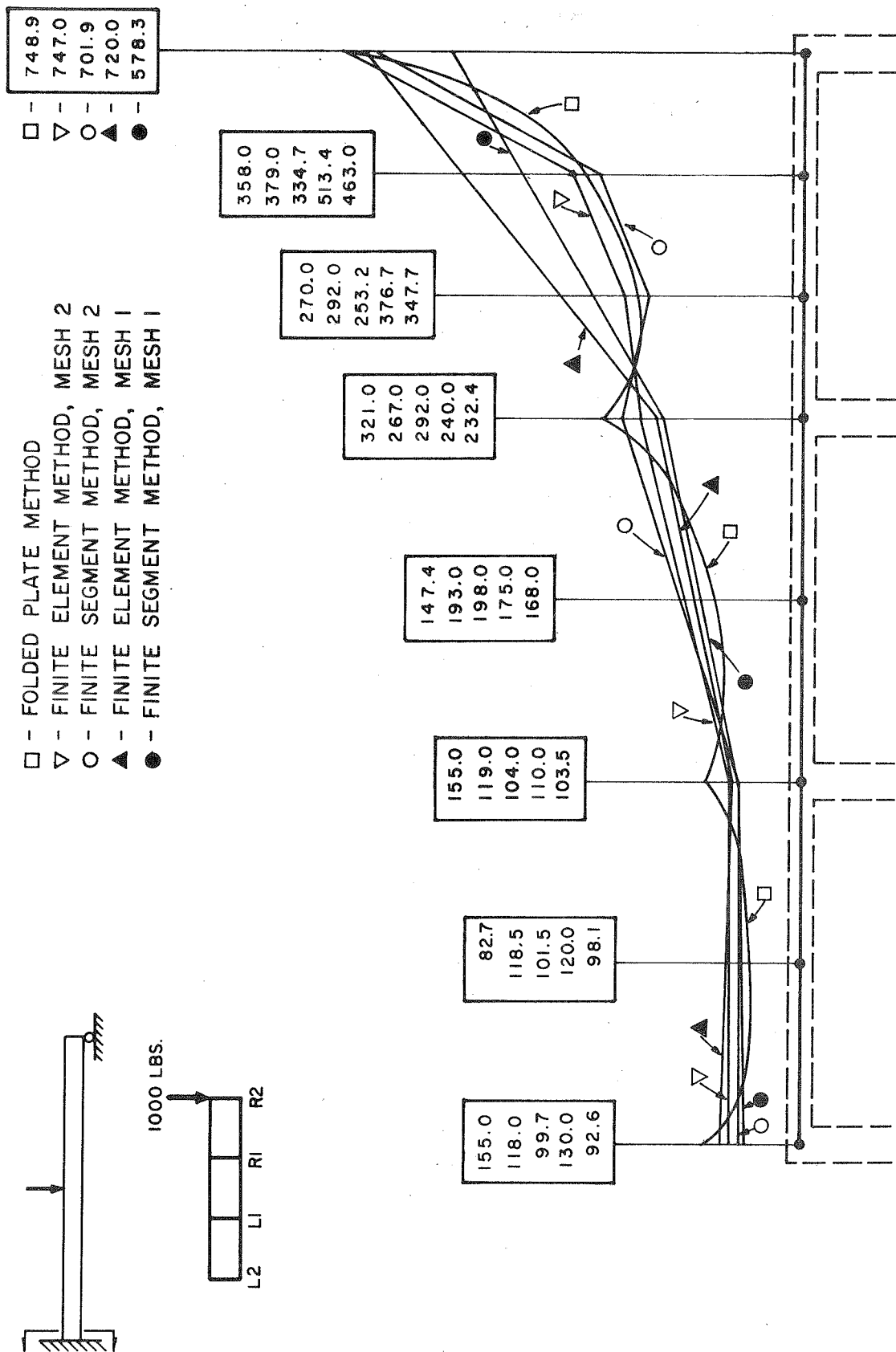


FIG. 46 TRANSVERSE DISTRIBUTION OF LONGITUDINAL STRESS σ_x (PSF) IN TOP SLAB AT FIXED END SUPPORT

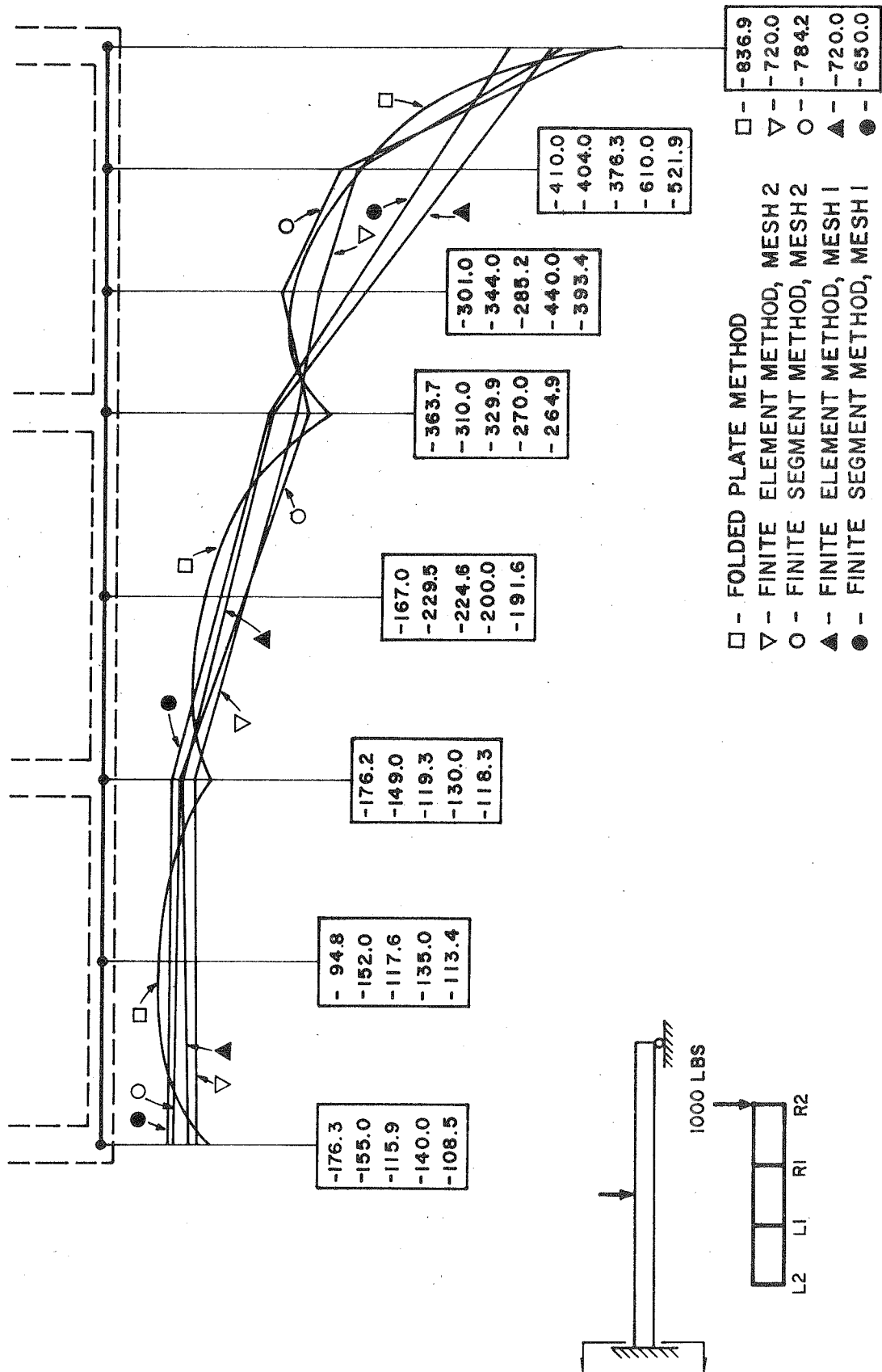


FIG. 47 TRANSVERSE DISTRIBUTION OF LONGITUDINAL STRESS σ_x (PSF) IN BOTTOM SLAB AT FIXED END SUPPORT

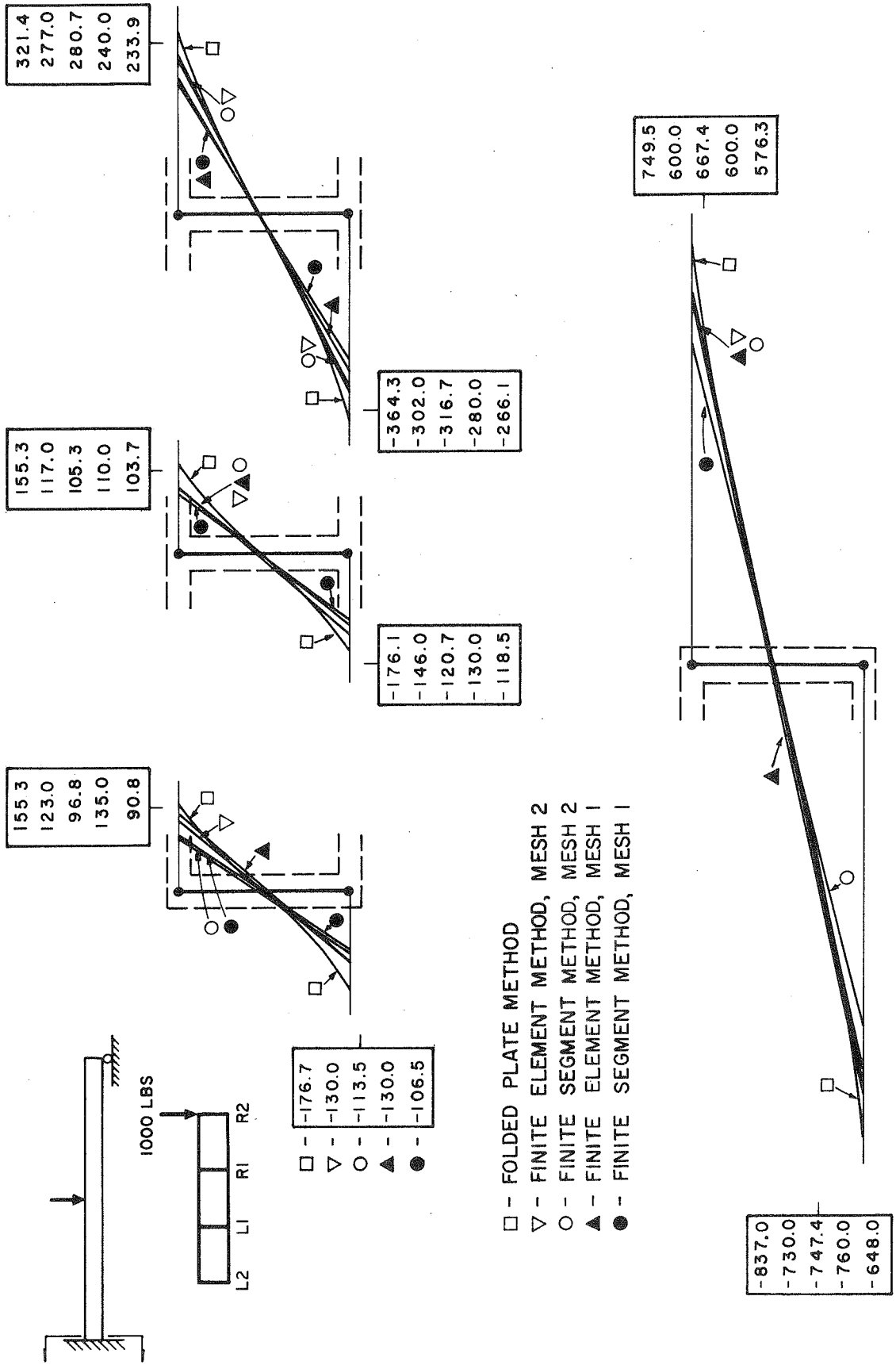


FIG. 48 TRANSVERSE DISTRIBUTION OF LONGITUDINAL STRESS σ_x (PSF) IN WEBS AT FIXED END SUPPORT

slab and web areas to obtain forces and then multiplying these forces by their respective lever arms to the neutral axis of the section. The girder moments, at a particular section, can then be summed to determine the total moment on an entire cross-section. This was done for sections at midspan and at the fixed end support. Each girder moment can then be divided by the total moment at a section to determine the percentage distribution to each girder.

The results of the above procedure for all five analyses are given in Table 1. It can be seen that the results for both Mesh 1 and Mesh 2 by the finite segment method are in good general agreement with those found by the folded plate method. For the finite element method, the results for the coarse Mesh 1 tend to overestimate the moments taken by girders R_1 and R_2 ; however, the results for the fine Mesh 2 are in good agreement with those found by the folded plate method.

5.6 Transverse Slab Moments

In evaluating the transverse slab moments from the computer output, plots of moment M_y at each element edge versus distance from the fixed support were made for all element edges in the cross section. Typical plots of this type are shown in Figs. 49, through 52 for points in the top slab, bottom slab and web of the loaded cell. The curves for the folded plate method were plotted directly from results at specified sections in the computer output. For the finite element method, values averaged longitudinally at the nodal points and values at the midpoints of each longitudinal element edge were used to plot the curves. Values at the midpoints of the longitudinal segments were used in plotting the curves for the finite segment method.

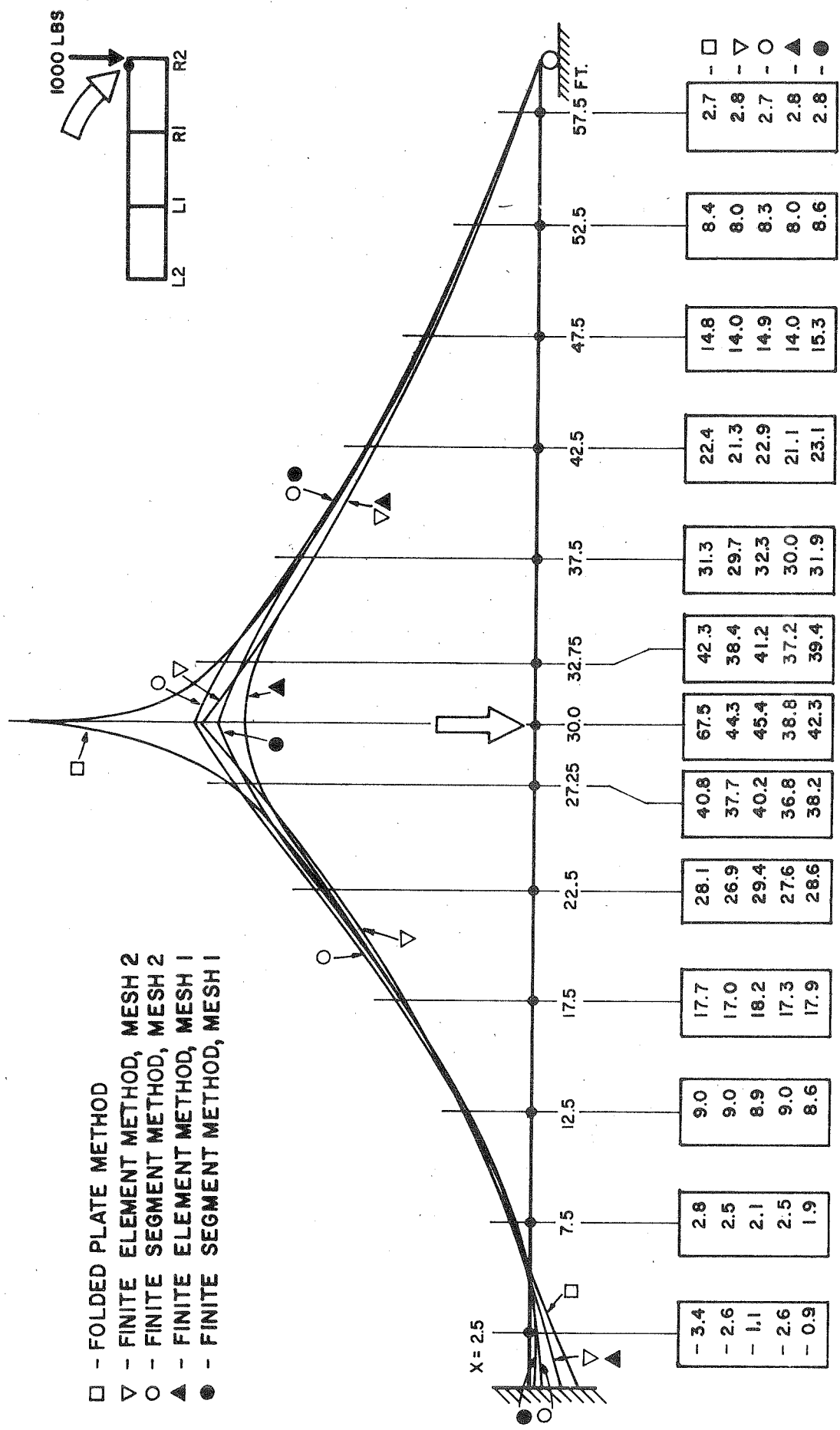


FIG. 49 LONGITUDINAL DISTRIBUTION OF TRANSVERSE MOMENT My (FT-LB/FT) IN TOP SLAB

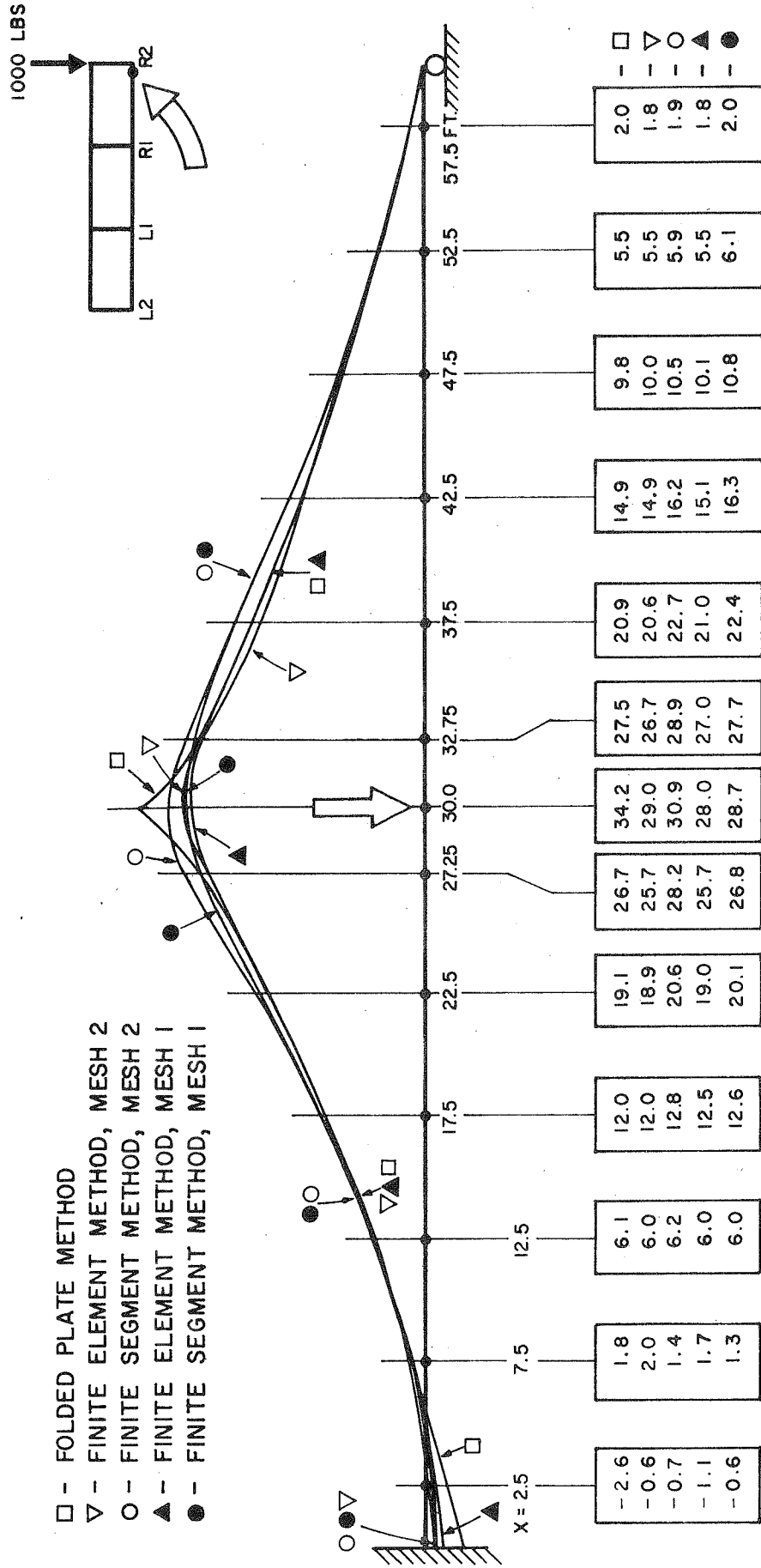


FIG. 50 LONGITUDINAL DISTRIBUTION OF TRANSVERSE MOMENT M_y (FT-LB/FT) IN BOTTOM SLAB

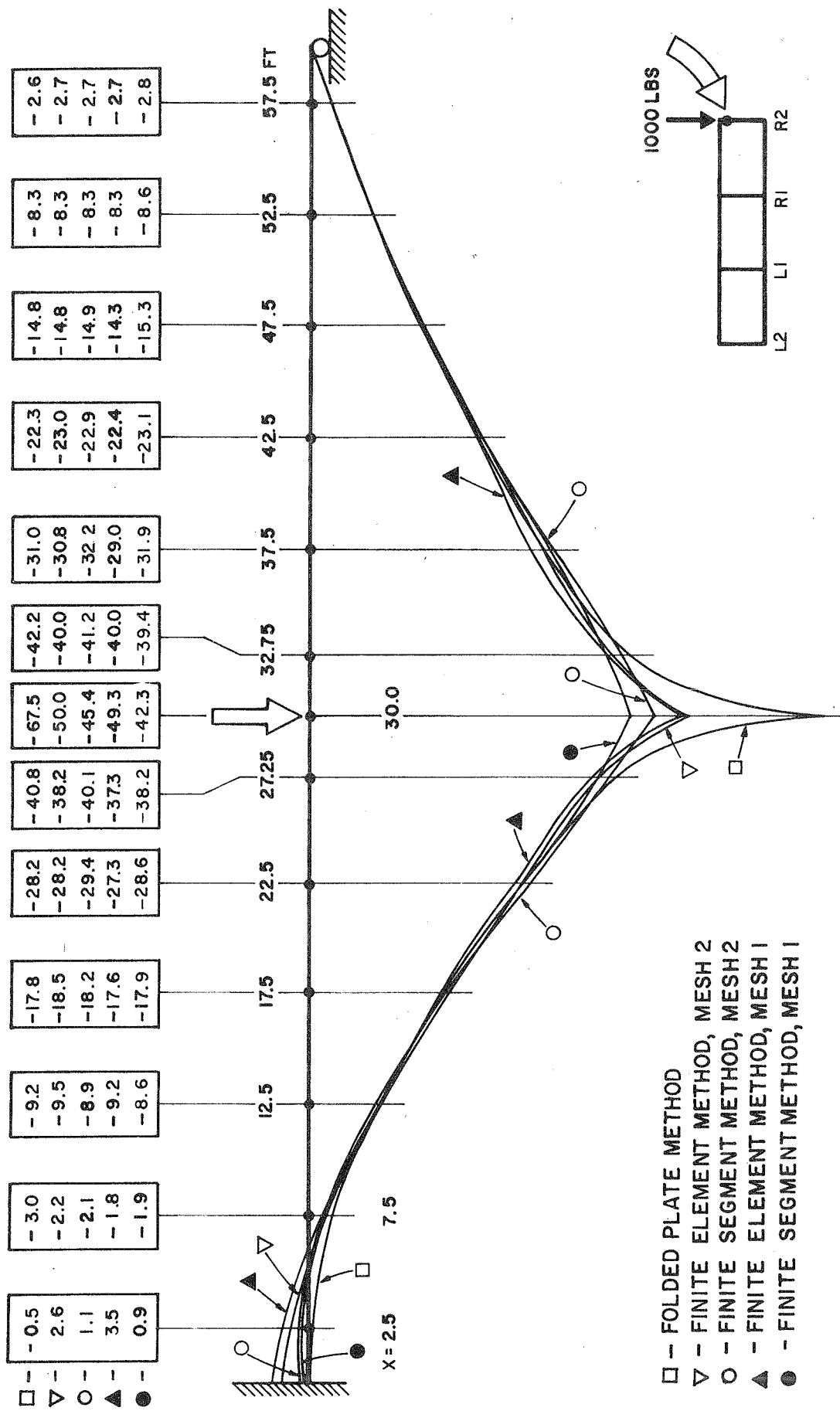


FIG. 51 LONGITUDINAL DISTRIBUTION OF TRANSVERSE MOMENT My (FT-LB/FT) AT TOP OF EXTERNAL WEB

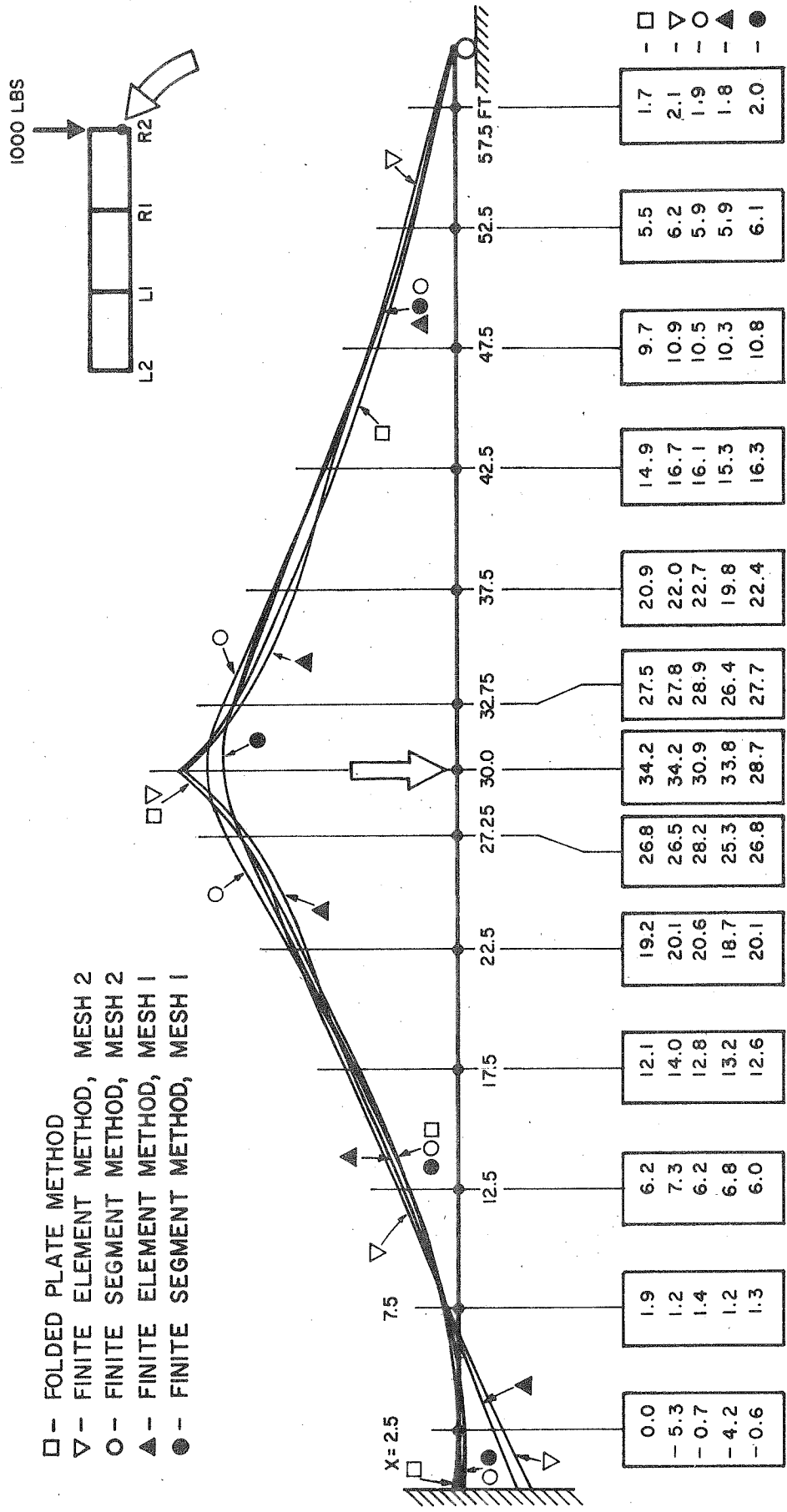
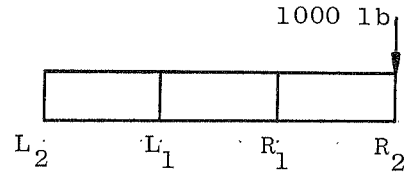


FIG. 52 LONGITUDINAL DISTRIBUTION OF TRANSVERSE MOMENT M_y (FT-LB/FT) AT BOTTOM OF EXTERNAL WEB.

TABLE 1: DISTRIBUTION OF MOMENTS TO EACH GIRDER
FOR 3-CELL BRIDGE UNDER ECCENTRIC LOAD
(FIXED-SIMPLE END SUPPORT CONDITIONS)



| Section | Girder | Folded Plate | | Finite Element | | | | Finite Segment | | | |
|---------------|------------------|--------------|-------|----------------|-------|------------|-------|----------------|-------|------------|-------|
| | | M ft-lb | % | Mesh 1 | | Mesh 2 | | Mesh 1 | | Mesh 2 | |
| | | | | M ft-lb | % | M ft-lb | % | M ft-lb | % | M ft-lb | % |
| Midspan | C L ₂ | 412 | 4.3 | 424 | 3.9 | 412 | 4.5 | 383 | 4.1 | 421 | 4.4 |
| | H L ₁ | 1265 | 13.3 | 1287 | 11.9 | 1251 | 13.6 | 1150 | 12.3 | 1242 | 13.1 |
| | H R ₁ | 2925 | 30.8 | 3566 | 32.9 | 2829 | 30.8 | 2824 | 30.2 | 2804 | 29.5 |
| | J R ₂ | 4894 | 51.6 | 5568 | 51.3 | 4690 | 51.1 | 4994 | 53.4 | 5045 | 53.0 |
| | Total | 9496 | 100.0 | 10845 | 100.0 | 9182 | 100.0 | 9351 | 100.0 | 9512 | 100.0 |
| Fixed Support | C L ₂ | 914 | 8.3 | 1040 | 8.4 | 1074 | 9.3 | 818 | 7.4 | 860 | 7.8 |
| | H L ₁ | 1994 | 18.2 | 2051 | 16.6 | 2258 | 19.5 | 1879 | 17.0 | 2007 | 18.2 |
| | H R ₁ | 4023 | 36.7 | 4383 | 35.5 | 4204 | 36.3 | 4101 | 37.1 | 4140 | 37.5 |
| | J R ₂ | 4040 | 36.8 | 4870 | 39.5 | 4040 | 34.9 | 4256 | 38.5 | 4034 | 36.5 |
| | Total | 10971 | 100.0 | 12344 | 100.0 | 11576 | 100.0 | 11054 | 100.0 | 11041 | 100.0 |

A study of Figs. 49 to 52 indicates good agreement between the results of all five analyses except in the sensitive vicinity of the concentrated load at midspan. In this vicinity a refinement of the mesh from Mesh 1 to Mesh 2 for both the finite element and the finite segment methods generally improves the comparison with the results of the folded plate method.

Static equilibrium requires that the sum of the transverse moments acting on a longitudinal joint should be zero. Thus, for a longitudinal joint at the top or bottom of the exterior web, the transverse moments in the slab should be equal and opposite to those in the web. Comparing these moments in Figs. 49 to 52, it can be seen that both the results of the folded plate and finite segment methods accurately satisfy static equilibrium, while for the finite element method this requirement is only satisfied approximately.

The transverse distribution of the transverse slab moments at midspan are shown in Figs. 53, 54 and 55. Both the folded plate and the finite element methods, which assume two way slab action, give distributions which are distinctly non-linear in the slabs of the loaded cell. The high moments directly under the concentrated load are clearly given by the folded plate method. The finite segment method, because of its assumption of one way slab action, gives transverse distributions in the slabs which are linear between the web supports. Thus the peak moments directly under the concentrated load cannot be found by this method.

5.7 Computer Times

The execution times, using an IBM 7094 digital computer, for each of the five analyses described in this chapter, were as follows:

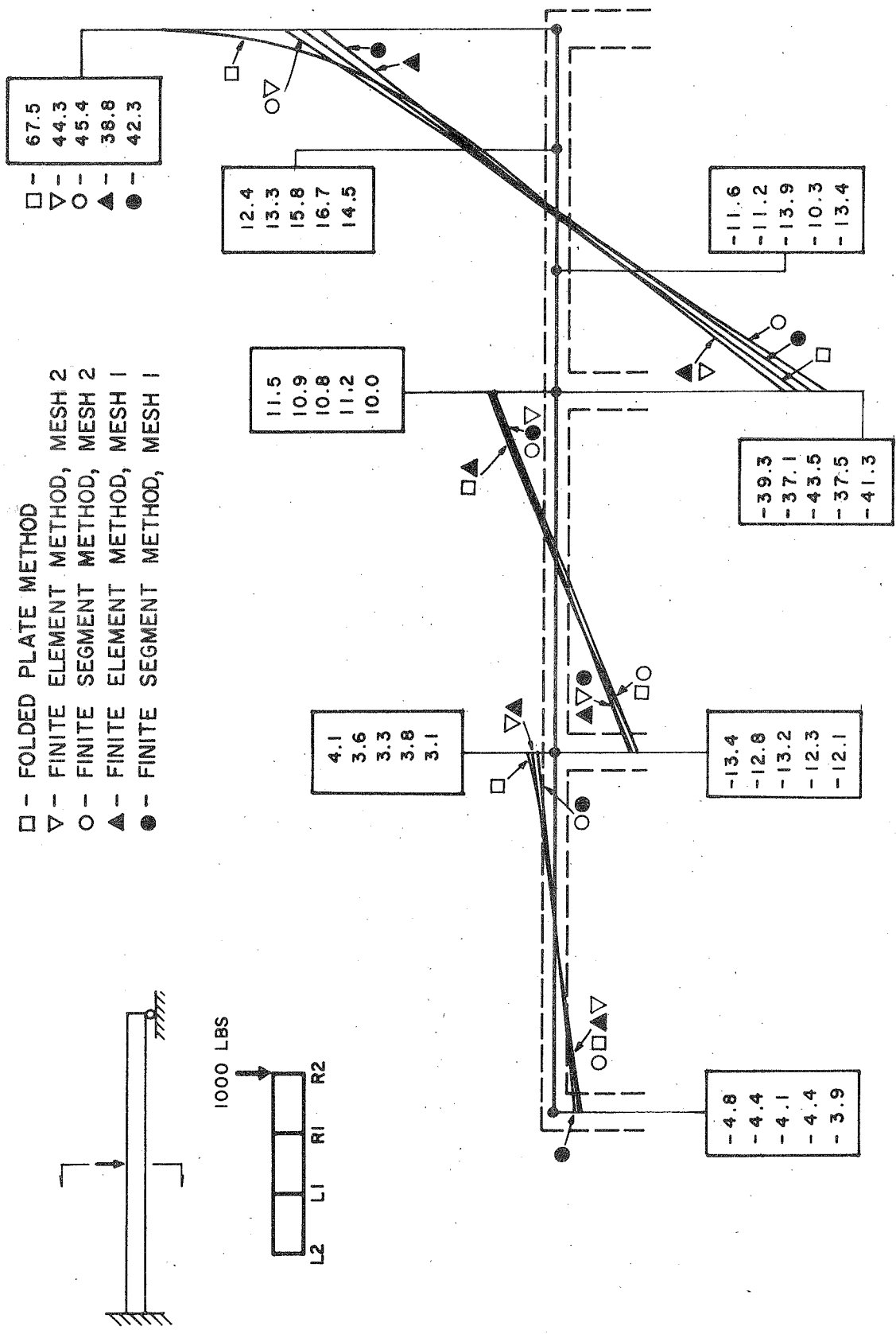


FIG. 53 TRANSVERSE DISTRIBUTION OF TRANSVERSE SLAB MOMENT M_y (FT-LB/FT) IN TOP SLAB AT MIDSPAN.

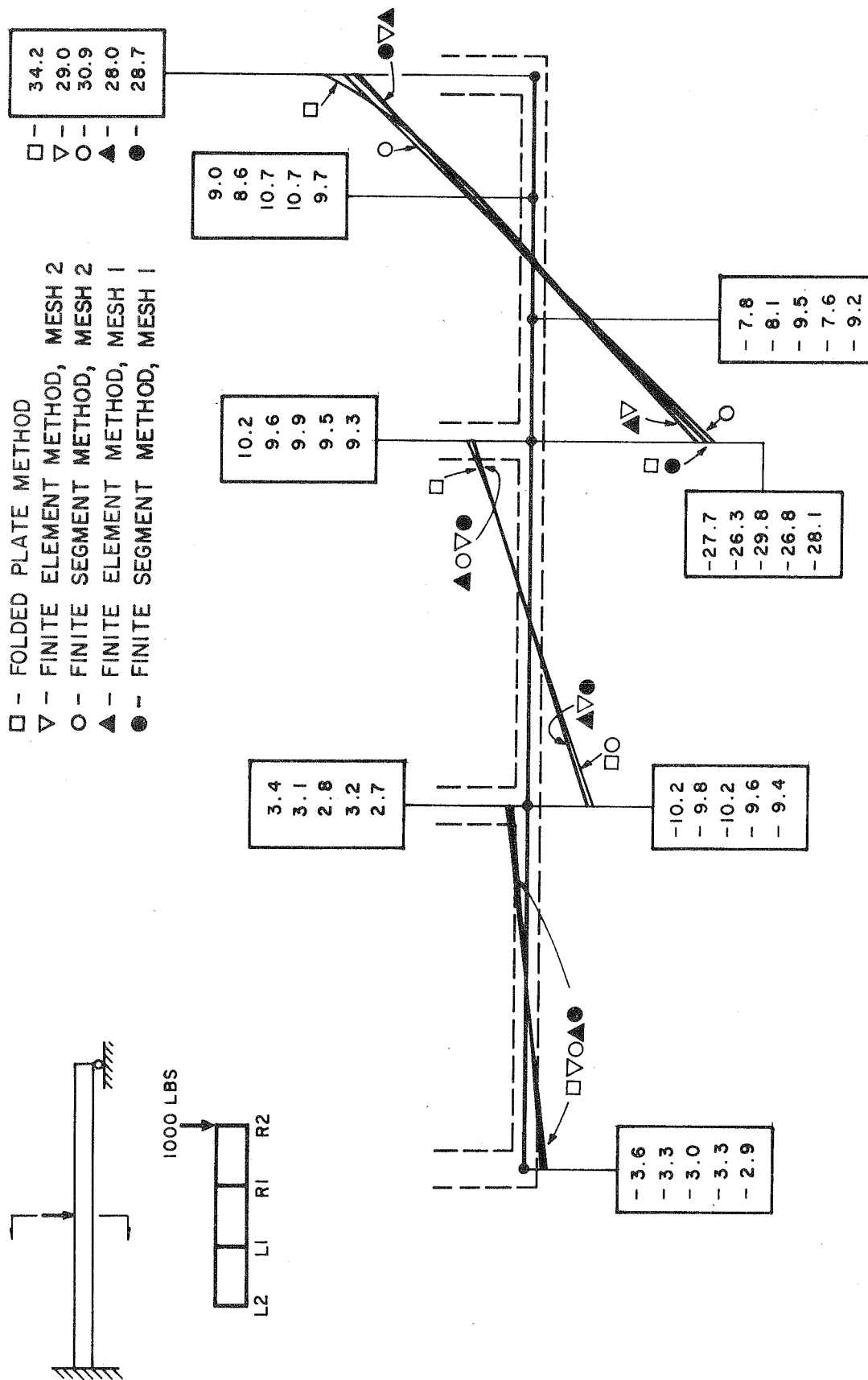


FIG. 54 TRANSVERSE DISTRIBUTION OF TRANSVERSE SLAB MOMENT M_y (FT-LB/FT) IN BOTTOM SLAB AT MIDSPAN

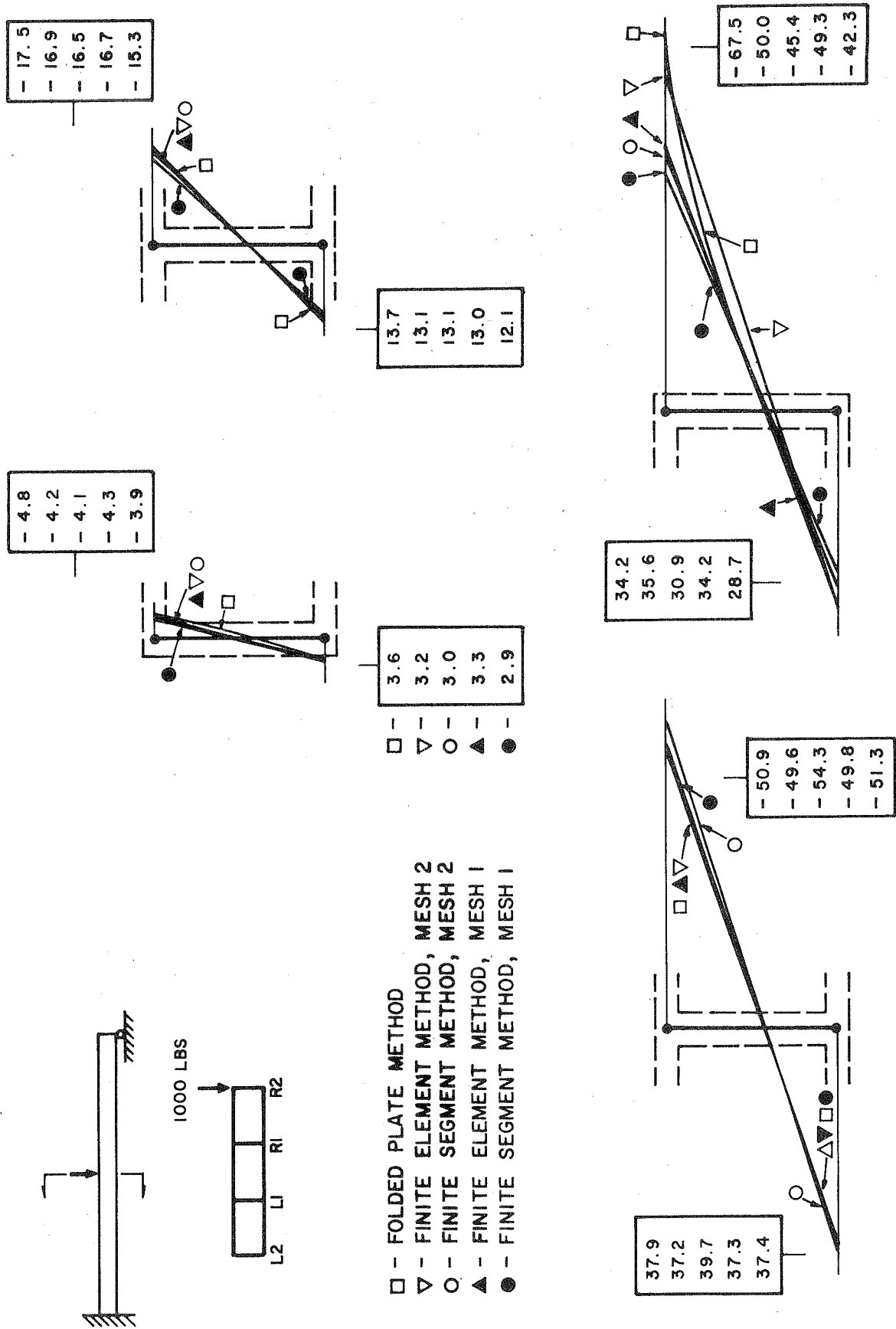


FIG. 55 TRANSVERSE DISTRIBUTION OF TRANSVERSE SLAB MOMENT M_y (FT-LB/FT) IN WEBS AT MIDSPAN.

| | |
|--------------------------------|-----------------|
| Folded Plate Method | 4 min. 27 sec. |
| Finite Element Method - Mesh 1 | 5 min. 50 sec. |
| Finite Element Method - Mesh 2 | 18 min. 17 sec. |
| Finite Segment Method - Mesh 1 | 2 min. 35 sec. |
| Finite Segment Method - Mesh 2 | 5 min. 48 sec. |

It can be seen that for a given mesh size the computer times required by the finite segment method are much less than by the finite element method. Also as the mesh size is refined the computer times required increase much more rapidly by the finite element method than by the finite segment method.

Wherever applicable, the folded plate method should be used, since it gives the most accurate results and requires a reasonable amount of computer time. Wherever structural geometry, variations in material properties, end support conditions and interior supports preclude the use of the folded plate method, the finite segment method should be used if the assumptions of the ordinary theory of folded plates are acceptable. Where these are not acceptable, the finite element method must be used, in which case, care must be taken to insure that an adequately refined mesh size is used to yield sufficiently accurate results.

6. STUDY OF 3-CELL AND 6-CELL BRIDGES

6.1 General Remarks

Of particular interest in the present study is the effect of longitudinal continuity on the load distribution in box girder bridges. In present design methods, a typical repeating segment of the cross-section, consisting of a top and bottom flange and a single web, is taken from the cross-section and is treated as an independent longitudinal girder. For wheel loads placed on the bridge deck, empirical formulas are used to determine the load distribution to the independent girder, which is then analyzed as a continuous beam to determine positive and negative moments for design. The load distribution factors presently used for concrete box girder bridges are based solely on a single parameter, the center to center spacing of the webs in the box girder cross-section, and the same factor is used for both positive and negative moments in the independent girder.

In order to make a rational study of the problem of load distribution in a multi-celled continuous box girder bridge subjected to a single concentrated load at midspan, two basic questions need to be answered.

1. What is the division of the total statical moment in a given span between the total positive moment at the midspan section and the total negative moments at the support sections?

2. What is the transverse distribution of the above total positive or negative moments at a section to each of the independent longitudinal girders?

Many factors may influence the answers to these questions besides the single parameter of the center to center spacing of webs in the cross-section.

Among these factors may be the geometry and dimensions of the bridge, the number of cells in the cross-section, the transverse position of the concentrated load on the bridge deck, and the degree of longitudinal continuity at the supports.

6.2 Description of Example Bridges Analyzed.

A 3-cell and a 6-cell bridge cross-section were selected as the two basic bridge types for the parameter studies. The cross-sectional dimensions of these bridges, shown in Fig. 56, are identical to those used for some of the example bridges in the initial report on simply supported bridges [1]. A single 60 ft. span was analyzed with three different sets of end conditions. The end conditions used were simple-simple, fixed-simple and fixed-fixed as shown in Fig. 57. These conditions give a range of results which can be extrapolated to the variations in end conditions found in spans of an actual continuous bridge. Two loading conditions were studied involving a single midspan load of 1,000 lb. distributed over a 1 ft. length and placed at two transverse positions on the bridge deck, Fig. 56. The first load position, designated 1, was at a central lateral position and the second load position, designated 4, was at an extreme eccentric lateral position over an exterior web. These designations correspond with those used in the initial report [1].

A total of 23 separate computer analyses were performed; eight by the folded plate method; three by the finite element method; and twelve by the finite segment method. The cases analyzed are summarized in Table 2. Note that the fixed-fixed support condition cannot be analyzed by the folded plate method because the method is limited to structures with simply supported ends. Only the 3-cell cross-section was analyzed by the finite element method because of the excessive computer times required for the 6-cell cross-section. All cases were analyzed by the finite segment method. A modulus of elasticity equal to 3,000,000 psi was used for all the analyses, while Poisson's ratio was assumed as 0.15 for the folded plate and finite element methods and as zero for the finite segment method.

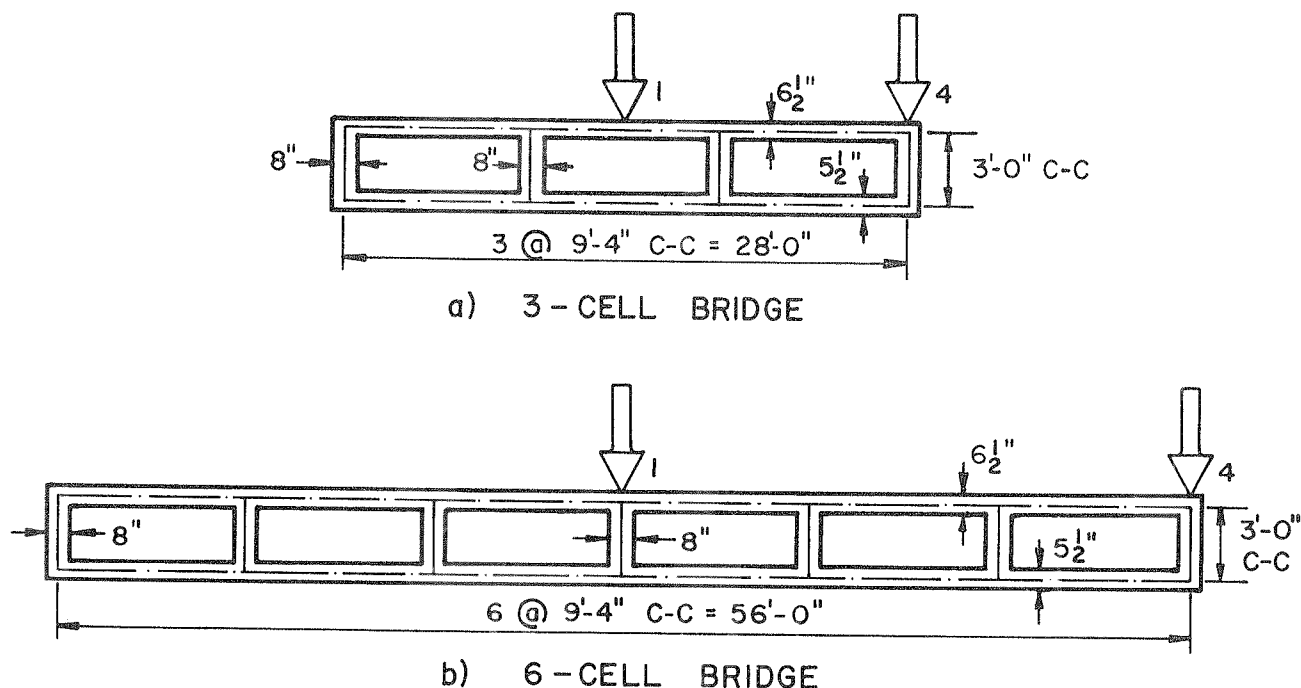


FIG. 56 TRANSVERSE SECTION DIMENSIONS AND LOAD POSITIONS FOR EXAMPLE BRIDGES

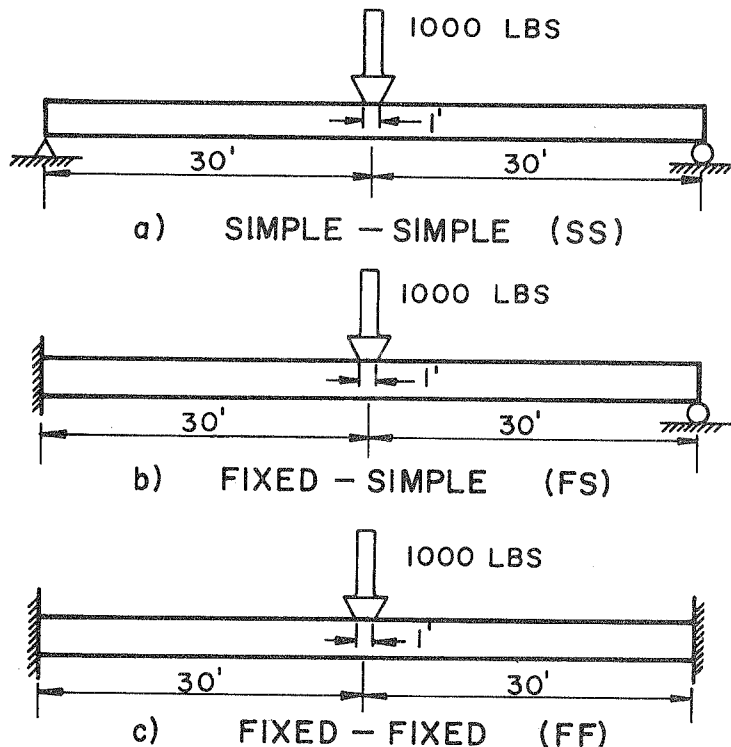


FIG. 57 END CONDITIONS FOR EXAMPLE BRIDGES

For each of the computer analyses listed in Table 2, analytical models had to be selected which divided the structure into a series of plates, finite elements, or finite segments, interconnected at joints. For the folded plate analysis 99 harmonics were used to represent the applied load and the reactions. The longitudinal subdivisions into finite elements and finite segments for all cases were the same as those shown in Figs. 31 and 33. The transverse element subdivisions and locations of longitudinal joints for the various cases are shown in Figs. 58, 59, and 60. For the 3-cell bridge, Fig. 58, the full cross-section was used.

For the 6-cell bridge under an eccentric load, Fig. 59, the solutions by both the folded plate method and the finite segment method were obtained by the superposition of symmetric and antisymmetric loading cases so that only half of the cross-section had to be used in the computer analyses. The boundary conditions imposed at the joints lying on the plane of structural symmetry are shown in Figs. 59b and 59c. For the symmetric load case the horizontal joint displacements and the rotations about the longitudinal joints are set to zero. For the antisymmetric load case the vertical and longitudinal joint displacements are set to zero. In addition, for the web member lying on the plane of structural symmetry, the in-plane plate stiffness must be halved for the symmetric load case and the slab stiffness must be halved for the antisymmetric load case. This is most easily accomplished by assigning this member a modulus of elasticity equal to one-half that used when analyzing the entire cross-section. Due account of this has to be taken when interpreting the computer output for internal forces in this member. For the 6-cell bridge, under a central load, Fig. 60, once more, advantage was taken of symmetry so that only one-half of the structure had to be analyzed by the computer.

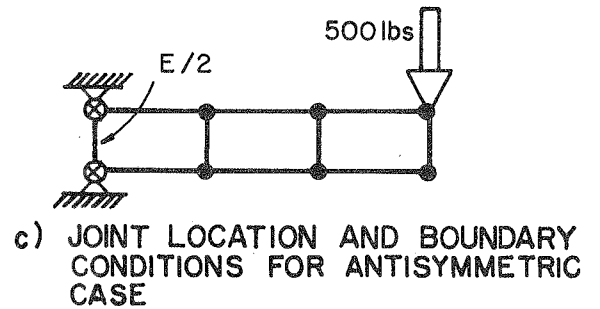
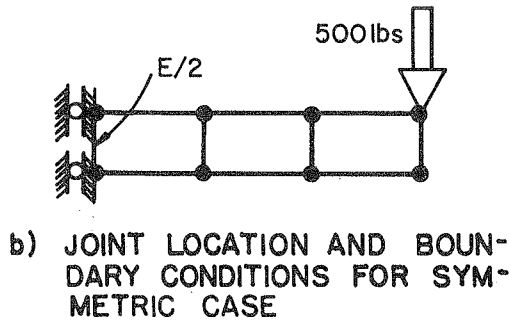
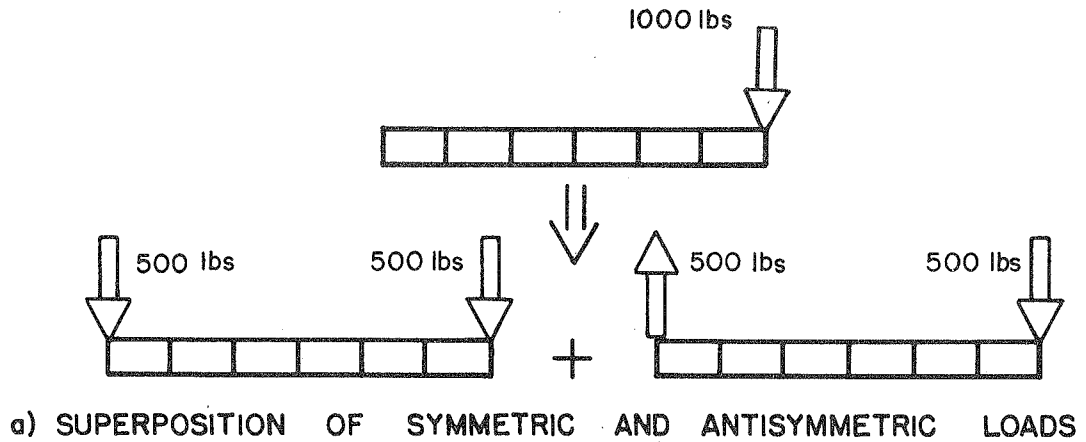


FIG. 59 TRANSVERSE ELEMENT SUBDIVISION OF 6-CELL BRIDGE UNDER ECCENTRIC LOAD FOR FOLDED PLATE AND FINITE SEGMENT ANALYSES

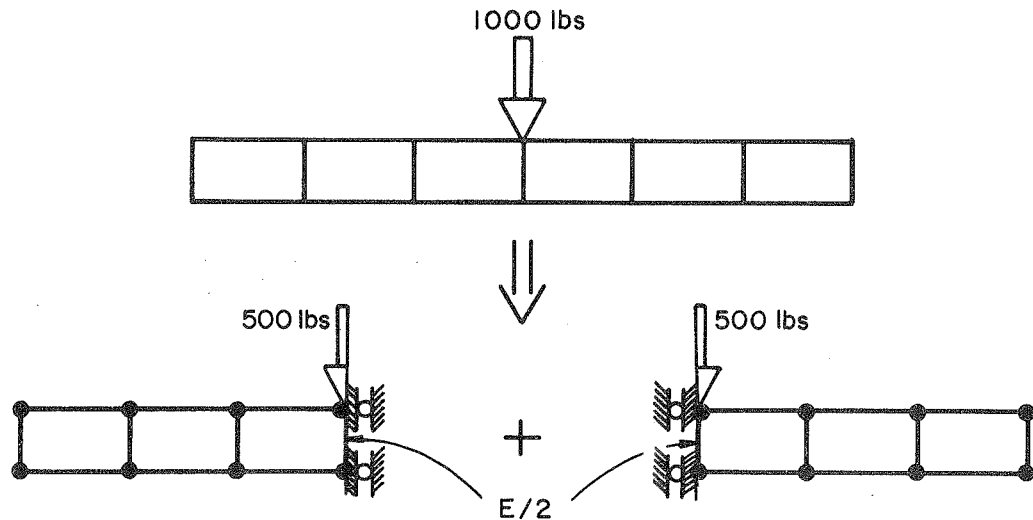


FIG. 60 TRANSVERSE ELEMENT SUBDIVISION OF 6-CELL BRIDGE UNDER CENTRAL LOAD FOR FOLDED PLATE AND FINITE SEGMENT ANALYSES

TABLE 2: SUMMARY OF COMPUTER ANALYSES PERFORMED
ON EXAMPLE BRIDGES

| Case | End Support Conditions ¹ | Number of Cells | Transverse Load Position ² | Folded Plate Method | Finite Element Method | Finite Segment Method |
|-----------|-------------------------------------|-----------------|---------------------------------------|---------------------|-----------------------|-----------------------|
| 60-3-1-SS | SS | 3 | 1 | x | x | x |
| 60-3-1-FS | FS | 3 | 1 | x | x | x |
| 60-3-1-FF | FF | 3 | 1 | | x | x |
| 60-3-4-SS | SS | 3 | 4 | x | | x |
| 60-3-4-FS | FS | 3 | 4 | x | | x |
| 60-3-4-FF | FF | 3 | 4 | | | x |
| 60-6-1-SS | SS | 6 | 1 | x | | x |
| 60-6-1-FS | FS | 6 | 1 | x | | x |
| 60-6-1-FF | FF | 6 | 1 | | | x |
| 60-6-4-SS | SS | 6 | 4 | x | | x |
| 60-6-4-FS | FS | 6 | 4 | x | | x |
| 60-6-4-FF | FF | 6 | 4 | | | x |

1. SS = Simple-Simple; FS = Fixed-Simple; FF = Fixed-Fixed

2. 1 - Central load; 4 - Eccentric load over exterior web.

6.3 Distribution of Moments to Each Girder

The distribution to each individual longitudinal girder of the total longitudinal moment at the midspan and the fixed end support sections was calculated by the procedure described in Section 5.5. The results of these calculations for all of the cases listed in Table 2 are presented in Tables 3, 4, 5 and 6. Based on a study of these results a number of points are discussed in the sections that follow.

6.3.1 Comparison of Results by Different Methods

Results obtained by the folded plate and the finite segment methods are close to each other for both the total moment at a section and the percent of this total taken by each girder. Differences between the results by the two methods are of the order of 1 to 2%. Results by the finite element method, given in Table 3, tend to be on the high side especially for the moments taken by Girders R_1 and R_2 . A refinement of mesh size as discussed in Section 5.5 is required to get more accurate results by this method.

Since the finite segment method gives accurate results, it can be used to make extensive studies of this type for arbitrary end and interior boundary conditions. Further discussion of Tables 3, 4, 5 and 6 will be based on the results by this method.

6.3.2 Longitudinal Division of Total Statical Moment Between Positive and Negative Moments.

The moment diagrams for a beam subjected to a midspan concentrated load of 1000 lbs. with end conditions of simple-simple, fixed-simple, and fixed-fixed are shown in Figs. 61, 62, 63. It is of particular importance to compare the moments at midspan and at the supports given in these figures with those obtained for the total moments at a section given in Tables 3, 4, 5 and 6. It is seen that the results are essentially the same, being within 1 or 2% of each other for all cases. The following conclusions may be drawn:

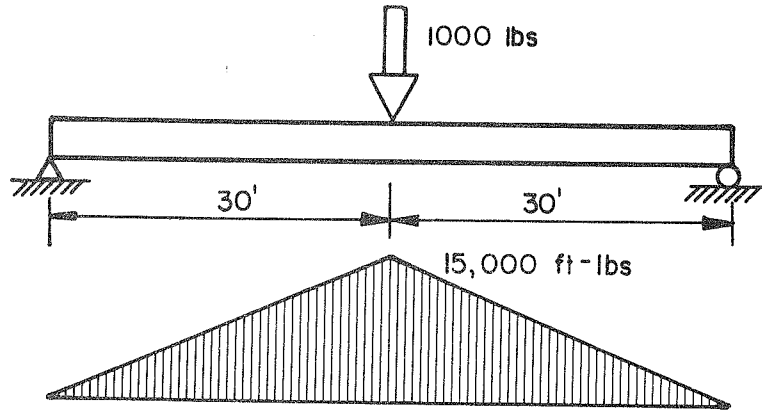


FIG. 61 BEAM MOMENT DIAGRAM FOR SIMPLE-SIMPLE CASE

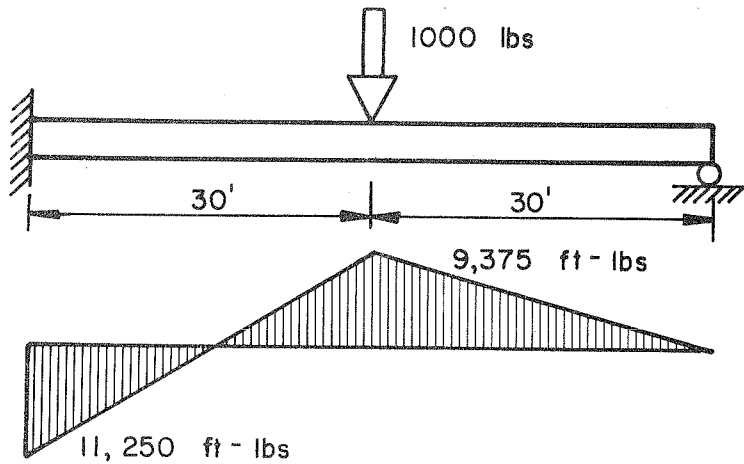


FIG. 62 BEAM MOMENT DIAGRAM FOR FIXED-SIMPLE CASE

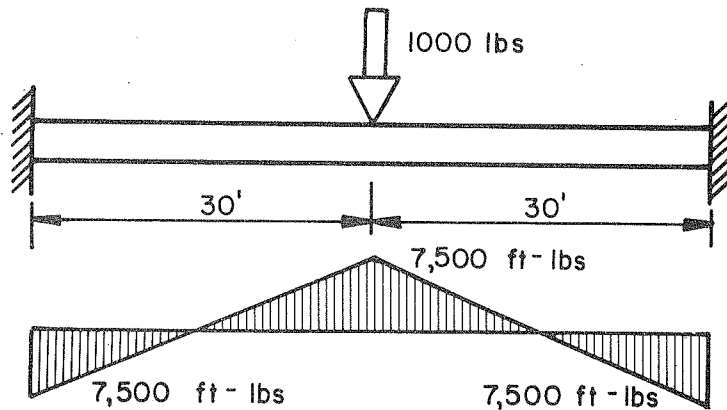
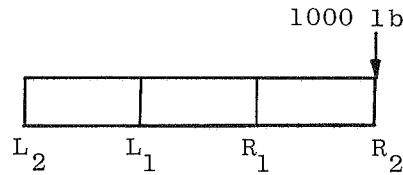


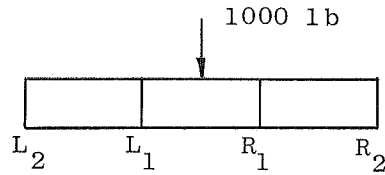
FIG. 63 BEAM MOMENT DIAGRAM FOR FIXED-FIXED CASE

TABLE 3. DISTRIBUTION OF MOMENTS TO EACH GIRDER
FOR 3-CELL BRIDGE UNDER ECCENTRIC LOAD



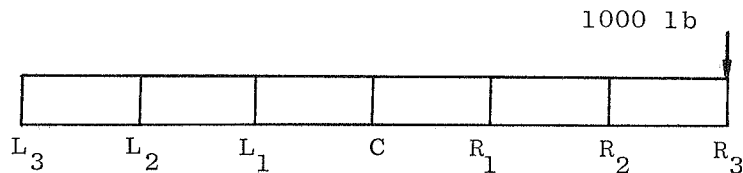
| Method | Section | | At Midspan | | | | | | At Support | | | |
|----------------|--------------------|----------------|---------------|-------|--------------|-------|-------------|-------|--------------|-------|-------------|-------|
| | Support Conditions | | Simple-Simple | | Fixed-Simple | | Fixed-Fixed | | Fixed-Simple | | Fixed-Fixed | |
| | Girder | | M ft-lb | % | M ft-lb | % | M ft-lb | % | M ft-lb | % | M ft-lb | % |
| Folded Plate | C | L ₂ | 1324 | 8.9 | 412 | 4.3 | | | 914 | 8.3 | | |
| | H | L ₁ | 3037 | 20.4 | 1265 | 13.3 | | | 1994 | 18.2 | | |
| | H | R ₁ | 4810 | 32.3 | 2925 | 30.8 | | | 4023 | 36.7 | | |
| | J | R ₂ | 5713 | 38.4 | 4894 | 51.6 | | | 4040 | 36.8 | | |
| | Total | | 14884 | 100.0 | 9496 | 100.0 | | | 10971 | 100.0 | | |
| Finite Element | C | L ₂ | 1351 | 8.2 | 424 | 3.9 | 101 | 1.1 | 1040 | 8.4 | 385 | 4.7 |
| | H | L ₁ | 3032 | 18.4 | 1287 | 11.9 | 667 | 7.3 | 2051 | 16.6 | 1030 | 12.6 |
| | H | R ₁ | 5431 | 33.0 | 3566 | 32.9 | 2937 | 32.3 | 4383 | 35.5 | 3016 | 36.9 |
| | J | R ₂ | 6657 | 40.4 | 5568 | 51.3 | 5394 | 59.3 | 4870 | 39.5 | 3735 | 45.8 |
| | Total | | 16471 | 100.0 | 10845 | 100.0 | 9099 | 100.0 | 12344 | 100.0 | 8166 | 100.0 |
| Finite Segment | C | L ₂ | 1310 | 8.8 | 383 | 4.1 | 66 | 0.9 | 818 | 7.4 | 307 | 4.1 |
| | H | L ₁ | 2933 | 19.7 | 1150 | 12.3 | 538 | 7.3 | 1879 | 17.0 | 900 | 12.0 |
| | H | R ₁ | 4675 | 31.4 | 2824 | 30.2 | 2125 | 28.8 | 4101 | 37.1 | 2834 | 37.8 |
| | J | R ₂ | 5970 | 40.1 | 4994 | 53.4 | 4648 | 63.0 | 4256 | 38.5 | 3456 | 46.1 |
| | Total | | 14888 | 100.0 | 9351 | 100.0 | 7377 | 100.0 | 11054 | 100.0 | 7497 | 100.0 |

TABLE 4: DISTRIBUTION OF MOMENTS TO EACH GIRDER
FOR 3-CELL BRIDGE UNDER CENTER LOAD



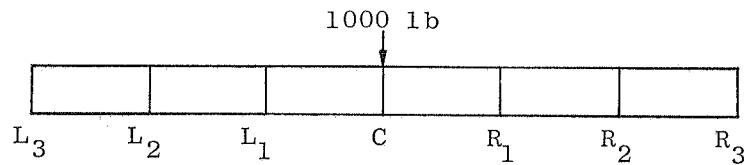
| Method | Section | | At Midspan | | | | | | At Support | | | |
|----------------|--------------------|----------------|---------------|-------|--------------|-------|-------------|-------|--------------|-------|-------------|-------|
| | Support Conditions | | Simple-Simple | | Fixed-Simple | | Fixed-Fixed | | Fixed-Simple | | Fixed-Fixed | |
| | Girder | | M ft-lb | % | M ft-lb | % | M ft-lb | % | M ft-lb | % | M ft-lb | % |
| Folded Plate | C | L ₂ | 2104 | 14.0 | 1129 | 12.0 | | | 1682 | 15.7 | | |
| | H | L ₁ | 5447 | 36.0 | 3570 | 38.0 | | | 3682 | 34.3 | | |
| | H | R ₁ | 5447 | 36.0 | 3570 | 38.0 | | | 3682 | 34.3 | | |
| | J | R ₂ | 2104 | 14.0 | 1129 | 12.0 | | | 1682 | 15.7 | | |
| | Total | | 15102 | 100.0 | 9398 | 100.0 | | | 10728 | | | |
| Finite Segment | C | L ₂ | 2110 | 14.1 | 1142 | 12.1 | 780 | 10.5 | 1680 | 15.2 | 1036 | 13.8 |
| | H | L ₁ | 5372 | 35.9 | 3578 | 37.9 | 2935 | 39.5 | 3846 | 34.8 | 2717 | 36.2 |
| | H | R ₁ | 5372 | 35.9 | 3578 | 37.9 | 2935 | 39.5 | 3846 | 34.8 | 2717 | 36.2 |
| | J | R ₂ | 2110 | 14.1 | 1142 | 12.1 | 780 | 10.5 | 1680 | 15.2 | 1036 | 13.8 |
| | Total | | 14964 | 100.0 | 9440 | 100.0 | 7430 | 100.0 | 11052 | 100.0 | 7506 | 100.0 |














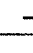
TABLE 5: DISTRIBUTION OF MOMENTS TO EACH GIRDER
FOR 6-CELL BRIDGE UNDER ECCENTRIC LOAD



| Method | Section | | At Midspan | | | | | | At Support | | | |
|----------------|--------------------|----------------|---------------|-------|--------------|-------|-------------|-------|--------------|-------|-------------|-------|
| | Support Conditions | | Simple-Simple | | Fixed-Simple | | Fixed-Fixed | | Fixed-Simple | | Fixed-Fixed | |
| | Girder | | M ft-lb | % | M ft-lb | % | M ft-lb | % | M ft-lb | % | M ft-lb | % |
| Folded Plate | C | L ₃ | 239 | 1.6 | 26 | 0.3 | | | 78 | 0.7 | | |
| | H | L ₂ | 551 | 3.7 | 92 | 1.0 | | | 169 | 1.5 | | |
| | H | L ₁ | 807 | 5.5 | 197 | 2.1 | | | 350 | 3.2 | | |
| | H | C | 1312 | 8.9 | 451 | 4.7 | | | 783 | 7.1 | | |
| | H | R ₁ | 2236 | 15.2 | 1073 | 11.3 | | | 1717 | 15.7 | | |
| | H | R ₂ | 4214 | 28.6 | 2811 | 29.6 | | | 3887 | 35.5 | | |
| | J | R ₃ | 5381 | 36.5 | 4834 | 51.0 | | | 3974 | 36.3 | | |
| | Total | | 14740 | 100.0 | 9484 | 100.0 | | | 10958 | 100.0 | | |
| Finite Segment | C | L ₃ | 326 | 2.2 | 19 | 0.2 | 0 | 0.0 | 66 | 0.6 | 7 | 0.1 |
| | H | L ₂ | 830 | 5.6 | 66 | 0.7 | 0 | 0.0 | 121 | 1.1 | 7 | 0.1 |
| | H | L ₁ | 875 | 5.9 | 159 | 1.7 | 15 | 0.2 | 287 | 2.6 | 59 | 0.8 |
| | H | C | 1260 | 8.5 | 433 | 4.3 | 110 | 1.5 | 684 | 6.2 | 259 | 3.5 |
| | H | R ₁ | 2046 | 13.8 | 985 | 10.5 | 501 | 6.8 | 1655 | 15.0 | 894 | 12.1 |
| | H | R ₂ | 3854 | 26.0 | 2748 | 29.3 | 2115 | 28.7 | 3994 | 36.2 | 2824 | 38.2 |
| | J | R ₃ | 5633 | 38.0 | 5000 | 53.3 | 4629 | 62.8 | 4226 | 38.3 | 3341 | 45.2 |
| | Total | | 14824 | 100.0 | 9380 | 100.0 | 7370 | 100.0 | 11033 | 100.0 | 7391 | 100.0 |

TABLE 6: DISTRIBUTION OF MOMENTS TO EACH GIRDER
FOR 6-CELL BRIDGE UNDER CENTER LOAD



| Method | Section | At Midspan | | | | | | At Support | | | |
|----------------|--|---------------|-------|--------------|-------|-------------|-------|--------------|-------|-------------|-------|
| | Support Conditions | Simple-Simple | | Fixed-Simple | | Fixed-Fixed | | Fixed-Simple | | Fixed-Fixed | |
| | Girder | M ft-lb | % | M ft-lb | % | M ft-lb | % | M ft-lb | % | M ft-lb | % |
| Folded Plate |  L ₃ | 700 | 4.7 | 243 | 2.5 | | | 487 | 4.5 | | |
| |  L ₂ | 1579 | 10.6 | 706 | 7.4 | | | 1059 | 9.7 | | |
| |  L ₁ | 2490 | 16.6 | 1577 | 16.5 | | | 2076 | 19.0 | | |
| |  C | 5420 | 36.2 | 4498 | 47.2 | | | 3678 | 33.6 | | |
| |  R ₁ | 2490 | 16.6 | 1577 | 16.5 | | | 2076 | 19.0 | | |
| |  R ₂ | 1579 | 10.6 | 706 | 7.4 | | | 1059 | 9.7 | | |
| |  R ₃ | 700 | 4.7 | 243 | 2.5 | | | 487 | 4.5 | | |
| | Total | 14958 | 100.0 | 9550 | 100.0 | | | 10922 | 100.0 | | |
| Finite Segment |  L ₃ | 684 | 4.6 | 215 | 2.3 | 66 | 0.9 | 408 | 3.7 | 157 | 2.1 |
| |  L ₂ | 1532 | 10.3 | 634 | 6.8 | 332 | 4.5 | 980 | 8.9 | 495 | 6.6 |
| |  L ₁ | 2454 | 16.5 | 1521 | 16.3 | 1172 | 15.9 | 2115 | 19.2 | 1462 | 19.5 |
| |  C | 5533 | 37.2 | 4590 | 49.2 | 4233 | 57.4 | 4009 | 36.4 | 3270 | 43.6 |
| |  R ₁ | 2454 | 16.5 | 1521 | 16.3 | 1172 | 15.9 | 2115 | 19.2 | 1462 | 19.5 |
| |  R ₂ | 1532 | 10.3 | 634 | 6.8 | 332 | 4.5 | 980 | 8.9 | 495 | 6.6 |
| |  R ₃ | 684 | 4.6 | 215 | 2.3 | 66 | 0.9 | 408 | 3.7 | 157 | 2.1 |
| | Total | 14873 | 100.0 | 9330 | 100.0 | 7373 | 100.0 | 11015 | 100.0 | 7498 | 100.0 |

(1) The results from the computer analyses satisfy statics.

(2) The division of the total statical moment in the box girder bridges between the total positive moment at midspan and the total negative moment at the support is the same as that found in a beam subjected to the same loading. Furthermore, it appears that this is true irrespective of the number of cells in the bridge or of the transverse position of the load on the bridge deck. Thus, only the transverse distribution of these total moments at a section to each girder need be further studied.

The second conclusion could be deduced approximately by the following simplified reasoning. First, assume the continuous box girder bridge to be cut along longitudinal lines in the top and bottom slabs at the midpoint between the webs, thus dividing the bridge into several individual and independent girders. If all of these girders have the same longitudinal variations of flexural and shear stiffness and ratios of these stiffnesses, similar moment diagrams would exist for each of the girders for similar loadings. The loadings on the girders consist of the applied external loading plus equal and opposite interaction forces at the cuts between the girders. The moment diagram due to the applied loading is the same as that in a continuous beam under the same loading, while the moment diagrams due to the equal and opposite interaction forces between the girders will cancel each other out when summed for all the girders. This is what occurs in box girder bridges of usual span lengths. If the individual girders have substantially different longitudinal variations of flexural or shear stiffness or ratios of these stiffnesses then this would not be true.

6.3.3 Transverse Distribution of Moments to Each Girder

The transverse distribution of moments to each girder is influenced by whether the midspan or support section is being considered, the

end boundary conditions, the number of cells in the cross-section and the transverse position of the load on the bridge deck. For a uniform distribution across the section, the percentage moment taken by each interior girder would be approximately equal to 100% divided by the number of cells in the bridge, while that for the exterior girders would be half this value. These percentages for interior and exterior girders are thus 33.3 and 16.7% for the 3-cell bridge and 16.7 and 8.3% for the 6-cell bridge. From a study of Tables 3, 4, 5 and 6 the following comments may be made:

(1) For a given case, a more uniform and thus a better distribution is obtained at a support section than at a midspan section. The percentage moment taken by the most highly stressed girder at a support section is from 3 to 17% less than that at a midspan section for the same girder. Thus it would seem that different distribution factors should be used at these two sections.

(2) For a given span, the results for different end boundary conditions show that increasing the fixity at the supports gives a poorer distribution of moments. This is to be expected since the ability of a bridge to distribute a concentrated load transversely is a function of the ratio of the relative stiffnesses in the transverse and longitudinal directions. As this ratio is decreased the distribution becomes poorer and vice-versa. An increase in end fixity or a decrease in span length increases the longitudinal stiffness resulting in a poorer distribution. Thus different distribution factors should be used for simple and continuous bridges having the same span lengths between supports. Further studies may show that the same distribution factors could be used at midspan for bridges with the same equivalent simple span between points of inflection.

(3) A load at position 4, over the exterior girder web, is the most severe loading case for the exterior web. Furthermore, comparing the results for the 3-cell and the 6-cell bridges in Tables 3 and 5, for any given set of end boundary conditions the percentages of the total moment taken by the exterior girder are within 1 or 2% of each other. This indicates the localized effect of this loading.

6.5 Midspan Deflections

The midspan vertical deflections found from the computer analyses of the cases listed in Table 2 are given in Table 7.

The agreement between the results for a specific case as obtained by the three methods of analysis is generally good for all loading cases.

Comparing the transverse distribution of deflections in Table 7 it is seen that increasing the fixity at the end supports has two distinct and obvious effects.

- (1) The maximum deflection under the load is decreased.
- (2) The deflection damps out more rapidly in a transverse direction.

While the transverse distribution of deflections and of the total moment at a midspan section to each girder have the same general trend, no relationship was found that would simply and accurately relate these two quantities.

TABLE 7. MIDSPAN VERTICAL DEFLECTIONS IN FT. $\times 10^4$ FOR
ECCENTRIC AND CENTER LOADS ON 3 AND 6-CELL BRIDGES

| Support Conditions | | Simple-Simple | | | Fixed-Simple | | | Fixed-Fixed | |
|---------------------------------|----------------|---------------|-------------|--------------|--------------|-------------|--------------|-------------|--------------|
| Method | | Folded Plate | Finite Seg. | Finite Elem. | Folded Plate | Finite Seg. | Finite Elem. | Finite Seg. | Finite Elem. |
| Case | Gird. | | | | | | | | |
| 3-Cell Bridge Eccentric Load | L ₂ | 0.992 | 0.934 | 0.994 | 0.277 | 0.229 | 0.244 | 0.037 | 0.049 |
| | L ₁ | 1.173 | 1.122 | 1.115 | 0.412 | 0.359 | 0.366 | 0.120 | 0.131 |
| | R ₁ | 1.736 | 1.692 | 1.661 | 0.856 | 0.791 | 0.786 | 0.442 | 0.451 |
| | R ₂ | 3.051 | 3.051 | 2.933 | 2.069 | 2.047 | 1.956 | 1.614 | 1.540 |
| 3-Cell Bridge Center Load | L ₂ | 1.431 | 1.392 | | 0.614 | 0.561 | | 0.267 | |
| | L ₁ | 1.797 | 1.806 | | 0.976 | 0.967 | | 0.663 | |
| | R ₁ | 1.797 | 1.806 | | 0.976 | 0.967 | | 0.663 | |
| | R ₂ | 1.431 | 1.392 | | 0.614 | 0.561 | | 0.267 | |
| 6-Cell Bridge Eccentric Load | L ₃ | 0.180 | 0.337 | | 0.021 | 0.015 | | 0.000 | |
| | L ₂ | 0.210 | 0.286 | | 0.031 | 0.023 | | 0.000 | |
| | L ₁ | 0.312 | 0.329 | | 0.066 | 0.052 | | 0.006 | |
| | C | 0.510 | 0.484 | | 0.150 | 0.127 | | 0.027 | |
| | R ₁ | 0.871 | 0.805 | | 0.348 | 0.301 | | 0.114 | |
| | R ₂ | 1.528 | 1.414 | | 0.823 | 0.767 | | 0.440 | |
| | R ₃ | 2.874 | 2.719 | | 2.054 | 2.031 | | 1.612 | |
| 6-Cell Bridge Center Load | L ₃ | 0.510 | 0.484 | | 0.151 | 0.127 | | 0.027 | |
| | L ₂ | 0.604 | 0.581 | | 0.221 | 0.195 | | 0.071 | |
| | L ₁ | 0.901 | 0.883 | | 0.462 | 0.430 | | 0.254 | |
| | C | 1.619 | 1.639 | | 1.139 | 1.140 | | 0.925 | |
| | R ₁ | 0.901 | 0.883 | | 0.462 | 0.430 | | 0.254 | |
| | R ₂ | 0.604 | 0.581 | | 0.221 | 0.195 | | 0.071 | |
| | R ₃ | 0.510 | 0.484 | | 0.151 | 0.127 | | 0.027 | |

7. CONCLUSIONS

Three general methods for the elastic analysis of continuous box girder bridges have been presented and discussed. The methods are designated as the folded plate method, the finite segment method and the finite element method. General computer programs entitled MUPDI, SIMPLA and FINPLA have been developed and described which reduce the analysis by these methods to a simple matter of preparing basic input data on cards, which when used with the programs will yield the detailed output of all internal forces, moments and displacements at selected points.

Each of the methods developed has been shown to have certain advantages and disadvantages. The folded plate method, which is based on the elasticity theory for folded plates, is the most accurate of the methods developed. Where applicable it yields a complete solution in a reasonable amount of computer time. It is restricted to continuous structures with simple supports at the extreme ends and to cases in which the material and dimensional properties of each plate making up the cross-section are constant, both longitudinally and transversely.

The finite segment method, based on the ordinary theory of folded plates, may be applied to structures with arbitrary end and interior support conditions. For a reasonable mesh size, it requires a computer time for solution comparable to that by the folded plate method. It gives accurate results for deflections and for the distribution of the total moment at a section to each longitudinal girder. For a concentrated load over a web, a refinement of mesh size results in values of longitudinal stress and transverse slab moments which begin to approach those by the folded plate method except directly under the concentrated load. Because of the one way slab action assumed, it should not be used to predict local slab moments or deflections directly under a concentrated load applied between the webs.

The finite element method, based on the elasticity theory, is the most general of the methods presented. It can treat arbitrary loadings, boundary conditions, varying dimensional and material properties, and cutouts in the plates. It has the disadvantage, that it requires a greater amount of computer time to obtain a solution than the other two methods. It gives accurate results for deflections using a relatively coarse mesh size. For other results, such as the longitudinal stresses, the transverse slab moments, and the distribution of the total moment at a section to each longitudinal girder, a refined mesh size must be used to achieve accurate results, especially in the vicinity of concentrated loads. Unlike the other two methods, complete static equilibrium is not automatically satisfied by the finite element method, but it is approached as the mesh size in the analysis is refined.

Studies of the effect of longitudinal continuity on the load distribution in box girder bridges have been presented. These studies show that for continuous box girder bridges of usual proportions and irrespective of the number of cells or the transverse position of loads on the bridge deck, the longitudinal division of the total statical moment between positive and negative moments is the same as that found in a continuous beam under the same loading. The transverse distribution of the total moment at a section to each longitudinal girder for concentrated wheel loadings is dependent on the section being considered, the end boundary conditions, the number of cells in the cross-section and the transverse position of the load on the bridge deck and thus these factors should be considered in establishing load distribution criteria for design.

No attempt has been made in this report to make a critical evaluation of the criteria in the present specifications for the design of continuous

box girder bridges. However, it is evident from the results given in this report that the present method of basing load distribution in box girder bridges on the single parameter of the spacing of the webs is an over simplification of the problem. Computer programs such as those developed in this investigation may be used in two ways. First, they may be used as a direct method of elastic analysis of a specific bridge under a given loading and thus replace present semiempirical methods used in analyzing complex bridge systems. Second, they may be used as an aid in studying the effect of different parameters on certain internal forces, moments, or load distribution properties. This use could provide a means for developing improved simplified analysis procedures similar to those presently being used for design.

A continuing program of research on box girder bridges is being conducted at the University of California. To date, the studies have been restricted to straight simply supported and continuous bridges. Additional studies are now being conducted on skew bridges and future studies on curved bridges are contemplated.

8. ACKNOWLEDGMENTS

This research investigation was conducted under the sponsorship of the Division of Highways, Department of Public Works, State of California, and the United States Department of Commerce, Bureau of Public Roads, with the author as the Faculty Investigator. The opinions, findings and conclusions expressed in this report are those of the author and not necessarily those of the Bureau of Public Roads.

Close liaison and support from the Bridge Department, Division of Highways, State of California, was provided by Mr. J. G. Standley, Supervising Bridge Engineer and Mr. R. E. Davis, Senior Bridge Engineer, of the Special Studies and Research Section.

The detailed theoretical development for the folded plate and finite segment methods was carried out by Dr. K. S. Lo and for the finite element method by Dr. B. N. Abu Ghazleh as part of their Ph.D. research under the direction of the author.

A special acknowledgment is due Mr. C. A. Meyer and Mr. D. Ngo, Graduate Students in Civil Engineering, who participated extensively in various phases of the investigation and especially in the development of the computer programs and the computer analyses carried out as part of the research program. Mr. A. Chou, Undergraduate Student in Civil Engineering, assisted in the reduction and plotting of data.

9. REFERENCES

1. Scordelis, A. C., "Analysis of Simply Supported Box Girder Bridges," Structures and Materials Research Report, SESM 66-17, Division of Structural Engineering and Structural Mechanics, Department of Civil Engineering, University of California, Berkeley, October 1966.
2. Wright, R. N., Abdel-Samad, S. R., and Robinson, A. R., "Analysis and Design of Closed Section Girder Bridges with Diaphragms," Research Report, Department of Civil Engineering, University of Illinois, March 1967.
3. Vlazov, V. Z., "Thin Walled Elastic Beams," 2nd Edition, Moscow, 1959, published for the National Science Foundation, Washington, D.C. and the Department of Commerce, U.S.A. by the Israel Program for Scientific Translations, Jerusalem, 1961.
4. Mattock, A. H. and Johnston, S. B., "Lateral Distribution of Load in Composite Box Girder Bridges," Highway Research Abstracts, Vol. 36, No. 12, December 1966.
5. Johnston, S. B. and Mattock, A. H., "An Analytical and Model Study of Composite Box Girder Bridges," paper presented at the ASCE Structural Engineering Conference, Seattle, Washington, May 8-12, 1967.
6. "Phase I Report on Folded Plate Construction" Task Committee on Folded Plate Construction, Journal of the Structural Division, ASCE, Vol. 89, No. ST6, Proc. Paper 3741, December 1963.
7. DeFries-Skene, A., and Scordelis, A. C., "Direct Stiffness Solution for Folded Plates," Journal of the Structural Division, ASCE, Vol. 90, No. ST4, Proc. Paper 3994, August 1964.
8. Gruber, E., "Die Durchlaufenden Prismatischen Faltweike," International Association of Bridge and Structural Engineers, Memoirs, Vol. 12, 1952.
9. Yitzhaki, D., "The Design of Prismatic and Cylindrical Shell Roofs," Haifa Science Publishers, Haifa, Israel, 1958.
10. Beaufait, F. W., "Analysis of Continuous Folded Plate Surface," Journal of the Structural Division, ASCE, Vol. 91, No. ST6, Proc. Paper 4555, December 1965.
11. Pultar, M. "Analysis of Continuous Folded Plate Structures," Ph.D. Thesis presented to the Department of Civil Engineering, Princeton University, Princeton, New Jersey in October 1964.
12. Lee, R. H., "An Analytical and Experimental Study of Continuous Folded Plates," Ph.D. Thesis presented to the Department of Civil Engineering, Purdue University, Lafayette, Indiana in January 1965.

13. Abu-Ghazaleh, B. N., "Analysis of Plate Type Prismatic Structures," Ph.D. Thesis presented to the Division of Structural Engineering and Structural Mechanics, University of California, Berkeley in January 1966.
14. Lo, K. S., "Analysis of Cellular Folded Plate Structures," Ph.D. Thesis presented to the Division of Structural Engineering and Structural Mechanics, University of California, Berkeley in January 1967.
15. Pestel, E. C. and Leckie, F. A., "Matrix Methods in Elastomechanics," McGraw-Hill Book Co., Inc., New York, 1963.
16. Zienkiewicz, O. C., "The Finite Element Method in Structural and Continuum Mechanics," McGraw-Hill Publishing Co. Ltd., London, 1967.
17. Rockey, K. C. and Evans, H. R., "A Finite Element Solution for Folded Plate Structures," Preprint, International Conference on Space Structures, September 1966, Department of Civil Engineering, University of Surrey, London, England.
18. Timoshenko, S. and Goodier, J. N., "Theory of Elasticity," McGraw Hill Book Co., New York, 2nd Edition, 1951.
19. Timoshenko, S. and Woinowsky-Krieger, S., "Theory of Plates and Shells," McGraw Hill Book Co., New York, 2nd Edition, 1959.

APPENDIX A

Description of IBM 7040/7094 Computer
Program for the Analysis of Folded Plate
Structures by the Finite Segment Method
(Ordinary theory) -- SIMPLA

UNIVERSITY OF CALIFORNIA
Berkeley, California
July 1967

Department of Civil Engineering
Division of Structural Engineering
and Structural Mechanics

IBM 7040/7094 Computer Program for the Analysis of Folded Plate
Structures by the Finite Segment Method (Ordinary Theory).

1.0 IDENTIFICATION

- 1.1 Program Name: SIMPLA - A general computer program for the analysis of folded plate structures by the finite segment method (ordinary theory).
- 1.2 Programmed by: Kam-Shing Lo, Graduate Student.
- 1.3 Faculty Investigator: A. C. Scordelis, Professor of Civil Engineering.
- 1.4 References:
a) Lo, Kam-Shing, "Analysis of Cellular Folded Plate System," Ph. D. Dissertation, Division of Structural Engineering and Structural Mechanics, University of California, Berkeley, January 1967.
b) Scordelis, A. C., "Analysis of Continuous Box Girder Bridges," Structures and Materials Research Report, Division of Structural Engineering and Structural Mechanics, Department of Civil Engineering, University of California, Berkeley, SESM 67-25, November 1967.

2.0 GENERAL DESCRIPTION

- 2.1 Nature of Program: The program provides a complete analysis of prismatic cellular or open folded plate structures. The structure may be composed of one or more (up to 15) types of plates. The folded plate structure is defined transversely by the cross-section in terms of the dimensions of its plate elements and their joint interconnection, and longitudinally by the number of segments and the support conditions at the two ends and at intermediate points, if any. Line loads can be applied anywhere on the structure along the joints. A wide variety of boundary conditions can be accounted for. The input data is so arranged that only the properties of a typical cross-section need be specified, and any repeating segments can be indicated by a simple input format. Results for any particular segment to be output can also be specified by the user as desired.
- 2.2 Definitions:

Element - the plate member between I-Edge and J-Edge (see Figs. A 2 and A 5).

Joint - the edge of a plate element, or the junction of two or more plate elements (see Fig. A 3).

Origin - the vertical plane at the extreme left of the structure. This program treats the structure longitudinally from left to right (see Fig. A 1 and REMARK a in Section 6.0).

End - the vertical plane at the extreme right of the structure. This program treats the structure longitudinally from left to right, i.e., from Origin to End (see Fig. A 1 and REMARK a in Section 6.0).

Segment - each structure is divided longitudinally into a number of segments. While the cross-sectional configuration of each segment must remain the same, the length and the boundary conditions of the segments may vary (see Fig. A 1).

Joint Actions - the external loadings or displacements imposed at each joint of a given segment.

Stopover - a mathematical manipulation employed in this program to alleviate the problem of sensitivity in the progression method of solution of linear equations. By specifying a stopover in every other or third segment, the accuracy of the results can be assured, at the expense of a slight increase of computational time. (See also REMARK c in Section 6.0).

Interior Support - an intermediate support along the span. It must be specified at the end of a segment (see Fig. A 1 and REMARK a in Section 6.0). Treatment of point support is described in REMARK b in Section 6.0.

Plate Type - defined by a given orientation (horizontal and vertical projections), plate thickness and modulus of elasticity.

- 2.3 Sign Conventions: These are given in Figs. A 1 to A 6. It should be noted that Joint Actions (forces and displacements) are referred to a Fixed (global) Coordinate System, and plate elements are referred to a Relative (local) Coordinate System.
- 2.4 Method of Solution: The basic approach is based on the finite segment concept in which each plate element is divided into a finite number of segments longitudinally. Compatibility and equilibrium conditions are then satisfied along the four edges of each segment. Each segment of the plate is assumed to obey the ordinary theory of folded plate analysis. This means, slab action is defined by the behavior of a transverse one-way slab spanning between longitudinal joints, and membrane stresses produced in each plate by longitudinal plate action are calculated by the elementary beam theory. The stiffness matrix of

each plate element is obtained in this manner. The total structure matrix is formed by the direct stiffness method. Instead of using the direct band matrix solution technique, a segment progression method is used in this program to solve the resulting set of linear equations. After the unknown displacements have been found, the final internal plate forces can then be calculated. (A complete description of the method of solution can be found in the references cited in Section 1.4).

2.5 General Capabilities and Restrictions:

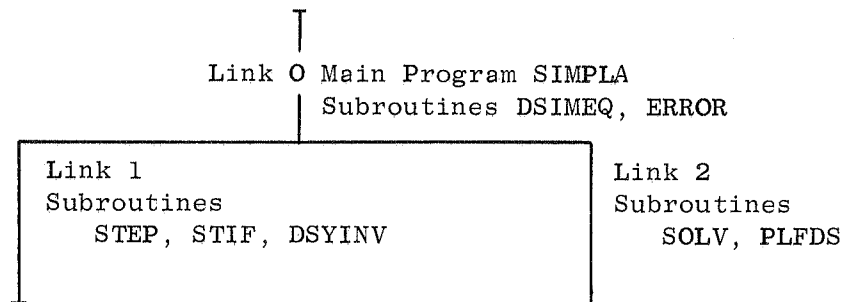
- a) The finite segment method provides for a wide variety of possible structural boundary conditions to be analyzed.
- b) Structures with overhangs and cantilevers can be treated.
- c) Imposed loadings must be applied uniformly along the full length of the joint of a particular segment.
- d) Due to the ordinary theory, torsional moments M_{xy} and longitudinal moments M_x are neglected. The longitudinal stress σ_x varies linearly over the width of each plate (see Fig. A 6). Poisson's ratio is taken to be zero.
- e) Compatibility conditions at the longitudinal joints are satisfied only at the center points of each segment.
- f) Each interior rigid diaphragm can have its own restraint conditions on the structure.
- g) The structure can have an arbitrary number of segments and stopovers.
- h) The maximum number of plates and joints is 15 and 16 respectively.
- i) The maximum absolute difference between the two joint numbers for any plate element is 4.
- j) Only one load case can be treated in each problem.

2.6 Error Checks: Only a limited number of error checks are built-in. The user should be cautious in checking the input data for each problem to be run.

3.0 PROGRAM STRUCTURE

3.1 Computer System and Language: This program is written for the B. C. (Berkeley Campus) Computer Center IBM 7040/7094 DCS (Direct Coupling System), in FORTRAN IV (Version 13) Language.

- 3.2 Double Precision: Double precision numbers are used in connection with the segment progression solution procedure.
- 3.3 Overlay System: Because of the large size of the computer program, an overlay system is used to separate the program into links. The arrangement of links and their subroutines is shown below:



- 3.4 Program Decks: The arrangement of program source (or binary) and data decks is in the following sequence:

```

$JOB
$IJOB
    SIMPLA
    SUBROUTINE DSIMEQ
    SUBROUTINE ERROR
$ORIGIN    ALPHA
    SUBROUTINE STEP
    SUBROUTINE STIF
    SUBROUTINE DSYINV
$ORIGIN    ALPHA
    SUBROUTINE SOLV
    SUBROUTINE PLFDS
$DATA
  
```

First Structural Data Deck

Second Structural Data Deck

etc.

Two Blank Cards

```
$EOF
```

- 3.5 Tapes Used: Tape Unit 2 is used for overlay. Tape Units 1, 3, and 8 are used for temporary data storage.

3.6 Disk Used: None.

3.7 Flow Charts and Name Codes: Flow charts are not shown in this write-up, but are available in the reference (a) cited in Section 1.4. Part of the name codes are shown in the INPUT DATA Section. A complete list of name codes is not available.

4.0 PROGRAM INPUT - DATA DECK

The program input is by means of keypunched cards. Continuous execution of several problems is possible using a single computer run (see Section 3.4). Each individual problem may not require all the data cards listed below. The user supplies only what is needed for a particular problem. Any extra data cards may result in an erroneous execution of the program. The sequential order of the input cards must also be strictly adhered to, and consistent units must be used throughout a problem.

4.1 Title Card - (12A6)

Col. 1 to 72 - TITLE(12), title of the problem to be printed with output; any acceptable FORTRAN characters may be used to identify the problem.

4.2 Control Card - (F10.0,3I4,F4.0,I4)

Col. 1 to 10 - SPAN, span length.

Col. 11 to 14 - NPL, number of plate types, maximum 15.

Col. 15 to 18 - NEL, number of elements, maximum 15.

Col. 19 to 22 - NJT, number of joints, maximum 16.

Col. 23 to 26 - SHEAR, index for shear deformation:

0 - to include shear deformation

1 - to neglect shear deformation

Col. 27 to 30 - NSEG, total number of segments along the longitudinal axis of the structure (no set maximum).

4.3 Plate Type Cards - One card for each plate type used in the structure under consideration. (I10,4F10.0)

Col. 1 to 10 - I, plate type number, an integer assigned by the user for each type of plate, must not be greater than 15.

Col. 11 to 20 - H(I), horizontal projection of the plate (see Fig. A 5 for sign convention).

Col. 21 to 30 - V(I), vertical projection of the plate (see Fig. A 5 for sign convention).

Col. 31 to 40 - TH(I), plate thickness.

Col. 41 to 50 - E(I), modulus of elasticity.

4.4 Element Cards - One card for each element, all elements in the cross-section of the structure must be described. (4I4)

- Col. 1 to 4 - I, element number, an integer assigned by the user for each element in the cross-section of the structure, and must be in consecutive ascending order.
- Col. 5 to 8 - NPI(I), joint number at I-Edge.
- Col. 9 to 12 - NPJ(I), joint number at J-Edge.
- Col. 13 to 16 - KPL(I), plate type number, must be one of those given previously under 4.3-Plate Type Cards.

4.5 Origin Boundary Cards - One card for each element in the cross-section. Each plate element is treated as a longitudinal beam. (I10,3F10.0,3I2)

- Col. 1 to 10 - I, element number.
 - Col. 11 to 20 - BCORI(1,I), given longitudinal axial force or displacement.
 - Col. 21 to 30 - BCORI(2,I), given transverse beam shear force or displacement.
 - Col. 31 to 40 - BCORI(3,I), given longitudinal beam moment or rotation.
 - Col. 42 - IORI(1,I), index for axial force or displacement.
 - Col. 44 - IORI(2,I), index for beam shear force or displacement.
 - Col. 46 - IORI(3,I), index for beam moment or rotation.
- | | |
|---|----------------------|
| } | 0 - for given force |
| } | 1 - for given displ. |

4.6 Segment Cards - One card for each segment. If joint actions differ from previous segments, 4.7-Joint Action Cards must follow. If interior support exists at the end of the segment, 4.8-Interior Support Card must follow. (4I4,F14.8,I4)

- Col. 1 to 4 - I, segment number, must start from 1 and be in consecutively ascending order, progressing from Origin to End (left to right).
- Col. 5 to 8 - IAJA, index for applied joint actions:
 - 0 - for repeating applied joint actions as in immediately preceding segment.
 - 1 - for a new set of applied joint actions (4.7-Joint Action Cards are needed).
- Col. 9 to 12 - ITRES, index to output results at the center of the segment:
 - 0 - to give final joint and plate forces and displacements.
 - 1 - to skip output of joint and plate forces and displacements.
- Col. 13 to 16 - ITSEG, index for segment length:
 - 0 - for repeating length as in immediately preceding segment.
 - 1 - for new segment length (give the length in next space).

- Col. 17 to 30 - TEMSEG, segment length, omitted if 0 is specified in ITSEG.
- Col. 31 to 34 - ITSTOP, index for interior support or stopover:
 - 0 - for no stopover nor interior support.
 - 1 - for stopover appearing at the end of this segment.
 - 1 - for interior support appearing at the end of this segment (4.8-Interior Support Card is needed).

4.7 Joint Action Cards - These cards are needed if a new set of joint actions is applied to the segment, i.e., when IAJA is set equal to 1 in 4.6 Segment Cards, one for each joint. (I10,4F10.0,4I2)

- Col. 1 to 10 - I, joint number.
 - Col. 11 to 20 - AJFOR(1,I), applied horizontal joint force or displacement.
 - Col. 21 to 30 - AJFOR(2,I), applied vertical joint force or displacement.
 - Col. 31 to 40 - AJFOR(3,I), applied joint moment or rotation.
 - Col. 41 to 50 - AJFOR(4,I), applied longitudinal joint force or displacement.
 - Col. 52 - LCASE(1,I), index for horizontal joint force or displacement.
 - Col. 54 - LCASE(2,I), index for vertical joint force or displacement.
 - Col. 56 - LCASE(3,I), index for joint moment or rotation.
 - Col. 58 - LCASE(4,I), index for longitudinal force displacement.
- } 0 - for applied uniform line load.
} 1 - for applied displacement at center of segment.

4.8 Interior Support Card - This card must follow the 4.6-Segment Cards or 4.7-Joint Action Cards if an interior support exists, i.e., when ITSTOP is set equal to -1 in 4.6-Segment Cards. (45I1)

- Col. 1 - IED(1), axial indicator
 - Col. 2 - IED(2), transverse indicator
 - Col. 3 - IED(3), rotation indicator
 - Col. 4 - IED(4), axial indicator
 - Col. 5 - IED(5), transverse indicator
 - Col. 6 - IED(6), rotation indicator
 - ...
- } for element no. 1
} for element no. 2
etc.

Continue in this fashion until last element in the cross-section.
Use: 0 - to indicate continuity.
1 - to indicate zero displacement.

4.9 End Boundary Cards - One card for each element in the cross-section. Each plate element is treated as a longitudinal beam. (I10,3F10.0,3I2)

| | | |
|---------------|--|---|
| Col. 1 to 10 | - I, element number. | |
| Col. 11 to 20 | - BCEND(1,I), given longitudinal axial force or displacement. | |
| Col. 21 to 30 | - BCEND(2,I), given transverse beam shear force or displacement. | |
| Col. 31 to 40 | - BCEND(3,I), given longitudinal beam moment or rotation. | |
| Col. 42 | - IEND(1,I), index for axial force or displacement. | } 0 - for given force 1 - for given displ. |
| Col. 44 | - IEND(2,I), index for beam shear force or displacement. | |
| Col. 46 | - IEND(3,I), index for beam moment or rotation. | |

5.0 PROGRAM OUTPUT

Printed output is furnished by this program. No punched output option is available. The input data is first given for an echo check. Final plate actions (forces and displacements) are given at the origin and at the end of the structure, and at the sections where stopovers or interior supports have been specified. Final plate forces and displacements are given for individual segments as specified by the user. It should be noted that the results for each segment are referred to the center of the segment in longitudinal direction.

5.1 Input Information - Title of the problem and all other input data are properly labeled and printed out for an echo check.

5.2 Final Plate Forces and Displacements for Longitudinal Plate Element at End. (See Fig. A 6 for sign convention.)

5.2.1 Plate Internal Displacements - the following displacements are given for each plate element:

Longitudinal displacement
Transverse displacement
Beam Rotation

5.2.2 Plate Internal Forces - the following forces and stresses are given for each plate element:

Beam moment
Transverse shear
Axial force
Longitudinal normal force per unit length at I-Edge, NX(I)
Longitudinal normal force per unit length at J-Edge, NX(J)
Longitudinal normal stress per unit area at I-Edge, SX(I)
Longitudinal normal stress per unit area at J-Edge, SX(J)

- 5.3 Final Plate Forces and Displacements for Longitudinal Plate Elements at End of Segment No. xx - These results are given only at the sections where stopovers or interior supports have been specified.
- 5.3.1.a Plate Displacements at Stopover - For sections where stopovers occur, the following displacements are given for each plate element:
- Longitudinal displacement
Transverse displacement
Beam rotation
- 5.3.1.b Plate Displacements and Reactions at Interior Support - For sections where interior support occurs, the following displacements and reactions are given for each plate element:
- Longitudinal displacement or reaction } indicated by:
Transverse displacement or reaction } 0 - for displ.
Beam rotation or reaction } 1 - for react.
- 5.3.2 Plate Internal Displacements - Same as listed in 5.2.1.
- 5.3.3 Plate Internal Forces - Same as listed in 5.2.2.
- 5.4 Final Plate Forces and Displacements for Longitudinal Plate Element at Origin
- 5.4.1 Plate Internal Displacements - Same as listed in 5.2.1.
- 5.4.2 Plate Internal Forces - Same as listed in 5.2.2.
- 5.5 Final Joint and Plate Forces and Displacements at Center of Segment No. xx - Results given only for the particular segments which have been specified by the user in the 4.6-Segment Cards.
- 5.5.1 Joint Displacements - The following displacements are given for each joint: (See Fig. A 4 for sign convention.)
- Horizontal displacement
Vertical displacement
Rotation
Longitudinal displacement
- 5.5.2 Plate Edge Displacements - The following displacements are given for each plate element: (See Fig. A 6 for sign convention.)
- Rotation at I-Edge
Rotation at J-Edge
Normal shear displacement at I-Edge, W(I)
Normal shear displacement at J-Edge, W(J)

Longitudinal shear displacement at I-Edge, U(I)
 Longitudinal shear displacement at J-Edge, U(J)
 Transverse membrane displacement at I-Edge, V(I)
 Transverse membrane displacement at J-Edge, V(J)

5.5.3 Plate Edge Forces - The following forces are given for each element: (See Fig. A 6 for sign convention.)

Transverse moment per unit length at I-Edge, M(I)
 Transverse moment per unit length at J-Edge, M(J)
 Normal shear per unit length at I-Edge, Q(I)
 Normal shear per unit length at J-Edge, Q(J)
 Longitudinal shear force per unit length at I-Edge, T(I)
 Longitudinal shear force per unit length at J-Edge, T(J)
 Transverse membrane force per unit length at I-Edge, P(I)
 Transverse membrane force per unit length at J-Edge, P(J)

5.5.4 Plate Internal Displacements - Same as listed in 5.2.1. (Note that these are at the center of the segment length.)

5.5.5 Plate Internal Forces - Same as listed in 5.2.2. (Note that these are at the center of the segment length.)

6.0 REMARKS

- a) The nature of the supports at the Origin, End, and Interior Support sections is considered for each plate element individually by this program, and therefore not all of the plate elements have to be subjected to the same boundary conditions at these sections. This provides a wide variety of boundary conditions that can be specified by the user.
- b) Interior point supports, such as resting on top of columns, can be handled in two ways:
 - i) Set the corresponding displacements imposed by the point support equal to zero in the appropriate column of the 4.8-Interior Support Card.
 - ii) Set the corresponding displacements imposed by the point support equal to zero at the center of a segment length in the appropriate 4.7-Joint Action Cards. A support between longitudinal joints is not allowed.
- c) A stopover need not be specified at the Origin, End, and at sections where an Interior Support exists. The minimum number of stopovers required to give accurate results depends on the size of the structure and on the suitable choice of locations for stopovers. Experience is needed to make a proper judgment.
- d) The number 0 (zero) is not considered as a subscript variable index. Thus, it can not be used as a joint, element, or segment number.

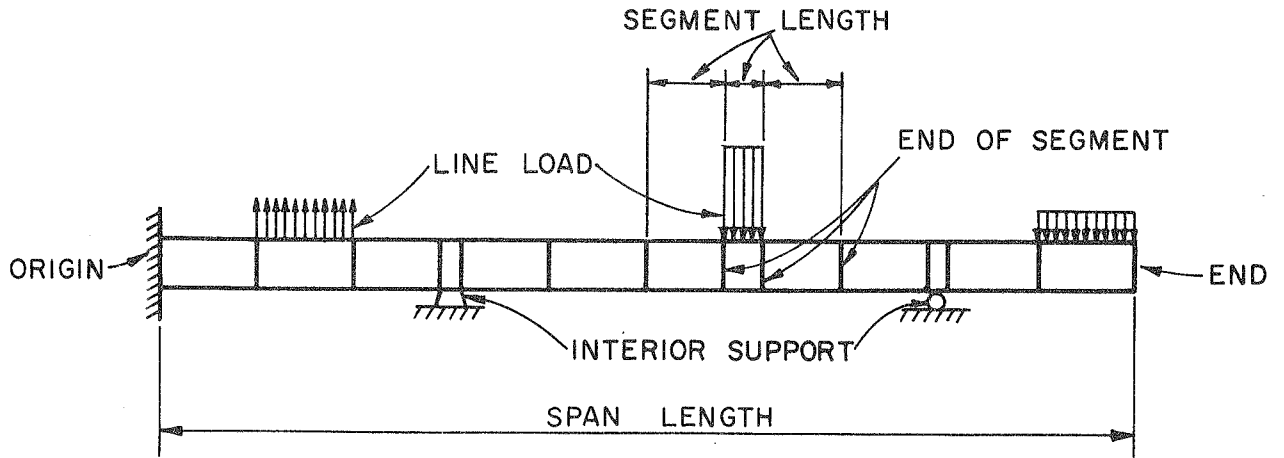


FIG. A1 LONGITUDINAL ELEVATION AND LOADING
(ALL LOADS MUST BE INPUT AS LINE
LOADS ALONG A LONGITUDINAL JOINT)

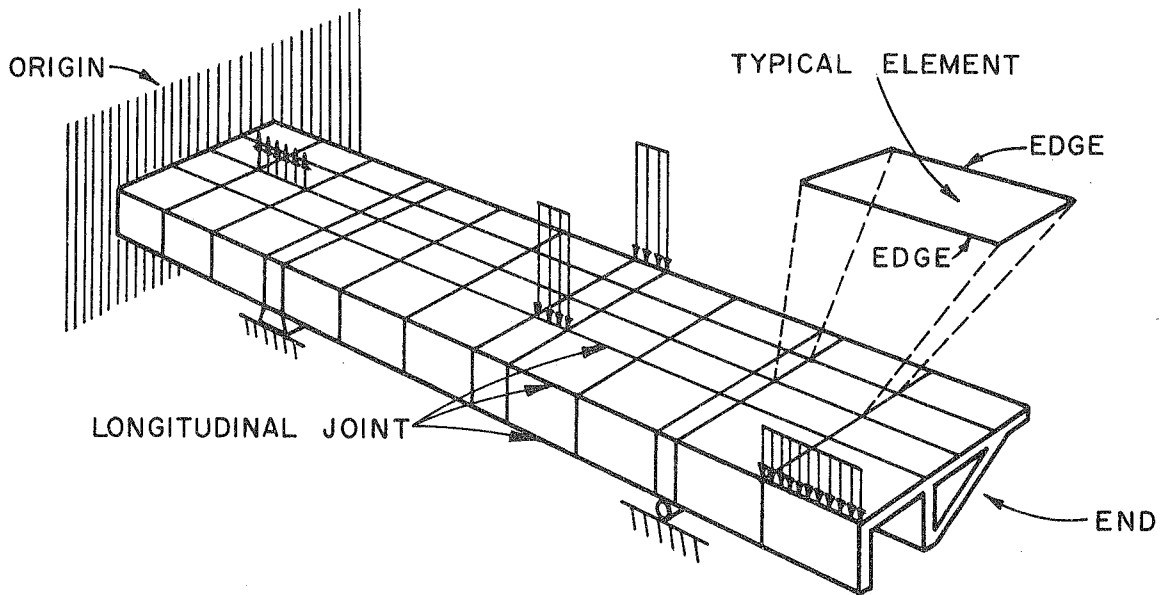


FIG. A2 GENERAL VIEW OF STRUCTURE

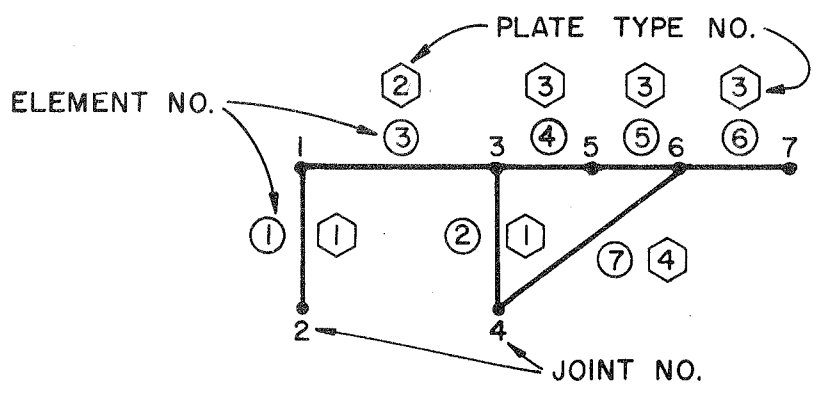


FIG. A3 CROSS SECTION IDEALIZATION USING ELEMENT, PLATE TYPE, AND JOINT NUMBERS. (SECTION IS TAKEN LOOKING TOWARD THE ORIGIN.)

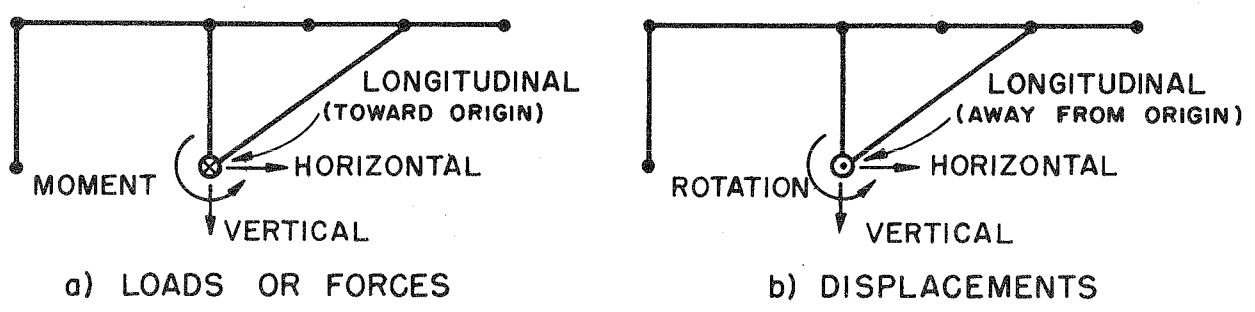


FIG. A4 POSITIVE JOINT ACTIONS IN FIXED COORDINATE SYSTEM. (COMMON DIRECTIONS FOR ALL JOINTS.)

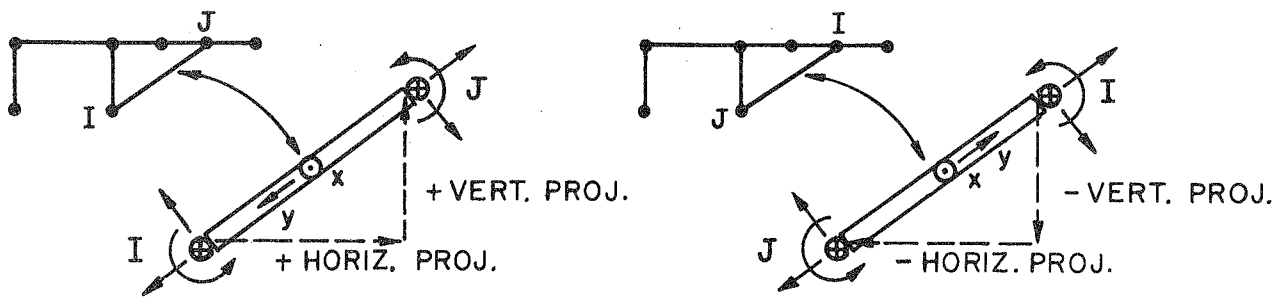
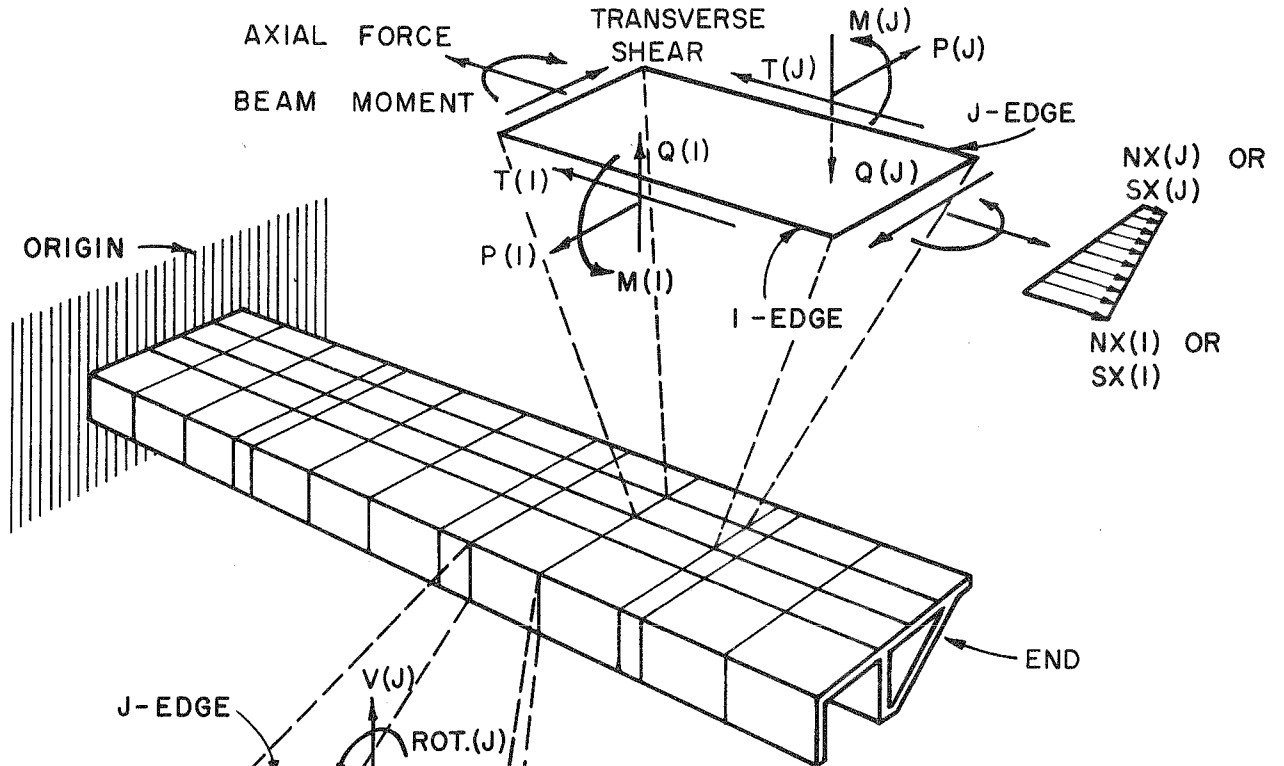


FIG. A5 SIGN CONVENTION FOR ELEMENT PROJECTION AND CORRESPONDING POSITIVE DIRECTION OF ELEMENT RELATIVE COORDINATE AXES AND POSITIVE PLATE EDGE FORCES.

b) FORCES



a) DISPLACEMENTS

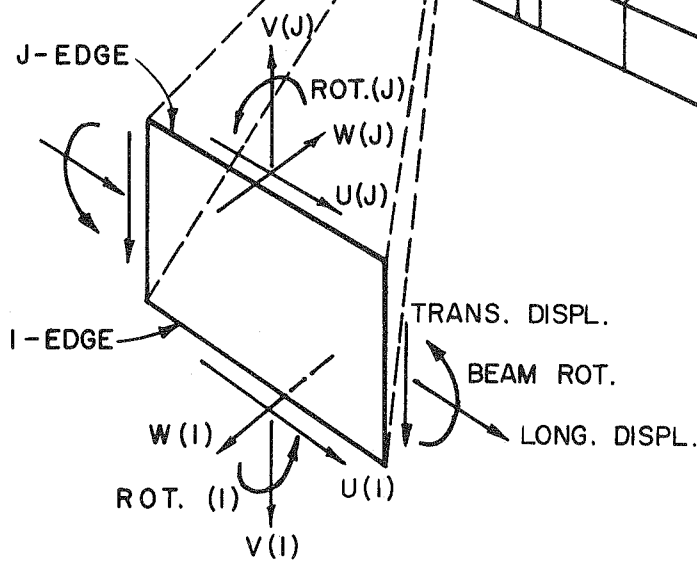


FIG. A6 POSITIVE INTERNAL BEAM END AND PLATE EDGE FORCES AND DISPLACEMENTS

APPENDIX B

Description of IBM 7040/7094 Computer
Program for the Analysis of Folded Plate
Structures by the Finite Element Method
(Elasticity theory) -- FINPLA

UNIVERSITY OF CALIFORNIA
Berkeley, California
August 1967

Department of Civil Engineering
Division of Structural Engineering
and Structural Mechanics

IBM 7040/7094 Computer Program for the Analysis of Folded Plate
Structures by the Finite Element Method (Elasticity Theory)

1.0 IDENTIFICATION

- 1.1 Program Name: FINPLA - A general program for the analysis of folded plate structures by the finite element method (elasticity theory).
- 1.2 Programmed by: B. Abu Ghazaleh and C. A. Meyer, Graduate Students.
- 1.3 Faculty Investigator: A. C. Scordelis, Professor of Civil Engineering.
- 1.4 References:
a) Abu, Ghazaleh, B. N., "Analysis of Plate Type Prismatic Structures", Ph.D. Dissertation, Division of Structural Engineering and Structural Mechanics, University of California, Berkeley, January 1966.
b) Scordelis, A. C., "Analysis of Continuous Box Girder Bridges," Structures and Materials Research Report, Division of Structural Engineering and Structural Mechanics, Department of Civil Engineering, University of California, Berkeley, SESM 67-25, November 1967.

2.0 GENERAL DESCRIPTION

- 2.1 Nature of Program: This program is capable of analyzing any prismatic cellular or open folded plate structure subjected to surface loads, line loads, concentrated loads or known displacements. All final nodal displacements and the internal forces and moments within the elements are printed out at points selected by the user. The input data is so arranged that only the properties of a typical cross-section need to be specified and only changes in these properties along the span need to be specified thereafter.
- 2.2 Definitions:
Finite Element - a rectangular element in the structure whose location is defined by its I and J nodal points on a typical cross-section and its interval position along the longitudinal span (see Fig. B3).

Nodal Point or Node - a joint at which finite elements are interconnected; these are defined by assigned numbers at a typical cross-section.

Finite Element Type - defined by a given orientation (horizontal and vertical projections), thickness, modulus of elasticity and Poisson's ratio (see Fig. B5).

Particular Element - a finite element whose element type or uniform loading differs from the corresponding element in the typical cross-section of the first interval along the span.

Group Displacement Component - a displacement in a given direction applied simultaneously to a designated group of nodal points at a specified section along the span.

Diaphragm - a transverse diaphragm, at a designated location along the span, which is made up of rectangular finite elements connected as specified to the folded plate structure.

- 2.3 Sign Conventions: These are given in Figs. B1 to B6. Reference is made to two right hand coordinate systems. The global (fixed) system XYZ, Figs. B2, B4, and B5, defines the positive directions of external loads, forces, displacements and the horizontal and vertical projections of an element. The local (element) system xyz, Figs. B5 and B6, defines the orientation of the element for the interpretation of the positive directions of internal forces, stresses and moments.
- 2.4 Method of Solution: The solution is based on a standard analysis by the finite element method. Rectangular elements with six degrees of freedom at each node are used in conjunction with a direct stiffness method to obtain a complete solution. A detailed description of the method of solution can be found in the references cited in Section 1.4.
- 2.5 General Capabilities and Restrictions:
- a) Restrictions as to the maximum number of elements, nodal points, loads, etc., are given directly in the input specifications, Section 4.0, and under remarks, Section 6.0.
 - b) External loadings may consist of uniform dead or live loads, line loads along a longitudinal joint, or concentrated loads at nodes.
 - c) Boundary displacement conditions may be imposed at each node independently or on a group of nodes at a section.
 - d) Each element in a transverse or longitudinal direction may have different dimensional or material properties and cutouts may be included by assigning a zero thickness or modulus of elasticity to an element.

e) Transverse diaphragms may be included at desired sections along the span.

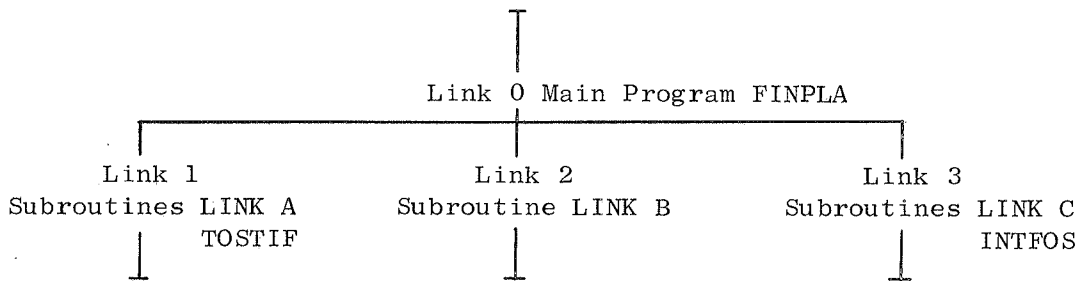
f) Only one load case can be treated in each problem.

2.6 Error Checks: Only a limited number of error checks are built-in. The user should be cautious in checking input data for each problem to be run.

3.0 PROGRAM STRUCTURE

3.1 Computer System and Language: This program is written for the B. C. (Berkeley Campus) Computer Center IBM 7040/7094 DCS (Direct Coupling System), in FORTRAN IV (Version 13) Language.

3.2 Overlay System: To increase the capacity of the program, an overlay system is used, separating the total program into several links. The arrangement of the links with their subroutines is shown below:



3.3 Program Decks: The arrangement of program source (or binary) and data decks is in the following sequence:

```

$JOB
$IJOB
  MAIN (FINPLA)
$ORIGIN ALPHA
  SUBROUTINE LINK A
  SUBROUTINE TOSTIF
$ORIGIN ALPHA
  SUBROUTINE LINK B
$ORIGIN ALPHA
  SUBROUTINE LINK C
  SUBROUTINE INTFOS
  
```

\$DATA

First Structural Data Deck

Second Structural Data Deck

etc.

Two Blank Cards

\$EOF

- 3.4 Tapes Used: Tape Unit 2 is used for the overlay system. Tape Units 1, 3, 8 and 9 are used for temporary data storage.
- 3.5 Disk Used: Element stiffness matrices are temporarily stored on disk. The write and read operations on disk are done by using a BCDISK subroutine supplied by the B. C. Computer Center in MAP language.
- 3.6 Flow Charts and Name Codes: Flow Charts are not shown in this report, but they are available for reference. Part of the name codes are shown in the INPUT DATA section. A complete list of name codes is not available.

4.0 PROGRAM INPUT - DATA DECK

The program input is by means of keypunched cards. Continuous execution of several problems is possible using a single computer run (see Section 3.3). Each individual problem may not require all the data cards listed below. The user supplies only what is needed for a particular problem. Any extra data cards may result in an erroneous execution of the program. The sequential order of the input cards must also be strictly adhered to and consistent units must be used throughout a problem.

4.1 Title Card - (12A6)

Col. 1 to 72 - Title of problem to be printed with output; any acceptable FORTRAN characters may be used to identify the problem.

4.2 Control Card - (F10.3,6I4)

Col. 1 to 10 - span length = SPAN.

Col. 11 to 14 - number of finite element types = NFEL, maximum = 90

Col. 15 to 18 - number of nodal points in a typical cross-section = NPTS, maximum = 20.

Col. 19 to 22 - number of finite element subdivisions along the X - axis = NUMELX, maximum = 40.

Col. 23 to 26 - number of finite element subdivisions normal to the X - axis = NUMELY, maximum = 28.

Col. 27 to 30 - number of transverse diaphragms = NDIAPH, maximum = 5.

Col. 31 to 34 - averaging index = INDAV, which is equal to
0 - if no final averaging of output forces is desired.

1 - if only longitudinal averaging of output forces is desired.

2 - if all permissible longitudinal and transverse averagings are desired.

(See Remark under Section 6.0d)

4.3 X-Coordinate Card - (10F7.3)

X-Coordinates of nodes along the X-axis = XDIST(I).
The origin 0.0 is not to be included. If there are more than 10 nodes along the X-axis, use another card (or third, etc.)

4.4 Element Type Cards (7X,I3,5F10.3) - One card for each type of finite element.

Col. 8 to 10 - type number = I.
Col. 11 to 20 - horizontal Y-projection of element = H(I) (See Fig. B5).
Col. 21 to 30 - vertical Z-projection = V(I) (See Fig. B5).
Col. 31 to 40 - element thickness = TH(I).
Col. 41 to 50 - modulus of elasticity = E(I).
Col. 51 to 60 - Poisson's ratio = FNU(I).

4.5 Element Cards (4I5,3F10.3) - One card for each element in the cross-section in the first interval along the longitudinal axis.

Col. 1 to 5 - element number = I.
Col. 6 to 10 - nodal point I = NPI(I) (must be smaller than J).
Col. 11 to 15 - nodal point J = NPJ(I) (must be larger than I).
Col. 16 to 20 - finite element type = KPL(I).
Col. 21 to 30 - dead load (load per unit plate area) = DL(I).
Col. 31 to 40 - load in Y-direction (load per unit of vertical projected area) = HL(5).
Col. 41 to 50 - load in Z-direction (load per unit of horizontal projected area) = VL(I).

4.6 Next Card (7X,I3)

Col. 8 to 10 - total number of particular elements (i.e., elements whose element types or uniform loadings are different from the corresponding elements in the first interval) = NPE, maximum = 62.

4.7 Particular Element Cards (4I5,3F10.3) - One card for each particular element. No cards required if there are no such elements. The numbering order must ascend in agreement with the ordinary element and interval numbering.

Col. 1 to 5 - number of particular element = I.
Col. 6 to 10 - element number corresponding to the first interval = NEL(I).
Col. 11 to 15 - interval number = INTER(I).
Col. 16 to 20 - element type = KNP(I).
Col. 21 to 30 - uniform dead load = DLP(I).
Col. 31 to 40 - uniform load in Y-direction = HLP(I).
Col. 41 to 50 - uniform load in Z-direction = VLP(I).

4.8 Next Card (7X,I3)

Col. 8 to 10 - number of concentrated or distributed line loads or displacements at the longitudinal joints = NCDL, maximum = 150. Only non-zero forces are counted.

4.9 Load-Displacement Cards (I5,3F10.3,2I5) - one card for each load or displacement component. No cards required if NCDL = 0. For transverse line loads use equivalent concentrated loads obtained by the tributary area concept.

Col. 1 to 5 - longitudinal joint number (nodal point number in the typical cross-section) = LJN(I).

Col. 6 to 15 - X-coordinate at which load (or displacement) starts = XLEN(I). Must begin at a node.

Col. 16 to 25 - length of load or displacement along the X-axis = XSTRCH(I). Must end at a node. Zero for concentrated loads or displacements.

Col. 26 to 35 - force intensity or displacement amount = DFINT(F) (use total amount if concentrated load).

Col. 36 to 40 - component indicator = INDIC(I), equal to:

- 1 - applied force or displacement in X-direction
- 2 - applied force or displacement in Y-direction
- 3 - applied force or displacement in Z-direction
- 4 - applied moment or rotation about X-axis
- 5 - applied moment or rotation about Y-axis
- 6 - applied moment or rotation about Z-axis

Col. 41 to 45 - action indicator = INDEX(I), equal to:

- 0 - for applied force or moment
- 1 - for applied displacement or rotation.

4.10 Next Card (7X,I3)

Col. 8 to 10 - number of applied group displacement components at a single cross-section = NTAD, maximum = 25.

4.11 Group Displacement Cards - two cards for each set of applied group displacements. Each displacement component requires a set of two cards. If all nodal points are affected, only one card.(a) First Card (3I5,2F10.3)

Col. 1 to 5 - displacement component number = I.

Col. 6 to 10 - component indicator = INDT(I) (for definition of indicator numbers see preceding card under 4.9).

Col. 11 to 15 - number of affected nodal points = NAN(I). If this equals the total number of nodal points in this cross-section, omit the second card.

Col. 16 to 25 - X-coordinate of applied displacement = XTD(I).

Col. 26 to 35 - displacement magnitude = DTIN(I).

(b) Second Card (20I3) - number designations of nodal points to which group displacement is to be applied = NAD(I,K).

If there are no transverse diaphragms, skip the cards 12, 13 and 14.

4.12 Diaphragm Indicator Card (2I5,5X,5I5)

Col. 1 to 5 - indicator = INDIAP, equal to:

- 0 - if all diaphragms are the same
- 1 - if one or more differ from the others.

Col. 6 to 10 - number of element types in diaphragms = NDIATY, maximum = 10.

Col. 16 to 40 - interval-numbers for location of diaphragms along the X-axis; zero for diaphragm at the origin = IDIAP(I).

4.13 Diaphragm Element Type Cards (7X,I3,5F10.3) - one card for each diaphragm element type.

Col. 8 to 10 - type number = I.

Col. 11 to 20 - element height = DIAH(I).

Col. 21 to 30 - element width = DIAL(I).

Col. 31 to 40 - element thickness = DIATH(I).

Col. 41 to 50 - modulus of elasticity = DIAE(I).

Col. 51 to 60 - Poisson's ratio = DIANU(I).

4.14 Diaphragm Cards - for each diaphragm one deck, if INDIAP = 1, otherwise one deck only for the first diaphragm.

(a) First Card (4I5)

Col. 1 to 5 - diaphragm number = I.

Col. 6 to 10 - number of elements = NDIAEL(I), maximum = 10.

Col. 11 to 15 - number of vertical sections per element for output of results = NXDIA(I), maximum = 4.

Col. 16 to 20 - number of transverse sections per element for output of results = NYDIA(I), maximum = 4.

(b) Second Card (6I5,F10.3) - one card for each element in diaphragm.

Col. 1 to 5 - element number = K.

Col. 6 to 10 - element type number = NTYPE(I,K).

Col. 11 to 15 - nodal point I = NPTI(I,K).

Col. 16 to 20 - nodal point J = NPTJ(I,K).

Col. 21 to 25 - nodal point K = NPTK(I,K).

Col. 26 to 30 - nodal point L = NPTL(I,K).

Col. 31 to 40 - Uniform dead load = DIADL(I,K).

Note: Nodal points are taken from typical section numbering and must be numbered counter-clockwise, when looking at typical section in + x direction.

4.15 Results Cards (3I5) - one card for each interval, indicating where results are desired. (See REMARK under Section 6.0d.)

Col. 1 to 5 - interval number = I.

Col. 6 to 10 - number of longitudinal sections per element = NSEGX(I), maximum = 4.

Col. 11 to 15 - number of transverse sections per element = NSEGY(I), maximum = 4.

5.0 PROGRAM OUTPUT

Printed output is furnished by the program, no punched output option is available. First, the input data are printed for an echo check. The final results consist of the nodal point displacements and internal force and stress quantities at locations specified by the user.

5.1 Input Check Printout: The complete input data is properly labeled and printed out for an echo check. Some error exits have been built in to stop execution in the case of bad data.

5.2 Final Nodal Point Displacements: The six displacement components δ_x , δ_y , δ_z , θ_x , θ_y , θ_z (see Fig. B4 for sign convention) are printed out in tabular form for all of the nodal points of the entire structure. (However, unknown nodal forces wherever the corresponding displacements have been specified are not given.)

5.3 Internal Forces: The internal forces N_x , N_y , N_{xy} , the moments M_x , M_y , M_{xy} , and the stresses σ_x , σ_y , σ_{xy} , (stresses are equal to the corresponding forces per unit length divided by element thickness) are printed out with proper headings in any interval and at as many intermediate points as have been specified by the user (see REMARK under Section 6.4). (For sign convention, see Fig. B6.)

5.4 Execution Times: The execution times for the three links of the program are printed out in seconds.

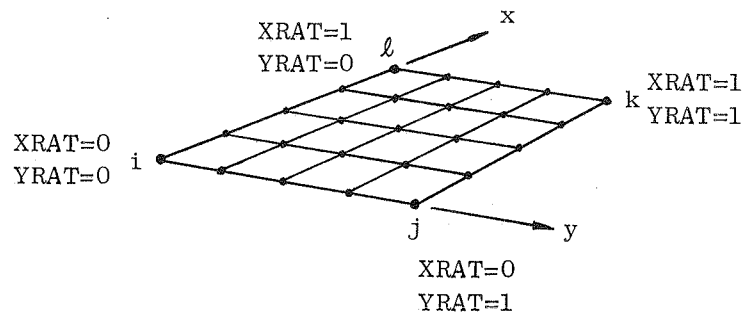
6.0 REMARKS

a) All cards are repeated in the same sequence for the next problem to be analyzed. Following the last problem, two blank cards have to be added.

b) Longitudinal averaging of output forces in two adjacent elements will be done only if specified in Section 4.2 and as long as no particular elements are involved. Transverse averaging of forces will not be done as soon as more than two elements meet at the joint under consideration. If two elements meet at an angle $\neq 180^\circ$, then only the transverse moments and longitudinal shears will be averaged if specified in Section 4.2.

c) Select the joint numbering of the elements so as to minimize the maximum absolute difference between the nodal point numbers for any element. The maximum absolute difference is 5 on a typical cross-section. Also note that a maximum of 20 nodal points can be used on a typical cross-section.

d) If internal forces are not desired in a certain interval, two 0's have to be punched for NSEGX and NSEGY in Section 4.15. Two 1's give results at the nodal points only. Additional subdivisions may be selected, up to NSEGX = NSEGY = 4, in which case results at 25 points will be printed with proper position labels as shown:



e) The number 0 (zero) is not considered as a subscript variable index. Thus, it can not be used as a joint, element, or diaphragm number.

f) The execution time can be estimated by the formula:

$$T(\text{seconds}) = cNM^2 + dP_n X_n Y_n$$

where N = maximum band width = 6 times the sum of the maximum absolute difference between the nodal point numbers on a typical cross-section for any single finite element plus the number of nodal points on the cross-section plus one.

P_n = average number of points within one element for which internal forces are output.

X_n = number of element intervals along the span.

Y_n = number of finite elements in a typical cross-section.

c = time factor = $(0.8 \text{ to } 1.2)10^{-4}$

d = time factor = $(2 \text{ to } 4)10^{-2}$

M = maximum band width = 6 times the sum of the maximum absolute difference between the nodal point numbers on a typical cross-section for any single finite element plus the number of nodal points on the cross-section plus one.

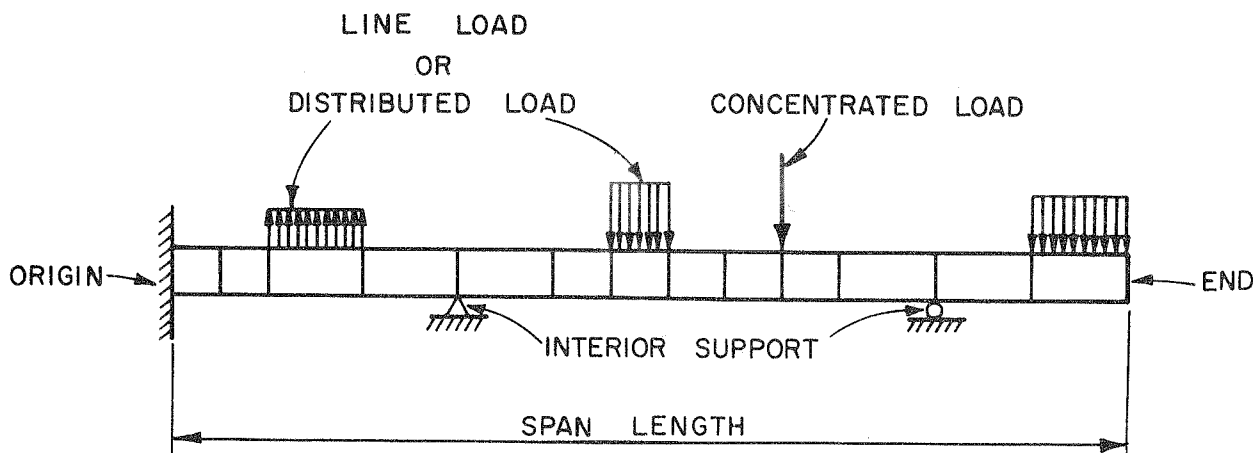


FIG. B1 LONGITUDINAL ELEVATION AND LOADING
 (LOADS MAY BE DEAD OR LIVE LOADS PER UNIT AREA, LINE LOAD PER UNIT LENGTH ALONG A LONGITUDINAL JOINT, OR CONCENTRATED LOADS AT A NODAL POINT)

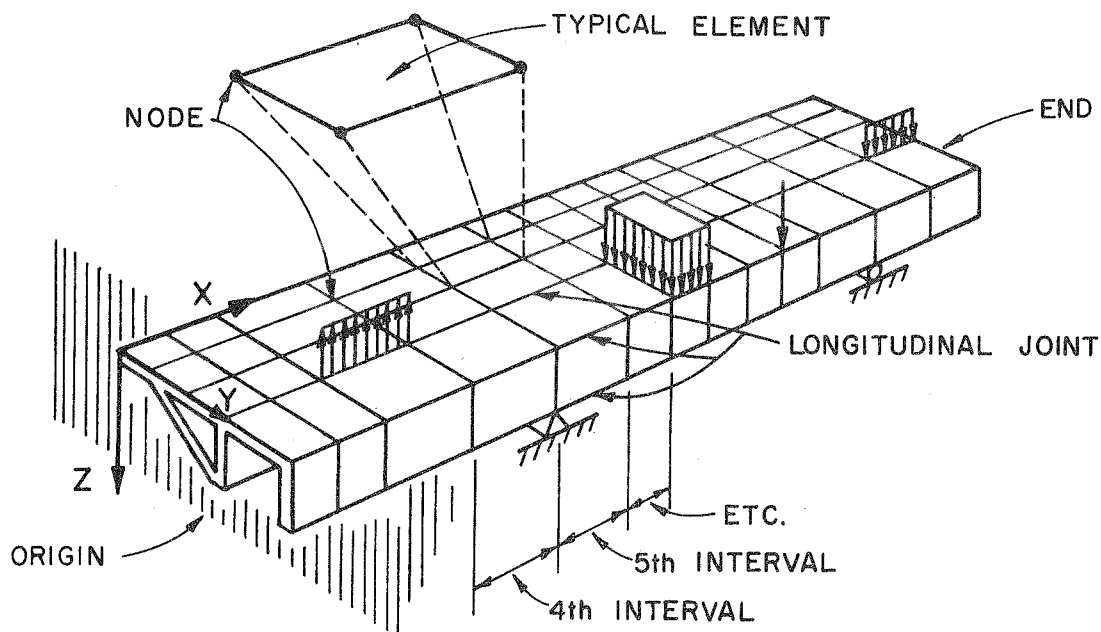


FIG. B2 GENERAL VIEW OF STRUCTURE SHOWING
 RIGHT HAND GLOBAL COORDINATE
 SYSTEM

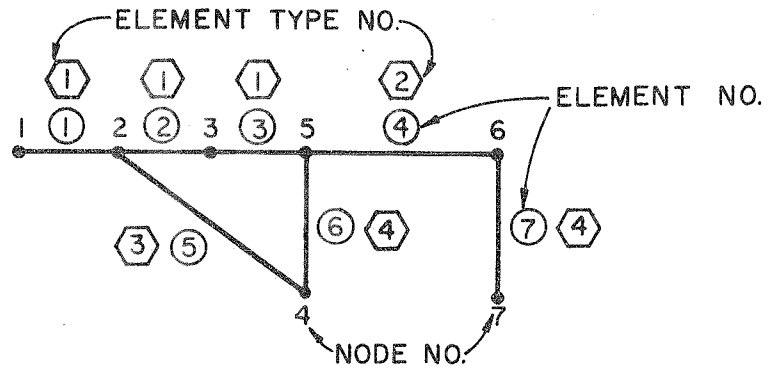


FIG. B3 FIRST INTERVAL CROSS-SECTION IDEALIZATION USING ELEMENT, ELEMENT TYPE, AND NODAL POINT NUMBERS. (SECTION IS TAKEN LOOKING AWAY FROM ORIGIN)

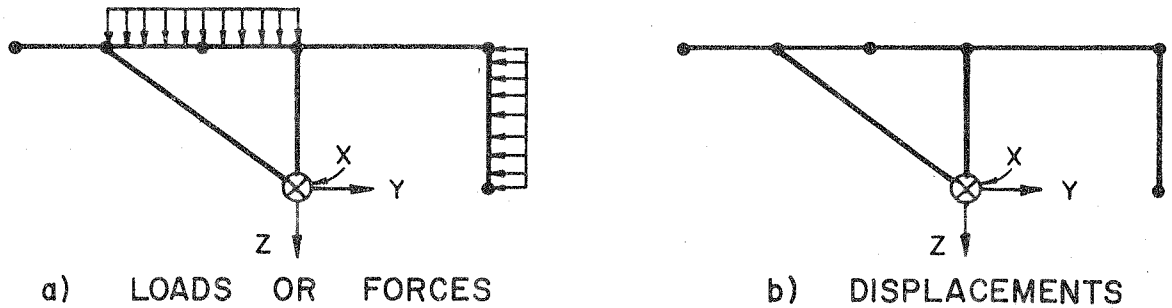


FIG. B4 POSITIVE DIRECTION OF ALL EXTERNAL LOADS AND DISPLACEMENTS. (SAME AS POSITIVE GLOBAL COORDINATE DIRECTION; USE RIGHT HAND RULE FOR MOMENTS AND ROTATIONS)

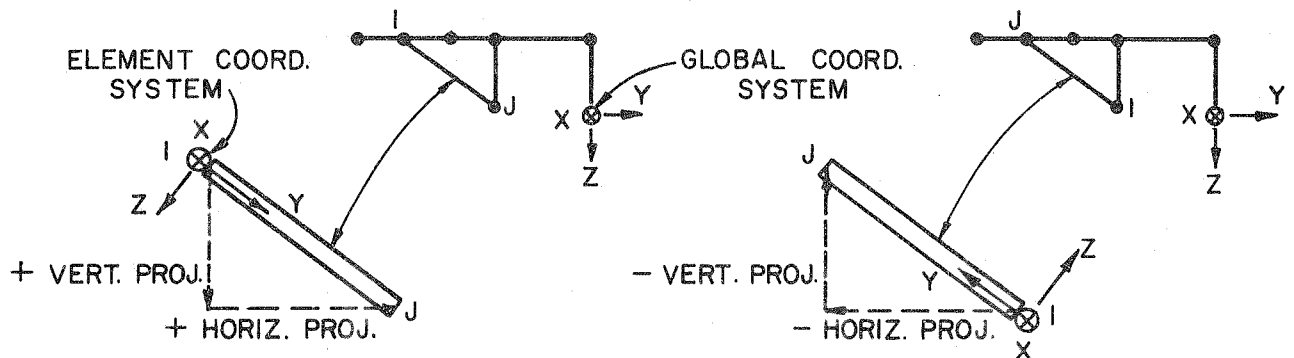
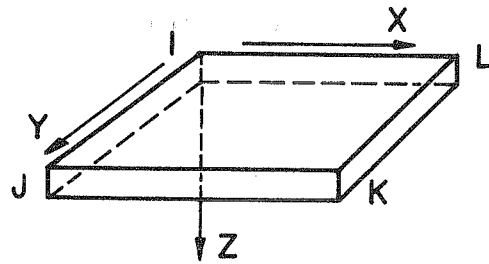
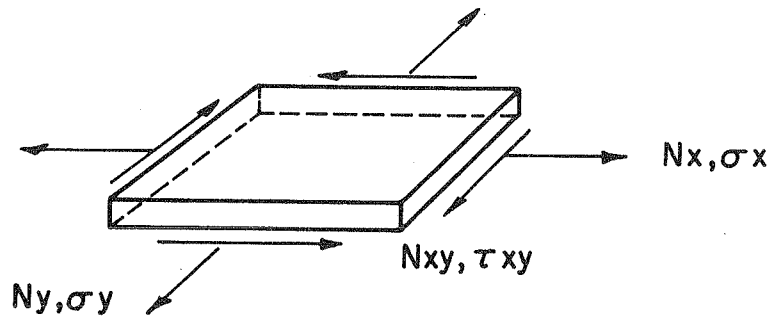


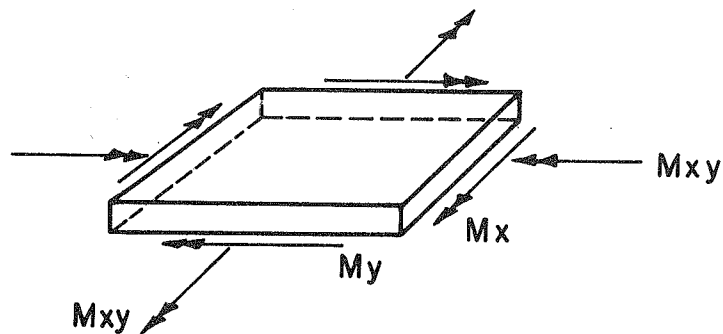
FIG. B5 SIGN CONVENTION FOR ELEMENT PROJECTIONS AND CORRESPONDING POSITIVE DIRECTION OF LOCAL ELEMENT COORDINATE AXES



a) ELEMENT COORDINATE AXES



b) N_x , N_y , N_{xy} ARE FORCES PER UNIT LENGTH.
 σ_x , σ_y , τ_{xy} ARE STRESSES EQUAL TO FORCES PER
 UNIT LENGTH DIVIDED BY ELEMENT THICKNESS



c) M_x , M_y , M_{xy} ARE MOMENTS PER UNIT LENGTH

FIG. B6 POSITIVE INTERNAL ELEMENT FORCES,
 MOMENTS AND STRESSES